



SBE16
MALTA
INTERNATIONAL CONFERENCE

**Europe and the Mediterranean
Towards a Sustainable Built Environment**

Chapter 5

Building Energy Performance

Current Status of Climate Change and Scenarios for Action

Nils Larsson

International Initiative for a Sustainable Built Environment

Email: larsson@iisbe.org

Abstract. This paper posits that the problems of climate change effects during the next 50-75 years will be coincident with scarcity and increasing costs of resources and increasing demand levels within the building sector. A case is made that climate change effects may arrive abruptly, which may cause public policy responses that are illogical and ineffective. Proposals are made for more logical responses for a rapid reduction of greenhouse gases under such emergency conditions.

1. GREENHOUSE GASES IN CLIMATE CHANGE

The anthropogenic driver of climate change is the increasing concentration of greenhouse gases (GHG) in the atmosphere, chiefly CO₂, but also including Methane, Sox and Nox gases. The World Resources Institute (WRI) estimates that buildings are directly responsible for 15.3 percent of global GHG emissions. To this should be added a share of industrial emissions (for materials) and for road transport. A very conservative estimate of building-related GHG share would therefore be in the range of 20 percent to 25 percent, and this would be higher in developed countries. A strategy for the diminution of GHGs must therefore include the building sector as main target for GHG reductions.

1.1. Energy and GHG emissions from buildings

The IPCC AR5 report on buildings¹ indicates that most global GHG emissions (6.02 Gt) are indirect CO₂ emissions from electricity use in buildings, and these have shown dynamic growth in the studied period in contrast to direct emissions, which have roughly stagnated during these four decades (Figure 1). For instance, residential indirect emissions quintupled and commercial emissions quadrupled.

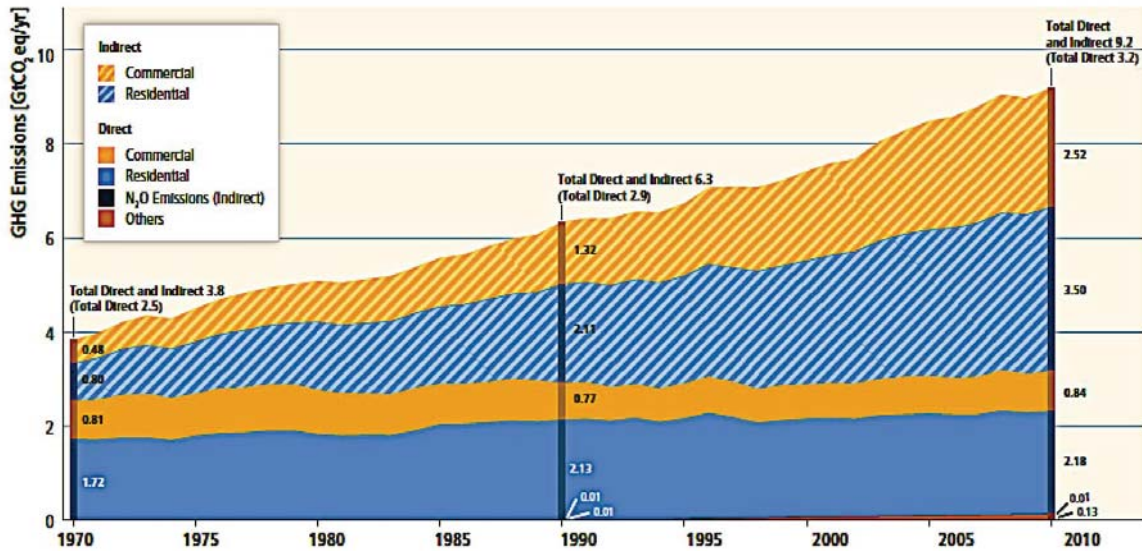


Fig 1: Direct and indirect emissions (from electricity and heat production) in the building subsectors (from IPCC WGIII, Chapter 9.2.1)

2. GLOBAL CLIMATE CHANGE IMPACTS

One of the sobering aspects of the work done by the IPCC is their exposition of the time scales involved. IPCC demonstrates that CO₂ emissions today have a positive feedback on global mean temperature that lasts for over 100 years, and the resulting sea level rise due to thermal expansion lasts well over a 1,000 years. Even if action to reduce GHGs is immediate, the effects of current emissions are still to come. Action is therefore needed, but in addition to the difficulty of obtaining political action, the slow rate of change in the building sector creates a special problem.

The overall impact is also clearly identified by IPCC, and identify some major global climate change projected impacts up to 2100, based on two different so-called *Representative Concentration Pathways* (RCP) that reflect differences in population and income growth as well as assumptions for technological change and energy intensity:

¹ IPCC Working Group III, Chapter 9.2.1

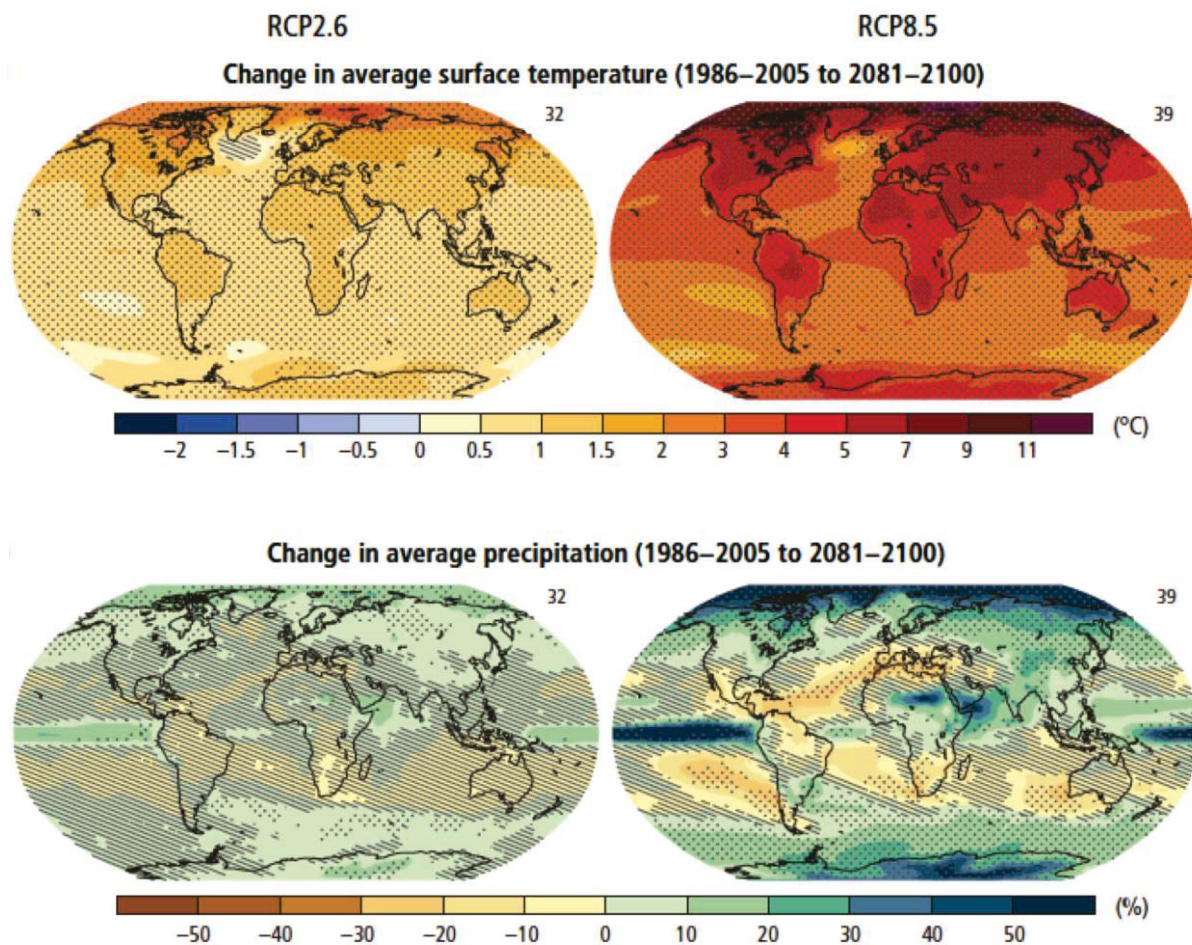


Fig. 2a and 2b: Changes to average global temperature and precipitation from the 1986-2005 period and projected to 2081-2100, from IPCC AR5 Summary for Policymakers, 2014.

3. CLIMATE CHANGE EFFECTS COMBINED WITH RESOURCE DEPLETION

3.1 Efficiency

Great strides are being made in improving the ecological performance of materials and mechanical systems are rapidly increasing in energy efficiency. Progress is also evident in the environmental performance of some new large buildings through changes in design practice, such as the adoption of *Integrated Design Process* protocols.

Performance improvements are mainly applicable to large and expensive new buildings, and more so in Europe than in North America or Asia. It should also be noted that new buildings in most regions represent only from 2% to 3% of the total building stock. Thus, high-performance exemplar projects represent only a very small portion of the total stock. Clearly, the stock of existing buildings should be the major focus of performance improvement efforts in the building sector but it is far more difficult to devise general prescriptions for performance improvements in existing buildings because of the

3.2 Consumption

Irrespective of efficiency gains in residential and non-residential buildings, the trend in developed countries to massively over-consume housing, and to develop it in a very low-density pattern, has required large quantities of materials for both infrastructure and buildings, with

consequent embodied and operating GHG emissions. The urban development of Las Vegas from 1973 to 2000, mainly from single-family housing, provides a striking example in Fig. 3.

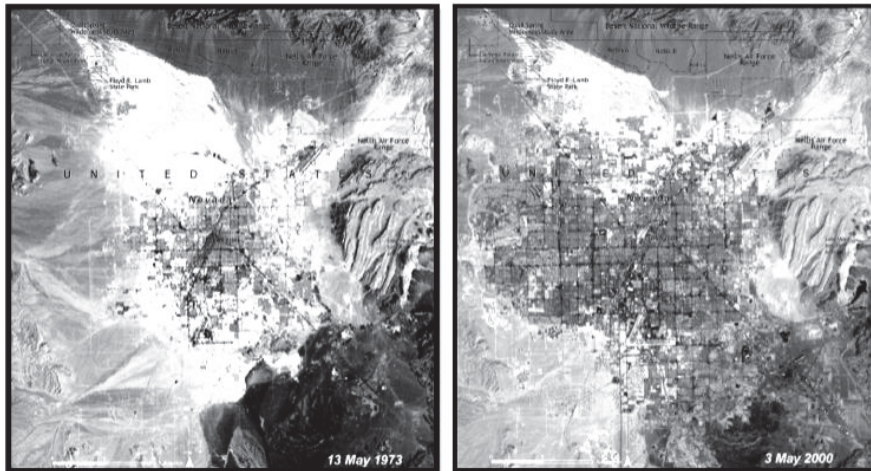


Fig 3: Aerial photos of urban development in Las Vegas in 1973 and 2000, from UNEP 2005

In the sub-sector of single-family houses (the most energy inefficient form of building) there has been considerable improvement in energy performance in North America over the last 15 years. However, there are compensating factors, as the data for single-family dwellings in the U.S.A indicate².

- Between 1950 and 2004, the size of the average new house in the US expanded by 135%, from about 93 m² to 218 m²;
- One in five new houses now comes in at more than 465 m². (The US National Association of Home Builders' 'showcase home' for 2005 was 553 m² or 15% bigger than the 2004 model.
- Forty-three per cent of new construction features 2.75 m ceilings compared with 15% in the 1980s.
- Meanwhile, between 1950 and 2003, average US household size fell from 3.7 to 2.6 people.
- This means that floor space per capita increased by over 230% from 25 m² to 84 m².

Such development patterns continue, and effectively wipe out efficiency gains. Although the recent recession has resulted in a reduction in the size of units, the problem is likely to worsen in other regions, with substantial urban growth forecast for regions such as Asia, Africa and Latin America, and with increasingly affluent populations striving for Western standards of accommodation. The sheer numbers, as shown below, will make solutions based on efficiency alone unlikely to succeed.

²From Rees, William E.(2009) *The ecological crisis and self-delusion: implications for the building sector*, in *Building Research & Information*, 37: 3, 300 — 311

4. THE DILEMMA

The overall situation is that, although impressive efficiency gains are being made in building and equipment performance, excess consumption is wiping out these gains. More troubling is that consumption is culturally determined, and cultural changes usually require a decade or more of substantial information and incentives. Some regions and countries, especially in Europe, have responded in a positive way, but major private sector emitters are not likely to respond to a sufficient degree, especially not within the very small narrow window of opportunity for mitigation that still exists. Add to this the need for substantial amounts of new construction in developing countries, and it is unlikely that global reductions in greenhouse gas emissions will be sufficient to result in levels below 450 ppm of GHG, which in turn will bring into play some of the more dire predictions of IPCC.

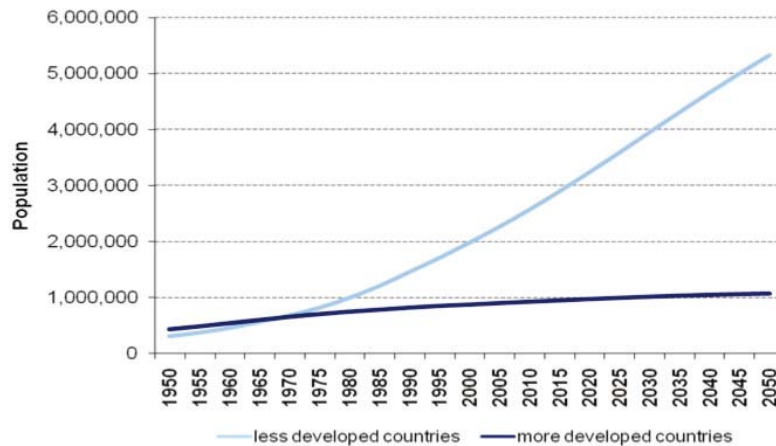


Fig 4: UN World Population Prospects: The 2006 World Urbanization Prospects: 2007 Revision

We therefore face a possibility of massive disruption of agriculture and industry and living and working conditions, possibly by mid-century and certainly by the end of the century. We are not likely to avoid this fate unless there is a major paradigm shift, and such shifts usually require major external events. It can be done: WW2 provides historical examples of such conditions³.

5. SCENARIOS FOR THE DEBUT OF CLIMATE CHANGE EFFECTS

A major problem in motivating decision-makers to act is that the harbingers of climate change in North America and northern Europe have been, until now, relatively gradual with benign effects. This sequence may cause us to become numbed by a gradually escalating series of climate-related incidents and not act decisively until it is far too late. However, climate change may also be announced by a series of major and sudden natural disasters, an outcome that is certainly within the bounds of projections made by the IPCC. If such a series of sudden catastrophes were to have direct impacts on elites in developed countries, especially in North America or Europe, there would likely be a strong and immediate public demand for effective responses to mitigate the effects of the events. This would provide a real opportunity to simultaneously deal with the greenhouse gas emissions that cause climate change, if key people and organizations had realistic plans and were ready to act.

Our assumption for the type of major events related to climate change that are likely to occur during the next decade include coastal storms with related storm surges, inland storms, flash floods, droughts and major forest fires.

³ See appendix 2 for an example of the kind of consumption restraints that proved acceptable in the U.S.A. during WW2.

5.1. *Business-as-usual scenario*

If a series of such events take place in first-world regions within the next decade, with extensive damage and multiple deaths, it is likely that the imminence of climate change will finally be accepted by the majority of decision-makers. Based on the history of catastrophic events of other types, we can assume that the shock effect will open the minds of the public and elites to radical measures. But such openness will last only for a few weeks, and desperate leaders will grab whatever plans are available. The result could be hasty, ad-hoc and poorly considered action. We have unfortunate examples of this kind of reaction from the collapse of the USSR, the 9/11 event, SARS, the recent recession, and even the current Gulf of Mexico oil spill.

5.2. *Responses under conditions of extreme and rapid climate change*

In the case of the forthcoming weather shocks from climate change effects, we may unfortunately face a similar situation, but the consequences may be even more serious. The immediate concern will be to care for injured populations and to carry out immediate repairs, and this is likely to push the need for adaptation and mitigation measures to the back burner.

Governments might be led to announce that, in addition to urgent repair and re-building efforts, national emissions must be reduced by large amounts over a very short period (say 80% by 2030 instead of 2050), along with promises of massive fines if targets are not met. Reaching such performance requirements would be very difficult, because strategies for such a rapid and deep reductions would have to be invented on the fly. We can foresee that such actions might be achievable in, for example, in the automotive or the consumer goods sectors, but it will be much harder to do so in the building sector. The building industry is very large and complex, with a few large players and very many small ones on the production side, and with control even more dispersed on the demand side. Finally, buildings, especially existing ones requiring renovation, are almost all unique, so global approaches need local modifications.

Given the scenario outlined above, a government might well push the construction and real estate sectors towards a rapid a drastic reduction in emissions, along with promises of large fines if targets are not met. Achieving such goals will be very difficult, because very few countries have central departments with direct responsibility for the building industry. Also, the industry is very large and complex, with a few large players and very many small ones on the production side, and with control even more dispersed on the demand side.

We can envision the results of these trends without too much speculation:

- First, we can expect a surge in demand for man and materials to carry out urgent repair, re-building and re-location needs which would, within a short time, deplete the supply of skilled and firms in the affected region;
- Manufacturers of building materials will be faced with urgent production requests, but would face greatly increased power costs, and might also have to cope with a disrupted labor force and plant conditions. Prices for materials and services of this type would therefore reach very high levels;
- Owners or managers of existing commercial buildings will have to reduce operating hours to meet GHG reduction targets;
- Residential owners of properties that do not meet very high performance standards may face mandatory energy cuts. When this is combined with the excessive size of many homes in North America, we can envision a surge in the sharing of accommodation;
- The value of buildings with poor energy efficiency will plummet. Suburban building land values will also face massive drops because of controls on new building and stringent limits on private vehicle emissions, which will bring new construction in outer suburbs to a halt.
- Many standards for good design and operations, such as adequate lighting levels, indoor comfort conditions, and work to preserve heritage buildings will fall by the wayside, at least temporarily (say for 20 years);

- Social tensions will rise to very high levels when those who want to pursue their normal paths (commercial building development, building your dream home) are faced with permit refusals, while climate refugees and families suffering from energy poverty are given priority;
- And the need to deal with repair and remedial work will lead governments to say that they cannot afford more GHG mitigation measures;

In the context of such a series of effects, it will be difficult to achieve substantial reductions in emissions.

5.3. A scenario for contingency planning

A leading academic, referring to recent evidence of rapid climate change in the Arctic and dealing with general social and political effects,¹ recently stated that ... *We need a much more deliberate Plan Z, with detailed scenarios of plausible climate shocks; close analyses of options for emergency response by governments, corporations and nongovernmental groups; and clear specifics about what resources — financial, technological and organizational — we will need to cope with different types of crises.*⁴

Some of these consequences can be avoided if quick and decisive action takes place, but such responses are likely to be effective only if action plans have been developed *before* the emergency occurs, and are ready for immediate implementation. Even though some government and many private-sector organizations have not been willing to take meaningful mitigation steps to date, they might be willing to prepare contingency plans for rapid reduction, as part of a due diligence process.

Such plans must support very rapid reductions in GHG emissions over a short time-frame – something like 75% over 5 years – but varying with the sector and specific cases. To be available when the time comes, such plans must be voluntarily developed *now* by a variety of public- and private-sector organisations, so they will be ready when needed. A large number of contingency plans will need to be prepared by individual governments and private-sector organizations, to cover most key sectors of the emission-producing economy.

Measures proposed do not include those that require lengthy planning or implementation times, such as the introduction of carbon taxes or risk assessment studies of existing urban areas and building stock with regard to possible climate change impact events, such as floods, wind storms, heat waves etc.⁵. Such work is a necessity for post-disaster recovery.

Excluding measures that require lengthy planning of implementation times, a selection of essential contingency plans will probably include plans for the *rapid* introduction of the following measures.

1. Immediately introduce carbon taxes, to reduce the carbon intensity of building-sector related goods and services; and simultaneously reduce existing income taxes;
2. Immediately ban the construction of new coal-fired generation power plants and the extension of existing plants, unless significant GHG sequestration is provided. It should be noted that much sequestration has been promised over the last decade, but very little has been delivered.
3. Rapidly reduce peak loads in electrical networks through the rate structure and through load ceilings, especially in manufacturing plants and commercial facilities, by means of changes in industrial processes, operating hours or other relevant means. This is intended to minimize the need for new power plants to handle peak loads.

⁴*Disaster at the Top of the World*, Thomas Homer-Dixon, New York Times, 22 Augsut, 2010

⁵See for example *Methods for risk assessment and mapping in Germany*, preface to special issue of *Natural Hazards Earth System Science* 6, 721-733, 2006, and also *Winter storm risk of residential structures - model development and application to German state of Baden-Württemberg*, P. Heneka, T. Hofherr, B. Ruck and C. Kottmeier, in *Natural Hazards Earth System Science* 6, 721-733, 2006.

4. Accelerate the introduction of feed-in tariff policies from decentralized renewable power sources, at rates that do not distort energy markets.
5. Ensure that facilities and services of critical importance, such as hospitals, public transportation systems, food supplies, water and sewage treatment and pumping systems, can remain functional at a basic level. This may require the provision of back-up electrical power, heat, water and other vital services on a decentralized basis.
6. Prepare for the relocation of key facilities such as docks⁶ and airports and of populations in areas vulnerable to flooding, storm surges or fire⁷. It should be noted that such projects may require 5 years or more to carry out, even on an urgent basis.
7. In developed countries, impose a *freeze* on new construction in un-serviced or low-density areas or potential flood areas, and a zero operating GHG emissions requirement for new construction that is permitted. This is undoubtedly one of the most important measures to minimize demand for scarce construction materials or land and also to minimize the generation of embodied emissions.
8. Ensure a rapid reduction programs in operating emissions of existing public buildings, private office, hotel and multi-unit residential buildings, through implementation of “shovel-ready” retrofit plans and better operating practices, all while minimising disruption or reduction in service levels to occupants.
9. Implement measures for the rapid and ambitious performance improvements in energy, peak loads and water consumption for existing single-family dwellings.
10. In areas designated for performance upgrading, establish immediate programs of urban infill to increase densities and renovation of existing buildings to greatly reduce GHG emissions (by at least 80%) and to improve water performance;
11. Launch programs for the rapid conversion of surplus office buildings to residential uses and identification of empty non-primary dwellings. Such a measure may be needed if residential areas are damaged or destroyed or if there is an influx of climate refugees.
12. Introduce measures to minimize short-term speculative price rises for construction materials. Under emergency conditions, free-market speculation can lead to material shortages and an inability to carry out urgent repair and upgrade projects.
13. Prohibit the sale of appliances and equipment that do not meet certain operating efficiency criteria (e.g. "A" label in Europe).
14. Establish priority training programs for regulators, renovation contractors, simulation specialists and others needed to upgrade performance in new and existing buildings.
15. Rapidly implement public education programs to promote conservation in energy, water and materials, for office tenants and residential owners or tenants.

The question of which of the measures outlined above will be the most effective is being partly addressed by major international organizations, such as IEA, OECD, the new Global Alliance for Building and Construction (Global ABC) and others, but there is little available so far that reflects the views of individual experts and knowledgeable individuals in diverse regions. The SBE partners, CIB, iiSBE, UNEP-SBCI and FIDIC are launching an international

⁶ The U.S. military is well aware of the dangers that many of its coastal bases are facing; see *National Security and the Threat of Climate Change*, CNA Corporation, 2007.

⁷ The dismal efforts at relocation and rebuilding in New Orleans are a reminder of how extensive and well coordinated the required efforts will have to be if they are to be successful;

survey in 2016 to address this issue⁸, building on the results of a pilot survey carried out in late 2015 by iiSBE. It is hoped that the analysis of this large-scale survey will supplement the top-down policy prescriptions that are being developed. No matter what measures emerge from the survey as considered most effective, they will have to be implemented by existing governments, professional associations and companies.

In any case, it is clear that the content of GHG rapid reduction plans proposed above would be a sensitive matter in some cases, where the leakage of information *under current conditions* might pose political difficulties because of limitations on personal freedom of action that are implicit in such measures, as well as harm that might occur to companies in a highly competitive market. It is therefore suggested that participating organizations would not be compelled to share their plans with any outside organization, but only to report that they have completed a plan that satisfies the content criteria established in the project. The main emphasis here is to ensure that workable and humane plans are available for *rapid* implementation when circumstances demand it. There are certain characteristics that such plans would have to be based on if they are to be effective.

- Measures proposed will have to be able to be very quickly implemented; beginning within weeks rather than months;
- The scope of proposed action will have to be defined (e.g. all or part of a property portfolio, certain segments of a customer base etc);
- Estimates of speed and amount of net reduction in GHGs emissions will have to be provided, projected on a year-by-year basis over a 5-year time frame;
- Plans will have to identify measures to minimize negative social disruption or other secondary impacts;
- Identify main obstacles or sources of likely opposition and suggest coping strategies;
- Complementary action required by governments, other regulatory authorities or financial institutions to facilitate implementation of the plan should be identified.

6. CONCLUSIONS

Some governments, especially in Europe, have launched ambitious plans to reduce GHGs, but it is not yet clear whether their voters will agree with the changes in lifestyle that will be necessary to meet these targets.

Excessive consumption will not easily be reduced, and is likely to lead us into global temperature increases that will be considerably greater than the desired target of 1.5 °C or even 2 °C;

It will probably require one or more climate-induced disasters of major proportions to shock governments and their populations into real action, especially in North America. When that happens, there will be an immediate demand for contingency plans to reduce GHGs in a very rapid way and to implement urgent measures for climate change adaptation.

In view of on-going government inaction, it is most logical for national and local governments, as well as private organizations to develop such plans and keep them ready. The alternative is to do nothing now, but to be forced to accept hastily developed and unsound plans when an emergency is declared.

⁸The draft plan can be downloaded from <http://www.iisbe.org/node/205#attachments>

Introducing the Portuguese Sustainability Assessment Tool for Urban Areas: SBTool PT – Urban Planning

Luis Bragança

University of Minho, School of Engineering, Civil Engineering Department, Guimarães, Portugal

Erika Guimarães

University of Minho, School of Engineering, Civil Engineering Department, Guimarães, Portugal

Email: braganca@civil.uminho.pt

Abstract. Given the accelerated urbanization process throughout the twentieth century, many of today's cities reflect a fast and disordered growth, which influences directly the demand for natural resources. For an indispensable change in the current urban infrastructure management models, it is necessary to quantify the sustainability level of actual practices and proposals. In this context, based on widespread methods, SBTool_PT Urban Planning represents an adaptation of the SBTool international method to the Portuguese context. This tool assesses the sustainability level of the practices promoted in urban projects with no size restrictions and is applicable to new urban development and/or urban renovation. The process is conducted by a rigorous analysis of requisites specifically developed to stimulate improvements on energy consumption, management of potable water, solid waste, urban soil and territory and air quality. Aiming at a full introduction of the tool, this article contextualizes its development and characterizes its assessment methodology. Additional application to a case study shows how the assessment of a proposed project is performed

1. INTRODUCTION

Cities are subjected to constant physic, social and economic changes, driven by various needs of societies and cause severe and irreversible disturbs on urban environment. Currently, given the accelerated population growth rates, the rhythm of imposed alterations is increasingly frenetic. The raise of urban population expands the existing urban networks and transforms rural areas, conducting sequential alterations in the environment. Beyond the immediate impacts, constant changes in urban environment deeply imbalance the quality of life of its inhabitants in the long term.

Given the rapid urbanization process of the latest twentieth century, today's cities reflect a fast and disordered development, which influences directly the need for resources and energy. Inevitably coincident with higher population densities, the increase of urbanization rates comes along with substantial raise in the demand of materials, water and energy sources and also affects the waste and effluent generation. Many urban infrastructure management models, internationally consolidated in industrialized countries, are strongly depended on non-renewable sources. Several studies demonstrate that the use of fossil fuel tends to enlarge in the short term, mainly in emergent countries, where economic development matches the increase of urbanization rates and population concentration.

It is thereby urgent to reassess the existing policies and regulation mechanisms through the establishment of social economic and environmental principles. To produce new, sustainable oriented, urban management models, it is necessary to quantify the sustainability level of proposed solutions. Sustainability assessment in urban areas must be made through the evaluation of priority criteria, which should base certification tools. This is an essential initiative to promote sustainable urban planning and governance.

The concept of urban morphology embraces everything that composes the urban network, such as the built heritage, the roads infrastructure, landscapes and open spaces. The shape of an urban community is the result of the interaction between those elements, through interventions of the inhabitants, local climate and other systems. In addition to stationary elements, movements and socioeconomic dynamics are implicit within the urban network. Thereby, an urban scenario scope is much more complex when compared to the assessment of a single building.

Based among others on the SBTool international method, a proposal to apply the SBTool methodology on urban areas was developed inside the scope of SBTool PT-STP project. The tool, called SBTool_PT Urban Planning (UP), presents a structure conceived towards the assessment of urban planning operations. Because of this specific scope, mainly at scale level, the tool has little similarities with the analogue tool designed for buildings (SBTool_PT Residential Buildings). However, its guidelines maintain the approach of several categories previously defined in accordance with existing international methodologies.

Hereinafter, this article presents the SBTool_PT-UP as an effective methodology for the assessment of urban communities. After a brief introduction on the basis for its development, an overall definition regarding the tool's overall aspects is made, regarding the main objectives, structure and calculation process. To achieve the purposes of a throughout presentation, the evaluation of a proposed project is followed in the form of a case study. The subsequent discussion of results acknowledges the main conclusions retrieved from the sustainability assessment performed by the tool.

2. METHODOLOGY BASIS

Prior to the presentation of the SBTool_PT for Urban Planning operations, it is necessary to analyse the different international methodologies in which the tool's development is based. Each methodology presents a proper structure, organized according to sustainability's dimensions. Also, the tool's assessment structure comes after the acknowledgement of different political strategies at national, European and international scale, and internationally accepted lists of sustainability indicators.

Thereby, the SBTool methodology for urban planning presents crosscut aspects with methods and practices recognized worldwide. In particular, BREEAM Communities, LEED for Neighbourhood Development and SBTool International Method must be highlighted.

2.1. *BREEAM Communities*

BREEAM Communities is an independent certification and assessment system that approaches sustainable concepts at social, economic and environmental levels, as well as the design requisites that impact practices within the built environment. The system provides credits according to the project's performance on sustainable objectives and planning policies. The summation of credits gives a final global score that varies from Pass, Good, Very Good, Excellent and Outstanding.

Certification is regulated by a "sustainability council", which represents a wide range of stakeholders of construction industry in the UK. BREEAM Communities certification standard embraces eight categories of assessment, described in table 1.

Table 1. Summary of BREEAM Communities Structure.

Category	Number of Indicators	Main objective
Climate and Energy	9	Reduce climate alterations
Community	4	Encourage community participation
Place Shaping	11	Conceive a local identify respecting local heritage
Ecology and Diversity	3	Protect site's ecological value
Transport	11	Provide sustainable transportation options
Resources	6	Ensure the efficient use and disposal of resources
Business	5	Supply site's economic needs and create local jobs offers
Buildings	2	Guide sustainable design of buildings

2.2. LEED for Neighbourhood Development

The objective of LEED for Neighbourhood Development is the promotion of healthy, lasting economic and environmentally rational practices on projects and construction of buildings. Based on the principles of the “New Urbanism” and on the theories of “Smart Growth” and “Sustainable Construction”, this tool focuses on the local selection, the association with existing buildings and infrastructure and the relation with the landscape. As shown in table 2, LEED for Neighbourhood Development is structured in three mandatory groups and two additional punctuation groups.

Table 2. Summary of LEED for Neighbourhood Development Structure.

Category	Number of Indicators	Main objective
Smart Location and Linkage	5 (mandatory) + 9 (credits)	Selection of the best location for the development concerning environmental and social priorities
Neighbourhood Pattern and Design	3 (mandatory) + 15(credits)	Emphasize social needs in the urban design process
Green Infrastructure and Building	4 (mandatory) + 17 (credits)	Highlights priority environmental and social aspects for the buildings' design
Innovation and Design Process (optional)	3 (credits)	Valorize higher performance practices
Regional Priority Credit (optional)	6 (credits)	Stimulate concern with site's specific environmental issues

2.3. SBTool International Method

The SBTool (Sustainable Building Tool) International Method is an initiative of the non for profit association iiSBE (International Initiative for the Sustainable Built Environment), developed in cooperation with teams from over 20 countries. The method establishes an overall frame to assess sustainable performance of buildings and developments and is a useful tool to help local organizations to develop SBTool-based sustainability evaluation systems.

The SBTool International Methodology is divided in two phases. The first, Evaluation of Project's Implantation Site, concerns the planning phase and supports macro issues related to local context. The second, Evaluation of Project and Building's Performance, refers to design, construction and operation phases and analyses parameters essentially related to local renovation/ regeneration, urban design and infrastructures and other built environment specific issues.

Likewise other assessment tools developed within the scope of the Portuguese context, SBTool_PT-UP is based in the structure of the SBTool international method, which is summarized in table 3.

Table 3. Structure of SBTool International Methodology regarding relevance for Urban Planning Operations (UPO).

Scope	Theme	Number of Categories / Indicators	Relevant Indicators for UPO
Evaluation of Project's Implantation Site	Location, Services and site's characteristics	3/26	6
Evaluation of Project and Building's Performance	Site's Development and Regeneration, Urban Project and Infrastructures	3/35	6
	Resources and Energy Consume	4/16	7
	Environmental Loads	5/25	17
	Indoor Environment Quality	5/19	16
	Service Quality	5/35	29
	Social and Cultural Aspects	3/15	9
	Economic Aspects	1/8	4

3. METHODOLOGY DESCRIPTION

3.1. Overview and Objectives

SBTool_PT-UP is applicable to urban planning projects that are not covered inside Urbanization Plans nor Detailed Plans scopes, and may eventually be framed as National Interest Plans (PIN). According to Portuguese laws, Urbanization Plans (PU) define the planning and urbanization policies for a large-scale urban territory Detailed Plans (PP) constitute specific parts of PU's, being subjected to municipal approval and promoted either by private or governmental initiatives. PIN's are projects that, among other objectives, promote positive impacts regarding the local development strategies or contribution to economic dynamics of economically disadvantaged regions.

The assessment made by the methodology focuses equally the development of new areas and interventions in existing urban communities, namely urban renovation or regeneration. Certification regards exclusively the project, where two phases are identifiable preliminary projects and detailed projects. The importance of a preliminary evaluation is given by the possibility of establishing the guidelines of sustainable urban areas.

The overall objectives of the sustainability assessment and certification methodology for urban planning concern:

- Improvement of space organization for urban network consolidation;
- Assurance of environment preservation and enhancement of environmental quality of urban entourage;
- Safeguard of the quality of life of urban communities' habitants;
- Fomentation of regional economic competition;
- Promotion of sustainability assessment of the built environment.

3.2. Structure

The general structure of SBTool_PT-UP is based on the hierarchy Dimension>Category>Indicator, as shown in table 5. The methodology presents 41 indicators, distributed among 14 categories within 3 main dimensions. The dimensions, related to the basis of sustainability, divide the categories in a macro scale. Categories, in turn, group indicators according to common issues and may also attend a life cycle analysis. Each one identifies the corresponding stage of life cycle (construction, operation and dismantlement), according to EN 15942. At last, indicators refer to impacts associated to specific aspects inside the respective category scope.

Each indicator assesses the impact of the urban area according to proper calculation methods, associated to individual functional units. The provided score represents an individual performance of the project. Posterior stage consists in comparing the score to the performance of reference urban areas. Such areas apply excellence, recognized practices inside sustainability

precepts, and thereby are acknowledged as benchmarks. The comparison is made using figures normalized through the Diaz-Balteiro equation, shown in equation (1).

$$\bar{P}_i = \frac{P_i - P_{*i}}{P_i^* - P_{*i}} \quad (1)$$

Where: P_i is the score on the indicator i ; P_{*i} and P_i^* correspond respectively to results of conventional and best practices for indicator i ; \bar{P}_i the normalized result.

Normalization method converts the parameters into a dimensionless scale, ranging from 0 (worst value) to 1 (best value). At last, the normalized result for each parameter is classified from A+ to E, according to the final score

To determine the score correspondent to the total performance, the individual values are summed up through a weighted system, which attributes different importance levels for indicators, categories and dimensions. The assigned weights are shown in table 4.

Table 4. General Assessment Structure of SBTool_PT-UP.

Dimension	Weight	Category	Weight	Indicator	Life Cycle Stage ^a	Weight		
Environmental	50%	Urban Design	20%	I.1	Passive Solar Planning	U	34%	
				I.2	Ventilation Potential	U	33%	
				I.3	Urban Network	U	33%	
		Use of Land and Infrastructures	15%		I.4	Land Natural aptitude	C; U	26%
					I.5	Flexible uses	C; U	14%
					I.6	Urban soil reutilization	C	23%
					I.7	Built heritage revitalization	C	17%
					I.8	Technical Infrastructure Network	C; U	20%
		Ecology and Biodiversity	20%		I.9	Green Spaces Distribution	U	26%
					I.10	Green Spaces Connectivity	U	29%
					I.11	Autochthone Vegetation	C; U	29%
					I.12	Environmental Governance	U	16%
		Energy	15%		I.13	Energy Efficiency	U	41%
					I.14	Renewable Energy	U	36%
					I.15	Centralized Energy Management	U	23%
		Water	15%		I.16	Potable Water Consume	U	40%
					I.17	Centralized Water Management	U	40%
					I.18	Effluent Management	U	20%
		Materials and Waste	15%		I.19	Material's Impact	C; D	39%
					I.20	Construction and Demolition Waste	C; D	22%
					I.21	Urban Solid Waste Management	U	39%
Social	30%	Exterior Comfort	20%	I.22	Air Quality	U	23%	
				I.23	Exterior Thermal Comfort	U	32%	
				I.24	Noise Pollution	U	18%	
				I.25	Light Pollution	U	27%	
				I.26	Safety in the Streets	U	50%	
		Safety	10%		I.27	Technological and Natural Risks	U	50%
					I.28	Service Proximity	U	37%
		Amenities	25%		I.29	Leisure Equipment	U	37%
					I.30	Local food production	U	26%
					I.31	Public Transportation	U	35%
		Mobility	25%		I.32	Pedestrian Accessibility	U	30%
					I.33	Cycling Network	U	35%
I.34	Public Spaces				U	42%		
Local and Cultural Identity	20%		I.35	Heritage Enhancement	C; U	26%		
			I.36	Social Inclusion and integration	U	32%		
Economic	20%	Employment and Economic Development	100%	I.37	Economic Viability	U	35%	
				I.38	Local Economy	U	35%	
				I.39	Employment	C; U	30%	
Extra Points	5%	Buildings	44%	I.40	Sustainable Buildings	C; U	100%	
		Environment	56%	I.41	Environmental Management	C; U; D	100%	

^a C – Construction; U – Use; D – Dismantlement

4. CASE STUDY

To characterize a practical application of the methodology and also demonstrate its performance as assessment tool, the analysis of an urban planning development is proposed as case study. The selected plan is Vila Lago Monsaraz Golf & Nautic Resort, which involves a land transformation for the purposes of touristic development.

Vila Lago Monsaraz Golf & Nautic Resort is a Detailed Plan (PP), also characterized as a National Interest Plan, located at the margins of Alqueva Dam, within Gagos and Xerez homesteads, at the Portuguese district of Monsaraz. Total investments involve about 170 million euros in a 15-year horizon, an area of 371,5 ha, 623 units related to hotel, touristic and commerce facilities and the creation of 700 job positions.

Placed inside a well-marked cultural landscape, the Alentejo region, the plan establishes the pre-requisites for a touristic intervention that aims natural, cultural and landscaped enhancement coupled with enjoyment of future users. These are important aspects to environmental and territorial valorization and the remarkable presence of water bodies improves the site's scenery features. The project has been positively distinguished by third-party Portuguese entities as the promoted sustainable practices overcome the standard practice in the country. Strategies related to local water management, use of local and recycled materials, solar orientation of the buildings (majorly North/South), vegetation as passive-shading components, and safe pedestrian pathways are the principal responsible for the good environmental performance.

Construction works had started in 2009 and when this analysis was made (2014) only technical infrastructure networks were completed. Thereby, the evaluation is focused exclusively on the project proposal. Table 5 presents the detailed scores and results.

Table 5. Final results for case study assessment.

Indicator	Score	Classification
I-1 Passive Solar Planning	0,45	B
I-2 Ventilation Potential	1,00	A
I-3 Urban Network	-0,74	E
I-4 Land Natural aptitude	1,00	A
I-5 Flexible uses	0,24	C
I-6 Urban soil reutilization	0,00	D
I-7 Built heritage revitalization	0,00	D
I-8 Technical Infrastructure Network	0,00	D
I-9 Green Spaces Distribution	0,32	C
I-10 Green Spaces Connectivity	1,00	A
I-11 Autochthone Vegetation	1,00	A
I-12 Environmental Governance	0,00	D
I-13 Energy Efficiency	1,00	A
I-14 Renewable Energy	0,20	C
I-15 Centralized Energy Management	0,53	B
I-16 Potable Water Consume	0,30	C
I-17 Centralized Water Management	0,96	A
I-18 Effluent Management	0,00	D
I-19 Material's Impact	1,00	A
I-20 Construction and Demolition Waste	0,58	B
I-21 Urban Solid Waste Management	0,00	D
I-22 Air Quality	1,00	A
I-23 Exterior Thermal Comfort	0,37	C
I-24 Noise Pollution	1,00	A
I-25 Light Pollution	0,42	B

I-26	Safety in the Streets	0,57	B
I-27	Technological and Natural Risks	0,33	C
I-28	Service Proximity	0,01	D
I-29	Passive Solar Planning	0,02	D
I-30	Ventilation Potential	0,08	D
I-31	Urban Network	-0,20	E
I-32	Land Natural aptitude	0,53	B
I-33	Flexible uses	0,29	C
I-34	Urban soil reutilization	28,69	A+
I-35	Built heritage revitalization	0,78	A
I-36	Technical Infrastructure Network	0,09	D
I-37	Green Spaces Distribution	0,22	C
I-38	Green Spaces Connectivity	0,15	C
I-39	Autochthone Vegetation	0,45	B
I-40	Environmental Governance	0,63	B
I-41	Energy Efficiency	0,00	D
Total			B

5. FINAL REMARKS

In the face of contemporary cities' needs, adopting sustainable guidelines in the development of urban management models is a verified new international trend. Nevertheless, many project designers are still unaware of this reality, which justifies investments on instruments for assessing and guiding urban areas towards sustainable performances.

In this ambit, assessment and certification tools stand out as suitable mechanisms for comparing practices adopted by existing proposals. SBTool Portuguese methodology for urban planning is pointed out as an adaptation of SBTool international method, as it modifies both the scale and scope of assessments. This conceptual change boosts its application and improves sustainability features for the built environment by defining sustainable parameters and comparing different solutions.

The results of a case study assessment showed that, although still under development and subjected to validation by iiSBE Portugal association, SBTool_PT-UP is a suitable method for evaluation of urban planning developments. The tool demonstrated a holistic approach in the sustainability assessment and allowed a good perception of project's performance at impact categories level.

REFERENCES

- Bragança, L., Araújo, C., Castanheira, G., Barbosa, J.A., Oliveira, P., "Approaching sustainability in the built environment" in International Conference SB13 Seoul - Sustainable Building Telegram Toward Global Society, 2013, pp. 17–25.
- J. A. Barbosa, L. Bragança and R. Mateus, "Assessment of Land Use Efficiency Using BSA Tools: Development of a New Index" *J. Urban Plan. Dev.*, vol. 141, no. 2, 2014.
- R. Mateus and L. Bragança, "Sustainability assessment and rating of buildings: Developing the methodology SBToolPT-H" *Build. Environ.*, vol. 46, no. 10, pp. 1962–1971, 2011.
- Ecochoice& LFTC UMinho, "SBTool PT: Metodologia para Planeamento Urbano - Relatório de desenvolvimento" 2013.
- BRE, "The Case for BREEAM Communities. BREEAM-UK" 2014.
- BRE, "Breeam Communities Technical Manual SD202 -1.0:2012" 2014. [Online]. Available: http://www.breeam.com/communitiesmanual/#_frontmatter/breeam_communities.htm%3FTocPath%3D_____1. [Accessed: 16-Nov-2015].

USGB, “Getting to know LEED: Neighborhood Development,” 2014. [Online]. Available: <http://www.usgbc.org/articles/getting-know-leed-neighborhood-development>. [Accessed: 13-Nov-2015].

USGB, “LEED v 4 for NEIGHBORHOOD DEVELOPMENT” 2014.

L. Bragança and R. Mateus, “Guia de Avaliação SBTool PT H v2009/1” 2009.

iiSBE, “SB Method and SBTool for 2015 - Overview” 2015.

Portugal, Decreto-Lei nº 316/2007. 2007.

Portugal, Decreto-Lei nº 76/2011. 2011.

iiSBE, “International Initiative for a Sustainable Built Environment” 2009. [Online]. Available: <http://www.iisbe.org/>. [Accessed: 13-Nov-2015].

Ecochoice & LFTC UMinho, “Relatório Técnico Científico Final - SBTool PT-STP – Ferramenta para a avaliação e certificação da sustentabilidade da construção” 2014.

The Contribution of Energy Performance Certificates to Resource Savings and Environmental Protection - Lessons from Germany

Thomas Lützkendorf

Karlsruhe Institute of Technology (KIT), Centre for Real Estate, Kaiserstraße 12, 76131 Karlsruhe, Germany

Peter Michl

Karlsruhe Institute of Technology (KIT), Centre for Real Estate, Kaiserstraße 12, 76131 Karlsruhe, Germany

David Lorenz

Karlsruhe Institute of Technology (KIT), Centre for Real Estate, Kaiserstraße 12, 76131 Karlsruhe, Germany

E-mail: thomas.luetzkendorf@kit.edu

Abstract. The provision of sufficient information is a requisite for rational decision-making. The role of Energy Performance Certificates (EPCs) as a policy instrument is considered for both, creating transparency in property markets on the energy characteristics of buildings as well as for motivating building owners to invest in energy efficiency retrofits. It is argued that transparency on the energy-related characteristics of buildings is a) required for rational planning and evaluation of energy policy in the building sector and b) is one of the necessary conditions to enhance the competitiveness of energy efficient **buildings** in the market place. If EPCs are to be effective, then they must be: a) available/accessible and widely disseminated, that their content is b) comparable and reliable, and c) relevant and generally understandable. The problems and barriers are considered for firmly embedding EPCs within the German real estate market between 1995 and 2012/2013, along with the latest policy responses to overcome some of these issues.

1. INTRODUCTION: EPCS AS PART OF EUROPEAN ENERGY POLICY

Political activities directed towards establishing a common energy policy of the European Community date back to 1974 and emerged as a response to the first oil price crisis in 1973. Until the 1990s the main focus was on reducing energy imports. Since then, an integrated energy and environmental policy has been pursued which is reflected in the triad of the key goals of a safe, reasonably priced, and environmentally friendly energy supply. To date, two main strategies are pursued in this context:

Energy demand: Reduction of final and primary energy consumption through measures focused on encouraging prudent and rational energy utilization as well as on saving energy.

Energy supply: Covering energy needs through a substitution of low-CO₂ and renewable sources for primary energy consumption.¹

The building sector is considered to be one of the most critical areas for achieving reductions in energy consumption. The main guidelines and directives of European energy policy for this sector display two prevalent approaches:

Development and further refinement of the *legal minimum requirements for the energy efficiency of buildings*. From 1976 onwards, the focus initially was on minimum requirements for insulation as well as on the efficiency of installations. Since 2002, these “singular” requirements have been replaced by minimum requirements concerning the overall energy efficiency of buildings. In 2010, these have been further extended by a *cost efficiency requirement*.

The provision of *technical facilities to measure and control energy consumption* as a basis for a *consumption-based invoicing of energy costs*. This area of regulation has been continuously further developed since 1976.

Beside these regulatory instruments, the requirement for energy performance certificates (EPCs) in member states first appeared in 1993. EPCs were designed as measures to *increase transparency in real estate markets* by providing information on the energy qualities of buildings.

The paper is structured as follows. First, EPCs are discussed as an instrument for improving market transparency and the problem of adverse selection is considered. This is followed by an explanation of the potential of EPCs for energy policy evaluation in the building sector. Against this theoretical background the utilization of EPCs in Germany is discussed in detail. Problems and barriers in firmly embedding EPCs within the German property (real estate) market during the time span from 1995 to 2012/2013 are identified and comments on latest policy responses to overcome some of these issues are provided.

2. THE IMPORTANCE OF MARKET TRANSPARENCY

In 1993, the Council of the European Union requested from member states within the Save-directive to develop and implement programs tailored at establishing EPCs for buildings. EPCs themselves were assigned the following functions: (1) Improving property (real estate) market transparency through the provisioning of objective information on energy-related characteristics of buildings, (2) Informing potential building users about efficient energy usage, and (3) Highlighting possibilities for improving energy-related characteristics. Since then, the requirements concerning EPCs have been further developed and specified within the Energy Performance of Buildings Directive and have then been transferred into the national laws and regulations of European member states.

Why is market transparency is one of the central conditions for the functioning of property (real estate) markets? In economics the model of perfect competition describes a set of premises under which a market leads to an efficient allocation of goods without the need of governmental interventions. However, the notion of market failure suggests that a non-efficient allocation can occur. One cause of market failure is asymmetric information and is related to the following two assumptions of the model of perfect competition (see, for example:):

homogeneity of goods: There are no quality, temporal and spatial differences between products. Furthermore, there are no personal preferences between market actors.

full market transparency: Sellers and buyers have complete, symmetric and free information about all market-relevant aspects, especially about the quality and prices of the goods.

Under asymmetric information as a cause of market failure, the violation of the assumption of homogenous goods plays only a minor role:

If goods are not homogeneous and full market transparency exists, then the price differentiation would reflect the differences in quality.

If the goods were not homogeneous and no full market transparency prevails, then there is no guarantee that prices reflect the quality differences. In this case, it is possible that high-quality goods are supplanted by low quality goods. The market for high-quality goods thus collapses.

The latter point briefly describes the problem of adverse selection, which was firstly shown by Akerlof. The problem of adverse selection mainly arises when consumers cannot actually observe the quality characteristics of goods (or when this is only possible with high effort/expenses). This particularly applies to the energy characteristics of buildings. For this reason, transparency on the energy characteristics of buildings is a necessary condition (but is not sufficient on its own) to enable market results (e.g. transaction prices, rents) to reflect these qualities. The competitiveness of buildings can also depend on these characteristics.

3. EPCS AND POLICY EVALUATION

Sensible planning and evaluation of energy policy in the building sector at the national and supra-national level requires – amongst other issues – the continuous monitoring of the energy quality of the building stock. In this context, the wide availability within a geographic region or country of EPCs for new and existing buildings can significantly contribute to establishing the necessary data sources. In order to illustrate this, the distinction between direct goals and potential positive/negative side effects of energy policy is helpful.

The direct goals of energy policy for the building sector can be summarized as the reduction of both, negative environmental impacts and dependence on energy imports through lowering primary- and final-energy consumption of the building stock. Consequently, the planning and evaluation of different energy policy instruments requires the continuous collection and analysis of data on (1) the energy quality of the building stock, (2) the rate of new construction, and (3) the rate of energy retrofitting the existing stock.

Beside direct policy goals, potential positive and negative side effects of energy policy need to be taken into account as well. So far, the focus of attention is on social and economic consequences; i.e. on questions relating to cost efficiency of energy retrofits and associated financial capabilities of building owners and tenants. In order to address such questions, data on the energy quality of buildings need to be combined with corresponding economic data (for example, on construction/refurbishment costs, transaction prices, rents and operating costs) and their interrelationships need to be analysed. In addition, addressing questions relating to financial capabilities of building owners and tenants requires taking into account additional data, for example on household income.

As such, linking economic data/parameters with data on the energy quality of buildings serves different purposes:

To evaluate the impact of EPCs; i.e. to assess whether and to what extent a differentiation of prices and rents is based on the energy characteristics of buildings.

To evaluate the cost efficiency and financial burden of minimum energy performance requirements and evaluate necessary financial subsidies (e.g. investment grants or subsidised loans).

For direct policy goals, an individual policy instrument or potential side effects to be evaluated, governments face the policy challenge of embedding a feedback mechanism within the real estate market. One fundamental difficulty here is that individual contributions of one specific policy instrument (e.g. EPCs) to overall policy goals usually cannot be precisely determined. This is because policy instruments are usually applied together as a bundle of instruments that often mutually depend and/or impact on each other. An additional, associated concern is the difficulty to relate positive or negative consequences back to one single instrument or even a bundle of instruments. This is because success or failure concerning the achievement of overall policy goals could also be caused by other factors. This particularly applies for EPCs which aim at influencing decision making by providing more/better information.

There is no straightforward link between market participants' level of information/education and the actions they take. Although an improved consciousness among market participants might lead to a change in behaviour taking place, a change in behaviour might have also been caused by other factors. This is what makes the evaluation of policy instruments a difficult undertaking and explains why the "success" of single instruments (in this case EPCs) usually cannot be evaluated in terms of their contribution to overall goals but only in terms of their contribution to achieving specific targets (e.g. improving market transparency by increasing the availability energy data).

EPCs have a special role since their widespread availability and dissemination is a necessary condition to evaluate whether overall energy policy goals (reduction of energy consumption and CO₂-emissions within the building stock) are being achieved. EPCs can only realise their full potential (in terms of establishing the necessary data sources and enabling feedback mechanisms at the policy level) if two conditions are met. First, they are legally embedded within the property market context. Second, they are linked to additional information/data gathered by governmental authorities and others (e.g. statistical bureaus, valuation expert committees, property market data providers, etc.).

4. EXPLOITING THE THEORETICAL POTENTIAL OF EPCS IN GERMANY

Legally binding requirements for EPCs were formulated for the first time within the German thermal insulation order of 1995 (Wärmeschutzverordnung). From 2002 onwards, the results of revisions, further developments and specifications of EPC requirements have been fed into the latest valid versions of the German energy savings order (Energieeinsparverordnung EnEV, version 2002, 2004, 2007, 2009, and 2013).

4.1. Current situation in Germany (1995-2012/2013)

To what extent are EPCs used in Germany a) by market participants as a basis for decision-making, and b) by governmental authorities and others as a basis for energy policy evaluation and real estate market analysis? The answer to this is structured according to three minimum requirements/conditions for a beneficial utilization of EPCs. EPCs need to be a) available/accessible and widely disseminated, and their content needs to be b) comparable and reliable, and c) relevant and generally understandable.

a) Availability/accessibility and dissemination of EPCs

Germany has no centralized database within which the content of EPCs is stored and which could serve as an information source for market participants and governmental authorities.

The demand for EPCs among market participants in Germany is also very low, in both letting (rental) and sales contexts. For example, the German association of housing companies recently estimated that in the past, less than 1% of potential tenants actively requested an EPC prior to renting a flat; and a study of the German energy agency estimated that only in 26% of the cases an EPC had actually been handed over prior to signing a rental or sales contract.

A low availability and dissemination of EPCs is also confirmed by the valuation expert committee of the city of Karlsruhe which stated (upon the authors' request) that EPCs were available for only a marginal fraction of transactions that have taken place in Karlsruhe during the past ten years. This corresponds with the situation in many other German cities: all current market reports (published through the respective valuation expert committees) for the 16 state capitals in Germany do not make any reference to EPCs and energy-related quality characteristics in connection with the (hedonic) analysis of real estate transaction prices.

In addition, 4 out of 16 current "Mietspiegel" (rental tables / representative lists of rents) for the state capitals do not refer to energy-related quality characteristics associated with the provisioning of information on average rental levels. Within the rental indices of 12 state capitals reference is made to energy-related quality characteristics; however, this is not done in a uniform/standardized manner and usually not in relation to actual EPC content. Instead, reference is made, for example, to single building features (e.g. availability of double-glazed windows, etc.), or to energy categories/classes.

A potential explanation for this low availability and dissemination of EPCs is that German legislators assumed that potential buyers and tenants would actually have an interest in EPCs and would therefore actively request them. Consequently, the respective energy saving orders focused on safeguarding an entitlement to see the EPC prior to signing a rental or sales contract; instead of enforcing actual handover. The strategy to start the information flow depended upon an obligation for existing building owners to obtain EPCs. However, the actual handover of EPCs depended upon the (voluntary) request from the potential buyers and tenants. These requests failed to materialise.

b) Comparability and reliability of EPCs

In Germany, two types of EPCs exist. One is based on the hypothetical calculation of energy demand; and the other is based on the average climate-adjusted, actual measured energy consumption. The demand for energy is ultimately calculated as a function of the energy characteristics, assuming a standardized climate and user behaviour. In contrast, the energy consumption is based on actual energy consumption over several (usually 3) periods normalized to an average reference-climate in Germany. Due to these different assumptions, deviations between both approaches as well as between the real energy consumption arise.

In addition, there were cases of incomplete, incorrect and even manipulated EPCs in Germany.

Furthermore, the rules/basis for calculating energy demand and average energy consumption are not constant/fixed. They have been constantly modified, starting from the initial to the current version of the German energy savings order. As a result, only the same types of EPCs which are based on the same calculation rules (or which refer to the same version of the energy savings order) are actually comparable.

All this hampers comparability of EPCs. Market participants are confused and this undermines the reliability of EPCs in Germany.

c) Relevance and understandability of EPCs

When discussing the relevance of EPC content it is necessary to distinguish between two different perspectives: policy and building users (i.e. potential buyers and tenants). From a users' perspective, *final energy consumption* determines costs and is therefore of particular interest. In contrast, energy policy goals are primarily focused on a reduction of *primary energy consumption* (non-renewable) and *CO₂-emissions* (which may also be of interest for users as additional information on the environmental impacts of a building). Consequently, three issues can be considered relevant: primary energy, final energy, and CO₂-emissions.

Different levels of aggregation exist for the content of EPCs. Generally, the higher the aggregation level of EPC content, the easier it is for non-experts (layperson) to understand and interpret. However, aggregation leads to a loss of information if the information/data on lower aggregation levels is not documented as well. In principle, three aggregation levels can be distinguished in this context. These are:

Level 1 (impact factors): the energy quality of a building depends on the characteristics of the building envelope (e.g. surface area, *U*-values of components), the technical parameters of equipment and appliances, and (in a wider sense) the energy source. Actual energy consumption depends on further exogenous factors like climatic conditions and user behaviour. For the issuing of both types of EPCs in Germany (demand-based/consumption-based), the climatic conditions are equalized. For the issuing of demand-based EPCs, also the user behaviour is equalized. However, both types of EPCs do not contain any information on the impact factors mentioned above.

Level 2 (indicators): This level comprises final energy, primary energy and CO₂-emissions. Only demand-based EPCs contain information on final and primary energy demand, and (on a voluntary basis) also on CO₂-emissions. In addition, transmission heat losses (HT') is displayed. Regarding consumption-based EPCs, only information on final energy consumption is contained (experts might be able to calculate primary energy consumption and CO₂-emissions on that basis, but this is usually not an option for layperson).

Level 3 (energy efficiency categories / classes): in principle, this level comprises a further aggregation of one or more indicators into a single qualitative energy efficiency category or class. Until 2013, German EPCs did not contain information at this level.

In summary, only demand-based EPCs in Germany contain relevant information for both, policy and users. The chosen medium level of aggregation can be considered as a compromise between understandability and attention to detail: while a higher level of aggregation might be useful for layperson, a lower level of aggregation might be useful for experts and allow for further analysis in the context of energy policy evaluation (see the conclusions section for additional explanation).

4.2. Policy responses

During the last two years (2013/2014) German legislators responded to some of the issues raised above by introducing legal changes; these are mainly focused on a) increasing availability/accessibility and dissemination of EPCs in the market place, b) on improving understandability and reputation of EPCs, and c) on strengthening the integration of buildings' energy characteristics into the transaction and rental price analysis carried out by public authorities.

a) Availability/accessibility and dissemination of EPCs

During 2010 and 2013 an intense discussion occurred in Germany on the further development of requirements for EPCs. On the one hand, German legislators needed to respond to new provisions from the European Commission's revised Energy Performance of Buildings Directive [2]; on the other hand, the identified shortcomings with EPCs in Germany needed to be remediated. The result was the current version of the German energy saving order (EnEV, 2014, published in 2013). The main changes include the obligation for sellers to actually show EPCs to potential buyers prior to signing a contract, to provide the EPCs when signing the contract as well as the obligation to include the key content from EPCs within real estate advertisements. This ensures that potential buyers will have access to the information from EPCs – even if they do not ask for them – and can take this information into consideration within their decision-making.

b) Understandability and reliability of EPCs

The new version of the energy savings order also includes the following specifications and amendments:

Introduction of energy efficiency categories / classes (A+ until H) in order to enable communication of EPC content in a highly aggregated format.

Introduction of a registration number for EPCs which will be issued after reporting to a central EPC registration office.

Extension of EPC content by allowing for voluntary indication of information on the economic efficiency of recommended energy retrofit measures (e.g. amortisation time / payback period; estimated costs for saved kilowatt hours final energy) in order to improve stakeholders knowledge on economic consequences of modernisation activities.

Extension of official random checks of EPCs regarding accuracy of form and content in order to improve overall quality and reliability of EPCs.

New penalty procedures to guard against the issuance of incorrect or misleading EPCs.

Introduction of a legal obligation to retain EPCs (2 years) for EPC issuers.

c) Integration of energy characteristics into real estate market analysis

In Germany, public authorities at the local/municipal level perform analyses of transaction and rental prices and publish the results in the form of market reports and rental tables in order to contribute to market transparency (this information is legally linked to German property valuation rules and also determines whether or not rent adjustments in the housing sector are legally permissible). The legal changes in this context particularly relate to:

the obligation (from 11 March 2013 onwards) to take energy-related quality characteristics into consideration whenever rental tables are created / issued (BGB, 2013, § 558 Abs. 2),

the explicit listing (already since 2010) of a building's *energy quality* as a value-influencing factor within the German property valuation order (ImmoWertV, 2010, § 6 Abs. 5); this implies the direct obligation for valuation professionals to take energy-related issues into consideration whenever valuation assignments are being carried out; this also implies the indirect obligation for local valuation expert committees to analyse the impact of buildings' energetic qualities on transaction prices.

In addition to these legal changes, the German Federal Ministry for Transport, Building and Urban Development (BMVBS) has published a guideline on how to integrate energy-related quality characteristics into the analysis of rental prices and proposed a standardized procedure for creating rental tables in order to obtain nationally comparable results (see [8]). All this shows that German legislators have actually responded to some of existing problems with EPCs and have undertaken steps to increase market transparency regarding the energetic qualities of buildings. This, in return, provides an improved basis for more rational decision-making among market participants and politicians.

5. CONCLUSIONS

EPCs have a potential role in improving market transparency and energy policy evaluation. To exploit the potential of the EPC as a policy instrument, several necessary conditions are vital to its design, use and success. Initially these conditions were not met in Germany which led to low impact. Recently (as of 2014), legislators have acknowledged these shortcomings. The result is that EPCs are more formally embedded within the property market - this was achieved by increasing the compulsion for actual handover of EPCs within transactions as well as by integrating energy-related building characteristics into property market analysis carried out by public authorities. However, some of the existing problems with EPCs in Germany remain unsolved and require further attention. This particularly applies to the following issues:

a) Accessibility of EPCs through a centralized database

Although a registration number for individual EPCs is now required to be reported to a central EPC registration office together with information on the EPC issuer, there still is no centralized database containing the actual content of EPCs. This is a “missed opportunity” since a centralized database would act as an information source for market participants and public authorities and also improve the accessibility of EPCs and their content.

b) Comparability of EPCs

The difficulty of comparing EPCs in Germany remains due to the two types of EPCs (demand-based and consumption-based EPCs) that building owners can choose. The comparison of EPCs remains problematic due to different calculation methods. The following two recommendations could improve the situation:

One type of EPC should be selected to avoid confusion and promote comparability. Consideration will have to be given to the benefits that arise from each type.

Additional information and transparency are desirable. EPCs should be equipped with an appendix containing information on the characteristics of the building envelope (e.g. surface area, u-values of components), on the technical parameters of equipment and appliances, and on the utilized energy sources. All this information is already gathered for calculating energy demand. The inclusion of this information would allow energy demand to be recalculated / reassessed according to future revisions of energy savings orders. In addition, this information could be used for further analyses within the context of energy policy.

From the experience of EPCs in Germany, it is evident that policy- and market-based approaches need to work together. Governments can set the framework conditions within which market participants can search for optimal solutions. Particularly through enforcing the provision/availability of appropriate information, governments can mitigate market failures in certain areas. Governmental regulation (in this case, EPCs) was necessary to enable market competition to account for the energy quality of buildings. The analyses of the relationships between energy-related characteristics of buildings and market results (e.g. transaction prices, rents, construction costs, etc.) enables additional insights for market-oriented regulation, e.g. setting the legal minimum requirements for the energy efficiency of buildings and financial support of specific technologies and energy concepts.

REFERENCES

- EC (2002), Directive 2002/91/EC of the European Parliament and of the Council of 16 December 2002 on the energy performance of buildings. In: Official Journal of the European Communities. Legislation. L 1, Volume 46, 4 January 2003.
- EC (2010), Directive 2010/31/EU of the European Parliament and of the Council of 19 May 2010 on the energy performance of buildings. In: Official Journal of the European Union. Legislation. L 153, Volume 53, 18 June 2010.
- EC (2006), Directive 2006/32/EC of the European Parliament and of the Council of 5 April 2006 on energy end-use efficiency and energy services and repealing Council Directive 93/76/EEC. In: Official Journal of the European Union. Legislation. L 114, Volume 49, 27 April 2006.
- Fritsch, M. (2014), Marktversagen und Wirtschaftspolitik. Mikroökonomische Grundlagen staatlichen Handelns. 9., vollständig überarbeitete Auflage. München. Vahlen, 2014.
- Akerlof, G. A. (1970), The Market for "Lemons", In: Quarterly Journal of Economics, Vol. 84, pp. 488-500.
- Sunnika-Blank, M. and Galvin, R. (2012), Introducing the prebound effect: the gap between performance and actual energy consumption. Building Research & Information, Vol. 40, pp. 260-273.
- TNS Emnid (2014), Umfrage zum Thema Energieausweis – Ergebnisbericht August 2014, Verbraucherzentrale Nordrhein-Westfalen. <http://www.vz-nrw.de/media230037A>
- BMVBS (2013), Hinweise zur Integration der energetischen Beschaffenheit und Ausstattung von Wohnraum in Mietspiegeln. Arbeitshilfen für die kommunale Mietspiegelerstellung. Bundesministerium für Verkehr, Bau und Stadtentwicklung (BMVBS), 01.06.2013.

Introduction of Sociology-inspired Parameters in the Energy Performance Certification Calculation Method

S Monfils

University of Liege, 20 rue de Pitteurs, 4020 Liege, Belgium

J-M Hauglustaine

University of Liege, 20 rue de Pitteurs, 4020 Liege, Belgium

Email: stephane.monfils@ulg.ac.be, jmhauglustaine@ulg.ac.be

Abstract. One of the existing tools that could help creating *smartenergy* policies is the Energy Performance Certification (EPC) of residential buildings, by introducing energy efficiency as a comparative criterion for real-estate purchase choices. It has been designed, at least, to influence real-estate market value, stimulate energy saving investments, move the housing market towards better energy efficiency and help create comprehensive databases which are fundamental for shaping smart strategies on urban / regional / national levels. But EPCs in their actual form, calculated with a standardized approach which purposefully (and understandably), gets human factor out of the equations, do not allow appropriation of the results by potential buyers or tenants. Often distant from reality, overestimating consumption, they usually result in a general misunderstanding and misuse of the document. This study aims at verifying that the actual calculation method used in certification could approach the objectives it has been designed for, by using additional data on occupants' behaviour and household characteristics. It first presents the two case studies of dwellings, and the additional data that has been gathered; the second part proposes a method to adapt the net heat demand calculation, and the comparative results between official (EPC) results, recalculated consumption evaluation and real consumption data.

1. INTRODUCTION

In order to reach energy efficiency at any level, human factor is crucial: on one hand, efficient solutions (regarding transport, building energy consumptions, water and waste management.) have to be implemented by an intelligent decision-making authority who understands the complexity of the urban context and its impacts on environment. On the other hand, smart cities authorities need smart citizens, who are aware of their environmental impact, to use smart solutions to their full potential. In the field of residential use of energy, people are therefore a crucial parameter of both the problem and its solution.

European Union's strategy for a sustainable growth makes the building sector energy consumption reduction a central objective for meeting the commitments taken under the Kyoto protocol on climate change. At a worldwide scale, this sector is thus regarded as one of the most cost-effective options for saving CO₂ emissions (IPCC, 2007). To target the existing buildings potential, the European Union introduced (through the 2002/91/CE European Directive) Energy Performance Certificates (EPC), which should provide clear information about the energy performance of a building when it is sold or rented, including reference values, allowing performance comparisons between buildings. The EPC also includes "clear" recommendations for technically possible improvements, in order to increase investments in energy efficiency, move the housing market towards greater energy efficiency, influence real-estate market value and help built up comprehensive benchmarking databases, fundamental for shaping smart strategies on a local ('smart cities'), regional ('smart regions') and national level.

Given necessary standardization, the calculation method does not provide realistic results, and this is confirmed by energy bills; in theory, two different families living in two identical

homes would receive identical EPCs, but in reality, their real consumption would vary from one to three or four (Hens, 2010), depending on occupants' behavior and household characteristics. As a consequence, crossing several studies that have been led in Belgium (Vanparys et al., 2012), the UK (Laine, 2011; O'Sullivan, 2007) or in Germany (Amecke, 2012) enlightens a general conclusion: the EPC is often considered unhelpful, unrealistic (and therefore mistrust), distant from reality, overestimating consumption, too long and technical, confusing...

Sociology of energy points the lack of appropriation of results as a missed opportunity. This study is therefore based on the assumption that, though acknowledging the importance of a standardized approach to allow building comparisons, other (and more accurate) results could be obtained from EPC inputs, by closing the gap between theoretical and real consumptions. A previous paper (Monfils, 2014) listed the uncertainty parameters of the EPC protocol and calculation method. It also proposed a method for the introduction of additional data (on the number of inhabitants, occupation patterns of the dwelling, levels and quality of electr(on)ic equipment and lighting) into a recalculation of internal gains and Domestic Hot Water (DHW) demand. This paper will propose to go further, with a re-evaluation of Net Heat Demand (NHD), based on extra information related to the dwellers' heating habits.

2. HYPOTHESES

2.1. Dwellings and households description

The study concentrates on two dwellings (Figures 1 and 2), an apartment in a small urban building and a row suburban house. We created, for these dwellings, an EPC with precision and respect to the regulation, then created "alternative" certificates by entering the calculation method and establishing different values for standardized parameters, in order to compare the results. Table 1 hereunder gathers some data describing the dwellings (parameters from the EPCs). Additional information may be found in (Monfils, 2014).

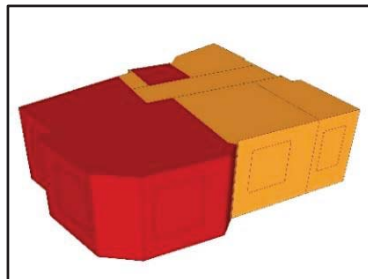
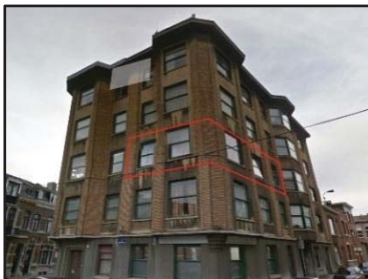


Fig 1. Apartment front façade and 3D model

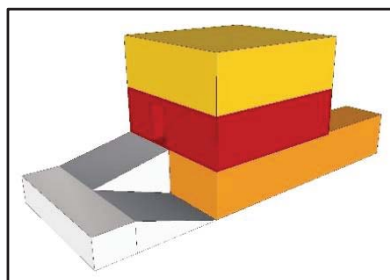


Fig 2. Row house front façade and 3D model

2.2. Tool

This study uses the regulatory EPC calculation method (Wallonia, 2013) provided by the Walloon public Administration in charge of the certification. With weather conditions being an important influence on the real consumption of dwellings, simulations have been made with climatic data for the region of Liege (where these dwellings are located), for the years 2010 – 2013 to compare the results with real consumption data for these years.

Table 1. Description of the dwellings

Data	Apartment	Row house
Heated volume (V_p)	330 m ³	612 m ³
Average U-value	2,2 W/m ² K	1,2 W/m ² K
Global heat η	51%	79%
DHW production η	40% (default)	75% (default)
Global DHW η	7% (hot water loop)	39% (default)
Number of inhabitants	1	4 (3)

2.3. Additional data

In order to “certify the building, not its users”, occupants’ behavior, comfort and building occupancy have been standardized in the official method: the whole dwelling is considered used and heated at all times, at a constant temperature of 18°C. Though permanent occupation increases internal loads, it also extends heating periods and, therefore, energy consumption. Reality, however, displays a wider range of behaviors: set temperatures and heating habits are bound to influence greatly the final energy consumption.

These information have been gathered from the dwellings owners. First, a series of 5 heating patterns (see Figure 3) were proposed to the owners, for them to characterize a typical winter week (indicating the number of days per week each pattern is used – 5 work days and 2 week-end days). The same patterns were used in (Monfils, 2014) to evaluate internal gains.

Pattern	Day-time occupation patterns of the house during typical winter days													Work days	Week ends					
	8h	9h	10h	11h	12h	13h	14h	15h	16h	17h	18h	19h	20h			21h	22h	23h		
1	4														4			0	0	
2	4												4		4			0	0	
3	4							week days : 3		4	4							4	0	
								weekends : 4												
4	4							week days : 3		4	4							1	1	
								weekends : 4												
5	4	week days : 3			week days : 3			week days : 3			4	4							0	1
		weekends : 4			weekends : 4			weekends : 4												

Fig 3. Occupation (and heating) patterns of the row house

A series of additional questions added extra information on:

- The repartition of heated rooms and their temperatures (if known) during each period of the patterns. This repartition can be seen on Figures 1 and 2; it displays day-time heated spaces (red), night-time heated spaces (yellow) and indirectly heated (orange).
- The presence of comfort control devices (thermostat, external probe), and their settings (such as set temperatures). These information allowed us to envision global temperature management or comfort-based manual control (mainly influencing set temperatures).
- The opening of spaces or staircases, to evaluate heat transfer between zones (mainly influencing the heat losses due to ventilation).
- The homogeneity of temperatures in considered zones
- The heating patterns during nights, in the absence of the occupants or in the bathroom

The results of this enquiry is visible in Table 2 hereunder.

Table 2. Data on behavior, heating and occupancy schedule and habits for the dwellings.

Additional data		Apartment	Row house
Global temperature management system?		No: Comfort-based management + thermostatic control	Yes: thermostatic control + thermostat + external probe
Annual heating period		October to April	October to April
Number of days (per week) for each pattern	1	1	0
	2	4	0
	3	0	4
	4	1	2
	5	1	1
Temperatures homogeneity?	Day zone	No ¹	Yes
	Night Zone	Yes (unheated)	Yes
Indirectly ² heated spaces?		Yes ³	Yes: basement ⁴
Never ⁵ heated spaces?		No	No
Open plan of the day zone?		Yes	Yes
Open staircase between zones?		No staircase → yes	Yes
Open staircase to unheated		No staircase → no	Yes
Maximal set temperatures	Day zone	20°C ⁶	21°C
	Night zone	-	21°C
	Bathroom	22°C	23°C
Minimal set temperatures	Day zone	-	16°C
	Night zone	-	16°C
	Bathroom	20°C	16°C

¹ Only the living room is heated; open plan indirectly helps heating circulations and kitchen
² Heated by adjacent rooms, without turning on the heating system in said room
³ Circulations, kitchen and bedrooms, when living room heated + presence of (very) hot water pipes distributing heat and DHW in upper floors (4th floor is highest demanding apartment of the building)
⁴ The son's bedroom has been considered indirectly heated during week days since 2011, as he integrated a boarding
⁵ Neither directly, nor indirectly
⁶ Comfort-based manual control: by default set temperature

2.4. Additional hypotheses:

Average temperatures are calculated in due ratio to the zones volumes:

$$T_{set,i} = \frac{\sum_j T_{set,i,j} * V_{p,j}}{\sum_j V_{p,j}} \quad (1)$$

where:

- $T_{set,i}$ = average set temperature for the “i” period of the heating schedule [°C];
- $T_{set,i,j}$ = set temperature in “j” room, for the “i” period of the heating schedule [°C];
- $V_{p,j}$ = part of the protected volume occupied by the “j” room [%].

By hypothesis, temperature in Indirectly Heated Spaces (IHS) depends on the temperature of adjacent Directly Heated Spaces (DHS). In this study, the difference empirically equals 2°C when there are DHS on the same floor, 3°C when DHS are on the lower floor, and 4°C when DHS are on the upper floor.

Heat losses due to ventilation are considered at 100% of the official calculation method evaluation at all times during heated periods. This hypothesis takes into consideration that both

dwelling present open spaces (and staircases for the houses), and that air tightness is a constant issue, as well as the inability in most dwellings to turn off a (almost) non existing ventilation system.

2.5. Net Heat Demand Calculation

The official calculation method estimates the Net Heat Demand (NHD) by evaluating the monthly balance between heat losses (due to transmission, airtightness and ventilation) and the heat gains (due to occupation and solar radiation):

$$Q_{heat,net,m} = Q_{T,heat,m} + Q_{V,heat,m} - \eta_{util,heat,m} (Q_{i,m} + Q_{s,m}) \quad (3)$$

where:

- $Q_{heat,net,m}$ = NHD for the “m” month [MJ];
- $Q_{T,heat,m}$ = monthly heat losses due to transmission (overall protected volume envelope)[MJ];
- $Q_{V,heat,m}$ = heat losses due to airtightness and ventilation (overall protected volume)[MJ];
- $\eta_{util,heat,seci,m}$ = monthly heat gains application rate; a taming factor that reduces the internal and solar gains when they are less needed (depending on the losses/gains monthly ratio) to be kept in this proposition, as it translates a behavioral approach on comfort management.
- $Q_{i,m}$ = monthly internal gains[MJ], see (Monfils, 2014) for proposed evaluation method;
- $Q_{s,m}$ = monthly solar gains[MJ].

This NHD is then submitted to systems efficiencies (see Table 1) to evaluate final (and primary) energy consumptions. In this steady state calculation method, studying the influence of users’ behavior can only pass through an adjustment of monthly heat losses via “real” dwelling occupancy schedule and heating habits data. The theory is to subdivide the protected volume in “heated zones”, characterized by their own average comfort temperature during a predefined heated period, and the percentage of the global heat losses they generate.

The heat losses by transmission are evaluated as follows in the official method:

$$Q_{T,heat,m} = H_{T,heat} * (18 - \theta_{e,m}) * t_m \quad (4)$$

where:

- $Q_{T,heat,m}$ = monthly heat losses through the envelope [MJ];
- $H_{T,heat}$: transmission heat losses coefficient [W/K];
- $\theta_{e,m}$ = monthly average exterior temperature [°C];
- t_m = length of the month [Ms].

In order to integrate multiple time periods, with different set temperatures and heat loss coefficient, we can split the number of seconds in a month (t_m) between infinite terms, and NHD can therefore be split the same way:

$$Q_{T,heat,m} = \sum_{i=1}^{i=\infty} \alpha_i * H_{T,heat,m} * (T_{set,i} - \theta_{e,m}) * t_{m,i} \quad (6)$$

$$\alpha_i = \frac{\sum_j H_{T,heat,j}}{H_{T,heat}} \quad (7)$$

where...

- α_i = multiplicative factor for thermal losses by transmission for the “i” period [-];
- $T_{set,i}$ = average set temperature for the “i” period (see equation 1);
- $t_{m,i}$ = length of the “i” period [Ms];

- $H_{T,heat,j}$ = heat losses by transmission through the envelope of the “j” room, directly or indirectly heated during “i” period;

The heat losses through ventilation are evaluated the same way as shown in equation (6):

$$Q_{V,heat,m} = \sum_{i=1}^{i=\infty} \beta_i * H_{V,heat,m} * (T_{set,i} - \theta_{e,m}) * t_{m,i} \quad (8)$$

where β_i factors = 1 at all heated times. The values obtained for each dwelling are in Table 3:

Table 3. Parameters variation for the studied dwellings

Period	% of DHS in	% of IHS in V_p	% of t_m	$T_{set,i}$ [°C]	α_i [%]	β_i [%]	
Apartment	1	5%	0%	4,2%	22	0%	100%
	2	44,7%	55,3%	6,2%	19,1	100%	100%
	3	39,6%	60,4%	22,3%	18,7	100%	100%
	4	0%	0%	67,3%	NH ¹	0%	0%
Row house	1	32,2%	0%	33,3%	15,3	38,5%	100%
	2	62,1%	37,9%	30,7%	19,2	100%	100%
	3	62,1%	0%	14,6%	17,6	100%	100%
	4	0%	0%	21,4%	NH ¹	0%	0%

3. RESULTS

The Tables 4 and 5 expose NHD and fuel consumption results for each dwelling for both official and proposed calculation methods (in this case, the result is the average of 2010 – 2013 simulations), as well as real consumption data (average of 2010 – 2013). Underneath, graphs (Figures 4 and 5) show the evolution of the comparison for the period 2010 – 2013.

The results show global improvements (with a reduction of the gaps between estimated and real consumption), as it was to be expected. But recalculated consumption is still 1,77 times the real consumption data for the apartment. This margin is still too important to overlook. It is far better in the row house case however (17% average margin); this can be explained by more precise and accurate input data in the calculation, for system efficiencies, for example.

The use of real annual climatic data is (globally) reflected in the real consumption data, except for the row house, where the 2013 variation still has to be explained. In the case of the apartment, the increase of real consumption in 2013 is explained by the owner as the year he renovated his kitchen, opening it to the rest of the apartment (which probably means it was better, though indirectly, heated).

Table 4. Results for the apartment

	[1] Official	[2] recalculated	[3] real	[1]/[3]	[1]/[2]	[2]/[3]
Net Heat Demand	12531 kWh	2917 kWh	-	-	4,3	-
Fuel consumption	39160 kWh	17404 kWh	9850 kWh	3,98	2,25	1,77

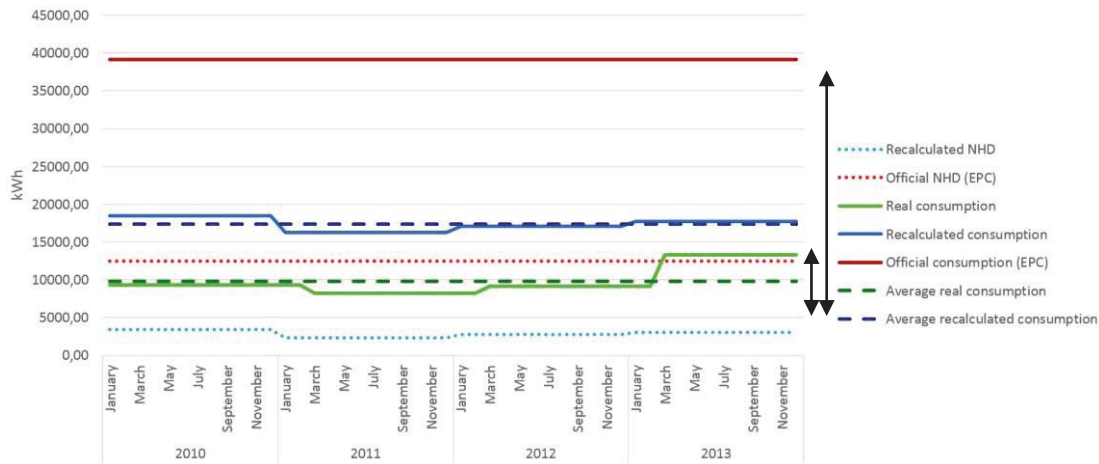


Fig 4. Evolution (2010 – 2013) of the comparison between official results, recalculated ones and real consumption data, for the apartment. The arrows indicate the differences between the average real consumption and the consumption estimations of both official and proposed calculation methods.

Table 5. Results for the row house

	[1] Official	[2] Recalculated	[3] Real	[1]/[3]	[1]/[2]	[2]/[3]
Net Heat Demand	29306 kWh	17507 kWh	-	-	1,67	-
Fuel consumption	39874 kWh	28495 kWh	24440 kWh	1,63	1,4	1,17

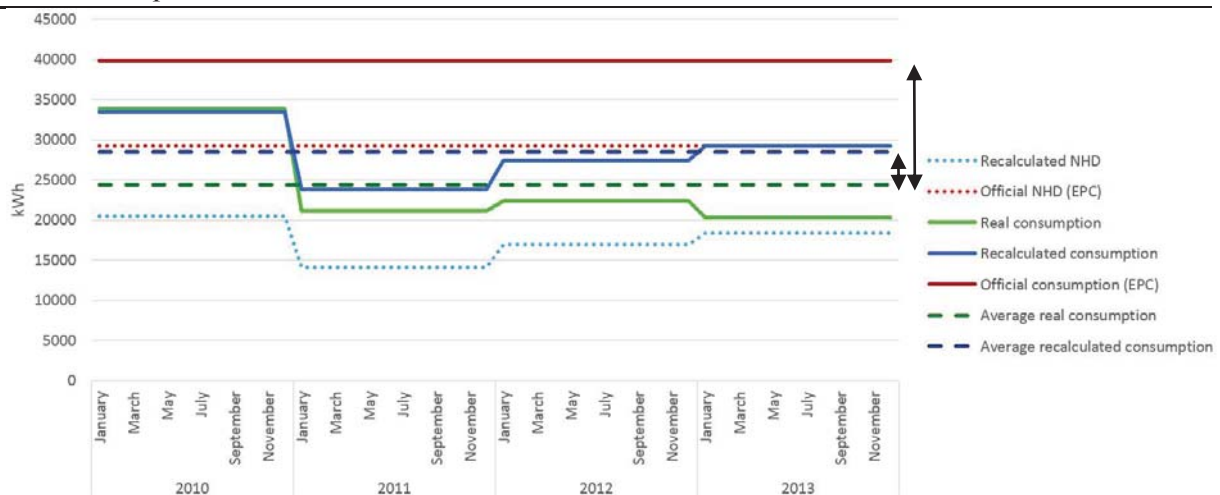


Fig 5. Evolution (2010 – 2013) of the comparison between official results, recalculated ones and real consumption data, for the row house. The arrows indicate the differences between the average real consumption and the consumption estimations of both official and proposed calculation methods.

4. DISCUSSION AND CONCLUSION

The Energy Performance Certification is a great opportunity for monitoring and trying to improve the housing stock, for whoever wishes to reduce its energy consumption. But that potential remains underexploited. In order for the scheme to reach its goals and be used to penetrate the decision-making process of potential buyers or tenants, it is essential to find a way to make it understandable and understood, trusted and used by anybody. Though acknowledging the necessity of presenting a “legal” result as a comparison base, following the approved standardized calculation method, it is believed that other results could be displayed, based on the building characteristics and a minimum of behavioural inputs, creating a closer bond between future renters/owners and the results displayed in the EPC.

The creation of a complementary (not replacing) “custom-made” certification, for example, could help raise energy consumers’ awareness of their energy consumption. The goal

of this study was therefore to see if the existing data is usable, and the method strong enough for this purpose.

The great difficulty in this method is in two parts:

- The adaptation of a steady-state method, with a defined set of input data. Multi-zone dynamic calculations would obviously render more precise (and probably closer) results, but
- The remaining pool of unknown parameters, which influence grows in the balance when other inputs are refined. An enlightening example in this study stands in the default values that are attributed to heating and DHW systems efficiencies (see Table 1), according to their type and age, and induce obvious reservation towards consumption results. The part of the DHW-related consumptions dramatically increase when the system is granted by very low efficiencies, and even more so when the number of inhabitants increase also. Another example lays in the ventilation rates, as no data on actual rates could obviously be given by the owners.

However, it seems that, with a small amount of additional data (on the number of inhabitants, the set temperatures, the heating schedules), the certification calculation method would be strong enough to approach real consumption data. These results are encouraging, without entirely closing the gap. This is normal: the uncertainties of the Energy Performance Certificate approach are not all behaviour-related, but also stand in other specificities of the protocol, though the variation in quality of the EPC itself can be considered negligible here: the EPCs have been made by the same person, with this study in mind...

The next step of this study would be to try and validate the method, by a qualitative survey of heating habits in different typologies of housing, and use statistics to globalize coefficients precisely calculated here for both dwellings.

5. ACKNOWLEDGEMENTS

Special thanks have to be given to the owners of the analysed houses, for their help and understanding when being interviewed.

REFERENCES

- 2010/31/UE, 2010, European Parliament and Council Recast Energy Performance of Buildings Directive, Moniteur, official journal of the European Union, L153/13 to L153/35.
- Amecke, H., 2012, The Impact of Energy Performance Certificate: A Survey of German Home Owners, Elsevier – Energy Policy 46, pp. 4 – 14.
- CPDT, 2005, Rapport final de la subvention 2004-2005, thème 2, Contribution du développement territorial à la réduction de l'effet de serre [trad. : Final report on subvention 2004-2005, theme 2, Contribution of urban development in the reduction of green house effect].
- Econotec, Consommations de chauffage du secteur résidentiel, in Institut wallon de développement économique et social et d'aménagement du territoire, À la rencontre de l'énergie – Le secteur résidentiel, Éditeur: J. Daras, Ministre wallon de l'Énergie et des Transports, 8 p., 2000.
- EPBD – Concerted Action, 2011, Implementing the Energy Performance of Buildings Directive (EPBD), Featuring country reports, EU Publications Office.
- Hens, H., Parijs, W., Deurinck, M., 2010, Energy consumption for heating and rebound effects, Elsevier – Energy and buildings 42 (2010), pp. 105 – 110.
- IPCC, 2007: Climate Change 2007: Synthesis Report. Contribution of Working Groups I, II and III to the Fourth Assessment Report of the Intergovernmental Panel on Climate Change [Core Writing Team, Pachauri, R.K and Reisinger, A. (eds.)]. IPCC, Geneva, Switzerland, 104 pp.
- ISO 7730:2005, Ergonomie des ambiances thermiques - Détermination analytique et interprétation du confort thermique par le calcul des indices PMV et PPD et par des critères de confort thermique local, International Standardisation Organisation, Switzerland, 52 p.
- Laine, L., 2011, As easy as EPC? Consumer views on the content and format of the energy performance certificate, Consumer Focus, United Kingdom.

- Monfils, S., Hauglustaine, J.-M., 2009, Etude énergétique et typologique du parc résidentiel wallon en vue d'en dégager des pistes de rénovation prioritaires, Reno2020 Research project scientific interim report, University of Liege.
- Monfils, S., Hauglustaine, J.-M., 2014, The Energy Performance Certification: A tool for smarter cities?, paper presented at the 9th International Conference on System Simulation in Buildings, Liege, 10-12/12/2014.
- O'Sullivan, A., 2007, Urban Economics, Boston, Massachusetts, McGraw-Hill, London.
- Vanparys, R., Niclaes, E., Lesage, O., 2012, Certificat énergie, la base d'un véritable audit ? , Test-Achats n°562, pp. 10 to 16.
- Wallonie, 2013, Arrêté du Gouvernement Wallon du 12 Décembre 2013, Annexe 1, Méthode de détermination du niveau de consommation d'énergie primaire des bâtiments résidentiels [trad.: Walloon Government Decree of the 12/12/2013, Annex 1, Method to determine the primary energy consumption level of residential buildings], Namur, 133 p.

A Fuzzy Control System for Energy Management in a Domestic Environment

Vincenzo Bonaiuto

Department of Industrial Engineering Engineering University of Rome Tor Vergata – via del Politecnico 1 00133 Roma Italy

Stefano Bifaretti

Department of Industrial Engineering Engineering University of Rome Tor Vergata – via del Politecnico 1 00133 Roma Italy

Luca Federici

Department of Electronic Engineering University of Rome Tor Vergata – via del Politecnico 1 00133 Roma Italy

Sabino Pipolo

Department of Electronic Engineering University of Rome Tor Vergata – via del Politecnico 1 00133 Roma Italy

Fausto Sargeni

Department of Electronic Engineering University of Rome Tor Vergata – via del Politecnico 1 00133 Roma Italy

Emil: vincenzo.bonaiuto@uniroma2.it

Abstract: An effective renewable energy sources management represents one of the key enabler for the usage reduction of fossil fuel and, consequently, of the greenhouse gas emissions. In this paper, a Fuzzy Logic controller properly tailored to manage the energy resources in a domestic microgrid is presented. In particular, it has been designed to ensure the thermal comfort and guaranteeing, at the same time, the maximization of the use of renewable energy sources together with the batteries life duration of the storage system.

1. INTRODUCTION

The future electrical distribution systems based on DER (Distributed Energy Resources) have to effectively manage the power fluxes so as to be able to exploit the potential of the micro-generation in the improvement of the power quality as well as the reduction of the losses due to the energy transport. On this topic, a microgrid (MG) is the set of loads and power sources able to operate as a single controllable system and useful to provide electricity and heat to the local area.

The electricity production from RES (Renewable Energy Sources), such as solar or wind generation, is classified as an intermittent energy production because it greatly depends on the availability of the sun (or wind) received at the time. So, in order to address the load requirements (mostly unpredictable), the usage of such a class of RES can be effectively employed only with a further addition of more controllable generation systems. In particular, the microgrid has to be designed with the addition of Energy Storage Systems (ESS) or by forming hybrid systems (e.g. by adding micro turbines, diesel generators, fuel cells, etc.).

In this scenario, the MG requires a proper control system for an effective and smart management of the power generators in order to minimize the ESS size (i.e. the batteries) as

well as the amount of energy obtained by the non-renewable sources. In this paper, a fuzzy controller specifically designed to manage the power fluxes on this MG will be described and some preliminary results will be shown.

2. MICROGRID AND SIMULATION ENVIRONMENT DESCRIPTION

The scheme of the domestic MG (shown in Fig.1) that has been accounted to design the controller is composed by a 5 kWp Photovoltaic array (PV), that represents the primarily power source, a storage system (a battery pack size 700Ah) as well as with a FC (a Fuel Cell generator composed of 3 cells of 1.2kW each for a total of 3.6kW) able to supply energy when both the RES and ESS are not capable to provide the amount of energy required by the load.

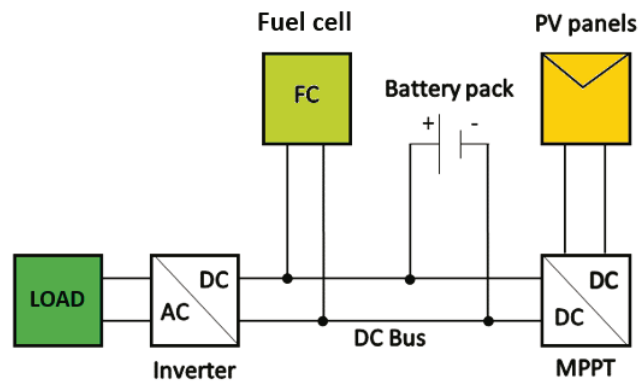


Fig 1– Microgrid scheme

Furthermore, the load has been considered as composed by two terms: the first one related to the electric appliances, including lighting and hot water production, while the second one is related to the consumption due to heating and cooling of the house. In particular, the first term has been estimated by using a statistic profile according to a typical house consumption of a small size family (Figure 2) at which some Gaussian noise has been added to take into account the feature of unpredictable behavior.

The controller has been simulated by using as case study a house with a surface of about 110m² (three rooms on the ground floor) and equipped with a HVAC system having a heat pump of 7 kWt.

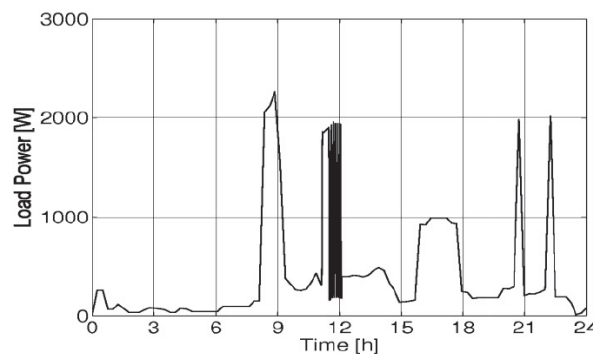


Fig 2 – Statistic profile of energy consumption for electric appliances and hot water production

The second term, due to the HVAC system, has been computed by the simulator taking into account the energy requirement for satisfy the thermal comfort inside the house with the varying of the outdoor temperature.

The weather data (temperature, air humidity and sun radiation) used in the simulations are real data acquired by the weather station of our university in the south area of Rome and relative to a couple of months in the summer (August) and winter season (January) respectively.

3. FUZZY CONTROLLER

The controller has been designed in order to satisfy the following main constrains:

- Assure the minimal thermal hygrometric discomfort in the buildings by controlling the Fanger indexes PMV (Predicted Mean Vote) and PPD (Predicted Percentage Dissatisfied).
- Maximize the use of RES.
- Minimize the amount operating hours for the FC and, at the same time, reduce the amount of its procedures of the switching on.
- Control the State of Charge of the battery (SoC) in order to grant the battery lifetime against deep discharging.

Moreover, the controller design has been carried out by taking into account the weather forecasts (provided by the Italian Air Force for the Rome Area) in terms of temperature (to estimate the electric load due to HVAC) and the solar radiation (to estimate the amount of energy supplied by the PV). In particular, the controller is able to take into account the forecast of load demand (electric and thermal) and/or of the production of energy for the next hour.

The controller is composed by two different section:

- Predicted Mean Vote Controller (PMV-C)
- Energy Management Controller (EM-C)

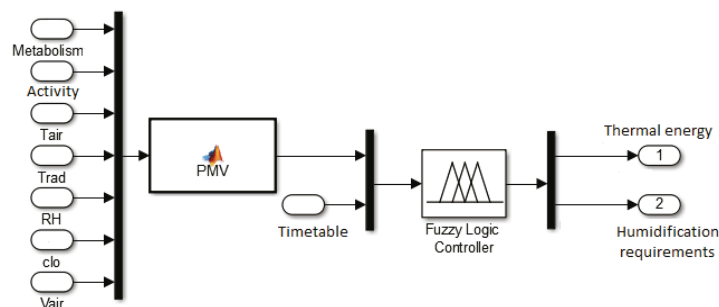


Fig 3 – Scheme of the PMV-C

The PMV controller estimates the value of the Predicted Mean Vote by using the Fanger's formula. This is able to estimate, on the basis of principles of body heat balance (i.e. metabolism, clothing, indoor temperature and humidity) a value comprised between -3 and 3 that represents the opinion of a person about his own thermal feeling.

The main goal on the basis of the rules of both fuzzy controllers are:

1. The thermal load is usually proportional to the distance from the situation of comfort;
2. Short events of slight discomfort can be accepted in particular conditions of energy demand (i.e. low production by PV or low SoC of the battery) together with suitable weather conditions;
3. If the SoC is very low, it is preferable avoiding deep discharge of the battery by tolerating slight thermal discomfort in case of favorable weather forecast together with few hours from the dawn (i.e. the start of the production of the PV);
4. The thermal load will be decreased allowing a slight discomfort in the case in which it will be expected a temporary energy shortage to avoid a deep discharge of the battery without the necessity to make operative the FC;

5. In the case that, in the next hour, it will be expected a wide production of energy by the PV, a temporary discharge of the battery can be accepted avoiding, in this way, that the FC is switched on.

In particular, the Fuzzy basic rules of the PMV-C can be summarized as follow:

- in case of extreme discomfort ($PMV < -2$ or $PMV > 2$) the heating/cooling will be always ON in order to restore the correct level of thermal comfort;
- in case of moderate level of discomfort ($-2 < PMV < -1$ or $1 < PMV < 2$), the behavior of the heating/cooling system will act in different way depending on the time slot: in fact, a further reduction of the PMV will be accepted in the morning of the working days and during the night in comparison with the occurring of the same the situation in the afternoon. This particular choice is based on main idea that in the morning of such days the house is not inhabited, while during the night, a feeling a light level of discomfort can be tolerated whereas it is sleeping and the value of the clo (the thermal insulation provided by clothing) is increased by the blankets;
- in case of thermal comfort ($-1 < PMV < 0$ or $0 < PMV < 1$), the system will be off in the morning and at night, while will operate at low level in the afternoon to approach as much as possible to the value of $PMV=0$.

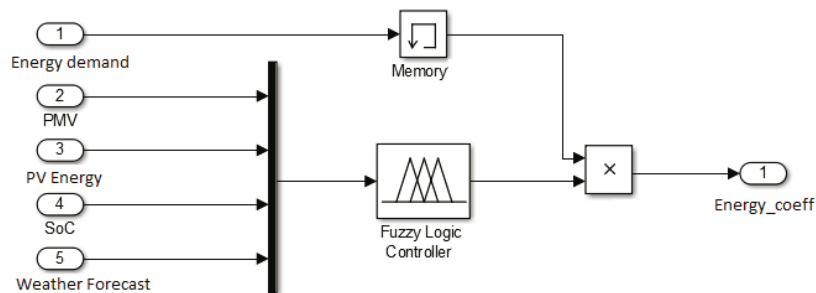


Fig 4 – Scheme of the EM-C

4. RESULTS

The controller has been simulated in a Matlab/Simuink environment. In particular, for the PV array has been used the simplified model reported in while, for the FC and the battery pack, the models available in the SimPowerSystems toolbox have been employed. Moreover, the HAMbase¹ software tool has been accounted to modeling the thermal behavior of the house.

¹HAMbase is a simulation building model developed by the Eindhoven University of Technology able to simulate heat flows in a multi-zonehouse.

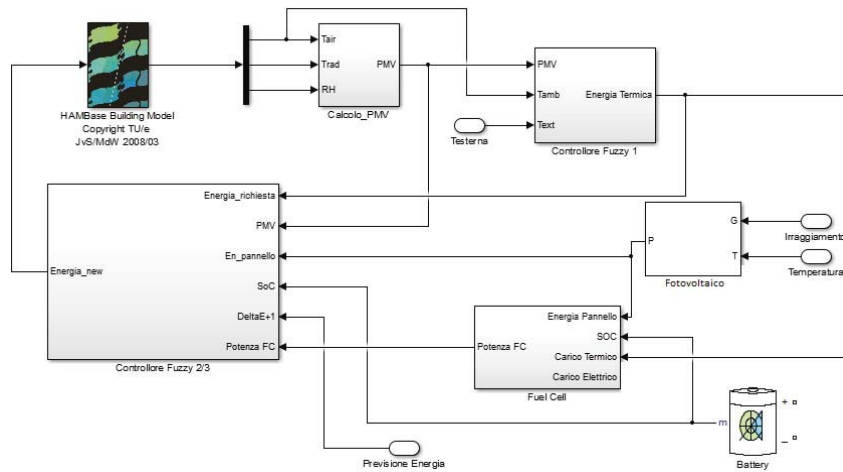


Figure 5 – Scheme of the Matlab/Simulink simulator

In particular, it has been set to the particular structure of the building (i.e. the thickness of the walls, the type and thickness of insulation materials, number and orientation of the windows, etc.).

The performances parameters have been identified, as suggested by, as follows:

- Amount of the hours in which there is a comfort violation ($-1 < PMV < 1$)²
- Amount of the operations of switching on for the FC;
- Amount of employed energy from RES.

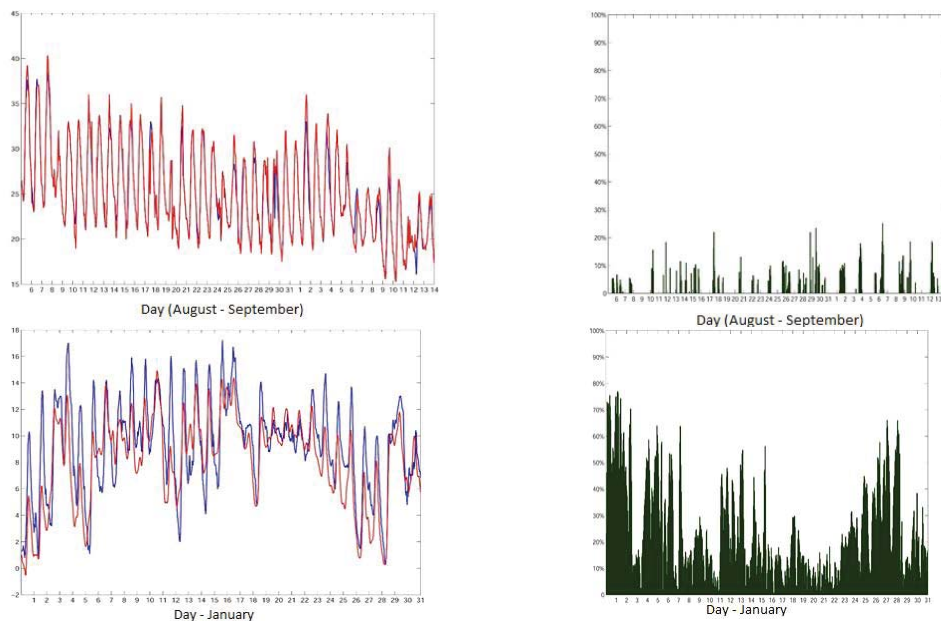


Fig 6 – Temperature (red = real value, blue = forecast) and error between forecast and real value

² As reported by ISO 7730:2005

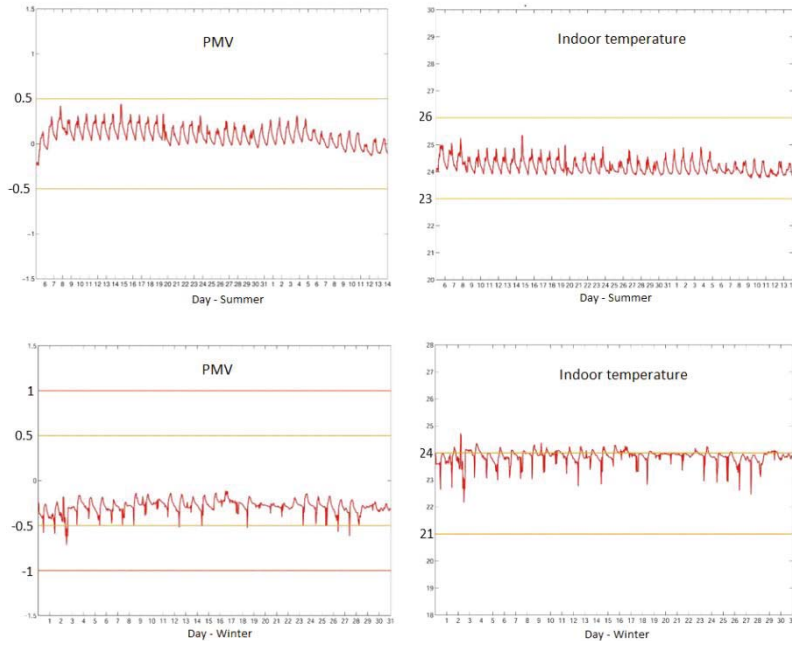


Fig 7 – PMV and indoor temperature

In the figure 6 are depicted the curves of the weather forecast for outdoor temperature of, respectively, the summer season (August-September 2014) and the winter season (January 2015). In the right section of the same figure the forecast error, with respect to the real temperature value, is illustrated. It is worth to notice that the weather forecast of the winter season are less accurate (mean error 22.7%) with respect to the same forecasting in the summer case (mean error 3.5%).

As shown in figure 8, the control system assures that the levels of hygrometric comfort are compliant to the values allowed by ISO 7730:2005 standard. In particular, there are no violation of the PMV in the summer as well as winter season while, for the indoor temperature during winter, it performs an overestimation of the thermal power that the system should provide.

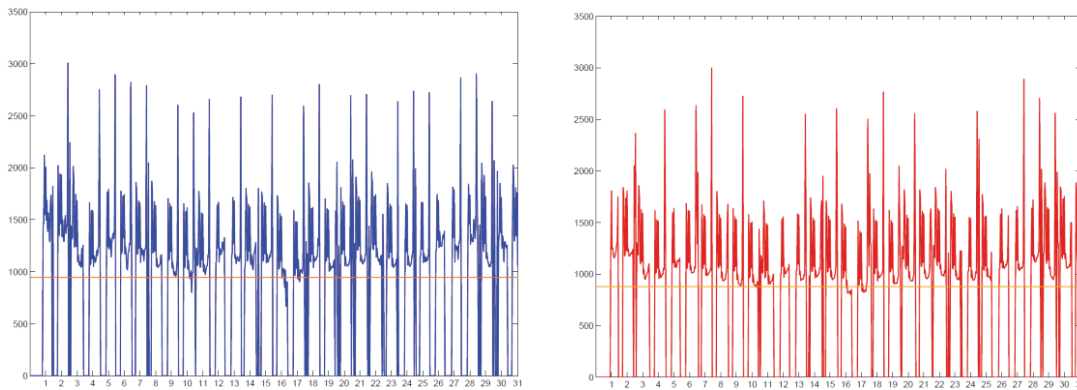


Fig 8 – Energy supplied by the FC in the winter case: (a) w/o forecast (b) w forecast

The efficiency of the system can be suitably evaluated through the performance indexes e_{f1} , e_{f2} and e_{f3} which describe the usage of the energy produced by the RES (i.e. PV in the MG).

$$e_{f1} = \frac{E_{RES \text{ used}}}{E_{load}} \quad e_{f2} = \frac{E_{RES \text{ used}}}{E_{RES \text{ tot}}} \quad e_{f3} = \frac{E_{no_RES \text{ used}}}{E_{load}}$$

The first parameter shows the ratio between the used RES with respect to the load demand while, the second one, is able to evaluate the amount of the RES used energy with respect to the whole amount of RES available energy in the MG. Finally, the third parameter shows the amount of the energy produced by non-renewable sources with respect to the load demand.

Table 1. Summary results

	w/o forecast	w forecast
e_{f1}	66.6%	77.6%
e_{f2}	72.8%	83%
e_{f3}	74.6%	69%
not utilized RES	27.2%	17%
FCt_{eqON}	697 h	642 h
PMV_{ave} (summer)	0.068	0.093
PMV_{ave} (winter)	-0.25	-0.56
PPD_{ave} (summer)	5.27%	5.48%
PPD_{ave} (winter)	6.4%	10.04%
SoC_{min}	70.58%	73.19%
SoC_{ave}	90.2%	91.54%

The simulation results are summarized in Table 1. In such a table are reported the results for two different fuzzy controllers that take or not into account the weather forecast for the next hour. It is worth to note that the introduction of the weather forecast evaluation slightly improves the performances of the system in term of more effective management of the RES as well as of the SoC of the battery pack. Moreover, it has been also reduced the amount of time in which has been used the FC. The value of t_{eqON} , reported in Table 1, takes into account both the switching on procedure as well as the time in which the FC is on. On the other hand, the slight discomfort tolerated in the case in which it will be expected a temporary energy shortage follows in an increase in the PPD (Predicted Percentage Dissatisfied) value.

5. CONCLUSIONS

A Fuzzy controller suited for the management energy in a domestic MG is presented in this paper. The goal of the controller rules are to improve the use of the RES with respect to the energy coming from fossil fuel avoiding, at the same time, a deep discharge of the battery pack and assuring the thermal comfort inside the house.

6. ACKNOWLEDGEMENT

Special thanks to ENEA (Italian National Agency for New Technologies, Energy and Sustainable Economic Development) for the data related to the forecasts about the solar radiation and to Aeronautica Militare (Italian Air Force) for the data about the weather forecast.

REFERENCES

- Lasseter R., Akhil A., Marnay C., Stephens J., Dagle J., Guttromson R., Sakis Meliopoulos A., Yinger R. and Eto J., "Integration of Distributed Energy Resources – The MicroGrid Concept", CERTS MicroGrid Review Feb 2002.
- Strasser, T., Andr n, F., et al., "A review of architectures and concepts for intelligence in future electric energy systems", *IEEE Transactions on Industrial Electronics*, 2015, 62(4), 2424-2438.
- Bertoldi P., Atanasiu B., Electricity Consumption and Efficiency Trends in European Union - Status Report 2009, European Commission, Joint Research Centre Institute for Energy, Renewable Energy Unit.
- De Almeida A., Fonseca P., Schlomann B., Feliberg N., Characterization of the household electricity consumption in the EU, potential energy savings and specific policy recommendations, *Energy and Buildings* 2011; 43:1884–1894
- Martin de Wit, "HAMBASE: Heat Air and Moisture model for Building And Systems Evaluation", Eindhoven University Press, Eindhoven, 2006.
- P.O. Fanger, "Thermal comfort", McGraw-Hill, 1972.
- A. Bellini, S. Bifaretti, V. Iacovone, and C. Cornaro, "Simplified model of a photovoltaic module," in *Applied Electronics*, 2009. AE 2009. IEEE, 2009, pp. 47–51.
- Bruni, G., S. Cordiner, and V. Mulone. "Domestic distributed power generation: Effect of sizing and energy management strategy on the environmental efficiency of a photovoltaic-battery-fuel cell system." *Energy* 77 (2014): 133-143.
- G. Bruni, S. Cordiner, V. Mulone, M. Galeotti, V. Rocco, M. Nobile, "Control Strategy Influence on the Efficiency of a Hybrid Photovoltaic-Battery-Fuel Cell System Distributed Generation System for Domestic Applications", *Energy Procedia*, 2013

Performance Monitoring of Energy Efficient Retrofits – 4 Case Study Properties in Northern Ireland

T E McGrath

Civil Engineering, Queen's University Belfast, BT7 INN, Northern Ireland, UK

S V Nanukuttan

Civil Engineering, Queen's University Belfast, BT7 INN, Northern Ireland, UK

D Soban

Civil Engineering, Queen's University Belfast, BT7 INN, Northern Ireland, UK

PAM Basheer

School of Civil Engineering, University of Leeds, England, LS2 9JT, UK

S Brown

Hearth Housing Association, Belfast, BT7 1BU, United Kingdom

Email: tmcgrath03@qub.ac.uk

Abstract. Approximately half of the houses in Northern Ireland were built before any form of minimum thermal specification (U-value) or energy efficiency standard were available. At present, 44% of households are categorized as being in fuel poverty; spending more than 10% of the household income to heat the house to an acceptable level. This paper presents the results from long term performance monitoring of 4 case study houses that have undergone retrofits to improve energy efficiency in Northern Ireland. There is some uncertainty associated with some of the marketed retrofit measures in terms of their effectiveness in reducing energy usage and their potential to cause detrimental impacts on the internal environment of a house. Using wireless sensor technology internal conditions such as temperature and humidity were measured alongside gas and electricity usage for a year. External weather conditions were also monitored. The paper considers the effectiveness of the different retrofit measures implemented based on the long term data monitoring and short term building performance evaluation tests that were completed.

1. INTRODUCTION

The UK Climate Change Act 2008 is legislation that enacts a long term legal framework, requiring a reduction of 80% by 2050 on 1990 levels of greenhouse gas emissions. As domestic buildings in the UK are the source of approximately a quarter of all CO₂ emissions, significant reductions will be required to achieve this ambitious target. According to the most recent Northern Ireland Housing Condition Survey there are 760,000 dwellings with a poor average energy efficiency SAP rating of D. Housing in Northern Ireland is old and inefficient with approximately 50% of houses built before the first minimum building thermal performance standards, introduced in 1973 (Northern Ireland Housing Executive, 2013). Whilst the energy efficiency of some dwellings may be easy to improve using relatively non invasive measures such as cavity wall insulation, loft insulation and double glazing other dwellings are categorised as “hard-to-treat”. Solid wall houses are categorised as “hard-to-treat” with cost effective energy efficiency improvements often difficult to implement. Across the UK there are approximately 6.5 million solid wall houses. The typical construction of these pre-1919 houses is single leaf solid red brick 225mm thick with a constructed U-value of 2.0 W/m²K. There are 87,600 solid wall houses in Northern Ireland, of which 95.3% have a SAP score lower than C. The two lowest possible bands of F and G represent 37.3% of all pre-1919 houses. To ensure we achieve the ambitious 2050 target, effective methods to improve the energy performance of such houses will be essential.

Another significant driver to improve the energy efficiency of domestic buildings in Northern Ireland is the issue of fuel poverty. A household is defined as being fuel poor if it needs to spend more than 10% of its income to heat the house adequately. The significant difference in fuel poverty levels in Northern Ireland compared to other regions, as shown in Table 1, is attributed to a number of factors including lower income, higher fuel prices and larger dependency on electric, solid fuel and oil. The rate of fuel poverty in Northern Ireland is amongst the worst in Northern Europe and 1,890 excess winter deaths over the last decade have been directly attributable to people living in damp and cold homes.

Table 1. Fuel poverty rates across UK regions

Country	Households in fuel poverty (%)
Northern Ireland	42
England	16
Scotland	28
Wales	29

This paper presents results of four solid wall homes based in Northern Ireland of which three have had significant energy efficient measures implemented. The fourth case study has undergone some conventional upgrades to the building fabric that would be typical for Northern Ireland. To understand the effects of the retrofit measures implemented long term performance monitoring of the internal conditions and energy consumption for space heating and electricity were measured.

2. CASE STUDY PROPERTIES

The properties are owned by a Social Housing provider, an organisation that provides housing to those on lower incomes. The houses are in close proximity to each other and are set in an urban environment.

2.1. Building fabric

In house 1, 2 and 3 the walls were internally insulated using a number of different materials as outlined below:

- House 1 - 100mm sheep wool, 50mm polyisocyanurate board and 6mm magnesium board.
- House 2 – 20mm aerogel board and 9mm magnesium board
- House 3 – 60mm wood fibre insulation board and 9mm magnesium board

In an effort to reduce thermal bridging at the junction of the internal insulation and the 1st floor level 300mm of sheep wool insulation was added next to the external wall in each house. In the roof space of house 1, 2, and 3, 200mm glass mineral wool insulation was laid down between floor joists. The underside of the roof space had 30mm PIR insulation and 6mm magnesium board fixed to the underside of the ceiling joists. In the roof space 200mm of glass mineral wool insulation was added in houses 1,2 and 3. Argon filled double glazing has been fitted in timber sash windows in house 1,2& 3. New insulated solid floors with expanded polystyrene insulation and concrete screed were added to all of the case study houses. House 4, which has undergone minimal retrofit, has a 10mm plasterboard fixed to 21mm expanded polystyrene board and vapour barrier. The windows in house 4 are timber framed single glazed sash windows.

2.2. Air permeability

Ventilation was provided in house 1, 2 and 3 through a Mechanical Ventilation and Heat Recovery (MVHR) unit with an efficiency 78.2%. Open fire places and chimneys in house 1,2

and 3 were sealed up and replaced with gas fires whereas the chimney in the living room of house 4 remains open. A number of diagnostic tests were completed on each property including air-tightness tests to the BS EN 13829-2001 standard. All vents and extract fans were temporarily sealed and drains filled with water. The results of the air-tightness tests are presented in last line of Table 2. UK building regulations stipulate that new homes should have a maximum design air permeability of $10\text{m}^3/\text{hr.m}^2$ under a pressure of 50Pa. There is no such design value for retrofits to houses. The four case studies all exceed this recommended air-tightness design value for new builds. As expected House 4 which has not undergone significant retrofit measures has the worst air-tightness value. This higher air permeability is likely to be caused in part by the open chimney in the living room. Difficulties with achieving air-tightness in energy efficient retrofits are well documented. A study of 102 retrofit properties has shown large variability in the air-tightness. Trends in age or wall type and air-tightness were not established. Pre-retrofit air-tightness results were between $2\text{-}23\text{ m}^3/\text{hr.m}^2$ and post-retrofit $2\text{-}15\text{m}^3/\text{hr.m}^2$ however some air-tightness results were marginally worsened with the report concluding that air-tightness measures need to be integrated better with other upgrades such as installation of floor/wall insulation or MVHR system.

According to make the most efficient use of any installed MVHR system the design air permeability should be between $2 - 4\text{ m}^3/\text{hr.m}^2$. Given the high air permeability of the case study houses 1, 2 and 3 it is likely that the MVHR will not be performing efficiently and may not even be required.

2.3. Space heating & domestic hot water systems

The space heating system and domestic hot water in houses 1, 2 and 3 was provided by a condensing gas boiler with a seasonal efficiency 89.5% with heat distributed through an underfloor heating system on the ground floor and radiator system on the first floor. Space heating and domestic hot water in house 4 was also provided by a condensing gas boiler with a seasonal efficiency of 89.2% and distributed through a radiator system.

Table 2. Summary of case study houses

	House 1	House 2	House 3	House 4
Wall U-value	0.22 W/m ² K	0.52 W/m ² K	0.45 W/m ² K	0.93 W/m ² K
Floor U-value	0.22	0.22	0.22	0.41
Roof U-value	0.16	0.16	0.16	2.07
Door U-value	2.2	2.2	3.0	3.0
Window U-value	3.10	3.10	3.10	5.4
Floor area (m ²)	102.85	62	58.2	56.55
Occupants	2 adults	2 adults & 1 baby	2 adults	1 adult
Occupancy hours	24 hour	Shift worker – occupancy pattern changes	Both workers	shift Occupant works part- time 11am-3pm
House type	Terraced	Terraced	Detached	Terraced
Air-tightness m ³ /hr.m ² at 50 Pa	15.04	14.14	10.52	17.21

2.4. Building performance evaluation

Temperature and humidity was measured at three locations in each of the properties; living room, bedroom and bathroom. Total gas and electricity consumption within the properties was also metered. The results of a yearlong monitoring period between the 1st August 2014 and 31st July 2015 are presented in this paper. As with any long term monitoring project a number of difficulties were encountered with data gathering due to a range of technical difficulties. Data was gathered using wireless sensors which sent data back to a central unit which transmitted the information to the cloud. In particular, gas data for house 2 and 4 was lost when the monitoring

device failed. In these cases data gathered from site visits, discussions with tenants and typical consumption patterns were used to estimate gas usage.

2.5. Relative humidity in case study houses

Relative humidity in range of 40 to 70% is considered acceptable for a comfortable environment. If humidity levels exceed 70% over long periods in a room the potential for the development of house dust mites, airborne fungi, mould and bacteria is increased. Mould growth is likely on surfaces if humidity levels are over 80% for than 6 hours of the day. These growths in turn emit spores, cells, fragments and volatile organic compounds. Chemical and biological degradation of materials is also initiated by dampness, which further pollute internal air. Dampness is considered to be a strong and consistent risk indicator for the development of asthma, respiratory infections such as bronchitis and allergies. Humidity levels may fall below 40%, particularly during spells of sustained cold weather, however associated risks appear minimal with an increased chance of static electric shocks for occupants. A summary of the measured relative humidity in the living room and bedroom of each property is presented in Table 3.

Table 3. Annual relative humidity in bedroom (BR) and living room (LR) of case study properties

Relative humidity (% hours in range in 1 year period)	House 1		House 2		House 3		House 4	
	BR	LR	BR	LR	BR	LR	BR	LR
≤40%	28.9	0.7	24.1	31.8	7	9.1	6.4	50.5
40%-70%	71.1	99.0	75.9	68.2	93	90.9	93.6	49.5
≥70%	0	0.3	0	0	0	0	0	0
Average winter relative humidity (%)	29.3	36.1	42	36	45.7	44.7	47.2	41.3
Average summer relative humidity (%)	36.3	43	42	47.5	45.6	43.2	50.9	38.4

None of the case study properties have sustained levels of high relative humidity and for the most part fall within the limits of CIBSE recommendations. House 3 has the highest percentage of time of hours in the 40% to 70% humidity range. This could possibly be linked to its relatively low air permeability value.

2.6. Internal temperature in case study houses

Internal temperatures between 17°C and 25°C are considered to be comfortable and are recommended by CIBSE. Prolonged exposure to low temperatures in houses have been linked with lowered resistance to infections with temperatures below 16°C being associated with respiratory issues and cardiovascular problems at temperatures below 12°C with the young children and elderly people most vulnerable. CIBSE also recommend summertime peak temperature and overheating criteria of less than 1% annual occupied hours in the bedroom and living room of 26°C and 28°C respectively. A summary of the measured temperature over the year-long monitoring period in the living room and bedroom of each property is presented in Table 4.

Table 4. Annual temperature in bedroom (BR) and living room (LR) of case study properties

		House 1		House 2		House 3		House 4	
Temperature									
%hours in 1 year period		BR	LR	BR	LR	BR	LR	BR	LR
≤17°C		9.8	0.7	12.6	0	12.9	30	40.4	43.1
18°C-25°C		89.3	98.9	87.4	100	87.0	70	59.6	56.9
≥26°C		0.9	0.4	0	0	0.2	0	0	0
Average	winter	21.1	19.3	17.6	20.5	19.0	16.4	14.3	14.2
temperature									
Average	summer	21.9	21.8	21.2	21.6	20.9	17.6	20.1	19.2
temperature									
% change of winter to		3.8	13.0	20.5	5.4	10.0	7.3	40.6	35.2
summer temperature									

The low internal temperatures of house 4 are particularly concerning with the living room having temperatures below 17°C for 43.1% of the time, with temperatures below 12°C for 8.3% of the time monitored. Temperatures increase from the winter to summer temperatures as would be expected with a changing ambient temperature. House 4 also sees the largest seasonal variation with bedroom and living room temperature increasing 5.8°C and 5°C from winter to summer respectively. The bedroom temperature in house 2 also has a significant change with a 20% increase in temperature; however this may be explained in part by the arrival of a new baby around that time period. The average living room temperature is also marginally below recommended temperatures.

The rate and pattern of heat loss associated with house 4 is markedly different from the other case study houses as shown in Fig 1. Over a period of a week in the month of January the living room temperature of House 4 has a steep, almost exponential, decline of heat daily. The temperature decline in other case studies whilst having a similar cyclical pattern of decreasing temperature at night are significantly less pronounced. Using the CIBSE criteria overheating is not an issue in any case study.

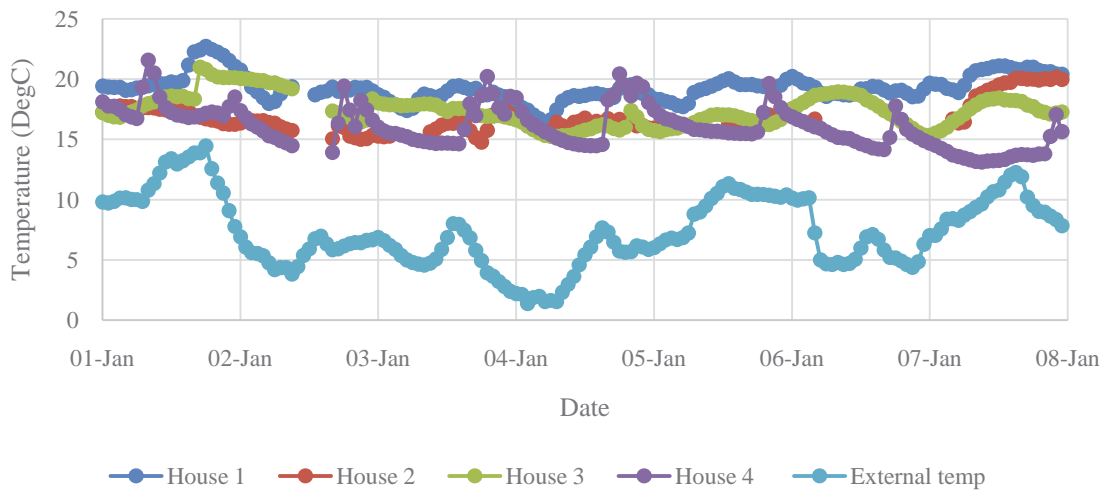


Fig 1. Hourly temperature profile of living room temperature of case study properties and external temperature

2.7. Gas consumption in case study houses

The UK regulator for gas and electricity markets OFGEM has published typical domestic annual consumption values for gas. Users are categorised as “low”, “medium” or “high” consuming 8,000 kWh, 12,500 kWh and 18,000 kWh respectively. Given the wide variety of age and type there is a lot of complexity associated with improving energy efficiency of existing houses. The “performance gap” between design and actual values also means it is difficult to

benchmark energy use in domestic retrofits. The Low Energy Building Database has compiled information on 33 UK domestic refurbishments and lists a range of actual primary energy use of 37.5 kWh/m²/yr to 283 kWh/m²/yr. This large range makes it difficult to establish what a realistic and achievable standard in retrofitting houses is. For new builds in the UK the Fabric Energy Efficiency Standard (FEES) have set good practice maximum space heating energy demand to be 39kWh/m²/year for apartments and mid-terrace houses and 46kWh/m²/year for end of terrace, semi-detached and detached houses. This standard has been created to allow for the efficient implementation of zero carbon or low carbon technologies in new domestic buildings and is therefore ambitious in the context of retrofitting properties. A summary of actual gas consumption and these benchmarks are presented in Table 5.

Table 5. Annual gas consumption for case study houses compared with benchmarks

	House 1	House 2	House 3	House 4
Gas consumption (kWh)	17724	7753 ¹	8514.7	5382 ²
OFGEM User Category based on actual gas consumption	Medium	Low	Medium	Low
FEES best practice (kWh)	4011	2418	2677	2205

¹ gas monitoring for this property was interrupted from the 28th October until the 16th December – a conservative estimate for usage based on typical gas consumption for the property is presented.

² gas monitoring for this property was interrupted from the 20th Jan until the 1st of May – a conservative estimate for usage based on typical gas consumption for the property is presented.

As expected gas usage in each of the four properties far exceed best practice FEES standard. Even though extensive retrofit measures were implemented in house 1,2 and 3 the effectiveness of these measures at reducing energy usage in the households is questionable. House 4 has exceptionally low gas consumption which when twinned with the consistently low internal temperatures is likely to signify that the occupant in this property is unable to afford to heat the house sufficiently and could be classified as being in fuel poverty.

2.8. Electricity usage in case study houses

To evaluate the actual electricity usage of the four houses a number of literature sources were used to establish typical or predicted electricity consumption patterns with results summarised in Table 6. The most recently published figures for typical annual electricity consumption from OFGEM, have been categorised as “low”, “medium” and “high” users who consume 2000kWh, 3100kWh and 4600kWh respectively. The report presents the findings of a survey of electrical energy consumption in 251 households. The average electricity consumption in households without electric heating was found to be 3638 kWh/year which when expressed in terms of house floor area resulted in 65kWh/m²/year. A study of 27 households in Northern Ireland found that electricity consumption had a strong relationship with the floor area of the building with the following correlation equation presented - $49(\text{Area m}^2) + 233 = \text{electrical kWh consumption}$.

The actual electricity consumption of the four house is presented alongside the predicted annual electricity consumption based on the previous literature (Zimmermann et al. 2012) and (Yohanis et al. 2008) as well as being grouped into a suitable OFGEM category in Table 6.

Table 6. Annual electricity consumption - Actual, predicted and % difference

	House 1	House 2	House 3	House 4
Actual	3094	3798 ¹	3056	1871
OFGEM User Category	Medium	Low	Low	Low
Predicted [12]	6685	4030	3783	3675
% difference	116	6	23.8	96.5
Predicted [11]	5272	3271	3084.8	3003
% difference	70	-14	1	61

¹ Data could not be gathered for August until December – the number presented is an estimate based on 6 months of data between January and June of 2015.

House 1 has the largest difference between actual and predicted electricity consumption. Given that the house is under occupied with only two adults present (one of whom is elderly and infirmed, spending significant time in bed) this is not surprising. House 4 has the lowest electrical consumption, despite the occupant using electrical radiators to boost heat in the living room. This low electricity use could be associated with low levels of occupancy and also an inability to afford to pay for electricity.

Fig 2 shows the average daily load profile over the monitoring period of electricity usage in the four houses is compared with an average UK load profile available from a report completed for the Energy Saving Trust (Zimmermann et al. 2012). The daily profile for house 2 and 3 appear to have relatively high electricity demand at night – both houses are occupied by shift workers which would explain this increased overnight demand.

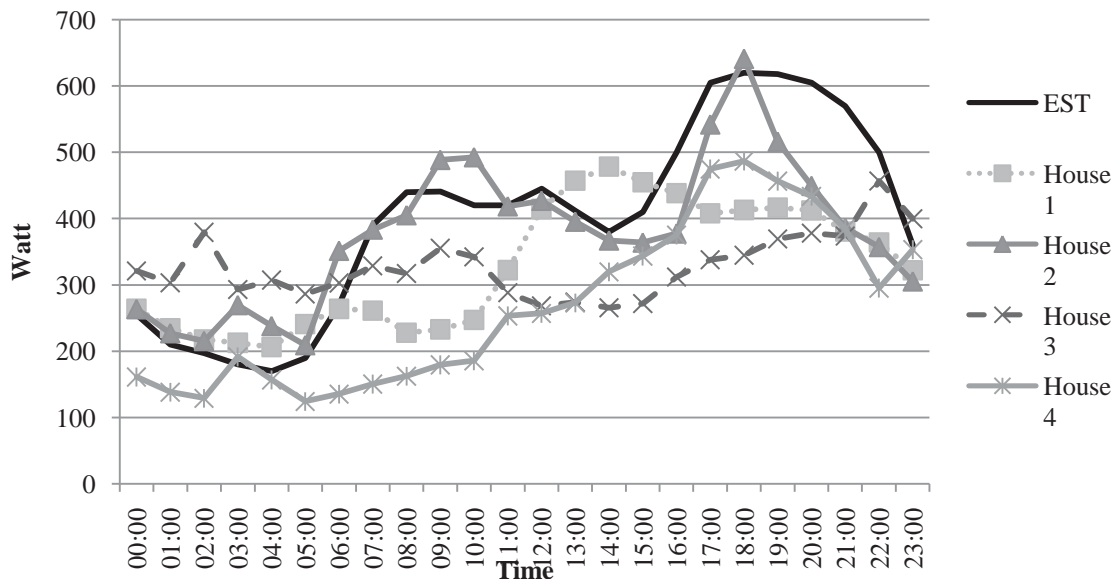


Fig 2. Average electricity profile of case study properties compared to typical UK profile

3. DISCUSSION AND CONCLUSIONS

The prolonged low internal temperature, high relative humidity and accelerated decline of internal temperature in house 4 overnight indicate, as would be expected, that it is the poorest performing property. The low internal temperatures and low gas usage would indicate that the householder is in fuel poverty and is unable to afford heating the house to a sufficient level. The relatively slow decline of overnight temperature from the other case study properties comparatively to house 4 indicate that retrofit measures have been effective at improving the building fabric. Gas consumption for houses 2 and 3 are categorised as low, and twinned with

generally good internal temperature ranges indicate that the retrofit measures implemented have improved the energy performance and comfort levels of the building. House 1 has the highest internal temperatures of any of the case studies coinciding with the highest gas usage. As one occupant is infirmed and the other is the care giver the priority is warm comfortable internal temperatures which they can achieve whilst still falling within the medium energy user category.

Whilst there are a number of sources of typical electricity consumption for households in the UK, there is less comprehensive data available that accurately predicts space heating consumption. Whilst large variations of space heating across homes is understandable due to a large range of variables (occupant preference, age/type/construction of building etc.) transparent benchmarks would be highly beneficial. To ensure we close the “performance gap” between design and actual energy usage we need more rigorous ways of estimating energy use in buildings.

The monitoring of these four case study properties is ongoing with further work planned considering dynamic modelling of energy usage in the buildings. Further work is required to consider the life cycle costing and environmental impact of the measures implemented to understand the financial and environmental benefit of such retrofit improvements.

4. ACKNOWLEDGEMENTS

The authors express their thanks to the sponsorship by Engineering and Physical Sciences Research Council (**EP/M506709/1**), Universities Ireland and internal funds provided by Queen’s University Belfast.

REFERENCES

- Northern Ireland Housing Executive, “Northern Ireland House Condition Survey 2011 - Main Report,” 2013.
- BRE, “A study of Hard to Treat Homes using the English House Condition Survey,” 2008. [Online]. Available: https://www.bre.co.uk/filelibrary/pdf/rpts/Hard_to_Treat_Homes_Part_I.pdf.
- Committee for Social Development, “Report on Fuel Poverty,” Belfast, 2012.
- Affinity Sutton & Energy Saving Trust, “FutureFit - Installation phase in-depth findings - Follow-up report,” London, 2011.
- Building Control Northern Ireland, “Building Regulations (Northern Ireland) 2012 Guidance - Technical Booklet K - Ventilation,” no. October. pp. 1–80, 2012.
- Chartered Institution of Building Services Engineers, Environmental Design Guide A, 7th Editio. Norwich: CIBSE Publications, 2006.
- World Health Organization Europe, WHO Guidelines for Indoor Air Quality: Dampness and Mould. Germany: Druckpartner Moser, 2009.
- J. Hills, “Getting the measure of fuel poverty: final report of the Fuel Poverty Review,” 2012.
- OFGEM, “Decision on revised Typcial Domestic Consumption Values for gas and electricity,” 2015. [Online]. Available: https://www.ofgem.gov.uk/sites/default/files/docs/2015/05/tdcvs_2015_decision_0.pdf.
- Zero Carbon Hub, “Fabric Energy Efficiency Standard,” 2014. .
- Y. G. Yohanis, J. D. Mondol, A. Wright, and B. Norton, “Real-life energy use in the UK: How occupancy and dwelling characteristics affect domestic electricity use,” *Energy Build.*, vol. 40, pp. 1053–1059, 2008.
- J.-P. Zimmermann, M. Evans, T. Lineham, J. Griggs, G. Surveys, L. Harding, N. King, and P. Roberts, “Household Electricity Survey A study of domestic electrical product usage,” 2012.

The Proper Design of Façade Openings for Occupant Satisfaction: Variance Based Sensitivity Analysis and Optimization of Model Output

R Albatici

University of Trento, Department of Civil Environmental and Mechanical Engineering, Via Mesiano 77, 38123 Trento, Italy

R Covi

Covi Costruzioni srl, Via del Plan del Sant 40, 38012 Mollaro di Taio (TN), Italy

A Gadotti

University of Trento, Department of Civil Environmental and Mechanical Engineering, Via Mesiano 77, 38123 Trento, Italy

Email: rossano.albatici@unitn.it

Abstract. The paper examines the relationship between energy efficiency and indoor comfort presenting an original methodology to assess data from simulation software. Recently, concerns about aspects related to occupant indoor comfort are arising near energy issues, usually considered the predominant key point for a sustainable construction. Various energy-oriented software are used, showing some main problems connected to the subjective nature of some parameters, the proper definition of input data, the output data management and options optimization. The research presented addresses these issues. It is based on the design and analysis of a free running single building. A brute force analysis was performed using EnergyPlus and an algorithm prepared with Wolfram Mathematica for the optimization problem. A variance-based sensitivity analysis was made considering the contribution of single variable to the amount of output uncertainty (first-order sensitivity index) and the uncertainty caused by interactions with other input variables (total effect index). Secondly, an optimal solution was evaluated, through the definition of an “objective function” considering both energy efficiency and indoor comfort.

1. INTRODUCTION

The concept of sustainability in the building sector has defined a new design approach that attempts, through a careful and conscientious consumption of resources, to minimize the environmental impact and reduce the energy demand during the whole life of the building. In this context, attention has been paid mainly on the energy efficiency aspect, not always with respect to indoor environment for users. However, the energy consumption of buildings depends significantly on the design criteria used for indoor environment, which also affect health, productivity and comfort of the users. In recent years concerns about all the aspects related to the wellness of the occupant and the comfort quality of living spaces have arisen. In order for a building to have success, both of the aspects have to be taken into account, dealing with the fact that they are intrinsically correlated.



Fig 1. Render of the concrete building under analysis.

Today's climate changes, which seem to lead to outdoor temperatures increasing constantly, winters becoming more temperate and wetter, and summers warmer, represent another key challenge for building designers. These changes will affect different aspects of the indoor environment, resulting above all in higher risk of summertime overheating. In the nearby future, buildings will probably require less heating in the winter and more cooling in the summer, leading to an increase use of air conditioning systems. Adaptation strategies should be investigated in order to minimize resources consumption and carbon dioxide production, while still assuring indoor thermal comfort. In this context, passive and active solar technologies for heating/cooling provide low-energy design solutions, which tend to be by definition more sensitive to external changes, presenting themselves as the most suitable strategies for facing the future scenarios, as they do not limit the adaptation to building installations only but react to the outdoor environment.

Building energy simulation is becoming more and more an established practice in recent years, due to the higher achievable accuracy of the dynamic tool, compared to the stationary calculations, and to the possibility of highlighting critical aspects, usually hidden in a monthly based analysis. However, the considerable amount of input required makes the simulation a complex tool to be handled by the designer. Among the main applications, such as comparing different building design alternatives, carrying energy retrofit analysis or predicting new buildings performance, the latter one presents more problematic uncertainty since schedules of occupants and consumption trends are unknown.

Various energy-oriented programs, that took center stage in building simulation, are now used also for the assessment and control of the indoor environment conditions. This approach shows some main great setbacks, connected to the subjective and qualitative nature of some parameters/variables, the amount of the input data required and not always available in early stage design, and the need to evaluate them balancing comfort and energy efficiency, which often collide. Finally a large output array must be managed and optimization carried out via different options.

Another difficulty lies in the climatic data used for simulation modelling. Predicted buildings performance and energy consumption are determined using a year representative of the weather, called test reference year (TRY), which consists of hourly data for 12 typical months, selected from approximately 20 year-data sets recorded as close to the project site as possible. Standard statistical calculations exclude extremes and lead to a typical climate file, which must concern the designer since it is not a real weather set and yet does not take into account forecasted climate changes. The conclusion drawn is that such data are no more suitable for the purpose of assessing building performance under future climate change conditions.

In this paper, the partial results of the CASA "Comfort for sustainable housing in the Alps" project are presented. The research is focused on the design and analysis of a free running single

building made of two distinct parts: an E-W oriented body with exposed concrete envelope and a timber element intersecting the first one (figure 1), with prevalent South-facing openings. The building will be located in Segno, town in Trentino, a typical alpine region in northern Italy. Specific attention has been paid to the effects on comfort conditions of openings, contemplating some significant parameters such as shading control, openings dimensions, transmittance, solar factor, shading types, aspect ratio, and varying them between a set of nominal values.

2. METHODOLOGY

A building simulation has been carried out in order to conduct a dual analysis of heating energy demand and comfort, using the software EnergyPlus, along with an algorithm prepared with Wolfram Mathematica for the optimization problem, in particular for managing inputs, interpreting outputs and producing resulting diagrams. The procedure is fully automated and yet scalable on as many processors available and as many parameters needed. Consumption of heating energy per heated net floor area is the first and most evident performance index of a building. Comfort performance is evaluated in terms of number of hours when the operative temperature exceeds of 2°C the category II range, according to the adaptive approach adopted by EN 15251. This theory recognizes that for natural ventilated buildings, but also for mixed mode buildings, people adapt to their environment and are comfortable over a much wider range of conditions than those predicted by Fanger’s theory.

A preliminary parametric analysis has been conducted, based only on openings contribution without considering any shading system. The variables considered have been percentage of South-facing openings, percentage of West-facing openings, thermal transmittance and solar factor of the glass. Then a second, more in-depth analysis has been carried out, taking into account also building shape and orientation, shading type and control automation. This allowed to highlight the most relevant parameters that have an influence on summer and on winter performances, and to estimate their effect.

Since the advanced design stage of the building and the limited number of variables, and given the high computational power available, for simplicity a brute-force analysis has been implemented, computing every combination of parameters. In this way, it has been possible to conduct a variance-based sensitivity analysis, considering the contribution of single variable to the amount of output uncertainty (first-order sensitivity index) and the uncertainty caused by interactions with other input variables (total effect index). Lastly, an optimal solution was evaluated, through the definition of an “objective function” considering both energy efficiency and indoor comfort.

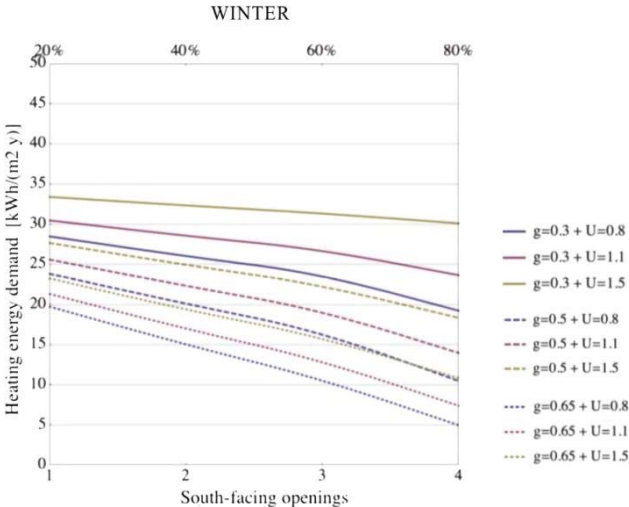


Fig 2. Heating energy consumption, assuming a percentage of W-facing openings of 40%

2.1. Simulation model

EnergyPlus, as a free simulation engine, does not come with a user friendly interface. Input geometry must be assembled within a third party graphical application, and thereafter exported. A plug-in for Trimble SketchUp developed by OpenStudio was adopted because it is an open source project and allows the user to assign many attributes directly on the model surfaces, shortening geometry modeling.

Since the building was in an advanced stage of design all the information about constructions and materials were provided. For a common energy analysis the building would have been divided in two thermal zones: night chambers and day living rooms. However, thermal comfort requires a more detailed breakdown and so each space was assigned to a different thermal zone, each one characterized by common schedule and set point.

Thermal zones exchange energy via conductive heat transfer only, but there is no convective factor since it was not implemented an inter-zone air flow network. Since the building runs without an HVAC, and no natural ventilation simulations were conducted at that point, an air flow exchange rate had to be supposed in order to take into account convective heat exchange, probably leading to an uncontrolled uncertainty source. However this approximation was accepted and since combinations did not show great temperature differences, it can be said that all cases were affected by this simplification about the same amount.

The north and west side of the building are in direct contact with the ground, but no ground historical temperature record where available for that location. A pre-processing analysis was conducted and an input undisturbed ground list of mean temperature by month was generated.

User schedules were developed based on the client habits and taking into account Alpine cultures. Schedules for natural ventilation were introduced for each season differently.

Other approximations, such as the green roof modeled as a dry ground layer, were made to simplify the model.

2.2. Preliminary analysis results

The preliminary analysis has varied 4 parameters – percentage of South-facing openings, percentage of West-facing openings, thermal transmittance U and solar factor g of the glass – for a total number of 576 combinations.

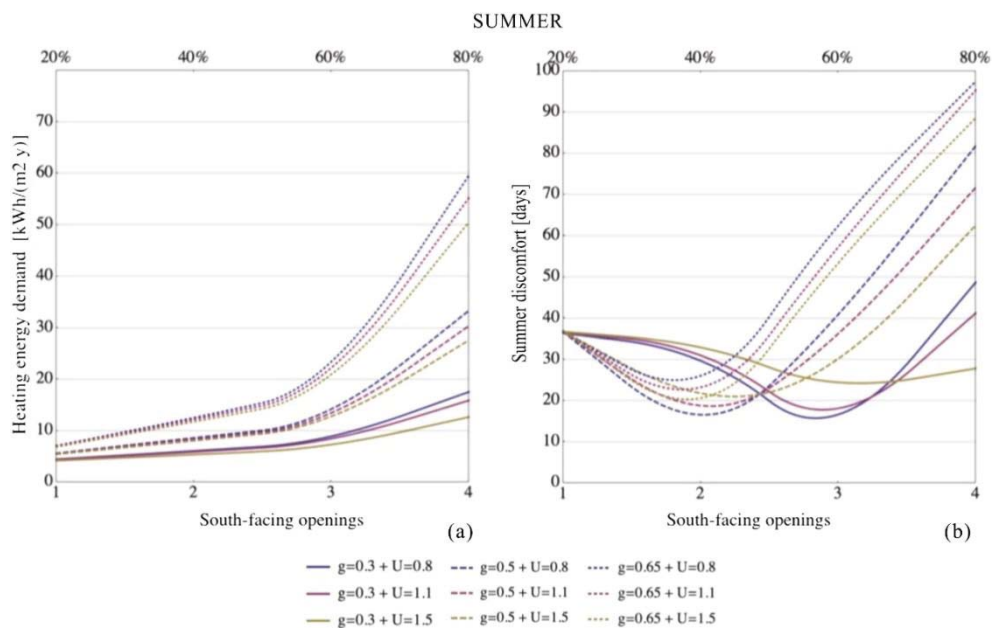


Fig 3. Summer performance in terms of cooling energy consumption (a) and in terms of comfort (b), assuming a percentage of W-facing openings of 40%

As shown in figure 2, heating energy consumptions decreases gradually with higher openings and the minimum value is reached with a combination of 80%S-80%W openings independently of transmittance or solar factor values. It can be drawn that the optimal combination during winter period is the one that maximizes solar heat gains and minimizing dispersions, with a glass with U-value as low as possible and g-value as high as possible.

Building summer performance has been evaluated both in terms of cooling energy consumption and of comfort. The figure 3(a) shows that cooling energy consumption trends are symmetrical to those of heating demand: in order to reduce consumption, solar factor should be low and thermal transmittance maximum. It can also be observed that g-value is the parameter that has the biggest influence on consumption trend. More interesting are the discomfort curves, which present, as shown in figure 3(b), a minimum point. It can be speculated that this tendency is due to the contribution of intermediate seasons, in which temperatures are still moderate and the increase of openings percentage brings a positive effect on comfort, while in summer, in absence of shading devices, large openings cause overheating and this justifies the fact that over a certain point discomfort curves start to increase again. Solar factor is confirmed, and it is clear from the diagrams, as the most relevant parameter governing the indoor quality during summer period.

This preliminary analysis, although far from being realistic inasmuch neglecting the effect of shading system, offered an interesting reflection on the importance of carrying out an analysis aimed to users comfort, and not merely on minimizing consumptions. This appears to be fundamental in light of the fact that cooling systems regulations are not always able to provide indoor comfort conditions and capable of adapting to variations in external conditions. Especially during intermediate seasons, when solar radiation starts to be relevant but outside temperatures are still low, it can be found that equipment calibrated on summer season can cause discomfort. With the aim of reducing their use to situations of real need only or, as an alternative, rethinking an automated controlled regulation as much adaptive as possible, an analysis in terms of comfort is therefore favorite.

2.3. Parametric analysis variables

The sensitivity analysis here presented took into account as many parameters as possible and run recursive routines in order to exclude those parameters that either do not affect others or impact little on the output. The first ones can be set independently for the project and give the design team a degree of freedom, the second ones can be appointed based on different concerns, such as costs or aesthetic.

For the purpose of this analysis only the parameters listed in table 1 were combined. A preliminary analysis with 43000 combinations was conducted to reduce to this more

Table 1. Set of parameters and values that can be assumed by parameters in the analysis

Parameters	Values								
	1	2	3	4	5	6	7	8	
Shading control	> 200	> 250	> 300	> 26 °C					
South openings	20%	30%	40%	50%	60%	70%	80%	90%	
West openings	20%	50%	80%						
Aspect ratio ^a	2:1	1:1	1:2						
Transmittance	0.8	1.1	1.5						
Solar factor	0.3	0.5	0.65						
Shading type	Sun blinds 30°	Sun blinds 60°	S. b. with tracking system	Ext. curtain	Int. curtain				

^aDefined as the ratio between North-South extension to East-West extension of the building.

manageable set of parameters. In particular, south opening were divided into 8 steps because of the south exposition of the building. Four shading control types were used, but many others could be chosen. This analysis shows the spreading impact of this variable and the necessity to investigate it more carefully.

3. RESULTS AND DISCUSSION

3.1 Winter analysis results

The winter thermostat set-point is 20 °C fixed with a constant schedule from the 15th of October to the 15th of April, following the typical heating period of the Alpine region. Comfort was not evaluated since the adaptive model does not work if a conditioning system controls the zone temperature.

All shading controls steps were let available even though energy saving measures do not advise it. Users usually activate the shading device to avoid excessing glare inside, and since the glare based activation control could not be fine-tuned, the solar on window and the outside temperature logics were kept in the analysis.

As resulted from the analysis (table 2), aspect ratio, window transmittance and west openings have little impact on both the first and total sensitivity indexes because the opaque envelope is well insulated and most of the heating removal is controlled. Window g-value is the second in order of impact. It regulates the amount of sun radiance that the glass let inside and since solar gains are free and great in value its influence was expected.

The surprising result is the little impact on variance of the south openings. It seems that this parameter does not influence much the energy performance of the building, which we know it is hardly true. This is all due to the effect of the shading device: running a parallel analysis without any shading device shows an influence on the S_i factor of 61.8% for the south openings. This explains also why the shading device has such an interaction with other parameters, with the South openings above all. The variance is most caused by the difference in activation time between the step regulated by the outside temperature (shading on if outside temperature above 26 °C, which never occurs during the heating period) and that controlled by the sun global radiation (in particular the first one, with shading on if global solar radiation greater than 100 W/m², which occurs during peaks in winter).

The shading control logic must take in great care this aspect and the design team should avoid situations of visual discomfort designing eaves with the right overhang. Also light inside shading device could help controlling glare, and in the meantime not preventing solar radiation from heating the zone.

Table 2. First-order sensitivity indexes, analysis on heating energy consumption (winter) [%]

	S_i	S_{Ti}
Shading control	38.5	45.7
South openings	2.1	13.4
West openings	2.4	5.8
Transmittance	15.9	13.4
Solar factor	28.1	23.8
Shading type	8.6	14.8
Aspect ratio	8.2	9.8

Table 3. First-order sensitivity indexes, analysis on comfort (spring, summer and fall) [%]

	S_i	S_{Ti}
Shading control	3.0	88.0
South openings	2.5	82.7
West openings	14.8	70.0
Transmittance	0.1	7.8
Solar factor	7.0	54.0
Shading type	0.3	8.1
Aspect ratio	1.4	26.2

3.2 Winter analysis results

As specified the building runs without a HVAC, therefore the adaptive comfort analysis could be run complementary to the heating season. Most part of spring and part of fall, as well as the whole summer time, were included and all the parameters listed were simulated. The results are summarized in table 3. The first order index shows the smallest impact on the output among all the parameters, while the total index is very high for Shading control, South- and West-facing openings and solar factor. This effect is due to the intermediate season: April has the same solar beam radiation of August, but much lower mean temperature. The Shading Control, relying in the first four cases on the solar beam intensity, would activate to protect the user from forecasted overheating, leading instead to discomfort due to low temperature. Intermediate seasons show a behavior that cannot be assimilated to summer and for this reason must be analyzed separately.

A summer analysis was conducted reducing the simulation period to 4 weeks, from the 15th of July to the 15th of August. The South-facing openings do not show the greatest first order index because the shading device is somehow always on, during peak temperature or peak solar radiation periods. To observe its real influence, a simulation without shading should be conducted. It is interesting to notice how the West-facing openings, on the other side, influence the output directly more than the South-facing ones. In conclusion, the total index effect in the previous analysis reached was over 50% in four cases, while in the summer specific analysis never reaches over 40%. Summer, like winter, shows one-way behavior: overheating must be avoided as much as possible. Intermediate seasons, for the reasons explained, caused situations of discomfort for low temperature, leading to a much more unstable output.

3.3 Optimal solution analysis

Having all the output combinations being evaluated, it was questioned what is in the pool the optimum solution. In building performance simulation (BPS), the term 'optimization' does not necessarily mean finding the globally optimal solution but rather indicates an iterative process, using computer simulation tools, aimed to achieve sub-optimal solutions, based on the chosen targets in respect of which the solutions will be evaluated. This attempt to express goals in mathematical terms for use in optimization studies is defined as 'objective function', and optimization problems can be classified as single-objective or multi-objective optimization depending on the number of objective functions they process.

In the presented case, it has been conducted a single-objective function, using weight factors to find optimal configurations of two variables, building energy demand and comfort conditions. An objective function was supposed, weighting summer comfort and heating demand of the building with different coefficients, from 0 to 1, giving for example equal importance to both of them (0.5-0.5 ratio) or prioritizing one over the other (0.3-0.7 ratio). As expected winter and summer require opposed solutions, while intermediate seasons could be included because the shading control logic is not adaptive to the season, as discussed.

The optimization took into account the winter and summer periods and showed that many combinations fell within a 5% interval from the best solution found. Since the uncertainty of many parameters reached 20%, due to user behavior, the first 30 optimum solutions were considered. The result is that, while winter solutions required the largest openings with very low transmittance, the summer optimum solutions were much closer because completely different combinations produce the same comfort result, without affecting the heating demand, mainly due to shading control and devices.

4. CONCLUSIONS

The sensitivity analysis is a powerful tool, yet not easy to set up for a professional use. Evaluating just the most important indexes, that sum the expected variance reduction due to fixing one parameter and the expected variance reduction due to fixing all other parameters except that one being considered, requires a great amount of computational time and a detailed input set up. There are tools on the market that let the designer interface EnergyPlus with optimization algorithms, but they always show some limitations.

Sensitivity analysis, even at this advanced stage of design, proved to be a very interesting design approach, discriminating those parameters that have no impact on the output, such as the thermal transmittance for a summer analysis or the aspect ratio for the winter period. These parameters can be evaluated outside the output optimization problem because they have no effect. On the other side, it shows which parameters do not interact with the rest of the pool, and are in fact uncoupled. These parameters can be set without concerning about the others. It is possible to evaluate second or higher order indexes for a specific group of parameters, in order to investigate the interaction within the limited pool. In this way the design team can exclude from the discussion those parameters that have no influence, recognize which parameters interact and on which degree, and eventually understand how these parameters interact within the specifics of the project.

It has been shown the importance of an object function approach. This is consistent with the increasing interest towards these methods, observed in the building design field of research. In the present work, it has been conducted a computation with an object function composed by two factors related to energy demand and comfort. In further work, a possible approach should be the elaboration of an overall object function for comfort, in which different weights are assigned to the different aspects influencing comfort, not only the thermal one.

5. ACKNOWLEDGMENTS

The present research is part of the CASA “Comfort for sustainable housing in the Alps” research project, a wider investigation on indoor comfort in residential buildings, aimed to develop a comprehensive assessment methodology for comfort evaluation and classification. Authors would like to thank CoviCostruzioni S.r.l, sponsor of the project.

REFERENCES

- Fisk WJ 2000 Health and productivity gains from better indoor environments and their relationship with building energy efficiency *Annu Rev Energ Env* 25(1) 537-566
- Corgnati SP Fabrizio E Filippi M 2008 The impact of indoor thermal conditions, system controls and building types on the building energy demand *Energ. and Buildings* 40 627-636
- Lai ACK Mui KW Wong LT 2009 An evaluation model for indoor environmental quality (IEQ) acceptance in residential buildings *Energ. and Buildings* 41 930-6
- IPCC 2014 Climate change 2014: Synthesis report, Summary for policy makers. Contribution of working groups I, II and III to the IV assessment report of the Intergovernmental Panel on Climate Change [Core Writing Team, R.K. Pachauri and L.A. Meyer (eds.)] IPCC Geneva, Switzerland
- Aries M and Bluysen P 2009 Climate change consequences for the indoor environment *HERON* 54-1 49-70
- Pernigotto G Prada A Costolab D Gasparella A and Hensenb JL 2013 Multi-year and reference year weather data for building energy labelling in north Italy climates *Energ. and Buildings* 72 62-72
- Holmes M and Hacker J 2007 Climate change, thermal comfort and energy: Meeting the design challenges of the 21st century *Energ. and Buildings* 39 802-814
- EN ISO 15251:2007 Indoor environmental input parameters for design and assessment of energy performance of buildings addressing indoor air quality, thermal environment, lighting and acoustics
- Deuble M and de Dear R 2012 Mixed mode buildings: a double standard in occupants' comfort expectations *Build. and Environ.* 54 53-60

- EN ISO 7730:2005 Ergonomics of the thermal environment - Analytical determination and interpretation of thermal comfort using calculation of the PMV and PPD indices and local thermal comfort criteria
- Saltelli A Annoni I Azzini F Campolongo M Ratto M and Tarantola S 2010 Variance based sensitivity analysis of model output. Design and estimator for the total sensitivity index *Comput. Phys. Commun.* 181 259-270
- Nguyen A-T Reiter S and Rigo P 2014 A review on simulation-based optimization methods applied to building performance analysis *Appl. Energ.* 113 1043-1058
- Evins R 2013 A review of computational optimisation methods applied to sustainable building design *Renew. Sust. Energ.* 22 230-245

Towards Sustainable Architecture: Lessons from the Vernacular. Case Study - the Traditional Houses of the Asir Province of Saudi Arabia.

Joseph Galea

Visiting Senior Lecturer, Architecture & Urban Design, Faculty for the Built Environment, University of Malta

Email: joseph.m.galea@um.edu.mt

Abstract: The current thrust in industrialized societies towards a sustainable Architecture is a result of a newly-found conscience about decades of wanton waste of natural resources to ensure buildings provide the comfort levels that society demands. This mismatch between design and comfort resulted from technologies that permitted any building to be made liveable irrespective of its context, albeit at an economic and environmental cost. The new trend towards a 'green' architecture, motivated by increasingly stringent regulations on energy use, has forced architects and designers to rediscover the relationships between building design and the environment. As Bernard Rudofsky states in his seminal book, "Architecture without Architects," '...there is much to learn from architecture before it became an expert's art.' This paper explores the lessons for sustainable architecture that the vernacular provides, through a brief investigation of the traditional buildings of the Asir Province of Saudi Arabia. Such buildings merit study not merely for their interesting forms or because of a misguided nostalgia. Neither is it for the inherent properties of their specific materials and technologies, which may or may not be realistically applicable today.

1. INTRODUCTION

The current thrust in industrialised societies towards a sustainable Architecture is a result of a newly-found conscience about decades of wanton waste of natural resources to ensure buildings provide the comfort levels that society demands. This mismatch between design and comfort resulted from technologies that permitted any building to be made liveable irrespective of its context, albeit at an economic and environmental cost. The new trend towards a 'green' architecture, 'encouraged' by increasingly stringent regulations on energy use, has forced architects and designers to rediscover the relationships between building design and the environment.

In the EU, buildings account for 40% of all energy use (Directive 2010/31/EU, 19 May 2010)

The figures are likely similar, if not higher, for other industrialized countries. Moreover, the major part of the built environment throughout the world is composed not of signature buildings – Architecture with a capital A – but of modest ones, comprising primarily the dwellings of the people. It follows therefore that the major part of energy use today is by housing, in all its different forms. Dwellings, today, often rely on mechanical means to achieve the comfort expected by their occupants.

Yet, it has not always been so.

2. THE VERNACULAR

In traditional societies man had, what N.J. Habraken calls, 'a natural relationship' with his dwelling (Habraken N. J., 1970.) He built forms of housing with readily available materials that responded to climatic forces and fulfilled his cultural "needs and values – as well as the desires, dreams and passion." (Rapoport. A. , 1969, p.2.) House forms evolved over a period of time using a limited palette of materials, with each iteration improving on the previous model, but continuing to abide with unwritten rules that gave a visual consistency and cultural coherence to vernacular settlements. (Galea, J.M., 1975, pp. 4-5.) (Galea, J.M., 1983, pp.230-249.) The result is what Pietro Belluschi called a "communal art, not produced by a few intellectuals but by the spontaneous and continuous activity of a whole people with a common heritage, acting under a community of experience." (Quoted in Rudofsky, B. , 1964.)

Furthermore, A. Rapoport states that "...vernacular seems to have the ability of being added to, subtracted from, or changed without losing its identity. " ('An Interview with Amos Rapoport,' 1979.)

By their very nature vernacular buildings were sustainable. This direct user-building relationship can still be found today in pre-industrial societies, although there are few areas where the internet and mass media has not intruded to contribute to the breakdown of traditional values.

However, even before the information revolution, tradition and its regulation of social norms were breaking down. Amos Rapoport in his seminal book, "House Form and Culture," identified three main reasons for this, namely: the proliferation of different "building types, many of which are too complex to build in traditional fashion," hence giving rise to specialised trades; the "loss of the common shared value system and image of the world;" and finally, the "originality, often striving for it for its own sake" that modern (not-traditional) cultures seek. (Rapoport, A., 1969 pp. 6-7.)

Vernacular architecture has long been admired by Architects and other 'cognoscenti.' However, this and the settlements it generated are often simply viewed as quaint developments with not much relevance to today's society, much like tourists look at and admire the old sections of town on their holidays, then go back to their home in the suburbs. "Our attitude is plainly condescending." (Rudofsky, B., 1964.)

Rudofsky rightly suggests that "the beauty of this architecture has long been dismissed as accidental but today we should be able to recognize it as the result of rare good sense in the handling of practical problems," and that, "there is much to learn from architecture before it became an expert's art." (Rudofsky, B., 1964)

Research has been carried out in Africa to "seek solutions from traditional architecture, in order to come up with cheaper and better ways of providing good standard sustainable buildings and spaces." (Mabaleka, B.G.) This is a laudable objective but one must be cautious not to fall into the trap of copying elements of the vernacular directly "without understanding what they mean or why they are good" (An Interview with Amos Rapoport.)

It is encouraging to see that the study of vernacular architecture is now being carried out, not only from a historical and visual perspective, but "as a source for teaching sustainable design" to future architects. (Forster, W., Heal, A. and Paradise, C., 2014, p. 203) The study of vernacular architecture can provide valuable general lessons "in response to climate, energy use and notions of environmental quality" (Rapoport, A. quoted in Forster, W. et al, 2014.) and, as importantly, to provide insights into the processes of people influencing the buildings they live in, which is the key to their satisfaction with their living environments. (Galea, J.M., 1975.) The challenge then is to apply the lessons learnt to design, to ensure that today's buildings and settlements are climatically appropriate, sustainable and meet the cultural and social needs of modern society.

3. CASE STUDY: THE HOUSES OF THE ASIR

The characteristic, traditional dwellings of the Asir Province of Saudi Arabia merit study for their reflection of the symbiosis of a people, their physical environment and their cultural requirements.

The following case study is the result of a 1980 trip that the author and two colleagues made to document these fascinating structures. Considering the length of time that has passed and the massive development in Saudi Arabia over the past decades several of the buildings photographed may have since disappeared. However, the lessons to be derived from them remain. At the time, these vernacular buildings were described in a paper by the author and others (Galea, J.M. and Boon, J.J., 1981.) What follows here depends heavily on that paper.

The land of the Asir province differs greatly from the harsh landscapes of the other provinces of the Kingdom. This is how that intrepid explorer of Arabia, Wilfred Thesiger described the Asir, the South Western Province of the Kingdom of Saudi Arabia.

“...a mountain-side forested with wild olives and junipers. A stream tumbled down the slope; its water ice cold at 9,000 feet, was in welcome contrast with the scanty, bitter water of the sands. There were wild flowers: jasmine and honeysuckle, wild roses, pinks and primulas. There were terraced fields of wheat and barley, vines and plots of vegetables. Far below....a yellow haze hid the desert to the east.” (W.Thesiger, 2007, p.17)

The province covers some approximately 104,000 sq. kms. It extends from south of Taif all along the Red Sea to Yemen on the south. To the east it merges with the Najd, the central region of Saudi Arabia where Riyadh, the capital of the Kingdom is located. Further east is the Empty Quarter, the *Rub al-Khali*, the desert that Thesiger refers to at the end of the above quote.

The western edge of the Province is defined by a narrow coastal plane, the Tihamah from which rise “a succession of high plateaux with steep scarp edges” (Kingdom of Saudi Arabia, 1982, p.12.) These are part of the mountain range with peaks rising to around 3,000m, which Philby called “the backbone of Arabia.” (Philby, H. St. J., 1976.) These topographical characteristics strongly influence the climate – a relatively mild tropical uplands climate, which contrasts sharply with the generally harsher climate elsewhere in the Kingdom.

The temperature in Abha, the provincial capital, averages 17.5 °C. In a year, the average rainfall is 278 mm. Temperatures average between 14 and 16 °C in January, to 22 -24 °C in July. The diurnal variation can be high, as much as 12 °C in September. Average Relative humidity is around a comfortable 65%. Rainfall is spread out throughout the year with the driest month being October, with 2 mm of rainfall, with peak precipitation in March with an average of 59 mm. (<http://en.climate-data.org/location/3634/>.) However, the distribution of the rainfall across the province varies as one moves from west to east.

The warm, moisture-laden air over the Tihama along the Red Sea, rises over the steep escarpment shedding its moisture in the form of heavy rains over the western part of the province. Here the rains often create temporary rivers in the wadis and green the landscape. Many wadis dry up shortly after the rains but some of the greenery persists. As one moves east across the province towards the desert, some 200 kms away, the amount rainfall rapidly drops off. This is clearly reflected in the type of dwellings that developed in different areas of the province. Although climate in general, and in this case amount of rainfall in particular, is a definite factor in the forms of vernacular houses that developed in the Asir, one has to be aware that “building form manifests the interaction of many factors” (Rapoport, A. ,1969, p.18) and cannot simplistically be determined or explained by climate alone.

The traditional houses of the Asir may be grouped into three broad categories. Each category is related to a particular area of the province and is influenced by, among other things, the materials available and the prevailing climate in the area. These three categories may, for convenience, be labeled as ‘Stone,’ ‘Mud’ and ‘Mud Slate.’ (Figure 1.) Intermediate forms of course exist, such as the ‘stone apron and mud’ houses, sometimes referred to as ‘Abha style’ houses. (Farsi, Z.M.A., 1989, p.63) These have a stone ground floor with mud or mud-slate upper floors. These buildings are significant because they demonstrate how within a similar context different forms may develop. However, for the purposes of this paper they are considered to be an exception.

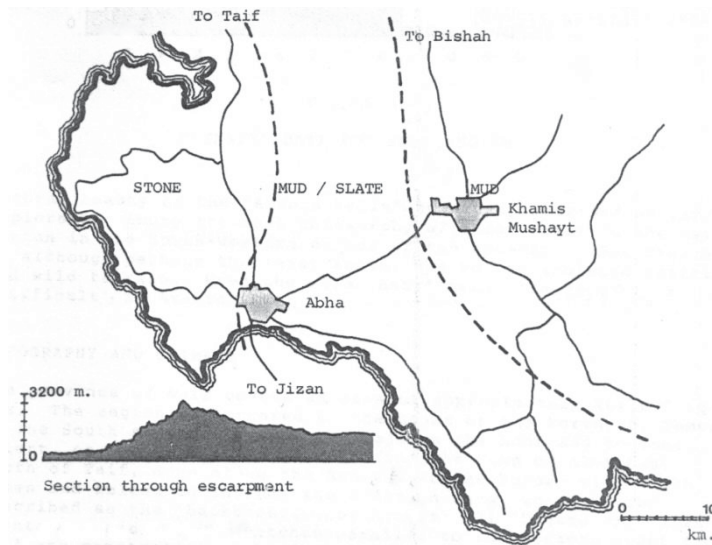


Fig 1. General distribution of the three broad categories of vernacular houses. (Borrowed from J.M. Galea and J.J. Boon 1981)

4. STONE HOUSES CASE STUDY

The stone houses are primarily located in the western part of the province where the rainfall is the highest. Here stone is abundant and is the primary material used for vernacular houses. Houses occur in small groupings in a fortress like mass, often located at the top of hills creating the impression of citadels. These settlements or house groups are often accessed via only one or two concealed and protected entrances. (Figure 2.) It is often difficult to distinguish and delineate individual dwellings. Entrances lead to a veritable warren of passages that thread their way through the structure.



Fig 2: Entrance to a 'stone' settlement



Fig 3: Reinforcing timbers in wall.

The houses themselves are usually one to two storeys high and have small internal courtyards. Certain areas can only be accessed by ladders across the roof. (Figure 4.) Internal rooms are lit and ventilated through a hole in the roof, formed in some cases by embedding a clay pot into the mud roof, covered by a slate when necessary. (Figures 5. 6)



Figure 4: Roofscape with ladder from an internal courtyard



Fig 5: Hole in roof formed by clay pot.



Fig 6: Slate covering for ventilation hole.

The walls may be 70cm thick at their base (Farsi, Z.M.A., 1989., p. 63) and taper slightly inwards as they rise, reinforcing the fortress impression, while increasing their structural

stability. Timbers, generally juniper or tamarisk, are often incorporated into the walls as reinforcement. (Figure 3.)

Construction of the walls is in dry rubble. Stones are trimmed to provide a smooth outer face. The interstices between the large stones are packed with small laminates of schist. Coursing is horizontal, albeit irregular, but the quality of workmanship is generally high. Vertical supporting elements are of rough timbers; in some instances consisting of complete tree trunks (Figure 2.) Roofs are again composed of a framework of rough timbers as primary and secondary load-bearing elements, carrying layers of bundled reeds, over which is a mud deck of c. 30cm thickness.

The upper surface of the roof is coated with a lime wash to protect it from the heavy rains in the area. Rain is shed from the roof by wooden spouts which project far beyond the face of the building. (Figure 7) In some instances water is taken to the ground down the walls along vertical, lime-plastered, mud channels. Doors and any external window shutters are solid timber and often inscribed with geometric designs or Islamic calligraphy. (Figures 8, 9) Apart from the carvings on doors and shutters the only other, simple but effective, decorative elements are quartz pebbles and small schists laid in careful arrangements above external openings. (Figures 10, 11)



Fig 7: Partly ruined dwelling showing rough timber primary roof supports and rainwater spout projecting beyond the wall.

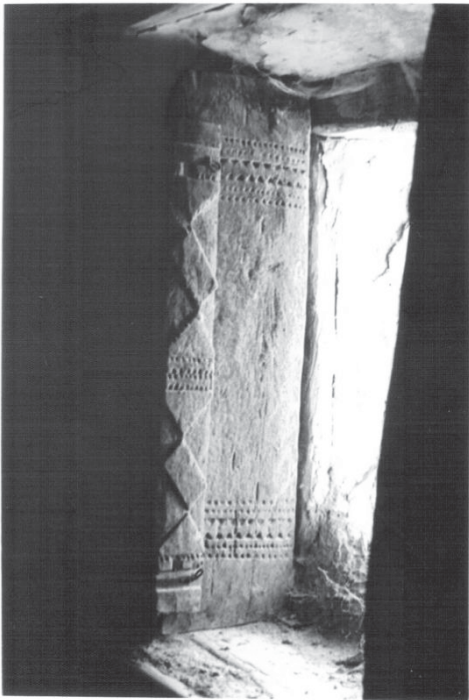


Fig 8: Carved window shutter



Fig 9: Door with geometric designs



Fig 10: Window decoration with lime wash window surrounds



Fig 11: Quartz decoration around window

The defensive nature of these houses and indeed of most of the house types in the Asir, have a historical reason. The Asir is the only area of Saudi Arabia that has been subject to several foreign invasions - by the Romans as early as 24 BC to the Ottomans in the early 19th century. (Galea, J.M. and Boon, J.J. 1981.) This, and inter-tribal conflicts, necessitated that houses and settlements could be easily and well defended. Although the Asir became part of the Kingdom of Saudi Arabia in 1934, under King Abdul Aziz ibn Saud, and the need for defense diminished,

the defensive characteristics of the dwellings persisted. This indicates the complex nature of the process responsible for house forms in vernacular societies.

5. MUD-SLATE HOUSES

As one moves further east and down from the rocky heights, the abundance of stone available for building diminishes. In this zone the traditional houses take on a different form. The defensive appearance remains but the houses become 3-4 storey, free-standing towers in small groups. They are built on stone footings but the primary building material is mud. Continuous mud courses, approximately 50cm high are laid, each course being allowed to dry before the next is laid. Since this zone still experiences heavy rainfall, bands of projecting pieces of slate, sloping outward, are laid between each course to shed water off the vulnerable wall surface. (Figure 12) This gives the houses a characteristic striped appearance. (Galea, J.M. and Boon, J.J. 1981.) This striped effect is enhanced in many cases by painting the wall surface between the slate bands coinciding with window lintels and sills in a white, and occasionally coloured, lime wash. The top of the walls and roof parapets are also finished with a lime wash to protect the edges. This white trim creates a particular appearance that T. Eigeland said resembled “cakes with icing on top.” (Eigeland, T., 1980.) (Figure 13)

Similar to what has been described for the stone houses, roofs are carried on rough timbers as the main vertical and horizontal structural elements with smaller, similarly rough, cross members over which are laid reed mats on which is laid a mud decking. (Figures 14, 15) The roof surface is again finished with a lime wash. The ubiquitous mud, on wood framing, is used also to form internal ‘built-in furniture.’ (Figure 16)



Fig 12: Horizontal bands of slate between courses.

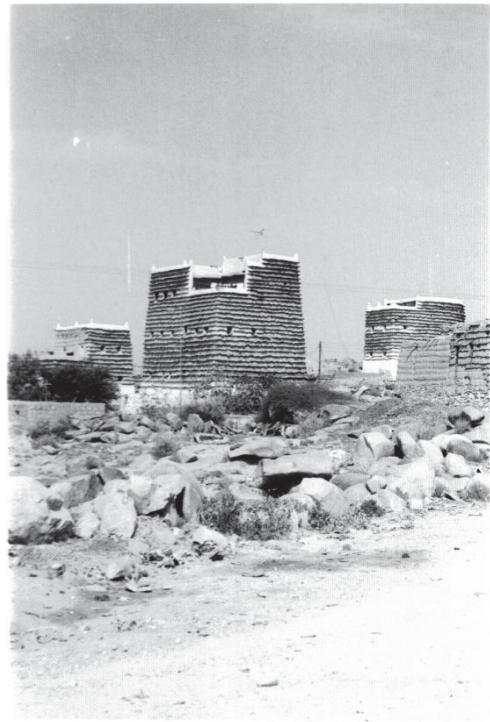


Fig 13: “Cakes with icing on top.”



Fig 14. Rough timber main structural elements



Fig 15: Reed mats over rough timber secondary elements

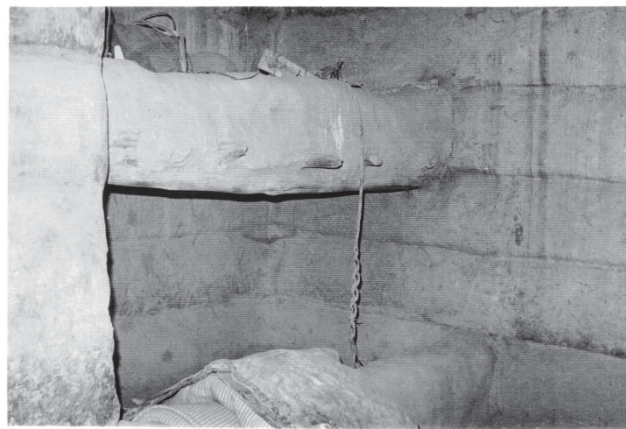


Fig 16: Mud 'built-in furniture.'

6. MUD HOUSES

The easternmost part of the province experiences much less rainfall. In this area the houses resemble the mud-slate houses of the central area, both in their construction technique as well as in their overall form. However, here the slate bands are not required. Therefore, here the houses are more 'monolithic' and vertical in appearance. Courses may be expressed or the whole wall may be given a coating of mud to provide a smooth surface. At the corners the courses are turned up to help guide rain away from the vulnerable building angles. Visually, this also emphasis the raised roof parapets at the corners. (Figure 17) (Galea, J.M. and Boon, J.J., 1981)

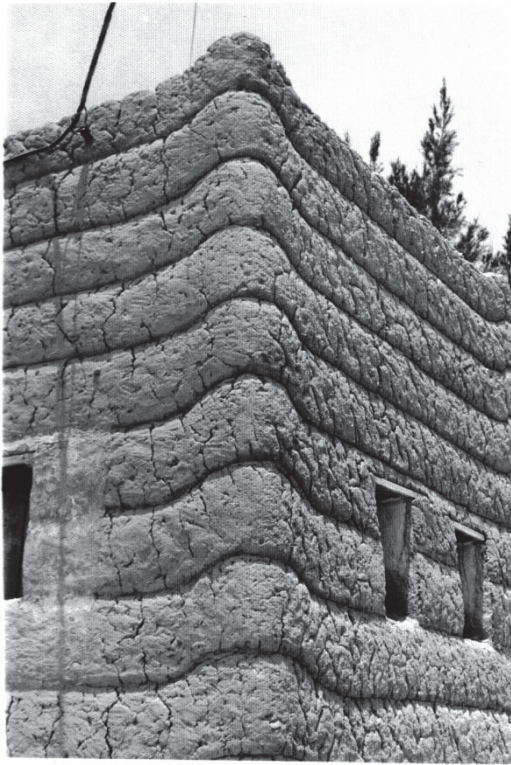


Fig 17: Coursing turned up at the corners

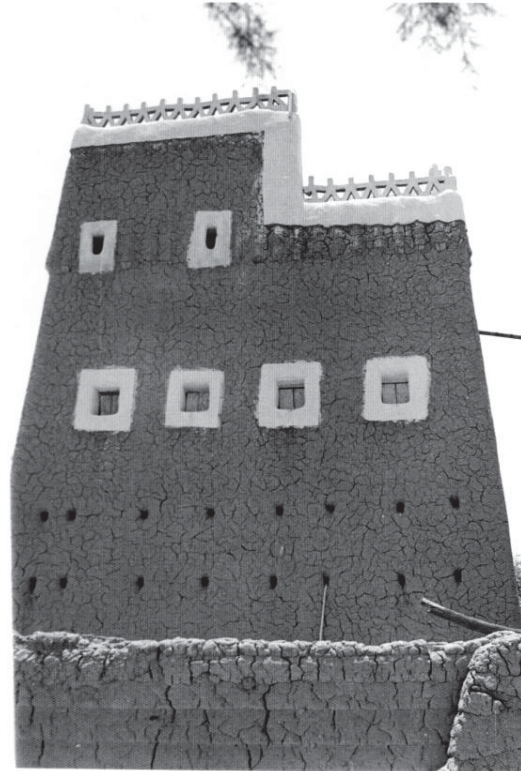


Fig 18: Lime washed window surrounds and roof parapets

Lime wash is again used at roof parapets as well at window surrounds, both for functional reasons but also for its obvious aesthetic value. Sometimes the lime wash may be applied over a whole wall surface or as a horizontal band going around the whole house, often emphasizing a row of windows. (Figures 19, 20)



Fig 19: Lime washed upper floor wall surfaces



Figure 20: Lime wash bands highlighting rows of windows

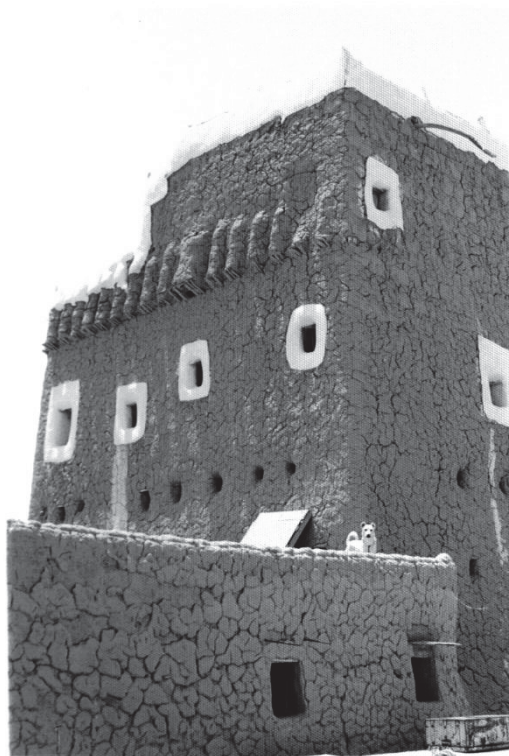


Fig 21: Mud on timber casings of primary beam ends

The ends of beams carrying the roof, and sometimes even the upper floor, are sometimes taken right through the walls to the outside face, perhaps to provide more bearing area for the beams. Here they are protected by a wood casing covered by mud. (Figure 21) The resulting pattern of wide vertical corrugations is sometimes carried around the four facades for aesthetic effect – a functional element exploited for its visual potential.

7. THE INTERNAL ORGANIZATION OF THE ‘QAS’

The internal organization of the ‘Qas’ or ‘Hisa’ (Arabic for ‘fort’,) as these houses are called, reflects the cultural and physical needs of their users and is based on the ‘purdah,’ the clear separation of public and private areas. Each house is generally surrounded by a wall delineating a courtyard from which open rooms for animals. The ground floor generally contains additional store rooms. The public area of the house is on the first floor, where the main sitting or guest reception room, the ‘majlis,’ is located. This room generally comprises a low seat around all the room, again formed in mud, covered by carpets and cushions. Walls and apertures (doors and windows) are often painted in bright colours, green being a favourite one. The upper floor/s contain the rooms for the family. The top floor is the women’s domain and comprises the kitchen and an open terrace, oriented according to the prevailing winds. The stairwell is often carried up to the flat roof area which provides additional private family space.

8. ‘QASABAHS’

It is worth briefly mentioning another building type that may be found, primarily in the central and eastern zones – the ‘qasabah’ (Arabic for ‘stick’ or ‘reed.’) This is a tall tower, approximately 12-15 metres in height, generally circular on plan, having a diameter of about 3 metres, although square examples are also found. These normally have a stone ground floor with their upper parts in mud, generally with slate bands, although all stone qasabahs may also be found. (Figures 22, 23)



Fig 22: Square, mud-slate qasabah on stone base



Fig 23: All stone, round qasabah

These towers likely served as watch towers to safeguard crops from marauding tribes (Talib, K., 1984, p.97) but may have eventually become a status symbol of their owners, (Galea, J.M. and Boon, J.J., 1981) retained and maintained even when their original purpose ceased to exist.

9. QASABAHS'

Vernacular architecture in general, and the traditional house of the Asir Province of Saudi Arabia in particular, demonstrates how people who are intimately connected to their physical environment manage to build habitations from materials that are readily available and generally re-useable, however limited the palette, that not only meet the climatic challenges of their particular environment but also satisfy their physical, social and cultural needs. Their results are a lesson in sustainability.

The lesson for architects, especially those working in economies of scarcity (Galea, J.M., 1980.) in the housing field is to work closely with the eventual users of their dwellings, and understand the complex system of forces that generate their vernacular buildings. Their primary role should not be that of introducing new forms of dwellings no matter how efficient they are deemed to be. Instead they should focus on improving and/or rationalizing existing technologies, so that their efforts become merely one more step in the vernacular continuum of buildings developing by a series of many, small changes in response to perceived shortcomings in the previous model. The work of Carin Smuts in South Africa (among others) is an example of this. (Frey, P., 2010, pp. 122-131.)

Let us not allow the current, admirable drive towards sustainability to be used as another excuse to push onto developing nations systems and products, whose primary purpose is the enrichment of the producers. As Victor Papanek said so long ago:

“Our responsibility as designers lies in seeing that emerging nations don’t emulate our own mistakes of misusing design talent as an ego trip for the rich and a profit trip for industry.” (Papanek, V., 1974, p. 122.)

Irrespective of context, examples of vernacular architecture provide architects and designers “a sort of enchanted catalogue of suggestions and germs of solutions on which their inventiveness can work.” (Frey, P., 2010, p.64.) Vernacular inspired teaching programmes in schools of architecture aimed at training students to combine “vernacular pragmatism and the resources of modern technology,” (Frey, P., 2010, p. 160) will hopefully lead to a new generation of architects who will, as a matter of course, design inherently sustainable buildings that, while being rooted in the community for whom they are meant, perform to contemporary green energy standards (such as LEED, BREEM, etc.) at an affordable cost.

REFERENCES

- 'An Interview with Amos Rapoport on Vernacular Architecture,' Creperie Bretonne, Louvain La Neuve, Belgium, July 13, 1979. *M.E.T.U. Journal of the Faculty of Architecture*, Vol. 5, No. 2, Fall 1979. Retrieved from http://jfa.arch.metu.edu.tr/archive/0258-5316/1979/cilt05/sayi_2/113-126.pdf, 19 November 2015
- Directive 2010/31/EU, 19 May 2010 on the energy performance of buildings
- Eigeland, T., 'Back to the Highlands,' *Aramco World*, September 1980
- Farsi, Z.M.A., *National Guide and Atlas of the Kingdom of Saudi Arabia*, 1989
- Forster, W., Heal, A., Paradise, C., "The Vernacular as a Model for Sustainable Design," in Weber, W. Yannos, S. (eds.) "Lessons from Vernacular Architecture," Routledge, London, 2014
- Frey, P. "Learning from Vernacular," Actes Sud, Tours, France, 2010
- Galea, J.M., "Homes and People", unpublished M.Arch. dissertation, University of Malta, 1975
- Galea, J.M., 'The Role of the Architect in Economies of Scarcity,' *International Journal for Housing Science*, Vol. 4, No. 6, 1980
- Galea, J.M., "The Development of the Domestic Architecture of Malta in Response to Technological and Economic Forces, in Ural, O., *International Journal for Housing Science and Its Applications*, vol. 7, no. 3, 1983
- Galea J. M. and Boon, J.J., "The Traditional Architecture of the Asir Province, Saudi Arabia," in Ural, O. and Krapfenbauer, O. (eds.), "Housing: The Impact of Economy and Technology," Pergamon Press, New York, 1981
- Mabaleka, B.G., "The Vernacular architecture as a model for Sustainable Design in Africa," retrieved from <http://www.scribd.com/doc/33702709/The-Vernacular-Architecture-as-a-Model-for-Sustainable-Design-in-Africa#scribd>, 26/11/2015
- Habraken, N.J. 'aap root mies huis' – 3 R's for Housing,' Amsterdam, Scheltema and Holkema, 1970
<http://en.climate-data.org/location/3634/>, retrieved 21/11/15
- Kingdom of Saudi Arabia, Stacey International 1982
- National Guide and Atlas of the Kingdom of Saudi Arabia
- Papanek, V., "Design for the Real World," Paladin, 1974
- Philby, H. St. J., "Arabian Highlands," De Capo Press NY 1976
- Rapoport, A., *House Form and Culture*, Prentice-Hall, Englewood Cliffs, N.J., 1969
- Rudofsky, B., *Architecture without Architects*, Doubleday, New York, 1964
- Talib, K., 'Shelter in Saudi Arabia,' Academy Editions, London, 1984
- Thesiger, W., *Arabian Sands*, Penguin Classics, 2007

Retrofit Opportunities for the Historical Back Bay Neighbourhood

Ornella Iuorio

University of Leeds, Leeds LS2 9JT, UK

Antonino Barbalace

Massachusetts Institute of Technology, Cambridge, MA02139, USA.

John Fernandez

Massachusetts Institute of Technology, Cambridge, MA02139, USA.

Email: O.Iuorio@leeds.ac.uk

Abstract. The housing stock in Back Bay holds a strong identity and cultural significance for Bostonians. This district is famous for its rows of Victorian brownstone homes and considered as one of the best-preserved examples of XIX century urban design in the United States. It is a quintessential part of the Bostonian aesthetic. As they were built at a time when the use of fossil fuels, emissions of greenhouse gases and the expectation of changes to our climate were not a concern, the building fabrics were not originally designed to retain heat energy particularly well either in the long cold winters or to cool down in the short humid and hot summers. This paper presents an evaluation of energy demand of the Back Bay historical neighbourhood and propose some guidelines for retrofit interventions. The paper is developed within a larger research project on "Smart retrofit for resilient historical cities". The project aims to develop a modelling tool that, given a retrofit target, compares different energy and hazard retrofit scenarios in terms of environmental and economic costs.

1. INTRODUCTION

There is an increasing international interest on reducing carbon footprint of building. This largely looks at the new buildings, and the upgrading and maintenance of existing buildings receive little attention in the contest of carbon reduction . Although it may contribute to a significant reduction especially when retrofit interest a large neighborhood intervention.

This paper aims to investigate the inflow of permanent materials that, over time, have contributed to the physical shaping of the Back Bay neighborhood and intend to demonstrate the beneficial effects of changing only a negligible amount of the existing materials. Therefore making the case that preserving the material legacy of a historic area can go hand in hand with improved environmental performance.

2. HISTORICAL DEVELOPMENT OF THE NEIGHBOURHOOD

A critical analysis of the historical development of the Back Bay neighborhood is essential to evaluate the construction material flow over centuries. The built history starts in 1813, when the "Boston and Roxbury Mill Corporation" received permission to build the Mill Dam with the intent to transform Boston from a harbor-bound provincial town into a modern city. By the mid nineteenth century Back Bay was heavily polluted, until 1849 when the Boston's Health Department demanded to fill the area for interests of the public welfare. Therefore, a portion of the Charles River was filled in mostly with granite gravel from Needham, Massachusetts, so that about 450 acres were added to the original 783 acre peninsula. The Back Bay neighborhood was built in this new area. A railroad connected to a gravel pit in Needham, nine miles from the Back Bay, was built to facilitate the land reclamation project. The scope of the earthwork

reached an average depth of 6 meters (20 feet) and more than 450 acres of area to be filled. Starting with the east end of the bay in 1857 by 1880, the entire lower basin was filled with solid ground. The Back Bay landfill was completed in 1890, closely resembling today's coastline (Figure 1). The houses were erected on wooden pile foundations driven through the made land and underlying mud to hard clay, typically 9 - 12m (30 to 40 feet) below the ground surface. About 270 piles were used for each house.



Fig 1. Aerial view of Back Bay

3. MATERIAL FLOW ANALYSIS

In order to properly estimate the amount of materials that went into the construction of Back Bay, a Boston geographic information system (GIS) map was adopted to collect information about the volumetric distribution of the area. Based on a section through the Mill Dam in *Gaining Ground*, three layers of fill were estimated and the weight of the filling materials charted in order to estimate the evolution over time (Figure 2).

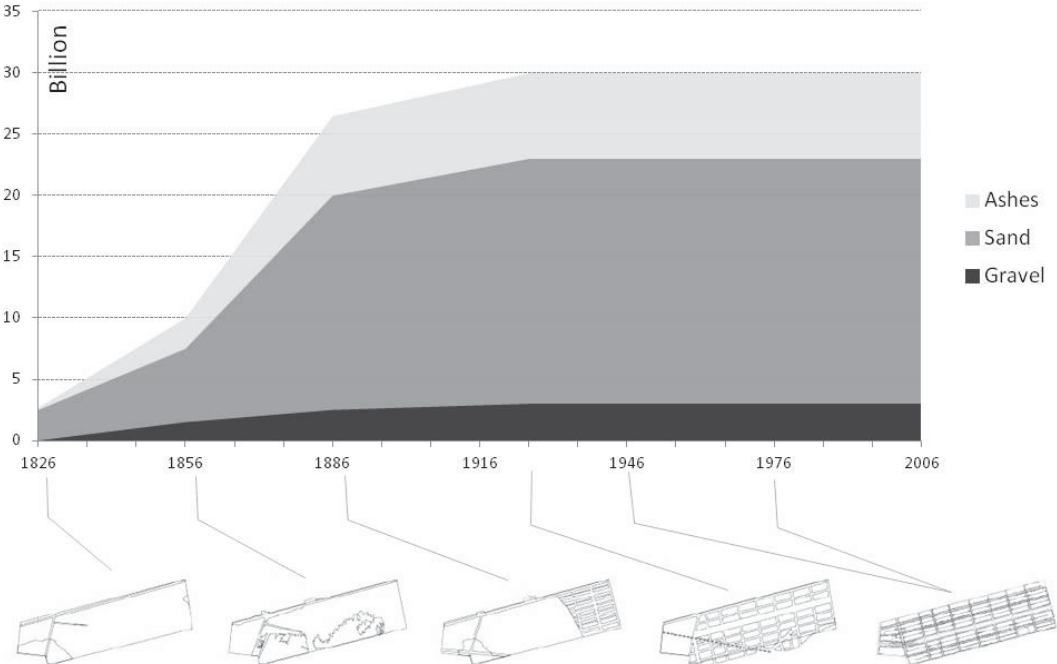


Fig 2. Accumulation of material weight for land filling.

The typical residential building in the Back Bay is the townhouse (Figure 3a). Usually arranged between four to six levels, these single family dwellings have a uniform setback from the street and feature a long narrow plan with side hallways and central staircases. The first floor is typically raised a few feet above the street level. The structure is triple-wythe (or more) load bearing brick masonry party and exterior walls. These walls rest on stone foundations that sit on wood piles (Figure 3b). The facades feature facing materials often distinguishing the first level from upper floors of the house, and whose material choices vary according to chronological trends and availabilities.

Terra-cotta hued facing brick prevailed in the earliest houses, prior to the frequent use of brownstone between the 1850s and 1860s. Different types of sandstones became popular in the 1870s, as well as an increased variety and experimentation of materials such as panel brick, glazed tile, pressed copper, and slate. Houses towards the end of the nineteenth century would often feature light colored limestone facades. The progression of the neighborhood's construction in terms of building weights is shown in figure 4.

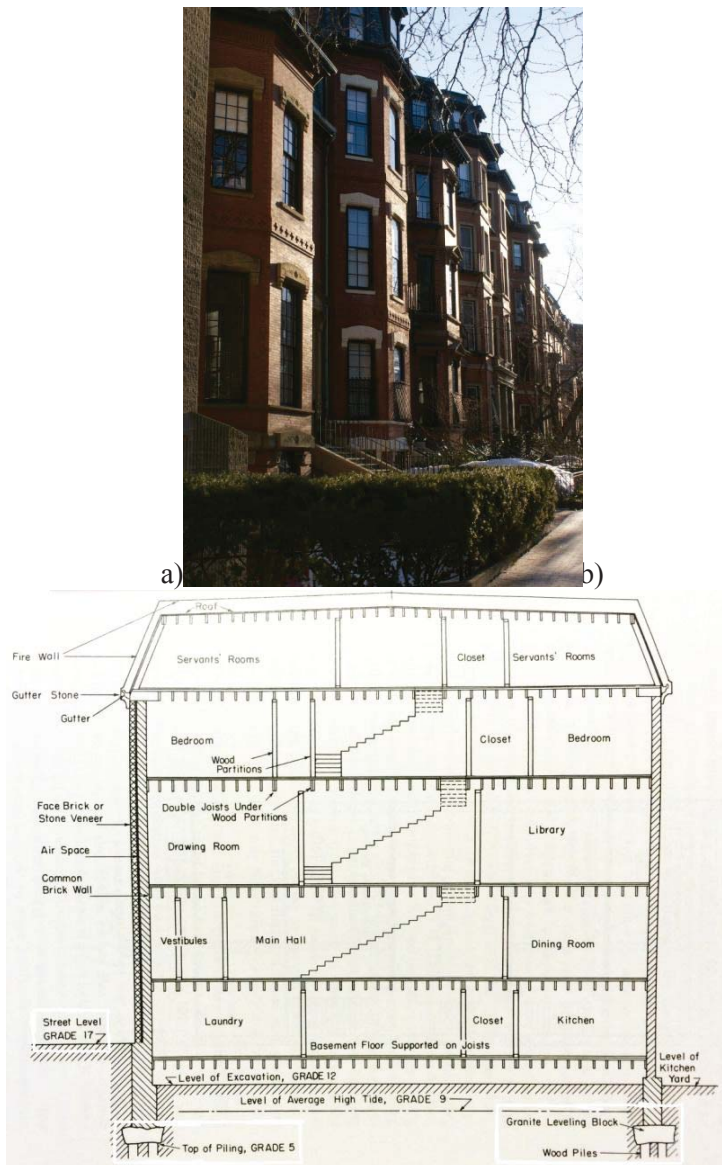


Fig 3. a) View of row houses; b) section of a typical Back Bay house showing the construction system.

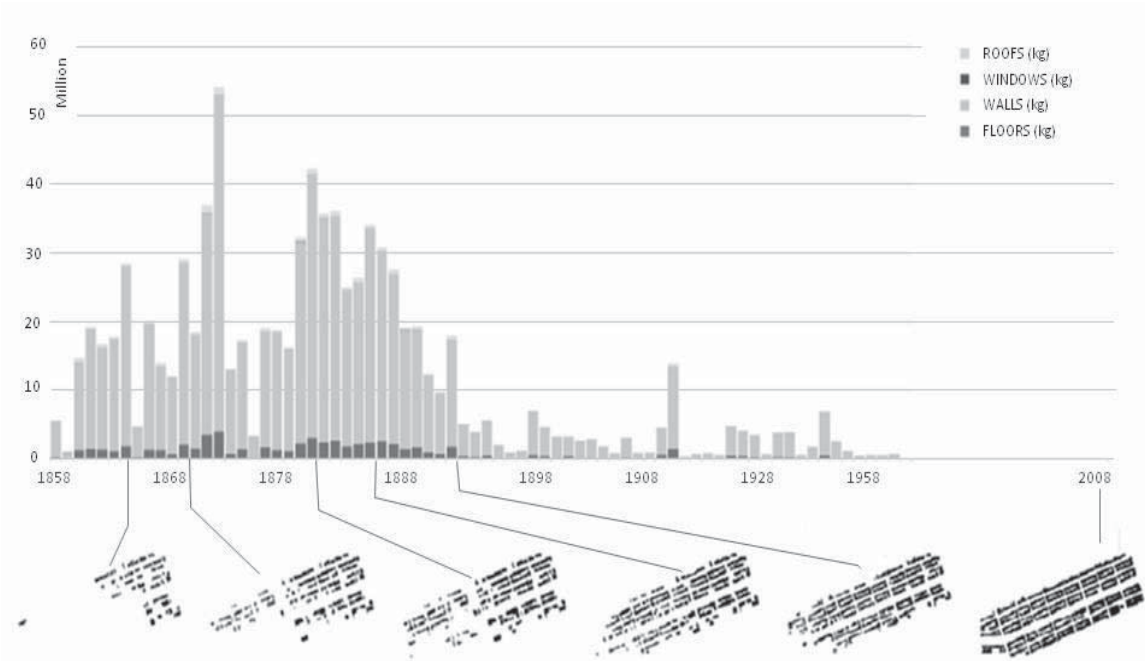


Fig 4. Accumulation of material weight for building.

4. RETROFIT

Carbon and energy savings in historic buildings are considered difficult to achieve due to limited retrofitting capability. In historical buildings, services are upgraded on a cyclic basis, whereas alteration of the building fabric can be very restricted, but when done, they can persist for an important portion of the life cycle of the building fabric. Therefore, in a logic of carbon reduction, any improvement of the thermal performance should be prioritized.

This work aims to investigate possible retrofit scenarios for the Back Bay neighborhood looking at the thermal performance, moisture balance and material intensity. In particular, this last is investigated in terms of material weight and associate embodied carbon (EE), where EE is calculated according to Inventory of Carbon & Energy (ICE).

4.1. Walls

The original Victorian buildings are of solid masonry walls made of 3wythe bricks and 1 brick or veneer layer toward to exterior and completed with gypsum plaster on the interior. This system presents a very transmittance value but, at the same time, the high rate of air infiltration prevents moisture build-up. Many buildings over the last century, have been transformed from single family houses in apartment buildings. In correspondence to this functional change, they were subjected to some refurbishments, which in many cases brought to replace the original internal gypsum plaster with dry walls that slightly improved the thermal comfort (Figure 5).

Better thermal performance can be achieved by adding insulations materials to the inner or outer of the masonry walls. However, as all the neighborhood lies in a conservation area, alteration of the external are not allowed. Therefore, only internal insulation can be added.

Three retrofit that are in line with preserving the architectural feature of the buildings are investigated (Figure 6): R1, removing the interior finish and replacing it with hydraulic lime; which improves the thermal resistance of the wall and, thanks its high porosity and water vapour permeability, can be considered 'breathable'. Moreover, lime is alkaline, which helps prevent mould growth and discourages rodents. R2, infill the drywall cavity with open cell spray insulation, allowing increasing thermal performance also preventing the occurrence of moisture and condensation; R3, infill the drywall cavity with loose mineral wool, allowing a very important improvement of thermal insulation, being at the same time naturally moisture – resistant and performing as a fire barrier, slowing down house fires. As shown in Table 1, the

third retrofit scenario is the one that let to achieve the current thermal requirements for new house ($U = 0.3 \text{ W/m}^2\text{K}$) and in terms of material, if compared to the original construction type 2, it only account for 3 kg per m^2 of added material and corresponding 46 MJ of EE.

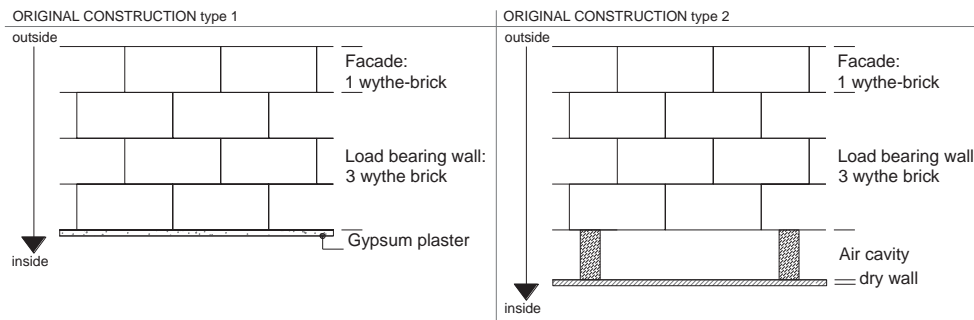


Fig 5. Wall sections of the original constructions.

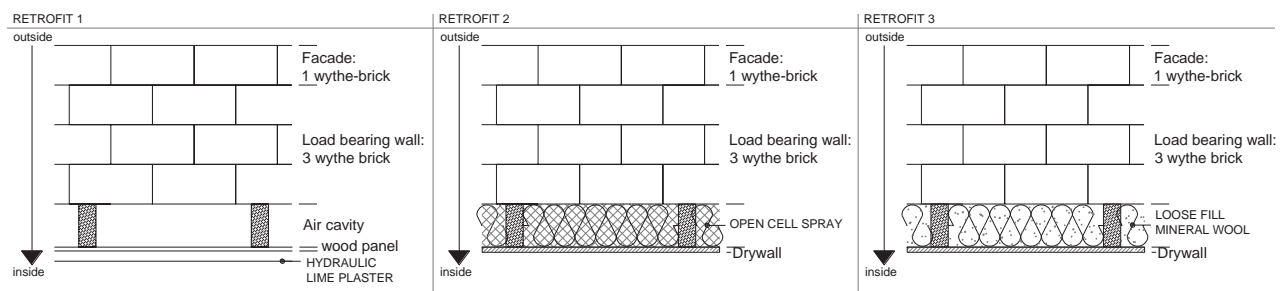


Fig 6. Retrofit scenarios

Table 1. Evaluation of the overall resistance, weight and embodied energy per unitary wall area of the original constructions and the retrofit solutions.

	Overall U value [$\text{W/m}^2\text{K}$]	Weight per 1m^2 wall area [kg]	EE per 1m^2 Wall area [MJ]
Original construction type 1	1.11	600	1880
Original construction type 2	0.91	612	1908
Retrofit 1: add hydraulic lime plaster	0.84	618	1928
Retrofit 2: add open cell spray	0.78	613	1999
Retrofit 3: add loose mineral wool	0.31	615	1954

4.2. Roofs

The roofs are usually the largest source of heating loss of a buildings. Therefore, roof retrofit presents an ideal opportunity to reduce energy consumption. In the extreme weather conditions of Boston with extremely cold snow winter, with temperatures below 0°C (up to -20°C) and hot and humid summers with temperatures around 30°C , roof thermal performance become an extremely important issue. In the Back Bay original constructions, the roof performance was extremely poor being built up mainly with wood boards, gravel and tar membrane (original construction type 1, figure 7) or slate tiles (original construction type 3, figure 7). In some cases, in a second phase, concrete fill and tiles were added to the wood and gravel roof, mainly for sound reduction, as can be read in the report by J Hickey Associates in 1972. This intervention (original construction type 2, figure 7) also produced an improvement of the thermal performance, which still does not meet the current requirements. Today, even if Back Bay buildings belong to conservation list, some roof modification for improvement purpose are

available. In this work two retrofit scenarios are developed with the aim to improve the performance but also respect the original slope, and avoiding excessive loading increment on the existing floor structure. Therefore, two solutions (R1 and R2) aim to substitute the gravel with an ECO XPS with closed cells and strong moisture resistance capacity (in particular, the Polyfoam ECO by knauf is considered). These solutions enable to fulfil the requirements for new roofs with a $U=0.18\text{W/m}^2\text{K}$ and with a reduction of the current dead load (Table 2). The Retrofit 2 differs from the first solution for the added light concrete layer for tile posing, with a consequent increment of dead load and EE, without any thermal improvement. The third solution, considers the adoption of CELENIT panels that are insulation panel made by wood and some cement, this allow an important improvement in the thermal performance but with a U factor slightly higher of the required for new constructions. The fourth investigated solution, instead aims to completely modify the actual condition to realize a ventilated roof, allowing a very high performance ($U = 0.16 \text{ W/m}^2\text{K}$).

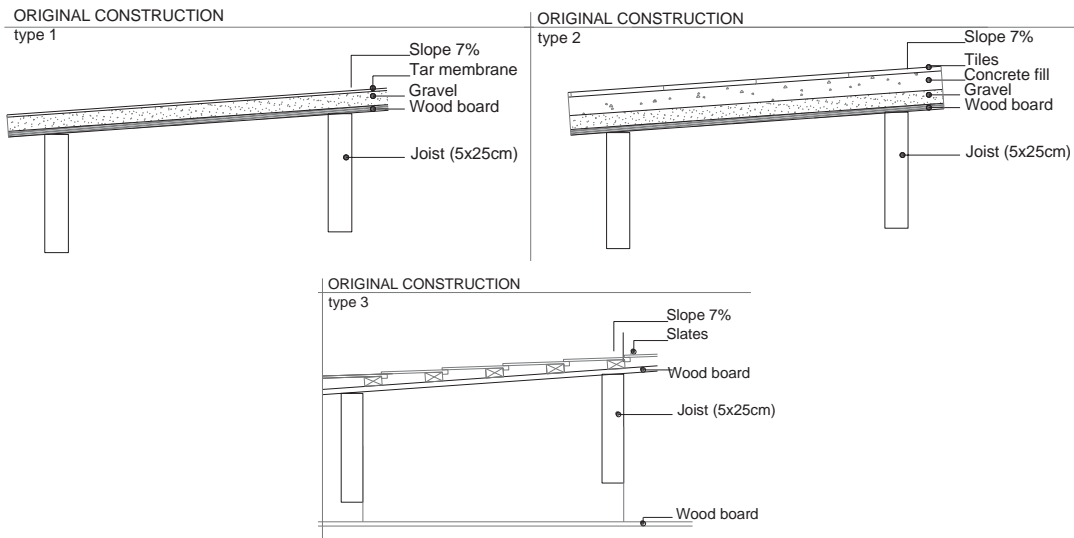


Fig 7. Floor sections of the original constructions.

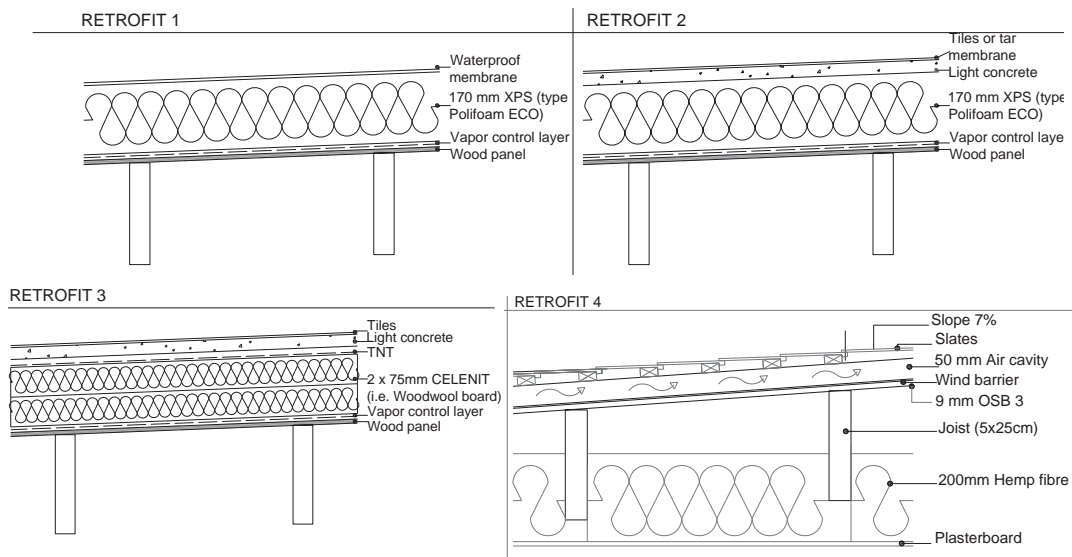


Figure 8. Retrofit scenarios.

Table 2. Evaluation of the overall resistance, weight and embodied energy per unitary roof area of the original constructions and the retrofit solutions

	Overall U value [W/m ² K]	Weight per 1m ² floor area [kg]	EE per 1m ² Floor area [MJ]
Original construction type 1	2.90	61	147
Original construction type 2	2.63	133	197
Original construction type 3	1.87	42	260
Retrofit 1	0.18	12	389
Retrofit 2	0.18	66	402
Retrofit 3	0.37	112	1174
Retrofit 4: ventilated roof with 200mm hemp fiber	0.16	102	1002

5. CONCLUSIONS

The enduring legacy of the Back Bay row houses, alongside with their solid construction, have enabled them to survive into the present day over a century they were built. But, to allow them to properly function for the future centuries providing a comfortable environment that fulfill the current standards requires retrofit and maintenance interventions. This paper, through a material flow analysis of the historical constructions and development of a range of retrofit scenarios for the main thermal components, aims to demonstrate that, changing interior finish materials and upgrading selective components of the building walls and floors, represents a relatively small change to the overall material weight picture, only 1% of the weight of the neighborhood's 1,228 townhouse building. But, when tested in terms of building operational energy, these minor upgrades can account for a significant improvement in building performance. In conclusion, it aims to propose a wider perspective to evaluate retrofit interventions and reinforce the John Sawhill essay that "*preserving history and saving energy are two sides of the same coin.*"

REFERENCES

- Forster A M, Carter K, Banfill P F G & Kayan B, Green maintenance for historic masonry buildings: an emerging concept, *Building Research & Information*, 2011.
- Filippi M, Remarks on the green retrofitting of historic buildings in Italy, *Energy and Buildings* 95 (2015) 15–22
- Seasholes N S. *Gaining ground: a history of landmaking in Boston*. Cambridge, Mass.: MIT Press, 2003.
- Bunting, Bainbridge. 1967. *Houses of Boston's Back Bay; an architectural history, 1840-1917*. Cambridge, Belknap Press of Harvard University Press, 1967.
- Forster A M, Carter K, Banfill P F G and Kayan B. Green maintenance for historic masonry buildings: an emerging concept. *Building Research & Information* (2011) 39(6), 654–664.
- Hammond G and Jones C, *Inventory of Carbon & Energy (ICE), Version 2*. Sustainable Energy Research Team (SERT), Department of Mechanical Engineering, University of Bath, Bath, United Kingdom, 2011.
- Miskin N. *The Carbon Sequestration Potential of Hemp-binder. A study of embodied carbon in hemp-binder compared with dry lining solutions for insulating solid walls*. Dissertation thesis. School of Computing and Technology, University of East London. 2010.
- The building regulations 2010, Approved Documents L, L1B Conservation of fuel and power in existing dwellings, HM Government, England.
- W Hickey Associates, 1972, *Investigation of collapse of the hotel Vendome prepared for City of Boston*, Boston Public Library.
- Back Bay Architectural Commission, 1990. *Guidelines for the residential district*.

Thermal Conductivity of an Unplanted Sustainable Green Roof System

Christina Said

Institute for Sustainable Energy

Paul Refalo

Department of Industrial and Manufacturing Engineering, University of Malta, Msida, Malta.

Luciano Mule`Stagno

Institute for Sustainable Energy

Charles Yousif

Institute for Sustainable Energy

Email: christinasaid@gmail.com

Abstract. Finding a balance between green open spaces and urban areas is important. In places where the density of buildings is high, greening of roofs can significantly improve the area. One of the main benefits of green roof systems, especially in warm climate countries, is the improved thermal performance of the building's envelope. The main purpose of this study was to evaluate the thermal performance of unplanted local growth media and a drainage layer used in green roof systems. Unplanted growth media consists of soil and other in/organic material without planted vegetation. Laboratory tests were carried out in a hotbox to study the energy performance of an unplanted green roof specimen at different moisture contents and soil surface temperatures. Results showed that the thermal conductivity of the specimen increased with both an increase in surface temperature as well as with an increase in the moisture content. It also resulted that a typical U-value of an unplanted soil layer is about $2.25 \text{ W/m}^2\text{K}$ in winter, while in summer it would be about $1.30 \text{ W/m}^2\text{K}$. This study gives an indication of the thermal performance of the soil layer of a green roof system had the up-keeping of the vegetation been ignored ending up with bare and unplanted media.

1. INTRODUCTION

Green roofs are regarded as visually attractive. However they are most often built for reasons other than aesthetics. They possess a great range of environmental advantages, which not only benefit the building where it is installed, but also the surrounding environment on a macro scale. Benefits on a micro scale, i.e. to the building itself, include: improvement of thermal insulation and thus reduction of building energy demand on space conditioning, increased lifetime of roof membranes by protecting them from solar radiation, improved aesthetics, amenity value and marketing. Moreover benefits on a macro scale, i.e. improvements to the overall quality of life in urban areas, include: reduction of the ambient temperature increase due to the Urban Heat Island (UHI) effect in cities, improved urban biodiversity, reduction of storm water runoff, improvement of air quality in cities, increase employment and commerce, social improvement, and recreational and educational development. In addition, planted roofs not only insulate but can also provide passive cooling for building interiors through evapotranspiration, which is the combined process of water loss from the growth media (evaporation) and vegetation (transpiration). In summer conditions, studies showed that evapotranspiration absorbed between 12-25% of the incoming heat flux.

R-Values calculated in field and laboratory experiments for extensive green roofs (7.5-15cm depths) varied from 0.37 to $0.85 \text{ m}^2\text{K/W}$. One study showed that the presence of moisture could increase the soil thermal conductivity since water is a better thermal conductor than air in the voids. However, when the soil is moist, evaporative cooling is enhanced resulting in a combination of the two effects. A study by Liu, which focused on the effect of soil moisture on green roofs, has shown that soil moisture in green roofs is important for evaporative cooling. To optimise building energy saving during summer, rather than keeping the thermal conductivity

low with dry soil, she found that it is more beneficial to irrigate the green roofs to increase evaporation .

The study in this paper focuses on the thermal performance of an unplanted local soil growth layer specimen (10 cm thick), a geotextile fabric sheet and a drainage layer made from polypropylene modules. To understand the performance of the unmaintained soil layer alone, the vegetation layer (plants) was excluded from this study.

2. THEORY AND METHODOLOGY

The thermal performance of green roofs could be investigated using three approaches: 1) field or laboratory experiments, 2) theoretical and numerical studies, and 3) a combination of laboratory or field experiments with numerical models [19]. Laboratory testing in a hot box was used in this study. The method chosen for the construction of the calibrated hot box and the testing of the specimen was based on ISO 8990:2000 - Thermal Insulation – Determination of steady state thermal insulation properties: Calibrated and guarded hot box. Fig 1 shows a schematic diagram of the hot box setup.

The growth-media specimen is placed between a hot and a cold chamber in which environmental temperatures are controlled. The method described in the standard is used to measure the total amount of heat transferred from one side of the specimen to the other, for a given temperature difference, irrespective of the individual modes of heat transfer. Based on the standard, the footprint of the soil layer specimen was taken as the minimum being 1.5m by 1.5m since the heat flow errors at its perimeter would increase with decreasing metered area. A sheet metal tray was constructed with these dimensions and with a depth of 0.25m.

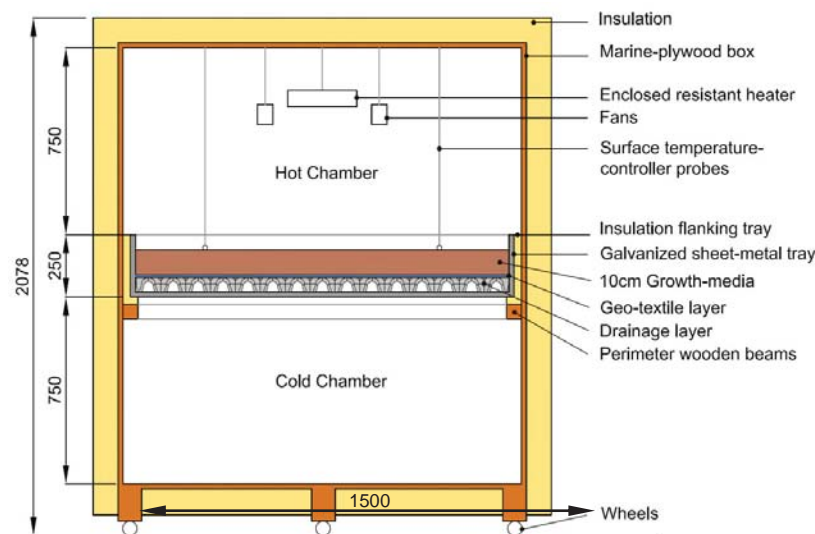


Fig 1: Section through hot box



Fig 2: Sealed hot box and thermal image

The specimen consisted of the following three layers:

Layer 1 - Drainage Modules: a modular array of lightweight polypropylene trays to drain out water quickly and store a substantial amount of water to support healthy plants.

Layer 2 – Geotextile fabric sheet: this layer segregates the vegetation and growth media from the drainage layer. It prevents the drainage from clogging and retains important organic materials.

Layer 3 – Growth Media: the substrate that sustains vegetation growth (a layer 10cm thick was used in this study). It is a mixture of inorganic material and soil with organic and mineral additives. The way in which heat is transferred through it is affected by soil depth, thermal

conductivity and temperature difference. Soil thermal conductivity is in turn affected by moisture content, density, mineral composition, size of particles and temperature. After discussions with a number of local garden and landscape consultants, it was suggested that for the local climate, the following composition should be used: 50% Local Soil (the largest percentage of the growth media was chosen as typical Maltese soil which is used for local agricultural purposes), 30% Expanded Clay (in order to create a lightweight mixture, a large percentage of expanded clay was added. Expanded clay is also important for good water drainage), 10% Peat (this improves the soil's structure and retains moisture in soil when it is dry), 10% Compost (to provide nutrients for the vegetation. Nagase suggests a 10% portion).

2.1. Hot box construction

For ease of manoeuvring, the hot box was designed to open up into two sections. The joints between the two boxes were carefully designed to fit into each other (tongue and groove) to create a good seal. Once the tray is inserted and the hotbox closed, the interior space is divided into two tight enclosures as required by the standard. The exterior walls of the box were insulated with 50mm expanded polystyrene sheets having a thermal conductivity of 0.035 W/mK. The box was tightened with ratchet straps to reduce heat losses from the joints. An infrared camera was used to check for thermal losses as shown in Fig 2.

2.2. Data Acquisition

Omega type T thermocouples ($\pm 0.5^\circ\text{C}$) were used to measure the temperatures at different locations. In order to calculate the temperature differences across the hot and cold sides of each layer, nine thermocouple sets were located over the metered area, as shown in Fig 3. Hukseflux heat flux (HF) sensors ($\pm 5\%$ accurate) were used to measure the heat transfer rate through the specimen.

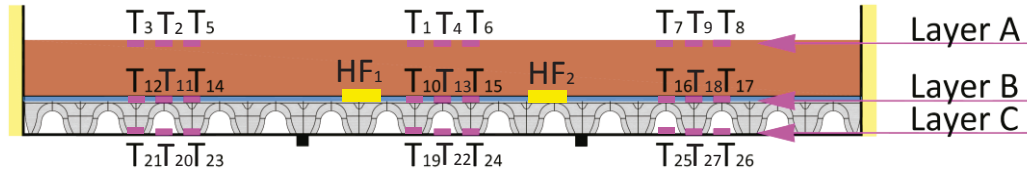


Fig 3: Section of the soil layer specimen showing the location of the thermocouples

2.3. Experimental procedure

The substrate was initially dried out in an oven to reduce its moisture content (MC). This was done to replicate the typical condition of local soil in summer. The tests with dry substrate were carried out first, followed by those with 40% and finally those with 80% moisture content (at 100% moisture content, the soil is saturated with water and any additional water would seep through). Each experiment was repeated for a more reliable result. The surface temperature was varied between 20°C and 50°C to replicate typical local climate conditions from winter to summer. These were varied together with the moisture content.

A typical experiment started by inserting the tray into the hotbox. Water was then sprinkled evenly over the entire tray area according to the moisture level to be tested. The hot box was then closed and tightened with the ratchet straps. The temperature controller was set at a specified temperature to heat the substrate's surface. This temperature represented the upper surface temperature (Layer A). Resistance heaters and fans were used to heat the upper chamber of the hot box. The hot box was situated in a room air-conditioned at a constant temperature of 16°C . This ensured that the cold chamber reached steady state at a constant low temperature. The insulation of the cold chamber results in a longer time for the cold chamber, and subsequently also the hot chamber, to reach steady state conditions. However, if the cold chamber was not insulated, its temperature profile would follow that of the room more closely,

which in turn depends on the thermostat of the air-conditioner. With an insulated chamber, the temperature of the cold chamber reaches a smooth, constant profile.

Data was collected using a dedicated LabVIEW programme, which measured all temperature and heat flux readings simultaneously. The recorded data was the average of readings taken every two minutes. The measurement period was continued until the hot box reached steady state. This was determined when the thermocouple and heat flux sensor readings remained constant for at least two hours. Full steady state readings took approximately 20 hours to reach. From the last two-hour set of steady-state measurements the heat transfer properties of the specimen were then calculated. Samples of soil were taken after every test and their mass was measured to ensure that the moisture content of the soil did not change.

3. CALCULATIONS

For each test, the temperature difference (dT) between different layers was calculated for the:

- Substrate (between Layer A and Layer B),
- Drainage Layer (between Layer B and Layer C),
- Total Specimen (between Layer A and Layer C).

The thermal conductivity, k , was then found by using the equation:

$$k = \frac{Q dx}{A dT}$$

where, Q/A is the heat flux measured by the heat flux sensor in W/m^2 ,

dx is the thickness of the soil layer in m ,

dT is the temperature difference across the specimen thickness, in K .

Once the k -value was known, the thermal resistance, R -Value (m^2K/W) and the thermal transmittance, U -Value (W/m^2K) were found from the following equations:

$$R = \frac{dx}{k} \text{ and } U = \frac{1}{R}$$

This resulting U -value does not include interior and exterior surface heat transfer characteristics as these vary heavily with building and weather conditions which were not factored in this study.

4. RESULTS

For a relatively dry substrate (0% moisture content MC), the k -value increased with an increase in temperature at the top surface from $20^\circ C$ to $30^\circ C$ as shown in Fig 4. However from $30^\circ C$ to $50^\circ C$, the k -value remained more or less constant at around $0.15 W/mK$. On the other hand the drainage layer's k -value had a larger increase when the surface temperature was increased. Therefore, for an increase in temperature, the total specimen's k -value increased. Fig 4 also shows a comparison of the substrate's k -value with different moisture contents. The k -value of the growth media increased with an increase in moisture and surface temperature. When the moisture content was increased to 40% and then 80%, the k -values also increased. At 80% moisture content the substrate's k -value was even higher than that of the drainage layer. The thermal conductivity of the dry substrate at $50^\circ C$ resulted in $0.14 W/mK$. With an increase of 40% moisture content, the k -value increased by 120% to $0.31 W/mK$, and at 80% moisture it increased to $0.60 W/mK$, a more than fourfold increase when compared to the dry state value. Figure 5 shows that the highest k -value of the drainage layer was also achieved at high moisture content and temperature. Even though the drainage layer did not have water inside it, the substrate's moisture content still had an effect on its k -value.

Fig 6 shows the resulting k -value of the total specimen. The overall effect is that with increasing moisture and temperature, the k -value increases. Fig 7 shows that the best U -value of $0.70 W/m^2K$, was achieved at a low temperature and when the substrate was dry. The worst U -

value was at a high temperature and high moisture content, which amounted to 3.70 W/m²K. Both situations are not very realistic when considering the Maltese or Mediterranean climate, since high temperatures usually occur for long periods in summer, thus the substrate would be relatively dry, whereas low temperatures usually occur in winter, when the substrate is often wet due to frequent precipitation.

The drainage layer improved the overall U-value of the soil layer specimen as shown in Table 1. At higher substrate moisture contents of 40% and 80%, the percentage increase of the overall U-Value was even larger.

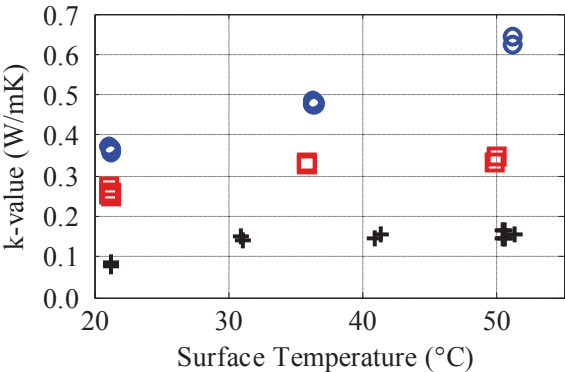


Fig 4: Thermal Conductivity of Substrate

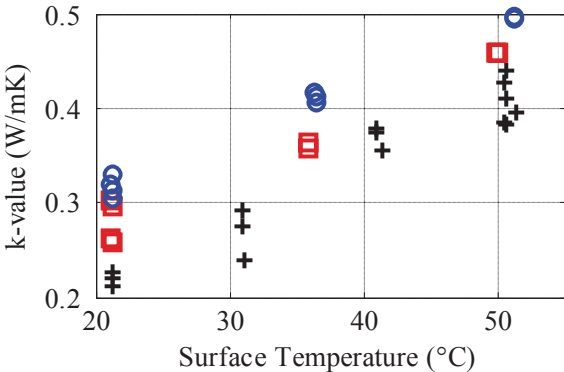


Fig 5: Thermal Conductivity of Drainage layer

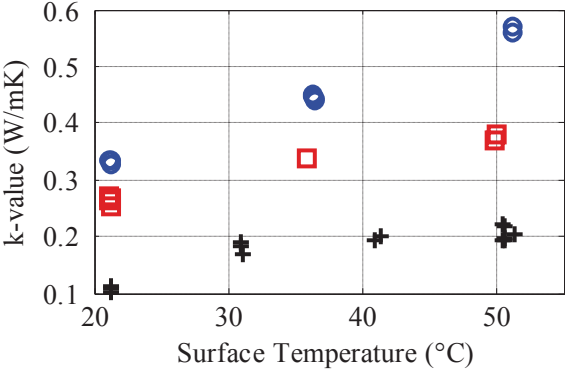


Fig 6: Thermal Conductivity of Total Specimen

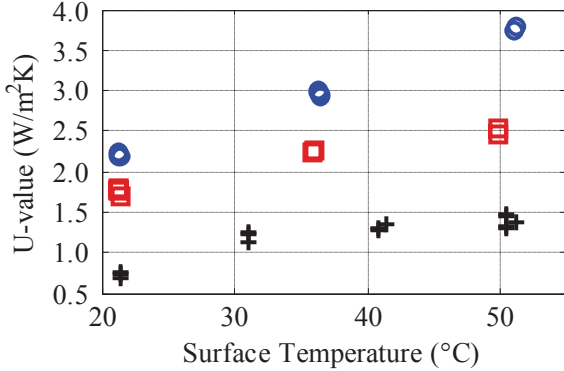


Fig 7: U-Value of Total Specimen

Table 1: Average U-Values at different moisture contents

Moisture Content	0%	40%	80%
Average U-Value of Substrate (W/m ² K)	1.59	3.45	5.29
Average U-Value of Substrate + Drainage (W/m ² K)	1.21	2.11	2.90
% change in U-Value due to Drainage Layer	-24%	-39%	-45%

Therefore from these results a typical winter U-value (low temperatures, moist substrate) would be about 2.25 W/m²K, while in summer (high temperature, dry substrate) it would result in a U-value of about 1.30 W/m²K. However it is important to note that in this study the substrate was not fully saturated, thus the drainage layer was dry. During heavy rainfalls, the modules of drainage layer would fill up with water, so the U-value during this situation would be different.

5. DISCUSSION

Both an increase in surface temperature and moisture content increases the thermal conductivity of the soil layer on top of green roofs. These findings agree with the research of Nakshabandi *et al.* that heat travels much better through water than through air. When the soil was relatively dry, heat transferred across the soil particles through points of contact, avoiding the air gaps. However when the moisture content was increased, the water droplets filling the voids helped bridge the gaps between the particles and thus the thermal conductivity increased. This finding also bears out the views of Alcazar and Bass, Sailor *et al* whose k-values of the substrate layer were very similar to the ones found in this work since vegetation layer was not considered. On the contrary to these findings are the results of Tabares-Velasco. Their data revealed that samples with high moisture content had lower conductive heat fluxes. However Tabares-Velasco included the vegetation layer. In fact, he concluded that evapotranspiration from the plants was the main controller of the heat flux intensity.

Furthermore, the findings of this study, which show that an increase in temperature increases the k-value of the specimen, are opposite to the findings of Cox (2010) and Bell *et al* (2009). Their studies conclude that when the ambient air temperature was increased, there was a reduction in the k-value. However, like Tabares-Velasco, they also concluded that this was likely due to evapotranspiration from the plants. This dispute on how the k-value fluctuates with regards to moisture content, as well as with regards to temperature, is mainly due to the variables involved when introducing the vegetation layer. The vegetation layer has a very important role since it significantly contributes to reducing the heat flux through the roof, by providing shade and evapotranspiration. This is very beneficial in summer for passive cooling. In fact Liu, concluded that to optimise building energy savings in summer, rather than keeping the thermal conductivity low with dry soil, she found that it is more beneficial to irrigate the green roofs to increase evaporative heat transfer.

A wet green roof has a good cooling performance. However dependence on rainfall does not ensure effective energy performance during dry summer seasons that are characteristic of the Mediterranean region. Therefore water management is important. For example, it would be ideal if a plant irrigation system is introduced to use grey water produced by the building itself. Besides contributing to evaporative cooling, moisture also increases the thermal mass of the green roof. The weight of the green roof system, including the growth media, moisture and the plants, all add to the thermal mass. Having such a thermal mass on the roof is beneficial because it acts as a heat sink. During summer conditions, it would absorb and store the external heat and then release it at night. Moreover, a wet heat sink above the roof would absorb the heat from the layer of warm air just beneath the room ceiling. However from an energy use point of view, having a moist green roof system in winter may not be as beneficial as during summer. Evapotranspiration and shading from the vegetation layer would not contribute to heat up the building below. However adding a green roof increases the thermal mass and thus may still be beneficial for the thermal performance. Also the vegetation layer creates air pockets and thus reduces the air circulation on the substrate's surface. Consequently the convective heat transfer caused by wind is minimised. In fact studies of green roof systems by Kotsiris *et al.*, Sailor and Spala *et al.*, all conclude that in winter, green roofs still improve the thermal performance of the building and save energy, albeit to a lower extent than in summer.

Another key result from this work was that the drainage layer significantly improved the U-value. When the substrate was dry it contributed to about 23% of the U-value, whereas when the thermal conductivity of the substrate was high with moisture, it contributed to about 45% of the total U-value. The channels within the polypropylene drainage modules created air gaps below the substrate layer, which contribute to the insulation effect of the green roof system. Vegetation, growth media, moisture, insulation, and the support structure are the key elements affecting the thermal performance of a green roof. The combination of these layers creates a dynamic green roof system that acts as a thermal mass on the roof. There is no unique answer as to which is the best combination and thicknesses of these layers, as these highly depend on the building's use, location, exposure and climatic factors. Therefore it is impossible to treat green

roof systems simply as an insulating material. This does not capture the transient thermal storage and evaporative cooling that take place on a green roof. Moreover the benefits associated with green roofs, such as shading, reduction in wind-related losses, storm water reduction and biodiversity restoration are equally important.

6. CONCLUSIONS

This study focused on how the thermal performance of an unplanted soil layer is affected by a change in surface temperature and moisture content. One can conclude that the thermal conductivity of a bare soil layer increases with both an increase in temperature and moisture content. Results showed that a typical Mediterranean winter U-value (low temperatures, moist substrate) for the studied 10 cm thick soil layer specimen would be about 2.25 W/m²K (assuming that the soil's surface temperature would be around 20°C), while in summer (high temperature, dry substrate), it would result in a U-value of around 1.3 W/m²K (at a soil surface temperature of 50°C). It also resulted that the drainage layer improves the overall U-value of the soil layer.

It is important to note that the steady-state U-values achieved from these experiments are useful as a benchmark, however they do not capture the dynamic aspects of the energy balance of a green roof. The thermal performance of a green roof is highly dependent on location, exposure, building use, the type of vegetation used, and many other variables. Therefore a green roof cannot be simply compared to an insulation material, nor can it be described by a single U-value. The improvement to the thermal performance of buildings is just one of many benefits that should be considered when evaluating the merits of green roof systems.

7. ACKNOWLEDGEMENTS

The authors would like to acknowledge the support of the laboratory officers of the Institute for Sustainable Energy (Manuel Aquilina) and of the Faculty for the Built Environment (Nicholas Azzopardi) of the University of Malta.

REFERENCES

- Energy efficiency for the 2020 goal. Accessed: 24/05/2013. Available: http://europa.eu/legislation_summaries/energy/energy_efficiency/en0002_en.htm.
- E. P. D. Barrio, "Analysis of the green roofs cooling potential in buildings," *Energy and Buildings*, Vol. 27, pp. 179-193, 4// 1998.
- N. H. Wong, D. K. W. Cheong, H. Yan, J. Soh, C. L. Ong, and A. Sia, "The effects of rooftop garden on energy consumption of a commercial building in Singapore," *Energy and Buildings*, Vol. 35, pp. 353-364, 5// 2003.
- M. Santamouris, C. Pavlou, P. Doukas, G. Mihalakakou, A. Synnefa, A. Hatzibiros, et al., "Investigating and analysing the energy and environmental performance of an experimental green roof system installed in a nursery school building in Athens, Greece," *Energy*, Vol. 32, pp. 1781-1788, 9// 2007.
- B. Bass and B. Baskaran, "Evaluating rooftop and vertical gardens as an adaptation strategy for urban areas," *Institute for Research and Construction*, p. 110, 2003.
- B. Yuen and W. Nyuk Hien, "Resident perceptions and expectations of rooftop gardens in Singapore," *Landscape and Urban Planning*, Vol. 73, pp. 263-276, 12/15/ 2005.
- N. H. Wong, Y. Chen, C. L. Ong, and A. Sia, "Investigation of thermal benefits of rooftop garden in the tropical environment," *Building and Environment*, Vol. 38, pp. 261-270, 2// 2003.
- H. Takebayashi and M. Moriyama, "Surface heat budget on green roof and high reflection roof for mitigation of urban heat island," *Building and Environment*, Vol. 42, pp. 2971-2979, 8// 2007.
- S. Brenneisen, "The benefits of biodiversity from greenroofs - key design consequences.," *Proceedings of the First North American Green Roof Conference*, pp. 323-329, 2003.
- E. L. Villarreal and L. Bengtsson, "Response of a Sedum green-roof to individual rain events," *Ecological Engineering*, Vol. 25, pp. 1-7, 7/20/ 2005.

- J. Mentens, D. Raes, and M. Hermy, "Green roofs as a tool for solving the rainwater runoff problem in the urbanized 21st century?," *Landscape and Urban Planning*, Vol. 77, pp. 217-226, 8/30/ 2006.
- A. Teemusk and Ü. Mander, "Rainwater runoff quantity and quality performance from a greenroof: The effects of short-term events," *Ecological Engineering*, Vol. 30, pp. 271-277, 7/2/ 2007.
- K. L. Getter, D. B. Rowe, and J. A. Andresen, "Quantifying the effect of slope on extensive green roof stormwater retention," *Ecological Engineering*, Vol. 31, pp. 225-231, 12/3/ 2007.
- C. Clark, P. Adriaens, and F. B. Talbot, "Green Roof Valuation: A probabilistic economic analysis of environmental benefits.," *Environmental Science and Technology*, Vol. 42, pp. 163-1628, 2008.
- A. Youngman, *Green Roofs: A Guide to their design and installation*. Wiltshire: The Crowood Press, 2011.
- L. Kelly, *Green Roof Construction and Maintenance: McGraw Hill Companies*, 2009.
- R. M. Lazzarin, F. Castellotti, and F. Busato, "Experimental measurements and numerical modelling of a green roof," *Energy and Buildings*, Vol. 37, pp. 1260-1267, 12// 2005.
- Z. Liu, "Prediction of soil layer R-Value dependance on moisture content," *Masters of Science in Mechanical Engineering*, Portland State University, 2011.
- P. C. Tabares-Velasco and J. Srebric, "A heat transfer model for assessment of plant based roofing systems in summer conditions," *Building and Environment*, Vol. 49, pp. 310-323, 3// 2012.
- A. Nagase and N. Dunnett, "The relationship between percentage of organic matter in substrate and plant growth in extensive green roofs," *Landscape and Urban Planning*, Vol. 103, pp. 230-236, 11/30/ 2011.
- F. P. Incropera, A. S. Lavine, and D. P. DeWitt, *Fundamentals of heat and mass transfer: John Wiley & Sons*, 2011.
- G. Nakshabandi and H. Kohnke, "Thermal Conductivity and Diffusivity of Soils as Related to Moisture Tension and Other Physical Properties.," *Agricultural Meteorology*, Vol. 2, pp. 271-279, 1964.
- S. Alcazar and B. Bass, "Energy performance of green roofs in a multi-storey residential building in Madrid. ," presented at the *Greening Rooftops for Sustainable City Conference*, 2005.
- D. J. Sailor and M. Hagos, "An updated and expanded set of thermal property data for green roof growing media," *Energy and Buildings*, Vol. 43, pp. 2298-2303, 9// 2011.
- D. J. Sailor, D. Hutchinson, and L. Bokovoy, "Thermal property measurements for ecoroof soils common in the western U.S.," *Energy and Buildings*, Vol. 40, pp. 1246-1251, // 2008.
- P. C. Tabares-Velasco, "Heat fluxes and water managment of a green and brown roof: Laboratory experiments," *Greening rooftops for Sustainable Communities*, 2009.
- P. C. Tabares-Velasco and J. Srebric, "Experimental quantification of heat and mass transfer process through vegetated roof samples in a new laboratory setup," *International Journal of Heat and Mass Transfer*, Vol. 54, pp. 5149-5162, 12// 2011.
- B. K. Cox, "The Influence of Ambient Temperature on Green Roof R-Values," *Masters of Science in Mechanical Engineering*, Portland State University, 2010.
- H. Bell and G. A. Spolek, "Measured Energy Performance of Green Roofs," presented at the *Greening Rooftops for Sustainable Cities Conference*, 2009.
- G. Kotsiris, A. Androutsopoulos, E. Polychroni, and P. A. Nektarios, "Dynamic U-value estimation and energy simulation for green roofs," *Energy and Buildings*, Vol. 45, pp. 240-249, 2// 2012.
- D. J. Sailor, "A green roof model for building energy simulation programs," *Energy and Buildings*, Vol. 40, pp. 1466-1478, // 2008.
- A. Spala, H. S. Bagiorgas, M. N. Assimakopoulos, J. Kalavrouziotis, D. Matthopoulos, and G. Mihalakakou, "On the green roof system. Selection, state of the art and energy potential investigation of a system installed in an office building in Athens, Greece," *Renewable Energy*, Vol. 33, pp. 173-177, 1// 2008.

The Effect of Different Glazing Apertures on the Thermal Performance of Maltese Buildings

T F Caruana

Institute for Sustainable Energy, University of Malta, Msida MSD 2080, Malta

C Yousif

Institute for Sustainable Energy, University of Malta, Msida MSD 2080, Malta

Email: caruana.trevor@gmail.com

Abstract. The aim of this work was to determine the effect of using different types of glazing on different orientations with different glazing to wall ratios as well as shading on the energy performance rating of buildings in Malta, using modelling with DesignBuilder EnergyPlus software for typical Maltese building models. All options have also been evaluated for their economic feasibility. A total of 864 simulations have been carried out. Results showed that the cooling load is by far larger than the heating and lighting loads. While single glazing has resulted in the worst total energy consumption, the addition of shading improves its performance drastically for most cases. The use of low U-value glazing types did not produce significant improvements, because the primary heat transfer was due to solar gains rather than internal heat losses by conduction or convection. A typical penthouse model showed that elongated building typologies have in general high total energy consumption and that glazing is not a primary factor in reducing this. It was concluded that for walls with up to 60% of glazed area, the use of single glazing with shading gives better thermal benefits than double-glazing, while the limit for an intermediate floor corner office is that of 40%.

1. INTRODUCTION

The scope of this study was to determine whether the approach of having large glazing areas as is normally used in contemporary architectural approaches, is adaptable to a sunny country like Malta, where direct solar radiation plays an important role in determining the internal temperature conditions and hence comfort levels of buildings. The effect of using single and double glazing in the Maltese context was also studied, both in terms of thermal insulation and light ingress as the ratio of glazing to wall area was increased. The effectiveness of external shading was also considered on both single and double glazing types.

This study was carried out using Energy Plus engine with Design Builder interface by carrying simulations of three different building models in order to simulate different glazing types in different orientations, dimensions, with and without external horizontal shading, throughout the year. The three building models were a hypothetical heavily insulated ten by ten metre square room with a window on one wall only, a typical one hundred (100) square metres intermediate floor corner office with windows on two sides and on an existing typical penthouse with traditional standard construction methods composed of masonry block walls and reinforced concrete slabs.

The scope was to find the limits that dictate the necessity for change from one type of glazing to another, based on the abovementioned variables, and to what extent shading plays a role in determining the optimum energy performance of buildings, as well as finding which variables have a substantial effect, and which don't.

The study was accompanied by an economic analysis based on the year 2015 in order to establish which glazing type is best suited for the different conditions tested, by taking in consideration the resulting heating/cooling/lighting loads calculated for each case.

2. LITERATURE REVIEW

2.1. Local climate

The Maltese climate can be described as Mediterranean and characterised by dry, hot summers with the hottest month being July, and mildly cold, with some rainy days in winter.

Extreme temperatures recorded have been 1.4°C and 43.8°C, with an increasing trend in temperature over the past fifty years of around 1.2°C. The average annual temperature for the Maltese Islands is that of 18.6°C. Highest cloud cover in Malta is mostly experienced in the winter months, with the lowest being experienced in the summer months. The Maltese climate is characterised by high levels of sunshine hours, especially during the summer period.

2.2. Glazing performance and properties

Kontoleon et al studied the behaviour of double glazing oriented towards the south in a typical construction of a Greek room with 8 by 8m dimensions. Out of the three types of double glazing considered, namely normal double glazing, low-e coated double glazing and low-e coated double glazing having a reflective film, they came to the conclusion that in winter, with internal insulation, overheating would occur with a glazed opening percentage (GOP) greater than 70%. With external insulation, no overheating was experienced. To avoid overheating in summer, a GOP of less than 60% is to be used in conjunction with external insulation, while a low-e coated double glazing with a reflective film performed better than the other glazing types considered, as a GOP less than 80% could be used.

Kontoleon et al concluded (for a Greek climate) that with external insulation and low-e double glazing, a 70% GOP is the optimal size in terms of minimisation of energy consumption for winter, while for summer 40% GOP for the same conditions is the optimum (with low-e glazing with reflective coating this increases to 60% GOP).

Macka et al have carried out studies by using various types of double glazing with coatings/tints applied, used in two types of flats in high rise buildings in a cold climate in Ankara, Turkey. Comparison with normal double glazed clear glass showed that the best annual energy performance was obtained with a double glazed unit having a low-E coating on the internal side followed by the double glazed units with a reflective, low-E coating with a tint applied on the inner pane.

3. METHODOLOGY

3.1. Modelling and simulations

The three building models (figures 1, 2 and 3) were set in DesignBuilder and all appropriate inputs were assigned, together with the weather file for Malta. Different simulations were carried out by varying the orientation and the window-to-wall ratio (WWR), for different types of glazing and shading.

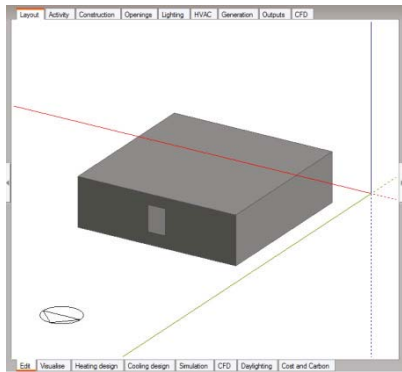


Fig 1: Heavily insulated square room

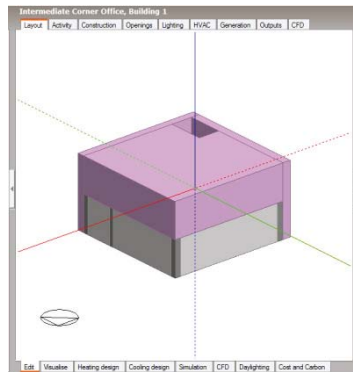


Fig 2: Typical corner office

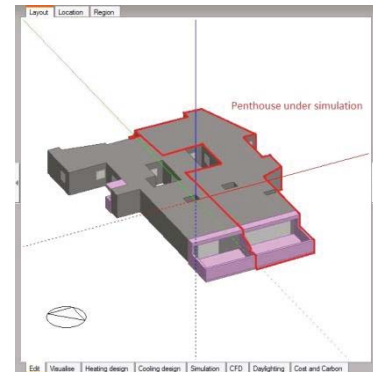


Fig 3: Typical penthouse

A comparison was then made for the total cooling, total heating, total lighting and transmitted solar energy changes. In this case, the total energy demand is the actual energy that needs to be removed or added in order to keep the indoor temperature at the set values of 18.5°C for winter and 26.5°C for summer, being close to the standard values used in the national Energy Performance Rating for Dwellings Malta (EPRDM). This procedure was carried out for the following glazing types as well as glazing and shading combination:

- a) Single Glazing consisting of a 4mm thick clear float glass with an aluminium frame.
- b) Double Glazing consisting of two 4mm thick clear float glass having an air cavity of 6mm (4-6-4), with an aluminium frame with thermal break.
- c) Double Glazing 4-13-4 air gap, with an aluminium frame and thermal break.
- d) Double Glazing 4-6-4 argon-filled gap and low-e coating with a uPVC frame.
- e) Double Glazing 4-13-4 argon-filled gap and low-e coating with a uPVC frame .

Glazing types c and e have been carried out only for the hypothetical heavily insulated ten by ten metre square room. Simulations of the heavily insulated room with no occupancy or appliances were carried out to gauge the effect of WWR when no other effects are taken into consideration. Further simulations with external automatic shading with horizontal medium reflectivity blinds having a "Cooling" control option have been carried out in conjunction with glazing options a and b. The "Cooling" shading control option offered by the Design Builder simulation software considers one factor that when the rate of cooling in a previous time step is not zero, shading is activated.

4. RESULTS

General results obtained from all three models were:

- i) Cooling constituted the largest load when compared to heating and lighting demand.
- ii) Given the mild climate of Malta, increasing the U-value of glazing is less important than shading.
- iii) Windows facing the south-east and moving clock-wise to south-west orientations contribute towards highest cooling as well as total energy demand, while minimum load results for the north facing window orientation, thus allowing greater window areas in this orientation.
- iv) Automated external shading was the most effective measure for reducing total energy consumption, when compared to the other unshaded glazing types.

4.1. Hypothetical 10x10m heavily insulated square room (HISR)

At WWRs greater than 20%, the total energy consumption increases at a steeper rate.

Tables 1 and 2 show the equivalent WWR for shaded clear single glazing and shaded clear double glazing respectively, when compared to 20% WWR unshaded glazing types, for the same total energy

consumption. These tables show that shading is the most effective measure, followed by double glazing with low-e coating (high performance double glazing).

Table 1: Equivalent WWR for clear single glazing with automated external blinds when compared to 20% WWR unshaded glazing types, for the same total energy consumption

Orientation (°)	Percentage WWR for shaded single glazing equivalent to 20% WWR unshaded single glazing	Percentage WWR for shaded single glazing equivalent to 20% WWR unshaded clear double glazing	Percentage WWR for shaded single glazing equivalent to 20% WWR unshaded high performance double glazing
0	43	35	30
45	61	53	46
90	75	67	58
135	87	75	64
180	80	69	60
225	93	81	69
270	83	73	63
315	65	56	48

Table 2: Equivalent WWR for clear double glazing (6mm air gap) with automated external blinds when compared to 20% WWR unshaded glazing types, for the same total energy consumption

Orientation (°)	Percentage WWR for shaded double glazing equivalent to 20% WWR unshaded single glazing	Percentage WWR for shaded double glazing equivalent to 20% WWR unshaded clear double glazing	Percentage WWR for shaded double glazing equivalent to 20% WWR unshaded high performance double glazing
0	58	49	42
45	80	69	59
90	96	84	72
135	>100	96	80
180	>100	88	76
225	>100	>100	89
270	>100	95	81
315	86	74	64

Table 3: Equivalent WWR for various orientations when compared to a 20% WWR for glazing facing North for the same total energy consumption

Orientation (°)	Single glazing equivalent WWR	Single glazing with external blinds equivalent WWR	Double Glazing 6mm air gap equivalent WWR	Double Glazing 6mm air gap with external blinds equivalent WWR	High performance double glazing 6mm argon gap equivalent WWR
0	20	20	20	20	20
45	10	15	9	13	9
90	6	13	5	11	5
135	5	11	4	9	4
180	6	13	5	11	5
225	5	12	4	10	4
270	6	15	5	13	5
315	10	15	9	14	9

4.1.1. External blinds control options.

Apart from the “Cooling” control option offered by the DesignBuilder software for the external automated blinds, another option was tested to see the effect of having a different control option. The other option simulated was the “Day Cooling + Solar” option, which is set to turn off shading at night, while during the day, shading is on whenever incident solar radiation on the window is greater than the

solar set point of 300W/m², and if the rate of cooling is non-zero in the previous time step. This regime is different from the "Cooling" shading control option because it only considers one factor that when the rate of cooling in a previous time step is not zero, shading is turned on. This has been carried out in combination with a single glazing window.

From results obtained for the total energy consumption for the two shading options considered it is noted that the Day Cooling and Solar shading control option is less energy efficient in all orientations and at all WWR's due to the higher cooling load. Refer to figures 5 and 6 for graphs obtained for the North and South orientations.

Hence it is concluded that the designer has to carefully consider the different design options for shading control given that the effect on space heating and cooling could be substantially different.

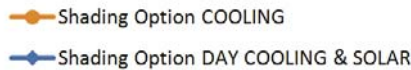


Fig 4: Legend for figures 5 and 6

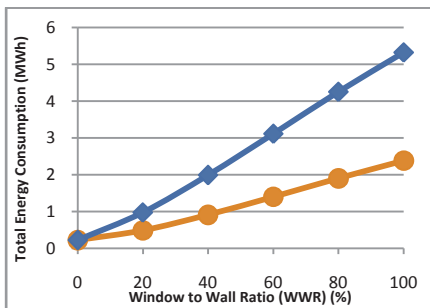


Fig 5: Shading Option Results for the North orientation

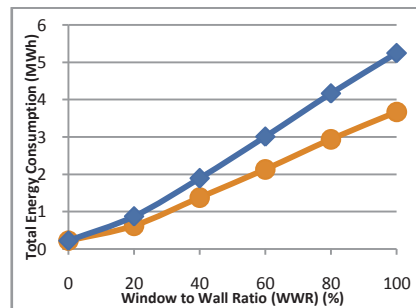


Fig 6: Shading Option Results for the South orientation

4.2. Typical 100 square metre intermediate floor corner office (IFCO)

For this model (refer to figure 2), the unshaded glazing types gave no practical improvement over single glazing. The only difference in total energy consumption was observed when external shading was applied, especially at larger WWRs and in orientations where there is higher exposure to sunshine. Notwithstanding, at 20% WWR or lower, shading did not make sense when compared to unshaded single glazing. Hence for any orientation at 20% WWR, no external shading is to be used given its detrimental effect on the total energy consumption for heating, cooling and lighting. For larger WWRs, shading is strongly advised.

Table 4 shows the equivalent WWR for various building orientations when compared to a 40% WWR for the 0° building orientation for the same total energy consumption, when using various glazing types.

Table 4: Equivalent WWR for various building orientations when compared to a 40% WWR for the 0° building orientation for the same total energy consumption

Orientation (°)	Single glazing equivalent WWR	Single glazing with external blinds equivalent WWR	Double Glazing 6mm air gap equivalent WWR	Double Glazing 6mm air gap with external blinds equivalent WWR	High performance double glazing 6mm argon gap equivalent WWR
0	40	40	40	40	40
45	30	22	29	22	29
90	27	35	27	33	27
135	24	25	24	25	24
180	30	56	29	54	29
225	35	40	34	38	34
270	47	64	46	62	45
315	40	24	40	24	40

Figures 8 to 10 show graphs plotting total energy consumption (TEC) with orientation for 20%, 60% and 100% WWR respectively. These show that when external shading was used, total energy consumption remained approximately constant for all orientations at any WWR, while for the unshaded glazing types an increase peaking at the 135° building orientation (windows facing South-East and South-West) as the WWR increased was noticed.

4.3. Typical penthouse (TP)

The TP model (refer to figure 3) had glazing areas on the front and back facades, with glazing area at the back facade being larger than that at the front facade for the same WWR. When building orientation is referred to, it means the direction in which the front facade glazing is facing.

Results showed that the greatest reduction in total energy consumption was obtained by introducing external shading, however, building orientations 0° (North), 180° (South) and 225° gave no significant reduction in total energy consumption. As for the rest of the orientations, external shading was seen to only make a difference beyond 60% WWR.

Low-e double glazing gave significant reductions in total energy consumption when compared to single glazing, and to a lesser extent for clear double glazing, with the greatest reduction being for building orientations 90°, 270° and 315°.

In general, high total energy consumption has been observed for all building orientations and WWRs when compared to results obtained for the Intermediate Floor Corner Office, irrespective of the glazing or shading being used. The application of any type of glazing or glazing/shading combination never gave a substantial reduction in the total energy consumption. This indicates that the glazing for such a building typology, is not the most important factor for reducing the total energy consumption, except for some WWRs greater than 60% for building orientations 45°, 90°, 270° and 315°. It was also noted that the rate of increase in total energy consumption was not steep, as WWR was increased from 0% to 100%, indicating that large WWRs can be accommodated without an extreme increase in total energy consumption, with the recommendation of using higher performing glazing types for the 45°, 90°, 270° and 315° building orientations.

Figures 12 to 14 show the total energy consumption (TEC) with orientation for WWRs of 20%, 60% and 100%. For legend refer to figure 11.

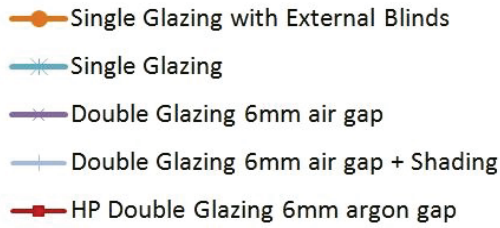


Fig 7: Legend for figures 12 to 14

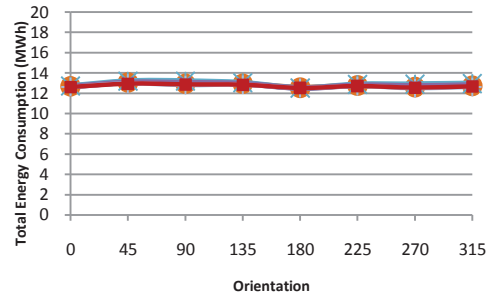


Fig 8: TEC - TP - 20% WWR

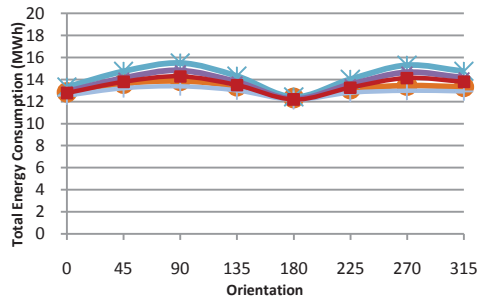


Fig 9: TEC - TP - 60% WWR

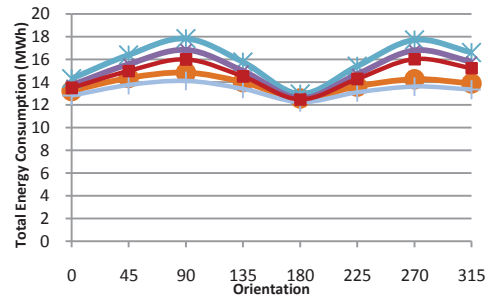


Fig 10: TEC - TP - 100% WWR

5. ECONOMIC ANALYSIS

Economic analysis results showed that when one takes into consideration the economic aspect from the property owner perspective, i.e. the energy savings at home, known as the delivered energy, it is evident that installing automated external shading devices and/or glazing other than single glazing are not financially feasible. The only exception was for the HISR, for shaded single glazing facing south-east and south-west (building orientations 135° and 225°) and having WWRs of 60% or greater and 40% or greater, respectively.

6. CONCLUSION

The study has shown that for a Maltese climate, the most detrimental factor is solar gains. The application of external shading at any orientation for WWRs of 60% or greater, nearly always resulted in substantial reduction in total energy consumption, especially for cooling. Although lower U-value glazing could reduce heating loads in winter, the overall effect is small to the extent that it does not justify investing in more expensive glazing apertures beyond single glazing.

Unshaded single glazing nearly always proved to have the worst energy performance of all the types considered, but the difference is relatively small, if one were to choose other glazing elements.

From the hypothetical HISR model, it was clear that improving the U-value of glazing elements makes more sense when the walls themselves have a low U-value. Given that dwellings usually do not have WWRs greater than 40%, and that a large number of dwellings have an elongated building typology, it is not useful to apply shading to windows or to replace single glazing with another type of glazing. In other words, one has to look at other building elements such as single leaf external walls and insulate them first.

Elongated building typologies like the TP model have high total energy consumption for all WWRs and orientations compared to building typologies based on a square plan. Also in such cases, glazing is not the most important factor in order to reduce energy consumption.

The economic results showed that none of the glazing options are cost effective, partly due to the mild climate of Malta and partly because the actual prices of high performance glazing elements are still expensive, and this is compounded by the fact that the price of electricity has been reduced recently, making investment in energy efficiency less attractive from an economical point of view. One can be prompted to change to better glazing and shading options if strong incentives are made available.

However by 2020 it will be mandatory for new buildings to be zero net energy, thus making the use of alternative options to single glazing attractive in order to obtain such a benchmark. Whether this would be the best cost-optimal option or not is open for debate and would require a completely separate study to compare the different options that one can use to reach zero net energy buildings.

REFERENCES

- Caruana T F. The effect of different glazing apertures on the thermal performance of maltese buildings [MSc Dissertation]. Malta: Univerity of Malta; Jun 2015
- DesignBuilder. Design builder - simulation made easy; DesignBuilder [Accessed 23 July 2015]. Available from: <http://www.designbuilder.co.uk/>.
- Malta Resources Authority. Climate change – introduction; 2012 [Accessed 09 September 2014]. Available from: <http://mra.org.mt/climate-change/climate-change-introduction/>.
- Galdies C. The climate of malta: statistics, trends and analysis 1951-2010. Valletta: National Statistics Office; 2011.
- Kontoleon K and Bikas D. Modeling the influence of glazed openings percentage and type of glazing on the thermal zone behaviour Energy and Buildings; 2002. pp 389-99.
- Macka S and Yasar Y. The effects of window alternatives on energy efficiency and building economy in high - rise residential buildings in cold climates Gazi University Journal of Science. Vol. 24, no. 4; 2011. pp 927-44.
- DesignBuilder. Window shading; DesignBuilder [Accessed 5 May 2015]. Available from: [http://www.designbuilder.co.uk/helpv4.2/#_Window_shading_internal_1.htm%3FTocPath%3DBuilding%2520Models%7CModel%2520Data%7CBuilding%2520Model%2520Data%7COpenings%2520Data%2520\(Windows%252C%2520Doors%252C%2520Vents%252C%2520Holes%252C%2520Sub-surfaces\)%7CE](http://www.designbuilder.co.uk/helpv4.2/#_Window_shading_internal_1.htm%3FTocPath%3DBuilding%2520Models%7CModel%2520Data%7CBuilding%2520Model%2520Data%7COpenings%2520Data%2520(Windows%252C%2520Doors%252C%2520Vents%252C%2520Holes%252C%2520Sub-surfaces)%7CE).

Occupant Behaviour at the Presidential Palace of San Anton, Malta: A Study Supporting the Development of a Methodology to Enhance Energy Efficiency in Heritage Buildings

A Wismayer

University of Bath, Claverton Down, Bath, BA2 7AY, UK

C S Hayles

INSPIRE @ UWTSO, Mount Pleasant Campus, Swansea SA1, Wales, UK

M Lawrence

University of Bath, Claverton Down, Bath, BA2 7AY, UK

N McCullen

University of Bath, Claverton Down, Bath, BA2 7AY, UK

V Buhagiar

Univerisyt of Malta, Msida, MSD 2080, Malta

Email: ambwism@gmail.com

Abstract. The eco-refurbishment of heritage buildings, which addresses energy efficiency, presents particular challenges to Euro-Mediterranean countries. This is compounded by sensitive adaptive reuse and occupant behaviour. This research seeks to develop a validated simulation model to profile the impact of proposed interventions and retrofitting solutions: an innovative assessment tool, enabling best practice decision-making, effective planning and optimal results in the drive towards maximising sustainability in historic buildings. The Presidential Palace of San Anton in Malta has been chosen as the case study. This national 17th century treasure represents a typology of heritage buildings, characterising the climatic and cultural profile of Mediterranean countries. Having undergone several transformations to accommodate its periodic reuse, the building is now an important multi-functional activity hub. This paper, which forms part of a wider study, will focus on the assessment occupant behaviour and comfort in this setting, an understanding of which is pivotal in identifying energy efficiency goals. The research will derive and test a methodology for examining users' perception, and how the internal environment is adapted to meet comfort requirements and functionality: this through the use of semi-structured interviews with building occupants.

1. INTRODUCTION

The building sector is responsible for approximately 40% of total primary energy use worldwide. Energy demand in itself has risen sharply as a result of advancing technologies and increasing population. Carbon dioxide emissions and climate change are both strongly related to energy consumption : residential buildings alone account for 10% of greenhouse gas emissions in the European Union. As a result, the development of strategies targeting a decrease in energy consumption in buildings has become an international priority.

Energy efficiency (EE) is a primary focus of European targets for 2020, 2030 and 2050, and commitment to sustainability goals is evident in European Directives such as the Energy Efficiency Directive and the Energy Performance of Buildings Directive. A recent revision of the latter specifically underlines the need for Energy Efficient Retrofitting (EER) of existing buildings. The importance of EER is obvious when considering the significant proportion of present building stock, coupled with a predicted lifespan of between 50 and 100 years. However, whereas studies have shown that significant gains may result through EER, rendering it an accepted means of achieving energy savings, a typical and practical strategy is rarely proposed.

In Europe, focus has been placed on renewable energy sources, including wind and solar power, as well as bio fuels, combined with the promotion of efficient energy use. In some cases, this approach has also been reinforced through a series of design standards addressing EE in residential buildings. However, established policies combining EE and renewables are generally lacking.

The potential for reducing energy demand and pollutant emissions is notably significant within the Mediterranean building sector. This is especially true in the case of heritage buildings. However, this typology presents a special and challenging case, as a result of the numerous factors that must be considered during such eco-refurbishment projects. One of these is the aspect of occupant behaviour, the impacts of which have proven to be difficult to identify accurately.

This study seeks to be of practical use by deriving innovative data in an identified area of local and international priority: the environment. The study will focus on the EE of a particular typology of heritage building, with awareness of local socio-economic aspects and within a globalised perspective. It is in line with the requirements of the Energy Efficiency Directive (2012/27/EU), and contributes to the drive to reaching energy targets for 2020 as stipulated by the European Union.

In this paper, the authors seek to outline a methodology for collating data to better understand the behaviour of the occupants of a typical Maltese palace, and the impact of such behaviour on the building's energy profile and performance.

2. OCCUPANT BEHAVIOUR

Occupant behaviour plays a pivotal role in reducing building energy use. Studies have shown that although improving the building envelope may result in lower gains, the presence of occupants will inevitably increase the total energy consumption. Research has highlighted the impact of occupant behaviour on adaptability and use of building technologies. Therefore, low energy consumption in buildings cannot be guaranteed through technology alone: rather, it should be supported by the appropriate interaction of occupants with the building.

Interactive adaptation, defined as the way in which occupants interact with their homes, has an impact on building performance and resource use. Studies have shown that energy consumption may be influenced by educating occupants to interact with the building in a more energy-conscious manner. The promotion of energy-saving measures may produce a 10% reduction in household electricity consumption as an outcome of improving user behaviour. This attitude, termed *green behaviour*, produces improved energy savings following positive behavioural changes.

Conversely, realised energy savings may fall short of predictions, as is often the case. A behavioural response known as the rebound effect may be a cause of this result. This occurs when consumers increase energy use following retrofitting interventions and/or policy changes designed to improve energy efficiency.

Another possible cause may be the inability to accurately replicate occupant behaviour patterns through simulation tools. The behaviour diversity and complexity of users cannot be imitated by computer-modelling software, which generally replicate patterns in a rigid manner. Energy consumption predictions are heavily influenced by the presence of occupants, and their interaction with building components, even when other controlling factors, such as climate, building characteristics and services, are clearly defined. Therefore, although the impact of occupant behaviour on building performance has been recognised and studied, knowledge gaps and restrictions to existing methodologies still exist.

The impact of human behaviour on building technologies and operation, and therefore on energy consumption, has been noted but not yet clearly defined. The inability to quantify the energy use attributable to building occupants is largely due to the variety of factors simultaneously influencing energy consumption. Yu et al. classify these into seven categories: climate, building characteristics, user characteristics, building services, occupant behaviour, socio-economic factors and the required indoor environmental quality. However, some of these

interlink substantially, and although compartmentalisation supports research methodologies, consideration must be given to the impact of integrated factors.

3. THE RETROFITTING REVOLUTION

In response to a heightened awareness of the impact that the construction industry has had, and continues to have, on the environment, several new technologies and innovative solutions are being developed and promoted in an attempt to reduce the carbon footprint of urban landscapes. One such tool comprises retrofitting – an intervention whose advantages over demolition have been highlighted. Advocated by Xing et al., it targets the refurbishment and reuse of existing stock, championing a saving in emissions during the embodied and operational lifecycle stages.

This implies that EE should be given equal importance in new and existing structures, as suggested by Yilmaz & Kundakcib. In fact, the existing building stock has been highlighted as a key area for potential energy-use reductions through eco-refurbishment and the same principle may be applied in Malta. Pertinently, the indicative national EE target for Malta calls for a revision of minimum energy performance requirements in both new and existing buildings.

It is estimated that 70% of existing buildings shall still be present in 2050. This raises interesting questions regarding their energy performance and retrofitting potential which, according to Filippi, are low and high respectively. However, the existing building stock in most Euro-Mediterranean countries varies dramatically, ranging from contemporary construction to heritage architecture. Sahin et al argue that EER should be implemented using different approaches according to typology, ensuring particular care for the historical, sociocultural and architectural values associated with heritage buildings.

4. ECO-REFURBISHMENT OF HERITAGE BUILDINGS

The eco-refurbishment of heritage buildings plays an integral role in the move towards a more sustainable future, by contributing to improving energy performance and occupant comfort. Studies have shown that significant energy savings can be achieved without impinging on the property's heritage value. Notwithstanding this, proposals designed to improve the energy performance of such structures must face the challenge of harmoniously merging several different aspects. These include protecting historic features, satisfying the modern requirements of the new use, retaining balanced environmental conditions for artefacts and achieving comfort requirements for occupants. The optimum result of a retrofit should comprise a rational balance of these components.

In addressing the heritage building typology, it is essential to define what may be considered to be a *heritage building*. A heritage building may be defined as a structure of architectural, social or heritage value, having features or characteristics the preservation of which is deemed desirable, and generally exhibiting traditional construction. It has also been contended that buildings pre-dating the large-scale reconstruction that followed the Second World War (i.e.: pre-1945), and the subsequent industrial revolution in Europe, may be classified as such. However, several sub-categories exist within this definition, having varying degrees of historical, architectonic and cultural value. EER interventions should be custom-designed to meet the unique needs of these typologies by developing a thorough understanding of the characteristics and use of each.

In order to address the requirements of both energy and heritage conservation, Ben & Steemers advocate a balanced approach to the eco-refurbishment of protected buildings. Key amongst the necessary considerations is the factor of occupant behaviour. Tackling this aspect is a vital part of the retrofitting process, since it has the highest energy savings potential in heritage buildings.

This context highlights the importance of maximising the EE of heritage buildings through eco-refurbishment. Restoration and adaptive re-use form the foundations supporting sustainable development. In fact, development without historic preservation is not sustainable. Internationally, the relationship between conservation and sustainability has been recognised.

The EE of heritage buildings has been targeted by the Architects Council of Europe, and discussed repeatedly by the Environment and Sustainable Architecture Work Group.

The Maltese archipelago's strategic location within the Mediterranean basin has imparted the islands with a rich history, reflected by the local architectural fabric. Given Malta's abundance of heritage buildings, there exists huge potential to exploit the benefits of EER in this context. However, whereas the regeneration and reuse of older properties is encouraged, the role of eco-refurbishment in this scenario remains generally unacknowledged. Despite the abundance of this category of building, Malta has yet to assess and achieve a balance between heritage and energy value.

5. CASE STUDY: THE PRESIDENTIAL PALACE OF SAN ANTON

It has been emphasised that public buildings should serve as role models in the shift towards retrofitting, thus incentivising the market. The Maltese government is the custodian of several heritage buildings. The eco-refurbishment of these may serve to demonstrate what can be achieved through EER, and provide an impetus for the private sector to take up the challenge.

As the constitutional head of state, the President of the Republic undertakes a leading role in Maltese society. The office calls for constant dialogue and open channels of communication with several sectors. The Presidential Palaces would, therefore, offer an excellent means of leading the eco-refurbishment of heritage buildings by example.

There are three Presidential Palaces. The Magistral Palace (Official Office) in Valletta is shared with other entities, whereas Verdala Palace (Summer Residence) in Dingli and San Anton Palace (Primary Residence) in Attard are both used solely by the President. Of these, the latter incorporates difference aspects of use and an architectural configuration typical of Maltese heritage buildings.

Currently the primary residence and main office base of the President, San Anton Palace was originally built in 1620 as a country retreat for Antoine de Paule, then Provençal Knight of St. John and later Grand Master of the Order. It is multi-functional building, catering to residential, administrative, office and service uses simultaneously for a population of approximately 100 occupants. The diversity of this working palace must merge harmoniously with the need to maintain the highest standards of heritage protection. It, therefore, presents a challenging case study, albeit comparable in its characteristics and layout to other buildings classified within the same typology.

6. METHODOLOGY

A mixed-method approach, based on methodological triangulation, was adopted to gather data for the wider research project. However, for the purpose of this paper, the methodology will focus on the semi-structured interviews carried out with building occupants of San Anton Palace.

6.1. *The Case Study*

Initially the use of cross-sectional design was considered, whereby more than one case is evaluated simultaneously with the scope of identifying patterns of association. This option would have offered the opportunity to compare similar cases and derive a template through which conclusions may be extracted. However, due to the scale of the Presidential Palaces, as well as the variety and nature of influencing factors and materials, it was felt more appropriate for the research to focus on the intensive examination of a single case study representative of the selected building typology. Comparison is still present in the analysis of rooms used by each occupant group, having different characteristics.

6.2. *Semi-Structured Interviews*

The semi-structured interview was selected as a form of data collection. Although errors resultant from interviewer variability are minimised in structured interviews through the standardisation of questions, the semi-structured interview is one of the most frequently used qualitative research methods. It offers both flexibility as well as opportunity to obtain rich, detailed data. Open-ended interviews, which allow respondents to express their opinions freely and discuss related topics deemed to be pertinent, were therefore adopted as a research methodology.

A series of semi-structured interviews with palace occupants, comprising both staff and residents, were undertaken in order to assess the comfort levels and functionality of the building in its existing use framework. The information gathered will prove vital in analysing the impact of occupancy behaviour on the building's energy efficiency, and in establishing comfort levels.

6.2.1. Pre-Interview Statement. Prior to conducting the interview, an introductory statement was provided to participants with the scope of introducing the research and explaining the aims in terms of eco-refurbishment and energy savings. The brief was also designed to emphasise the importance of the interviewees' contribution and the eagerness of the interviewer to improve the quality of the internal climatic conditions. Moreover, definitions of particular terminologies used throughout the interview were included for the purpose of clarity and consistency.

6.2.2. Pilot Interviews. Pilot interviews were carried out with a member of each of the three primary occupant groups namely, palace-based administrative staff, service staff and Foundation staff. The results were analysed and the interview schedule was amended accordingly in order to clarify words/phrases and meanings (in the case of the latter, by providing examples). The method of conducting the interview was also revised slightly. During the pilot interviews, participants found it difficult to recall scale bar references in questions where it was required to rate comfort levels. Therefore, a copy of the scale bar was made available to the respondents, for reference, during subsequent interviews. Written definitions of comfort and functionality were also made available, since participants had trouble distinguishing between the two concepts.

6.2.3. Participant Selection. The option to design different schedules for selected occupant groups (for example, administration, service staff, security etc.) was considered. However, the selected method comprised a common interview structure, having open-ended questions and allowing the respondent the opportunity to further develop any relevant area. A total of 28 interviews have been carried out to date, comprising approximately 27% of the total population.

6.2.4. Contextualising Results. In order to contextualise the information compiled, particularly with regards to ratings, the relative humidity, internal air temperature and MET office readings were recorded on interview days in order to frame the comfort levels discussed by the respondents. The relative humidity and temperature was gathered using a portable data logger.

6.3. *Focus Groups*

The focus group method offers a number of advantages lacking in the group interview technique. According to Bryman, the former is more focused, targeting specific themes and issues, and is concerned with the interactions between participants. Although the distinction between the two methodologies is somewhat vague, the group interview method was discarded in view of the aforementioned benefits of the focus group technique. Focus group sessions will be carried out in order to further develop results derived from the interviews. During these discussions, the perspectives of individuals may stimulate alternative views, challenging

participants' responses and aggrandising the quality of data generated. The findings derived will be presented at a later stage.

7. DISCUSSION

In order to design a strategy for improving building performance, it is important to establish the expectations and requirements of users, as well as their perceptions of and interactions with the existing building layout and fabric. Feedback from occupants regarding interactive adaptivity is a vital building block towards green retrofits. It is also important to recognise that energy use in buildings is not solely a technical issue but, rather, one with a socio-technical dimension. The approach taken in this research is, therefore, well validated by the wider literature context.

The methodology adopted throughout this study aimed at being as inclusive as possible. This approach imparts three major benefits. Firstly, it was designed to engage occupants in the eco-refurbishment process at an early stage, such that they feel empowered and cooperate in bringing about positive change. Secondly, it motivated them to respond correctly during the interviews. The value of interviews with occupants may be reduced through distorted responses given, consciously or unconsciously, by the participants. Involving the occupants in a way that motivates them minimises the occurrence of this limitation. Thirdly, it creates a positive climate, supporting future behavioural change, as part of this process.

7.1. *Occupant Interviews*

Interviews were designed to collate data on a 'need-to-have' (rather than a 'nice-to-know') basis. This minimised the interview duration and reduced inconvenience to participants. The content of the interview schedule builds on published data to include all relevant factors. For example, Stevenson and Rijal outlined the following as pertinent aspects when evaluating interactive adaptivity: fabric performance, energy use, window opening activity, thermal comfort, indoor air quality, functionality and occupant behaviour. The initial information session afforded a consistent understanding of terminology amongst participants. This ensured robustness of findings, which may be assessed appropriately, at a later stage, in terms of the results, effectiveness and implications on other factors.

The adopted methodology results in building a relationship with the occupants, which is essential if the retrofit solution is to be effective. It also acts as a learning tool for all stakeholders, including building users who gain insight of their impact on energy efficiency through increased awareness and reflection. The findings enable evidence-based decision-making of appropriate retrofitting solutions through established knowledge of the needs, wants and practices of the users. As a result, a framework of intervention measures may be developed.

7.2. *Knowledge Transfer and Management*

Henryson et al. advocate the importance of information to motivate consumers to be more energy efficient. Therefore, once collated and analysed, the results of the interviews should be disseminated to all stakeholders including the keepers and users of the property, as well as building managers and designers/architects who may be called upon to intervene on San Anton Palace. Similarly, following the selection of appropriate eco-refurbishment interventions, decisions taken should be transmitted and explained to occupants in order to avoid them feeling detached and vulnerable.

The result of this research has implications for a wide diversity of stakeholders. The data must, therefore, be captured and managed effectively. Best practice knowledge management is illustrated through an evidence-based decision framework wherein the process and relative outcomes are clearly documented. Such a framework supports physical monitoring and post-intervention evaluation: this aspect is critical since studies have shown a tendency for behavioural change to revert. Knowledge derived through this framework can be shared with organisations, the construction industry, architects and academia. In particular, policy-makers

should have access to this supportive infrastructure: a valid tool to inform national strategy based on a socio-technical approach.

8. CONCLUSION

It was Malta's Prime Minister who first raised the issue of climate change internationally during the General Assembly of the United Nations in 1988, triggering several decades of climate negotiations. Climate change is now a recognised threat requiring immediate action. A response from the building sector is necessary in order to mitigate this issue.

The indicative national EE target for Malta calls for a revision of minimum energy performance requirements of existing buildings. This commitment should be implemented on the basis of a policy infrastructure encouraging stakeholders towards eco-refurbishment.

In this context, heritage buildings present particular challenges since they comprise complex systems exhibiting a balance between several factors. It has been postulated that there is insufficient information about the individual and combined influence of these factors on the building's energy profile. Technological solutions alone are inadequate: rather, retrofit decisions should also be derived from evidence-based data regarding occupant behaviour.

Ben and Steemers have demonstrated that significant energy savings may be achieved in listed properties through behavioural changes, far exceeding that resultant from physical interventions. Moreover, it has been argued that occupant engagement plays an integral role in achieving zero carbon targets in this sector. Therefore, the retrofit of heritage buildings must feature occupant consultation such that user perspectives and requirements may be identified to ensure viable solutions.

The methodology defined through this research ascertains that a structured approach has been adopted in order to identify and assess occupant views and needs. This should encourage responsible behaviour and safeguard evidence-based decision-making, implementation and monitoring. The next stage of the wider study will comprise a thorough analysis of the results derived through occupant interviews, consolidated by focus groups and the findings of a full-scale survey of the Palace. The outcomes of the integrated data will be bolstered by on-site monitoring and presented at a later date.

REFERENCES

- Hong T, Koo C, Kim J, Lee M and Jeong K 2015 A review on sustainable construction management strategies for monitoring, diagnosing, and retrofitting the building's dynamic energy performance: Focused on the operation and maintenance phase *Applied Energy* 155 671-707.
- Sahin C, Arsan Z, Tuncoku S, Broström T and Akkurta G 2015 A transdisciplinary approach on the energy efficient retrofitting of a historic building in the Aegean Region of Turkey *Energy and Buildings* 96 128-139.
- Caputo P, Costa G and Ferrari S 2012 A supporting method for defining energy strategies in the building sector at urban scale *Energy Policy* 55 26-270.
- Kolaitis D, Malliotakis E, Kontogeorgos D, Mandilaras I, Katsourinis D and Founti M 2012 Comparative assessment of internal and external thermal insulation systems for energy efficient retrofitting of residential buildings *Energy and Buildings* 64 123-131.
- Aste N, Caputo P, Buzzetti M and Fattore M 2015 Energy efficiency in buildings: What drives the investments? The case of Lombardy Region *Sustainable Cities and Society* 20 27-37.
- Wang Z, Ding Y, Geng G and Zhu N 2013 Analysis of energy efficiency retrofit schemes for heating, ventilating and air-conditioning systems in existing office buildings based on the modified bin method *Energy Conservation and Management* 77 233-242.
- Wang Y, Wang L, Liu Y, Ding P, Deng S and Long E 2015 Defining air-conditioning and heating seasons based on human thermal perception and building energy efficiency *Urban Climate* 14 (4) 544-553.
- Romani Z, Draoui A and Allard F 2015 Metamodeling the heating and cooling energy needs and simultaneous building envelope optimization for low energy building design in Morocco *Energy and Buildings* 102 139-148.

- Ascione F, Chechea N, De Masia R, Minichiello F and Vanoli G 2015 Design the refurbishment of historic buildings with the cost-optimal methodology: The case study of a XV century Italian building *Energy and Buildings* 99 162-176.
- Pisello A, Petrozzi A, Castaldo V and Cotana F 2014 Energy refurbishment of historical buildings with public function: pilot case study *Energy Procedia* 61 660-663.
- Yu Z, Fung B, Haghghat F, Yoshino H and Morofsky E 2011 A systematic procedure to study the influence of occupant behavior on building energy consumption *Energy and Buildings* 43 1409-1417.
- Ben H and Steemers K 2014 Energy retrofit and occupant behaviour in protected housing: A case study of the Brunswick Centre in London *Energy and Buildings* 80 120-130.
- Emery A and Kippenhan C 2006 A long term study of residential home heating consumption and the effect of occupant behavior on homes in the Pacific Northwest constructed according to improved thermal standards *Energy* 31 677-693.
- Yan D, O'Brien W, Hong T, Feng X, Gunay H, Tahmasebi F and Mahdavi A 2015 Occupant behavior modeling for building performance simulation: Current state and future challenges *Energy and Buildings* 107 264-278.
- Hong T, D'Oca S, Turner W and Taylor-Lange S 2015 An ontology to represent energy-related occupant behavior in buildings. Part I: Introduction to the DNAs framework *Building and Environment* 92 764-777.
- Stevenson F and Rijal H 2010 Developing occupancy feedback from a prototype to improve housing production *Building Research & Information* 38 (5) 549-563.
- Henryson J, Hakansson T and Pyrko J 2000 Energy efficiency in buildings through information – Swedish perspective *Energy Policy* 28 169-180.
- Ouyang J and Hokao K 2009 Energy-saving potential by improving occupants' behavior in urban residential sector in Hangzhou City, China *Energy and Buildings* 41 711-720.
- Doran S, Zapata G, Tweed C, Suffolk C, Forman T and Gemmell A Solid wall heat losses and the potential for energy savings: Literature review BRE 2014.
- Yu Z, Haghghat F, Fung B, Morofsky E and Yoshino H 2011 A methodology for identifying and improving occupant behavior in residential buildings *Energy* 36 6596-6608.
- Power A 2008 Does demolition or refurbishment of old and inefficient homes help to increase our environmental, social and economic viability? *Energy Policy* 36 4487-4501.
- Xing Y, Hewitt N and Griffiths P 2011 Zero carbon buildings refurbishment: A Hierarchical pathway', *Renewable and Sustainable Energy Reviews* 15 3229-3236.
- Sodagar B, Rai D, Murphy J and Altan H 2009 Role of Eco-refurbishment in Sustainable Construction and Built Environment. 3rd CIB International Conference on Smart and Sustainable Build Environments. Delft University of Technology (Delft) 15-19 June 2009.
- Yilmaz Z and Kundakcib A 2006 An approach for energy conscious renovation of residential buildings in Istanbul by Trombe wall system *Building and Environment* 43 2008 508-517.
- Ouyang J, Wang C, Li H and Hokao K 2011 A methodology for energy-efficient renovation of existing residential buildings in China and case study *Energy and Buildings* 43 2203-2210.
- Filippi M 2014 Remarks on the green retrofitting of historic buildings in Italy *Energy and Buildings* 95 15-22.
- Polo Lopez C and Frontini F 2013 Energy efficiency and renewable solar energy integration in heritage historic buildings *Energy Procedia* 48 1493-1502.
- BICC. Regeneration of Property. Available from: <http://www.bicc.gov.mt/en/Pages/Regeneration-of-Property.aspx> [Accessed 9th November 2015]
- Economidou M, Atanasiu B, Despret C, Maio J, Nolte I and Rap O Europe's buildings under the microscope: A country by country review of the energy performance of buildings. Buildings Performance Institute Europe: 2011.
- Freller T. The palaces of the grandmasters in Malta. Sta Venera: Midsea Books; 2009.
- Bryman A. Social Research Methods. Oxford: Oxford University Press; 2001.
- Chiu L, Lowe R, Raslan R, Altamirano-Medina H and Wingfield J 2014 A socio-technical approach to post-occupancy evaluation: interactive adaptability in domestic retrofit *Building Research and Information* 42 (5) 574-590.
- UN Web TV. Ban Ki-moon (UN Secretary-General) at the Commonwealth Heads of Government meeting 2015 - Joint Press Conference. Available from: <http://webtv.un.org/watch/ban-ki-moon-un->

secretary-general-at-the-commonwealth-heads-of-government-meeting-2015-joint-press-conference/4635785433001?page=2[Accessed: 28th November 2015]

Hayles C and Dean M 2010 A methodology to investigate adaptation for zero carbon living. Proceedings of the CIB 2010 World Congress: Building a better world. Salford Quays (United Kingdom) May 10th - 13th 2010.

Renovating Primary School Buildings in Malta to Achieve Cost-optimal Energy Performance and Comfort Levels

Damien Gatt

Sustainable Energy and Water Conservation Unit, Ministry for Energy and Health, Luqa, Malta

Charles Yousif

University of Malta, Institute of Sustainable Energy, Msida, Malta

Email: damiengatt@gmail.com, damien.gatt@gov.mt, charles.yousif@um.edu.mt

Abstract. The Energy Efficiency Directive requires that 3% of the floor area occupied by public buildings be renovated each year to meet the Minimum Energy Performance Requirements (MEPRS) based on the Cost Optimal Methodology (COMet) as defined by the EPBD. The MEPRS for the retrofitting of schools in Malta still have not been defined. In this study, an innovative and energy efficient COMet approach for the retrofitting of Public Primary School Buildings (PPSBs) in Malta has been applied. All current PPSBs are naturally ventilated and have diverse footprints and envelope constructions. This prompted us to move away from the commonly adopted COMet approach, which assumes that one or two Reference Buildings (RBs) are sufficient for defining the MEPRS for all schools and that the building is assumed to be mechanically ventilated with active heating/cooling sources to reach comfort defined by pre-determined temperature set-points. In contrast, this paper aims to achieve comfort using the EN 15251 adaptive thermal comfort approach for naturally ventilated buildings and provides an Excel tool that calculates the MEPRS based on the actual building construction and orientation. Results have shown that for summer, the PPSB can attain adaptive comfort if its glazing is externally shaded and night purging is applied.

1. INTRODUCTION

The EPBD recast highlights that buildings account for 40 % of the total energy consumption (EC) in the EU. The EU Commission aims at realising the full potential of energy savings of buildings by requiring MS to define the Minimum Energy Performance Requirements (MEPRS) of new buildings and buildings undergoing "major renovation" with a view to achieving Cost Optimal Levels (COLevs) which COLev is defined in as "*the EP level which leads to the lowest cost during the estimated economic lifecycle*" while ensuring comfort levels are met.

Furthermore, the Energy Efficiency Directive (EED) (2) requires that 3% of the total floor area owned and occupied by public buildings be renovated each year to meet at least the MEPRS of the EPBD recast, which public buildings should serve an exemplary role.

This exemplary role can be understood precisely for public primary school buildings (PPSBs), for their ability to spread a new style of sustainable living (3). However, the MEPRS for educational buildings in Malta based on COMet as required by the EPBD have not yet been set and consequently there are no guidelines of how such renovation shall be carried out. Renovation for PPSBs shall provide a good balance between EP and high levels of comfort as various studies have shown that comfort has a high degree of influence on student's academic achievements(4)(5).

A study of the various existing PPSBs around Malta shows the many diverse topologies and envelope constructions the different buildings are made up of. In addition, all the PPSBs are naturally ventilated. Given, these scenarios, this study moves away from the commonly adopted COMet approach and introduce an innovative and cost-effective approach to the COMet by:

(1) Aiming to achieve thermal comfort, using the EN 15251(6) adaptive thermal comfort approach using only passive means for naturally ventilated buildings. Dynamic building simulation modelling was also used instead of commonly used monthly quasi-steady state (QSS) simulation tools, which QSS tools automatically assume that the building requires to be mechanically ventilated with active heating/cooling sources to reach thermal comfort (TC) that is defined by pre-determined temperature set-points.

(2) Developing an excel tool that calculates the MEPRS based on the actual building construction and orientation, rather than assuming that one or two Reference Buildings (RBs) are sufficient for defining the MEPRS for all school buildings as is the usual adopted approach and

(3) Making use of Building Energy Optimization Tools (BEOPTS) in combination with Dynamic Building Software Simulation Tools (BSSTs) so as to consider thousands of combination of measures (COMs) and arrive at more accurate solutions instead of considering a few COMs as is considered in the commonly adopted COMet approach.

2. COMFORT ANALYSIS RESEARCH METHODOLOGY AND RESULTS

2.1. Defining RB Topologies for PPSBs

An investigation of existing PPSBs shows that all schools are naturally ventilated and have the same occupancy schedule. Despite this similarity, the building topology and envelope construction varies among the different schools.

Given the many variables, a representative MEPRS study for existing PPSBs in Malta will require many RBs to be defined. However, to keep the COMet simple, the study has used an innovative approach that defines only one RB, but still caters for the different variables among the different schools as follows. The Siggiewi Primary school shown in Figure 1 was the RB chosen as it contains classrooms facing all primary axis within $\pm 20^\circ$, and is made up of areas having 3 floors enabling one to study the way EP and comfort varies with orientation and floor level. The EP for the RB was then calculated using the EnergyPlus simulation tool for classrooms on a kWh/m²/year per orientation and floor basis, rather than simply on an overall kWh/m²/year basis. In order to represent the full spectrum of existing PPSBs envelope and constructions, this EP calculation included both the EP (per orientation and floor basis) for the chosen RB, where the existing envelope construction and equipment type is considered, as well as the EP when the same RB is simulated to have different envelope construction and equipment types. The considered simulations included constructions having both higher and lower U-values and different equipment to the chosen RB. The EP calculation for these thousands of variants was enabled by combining EnergyPlus with DesignBuilder optimization tools.

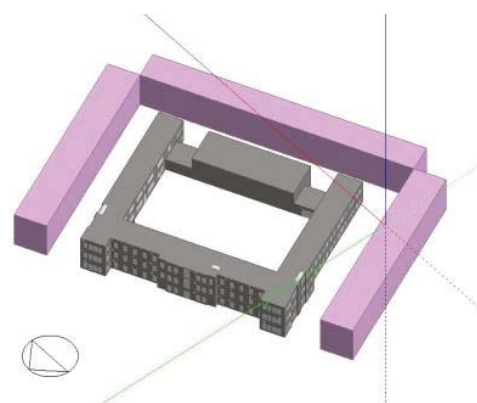


Fig 1: Plan view of of the Siggiewi Primary school (left) and DesignBuilder model of the school (right)

Such approach allows a customized MEPRS solution to any PPSB footprint under study having any area per orientation and floor when all gathered data from the different combinations was inputted in an excel tool. Once the user defines the building characteristics in the the Excel tool, the EP calculation of the existing PPSB and the required global cost (€/m²) required to

upgrade the building to the various superior construction and equipment variants is calculated automatically.

2.2. Comfort analysis and results for RB topologies

As a starting point, the comfort of the existing Siggiewi school building was analysed. Comfort was analysed both as means of validating the DesignBuilder school model and to identify the most adequate passive retrofitting options for the COMet. Comfort was analysed using two methodologies: questionnaires and dynamic BSSTs. The results from the two methods were then compared as a means of validating the results from the software to identify the suitability of the EN 15251(6) adaptive comfort model used for this study. The questionnaires were handed out to all teachers at the school. Thermal Comfort (TC) questions were designed using subjective evaluation/judgement scales as recommended by EN 15251(6).

The Siggiewi primary school RB was modeled using DesignBuilder, having the school's existing envelope construction¹ and Maltese climate weather file.

To assess the TC of the building, simulations for winter and summer typical weeks were carried out for representative classrooms and adjacent corridors of different floors and orientations. The analysis was carried out by plots of hourly mean operative temperature (OT) (generated by EnergyPlus) for the occupied and simulated periods in each of the analysed classrooms against the hourly adaptive comfort temperature (\pm EN 15251(6) Category II adaptive temperature limits) also generated by EnergyPlus.

During winter, for all the representative classrooms, adaptive comfort was not met as many OT points lie outside the lower OT limit (Refer to Figure 2 which shows the results for the Top Floor (TF) rooms). The lack of comfort during the winter period (with no active heating source) can be understood from the fact that 90% of the respondents use heaters during the winter period which compares well with the simulation results. From the heat balance plots generated by DesignBuilder it was in fact shown that the major sources of heat losses during the winter period are uncontrolled heat losses to the colder outside air when the windows were kept open. It was therefore determined that during winter it was required to introduce mechanical ventilation (MV) to control the heat losses from windows, with MV set up so as to exhaust classroom air while bringing the resulting warmer corridor air inside the classrooms so as to reduce the heating loads. An active heat source is also required during winter to ensure comfort.

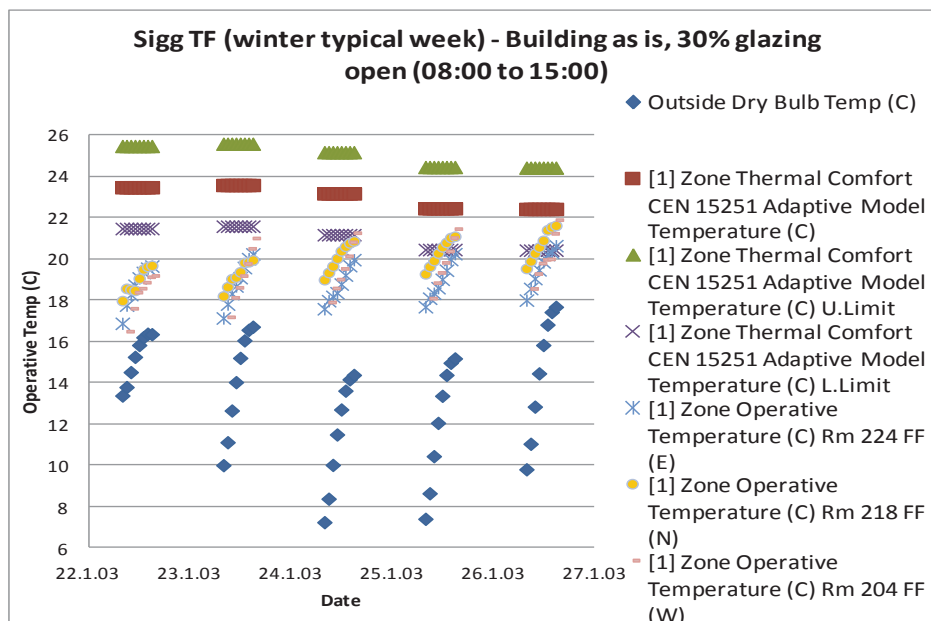


Fig 2: TF hourly mean OTs against hourly adaptive comfort temperature plot for for a typical winter week

¹RB existing construction: external wall U-Value: 1.5 Wm⁻²k⁻¹, Roof U-value:0.6 Wm⁻²k⁻¹, external windows : Al frame single glazed.

For summer, comfort was only met for representative rooms of the Lower Ground Floor (LGF) due to the lower solar gain from windows and heat losses from floors. Both the TF and Middle floor (MF) representative rooms failed to meet adaptive thermal comfort (Refer to Figure 3 which shows the results for the TF rooms). The questionnaire results also showed that the majority of the respondents disapproved of the June indoor environment, especially in the TF (due to the highest solar gains) which compares well with the simulation results. When the building was night purged and external shading was applied to both the external glazing and classrooms, with the windows kept open, adaptive comfort was generally met for both the MF and TF as shown in Figure 3. This means that comfort can be achieved passively during summer when ceiling fans are used to counteract the few hours when comfort is not met.

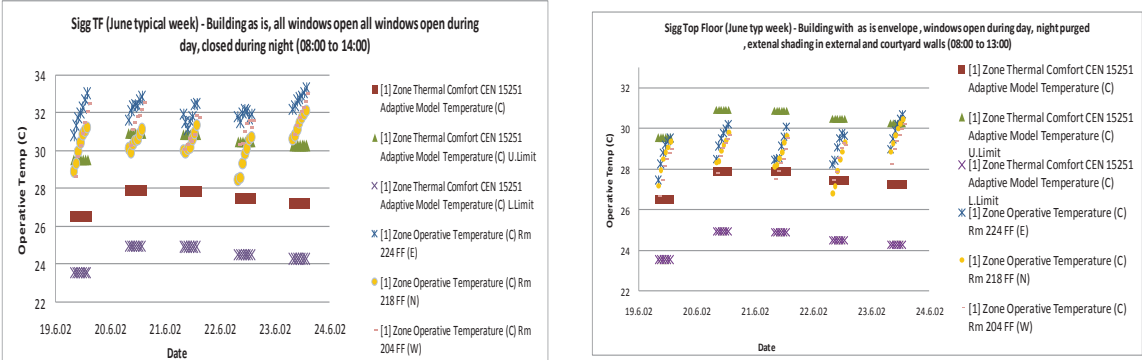


Fig 3: TF hourly mean OTs against hourly adaptive comfort temperature plot for for a typical winter week. Left figure shows comfort with the building as is and the right figure with external shading applied.

3. PPSBS COST-OPTIMAL STUDY RESEARCH METHODOLOGY AND RESULTS

The findings from the comfort analysis provided the basis to enable the cost-optimal approach to use the most effective retrofit measures and use only passive techniques to reach summer comfort.

3.1. Selection of Variants for Building Envelope and Equipment

The first step was to identify the selection of variants for the building envelope and equipment to be used for the cost-optimal study. Combinations of measures (COMs) were defined by the combination of the elements of differentiation shown in Figure 4 below. For each technical variant of measures, one option from each of the above elements was chosen. This led to a total number of 57,600 combinations of measures (COMs) when the above number of different options is combined. For each of the 57,600 COMs the energy demand (ED) was calculated on a per floor and per building orientation scenario as described in the below sections.

Equipment					Thermal quality of building envelope					
	Option 1	Option 2	Option 3	Option 4		Option 1	Option 2	Option 3	Option 4	Option 5
Lighting	Low standard template	T5 tubes with electronic Ballasts	T5 tubes with electronic Ballasts one Presence	T5 tubes with DALI Ballasts, with automatic dimming	Room external walls U-value ($Wm^{-2}k^{-1}$)	2.9	2.1	1.5	1.2	0.6
Space Heating/Mechanical Ventilation	30 % radiative, 70% convective electrical heating, Heating design load is automatically sized by EnergyPlus. Heating is combined with MV (ACH :10 L/s/pers)	Same as Option 1 but with 100% electric convective heating instead of the 30 % radiative electrical heating, automatically sized by EnergyPlus.	Portable electric radiation heaters, no MV, 30 % of windows opened (instead of MV) to allow for the required ACH.	Electric Far Infra-Red (FIR) panel heaters mounted on soffit, surface temperature of panels 100° C, 97 % radiative heating. MV was combined with the FIR panel heaters as described in option 1.	Internal partitions separating rooms from corridors (U-value ($Wm^{-2}k^{-1}$))	2.2	1.3			
					Flat roof (U-value ($Wm^{-2}k^{-1}$))	2.4	2	1.3	0.6	0.35
					Room window frames	Al Frame (no thermal break)	uPVC Frame			
					External windows glazing	3 mm clear glass	Double glazing (3 mm each pane+air gap)	Double glazing (3 mm each pane+ argon fill in gap)		
Passive space cooling (shading) for the summer period	Movable external shading on glazing for both classrooms and corridors) + Night purging									
Hot water	Electric storage heaters	Electric instantaneous water heaters	Flat plate solar water heaters with storage, Solar Fraction of 0.8 with							
RES electrical generation	No photovoltaic panels	Roof mounted Photovoltaic panels (with PV panels, incl. space between panels) covering	Roof mounted Photovoltaic panels (with PV panels, incl. space between panels) covering 40 % of total roof area	Roof mounted Photovoltaic panels (with PV panels, incl. space between panels) covering 60 % of total roof area						

Fig 4: Selection of variants for the building envelope (left table) and equipment (right table)

3.2. Primary Energy Demand (ED) Calculation for the Cost-optimal Study

In order to assess the energy performance (EP) of the existing building when updated with the COMs, EnergyPlus in combination with the optimization tools were utilised. The energy requirements for hot water were determined analytically using basic heat transfer equations. The energy needs considered in the calculations included those for space heating and MV (ED calculated for 1st Dec to 31st May), hot water, and lighting. The annual energy generated from PVs was also considered. The ED for space cooling purposes was not considered, because the building was considered to attain comfort during the summer period if external shading is used to control solar gains inside the building.

The EN15251 Category 2/ Cibse Guides comfort and activity criteria set points were set for the software simulations to determine the ED. Site energy to primary energy conversion was taken as 2.5 in view of the near future conversion to natural gas power stations.

3.3. Global Cost Calculation

The global cost was calculated as per methodology identified in the EPBD recast (1). The NPV was calculated on a 30 year period using a 6 % discount rate. The year 2015 Maltese market prices were considered for the calculations.

3.4. Calculation Tool to Identify the EP for PPSBs

Once all data was collected, an excel tool that includes all the EP data per orientation and floor for the various COMs (calculated from the above sections), was designed to enable one to determine automatically the cost optimal retrofitting solution/s and the MEPRS after inputting the area per floor and orientation, equipment and construction details of a specific building into the tool. The tool takes into consideration both the EP calculation of the initial PPSB and the required global cost ($€/m^2$)/ NPV (€) required to upgrade the building to the various superior construction and equipment variants. This approach therefore enables a customized solution to the COMet.

3.5. Determination of the MEPRS and Cost-optimal measures

	Group 1 RBs (as per Siggiewi school/Technical Guide F construction(7))	Group 2 RBs (low standard building)	Building configuration	Description
Roof U-value	0.6 Wm ⁻² K ⁻¹	1.3 Wm ⁻² K ⁻¹	Type 1	School building (with 2 floors) LGF and TF with a square configuration , each orientation has 600 m ² of classroom area (300 m ² per floor)
Classroom External Wall U-value	1.5 Wm ⁻² K ⁻¹	2.1 Wm ⁻² K ⁻¹	Type 2	Building (with 2 floors) LGF and TF with all rooms facing the North orientation and having 2,400 m ² of classroom area (1,200 m ² per floor)
Classroom Partition U-value	2.2 Wm ⁻² K ⁻¹	2.2 Wm ⁻² K ⁻¹	Type 3	Building (with 2 floors) ground and top floor with all rooms facing the South orientation and having 2,400 m ² of classroom area (1,200 m ² per floor)
Classroom window frame	Aluminium	Aluminium	Type 4	Building (with 2 floors) LGF and TF with all rooms facing the East orientation and having 2,400 m ² of classroom area (1,200 m ² per floor)
Classrooms glazing	Clear double glazing (air between panes)	Single glazing	Type 5	Building (with 2 floors) LGF and TF with all rooms facing the West orientation and having 2,400 m ² of classroom area (1,200 m ² per floor)
Classrooms lighting system	T5 Fluorescent (assumed always on during occupied periods)	Low standard lighting (assumed always on during occupied periods)		
Air heating system	Electric radiators -30 % radiative (ventilation via windows opening)	Electric radiators -30 % radiative (vent via windows opening)		
HW system	Electric storage heaters	Electric storage heaters		
% of roof area occupied by PVs	0%	0%		

Fig 5: Description of the constructions (left table) and building configurations (right table) used to establish the 10 case study buildings

In order to demonstrate typical examples for the calculation of MEPRS for PPSB's with the tool explained in Section 3.4, ten (10) case study buildings (RBs) were used (i.e. the five school building configurations types were demonstrated with both Group 1 and Group 2 constructions (refer to Figure 5)).

From the tool, the MEPRS and the Global cost required to achieve the MEPRS were calculated. Table 1 shows a summary of the starting RB ED, MEPRS, the Global Cost and NPV based on both site energy and primary energy required to achieve the cost-optimal level for all the 10 RBs.

Table 1: Summary of the MEPRS (kWh/m²/annum), the Global Cost (€/m²) and NPV (€) required to achieve the cost-optimal level for all the 10 RBs

Reference Building (RB)	RB starting Site Energy Consumption (kWh/m ² /yr)	RB Starting Primary energy Consumption (kWh/m ² /yr)	Cost-optimal energy consumption (Primary Energy) (kWh/m ² /yr)	Global cost (LCC) (€/m ²) required to obtain cost optimal energy consumption	NPV (k€) (no FIT) based on Site Energy to upgrade and achieve Cost-optimal energy consumption (30 yr. period)	NPV (k€) (no FIT) based on Primary Energy to achieve Cost-optimal energy consumption (30 yr. period)
Group 1 Type 1 RB (square config.)	76.37	190.93	0.6	143.75	446.56	1,582.25
Group 1 Type 2 RB (N facing)	62.25	155.63	-5.15	119.17	407.89	1,323.21
Group 1 Type 3 RB (S facing)	62.66	156.65	-2.19	151.94	254.66	1,156.63
Group 1 Type 4 RB (E facing)	97	242.50	-0.58	151.94	641.93	2,124.80
Group 1 Type 5 RB (W facing)	83.56	208.90	0.67	153.69	481.76	1,724.38
Group 2 Type 1 RB (square config.)	84.24	210.60	-0.58	163.12	446.04	1,708.93
Group 2 Type 2 RB (N facing)	74.95	187.38	-0.58	137.02	470.06	1,596.54
Group 2 Type 3 RB (S facing)	73.02	182.55	-1.42	169.79	291.6	1,366.87
Group 2 Type 4 RB (E facing)	92.78	231.95	1.67	175.69	497.84	1,892.52
Group 2 Type 5 RB (W facing)	85.84	214.60	1.79	174.47	543.14	1,995.74

The retrofitting measures required in order for the building to achieve the cost optimal MEPRS for each RB is similar for each of the 10 RBs as follows: 1) Introduce MV during the winter period and replace portable electric radiation heaters with FIR panel heaters, 2) Upgrade to T5 fittings with lux detectors, 3) Install PVs so as to occupy 20% of the roof area, 4) introduce SWHs having an overall Solar Fraction of 0.8. Building envelope is to be maintained as is.

3.6. Determination of the measures providing the highest and lowest NPVs

The tool described in Section 3.4 and the same 10 RBs were again used to determine, the maximum and minimum possible NPV's (shown in Table 2) and the measures required to achieve these.

Reference Building (RB)	RB starting Site Energy consumption (kWh/m ² /yr)	Site Energy consumption (kWh/m ² /yr) giving highest NPV (30 yr period)	Maximum NPV (k€) generated no FIT (30 yr period)
Group 1 Type 1 RB (square config.)	76.37	-73.67	820.03
Group 1 Type 2 RB (N facing)	62.25	-75.00	781.36
Group 1 Type 3 RB (S facing)	62.66	-73.82	628.13
Group 1 Type 4 RB (E facing)	97.00	-73.17	1,015.40
Group 1 Type 5 RB (W facing)	83.56	-72.68	855.23
Group 2 Type 1 RB (square config.)	84.24	-73.18	819.51
Group 2 Type 2 RB (N facing)	74.95	-74.55	843.52
Group 2 Type 3 RB (S facing)	73.02	-73.51	665.06
Group 2 Type 4 RB (E facing)	92.78	-72.27	871.30
Group 2 Type 5 RB (W facing)	85.84	-72.23	871.30

Table 2: Summary of the maximum achievable NPV (€) based on Site energy and the Site energy required to achieve maximum NPV (€) for all the 10 RBs

The same retrofitting measures for HVAC, lighting, hot water and building envelope required to achieve the cost-optimal MEPRS are to be implemented to achieve the highest NPV for all RB configurations. The only difference is that PVs are required to occupy 60% of the roof area instead of 20% in order to maximize the NPV. Measures that provide a low/negative NPV are common for all the 10 RBs analyzed. The measures are the following: 1) Maintaining natural ventilation during the winter period, 2) incorporate dimming (DALI), 3) not installing PVs, 4) not introducing SWHs (preferable) or instant heaters and 5) Replacing Al windows with ones having a uPVC frame and 6) insulating roofs and external walls to achieve lower than Technical Guide F(7) U-values

4. DISCUSSION

From Table 1, it can be seen that for each of the ten (10) RBs, there is a considerable difference in initial ED, with the highest demand resulting for the East facing glazing configurations due to the highest space heating demand. It can also be noticed from Table 1, that for all the 10 different RBs, the MEPRS is circa 0 kWh/m²/annum. However, despite this similarity, there is

major difference in the global cost (€/m²) and NPV (€) required to achieve the MEPRS for the different RBs.

RBs with S and N facing glazing building configurations achieve the lowest NPV, due to a lower demand for space heating, while E facing and W facing RBs achieve the highest NPV (€) over a 30 year period despite having the largest Global Cost (€/m²). The E facing and W facing RBs therefore have the largest investment potential from an investor's point of view when it comes to achieving MEPRS.

Given that the COMet of different RBs resulted in the same MEPRS with the same required retrofitting measures, defining multiple RBs is not required from a policy point of view. However, from an investor's point of view, given that the global cost and NPV are very dependent on the particular building orientation/construction, it is beneficial to have a tool as described in Section 3.4, where the resulting Global Cost and NPV to achieve MEPRS for any specific PPSBs can be found easily.

Positively, applying retrofitting measures to achieve cost-optimal MEPRS results in a significantly positive NPV (even when based on site energy) for all the 10 analysed RBs. This positive NPV means that the retrofitting of PPSBs to achieve MEPRS does have a possible investment potential. As is also depicted in Table 2, maximum NPVs coincided with the greenest energy ratings, so it makes sense from an investor's and policy perspective (to achieve 10% RES by 2020) to aim for the COMs that achieve maximum NPV rather than MEPRS. Measures that result in a low NPV (e.g. insulation) when based on site energy may however make sense from a Government point of view given that NPV based on the primary energy is much larger than that calculated based on the site energy, but incentives are required to be introduced for these measures to be attractive to the private investor.

5. CONCLUSION

The study has provided an innovative and energy efficient approach for the determination of MEPRS for PPSBs, by using an adaptive comfort approach and a customised approach for the determination of the MEPRS. It was shown that such customized approach may be more important from an economic rather than a policy point of view to facilitate the retrofitting implementation of PPSBs in Malta.

The results have shown that all existing schools of all orientations can achieve real zero-net energy and produce positive NPV over 30 years. The Excel tool that was developed can be used by any authority to choose the best set of EE measures that are best suited for different orientations of the different wings of the same school, as well as for the different floors within the same school.

The implementation of PVs is shown to be a good choice in terms of achieving high NPV results. However, one has to appreciate that the EE Directive is more concerned about EE and hence it should be stressed that EE measures have to go hand in hand with RES, also to ensure that the consumption of energy does not increase in the future, simply because renewable energy is being generated.

REFERENCES

- European Parliament. Directive 2010/31/EU of the European Parliament and of the council of 19 May 2010 on the energy performance of buildings (recast). 2010.
- European Parliament. Directive 2012/27/EU. Off J Eur Union. 2012;L315/1:1–56.
- De Santoli L, Fraticelli F, Fornari F, Calice C. Energy performance assessment and a retrofit strategies in public school buildings in Rome. *Energy Build* [Internet]. Elsevier B.V.; 2014 Jan [cited 2014 Jul 26]; 68:196–202. Available from: <http://linkinghub.elsevier.com/retrieve/pii/S0378778813005252>
- De Giuli V, Da Pos O, De Carli M. Indoor environmental quality and pupil perception in Italian primary schools. *Build Environ* [Internet]. Elsevier Ltd; 2012 Oct [cited 2014 Jul 17];56:335–45. Available from: <http://linkinghub.elsevier.com/retrieve/pii/S0360132312001163>

- Haverinen-Shaughnessy U, Moschandreas DJ, Shaughnessy RJ. Association between substandard classroom ventilation rates and students' academic achievement. *Indoor Air* [Internet]. 2011 Apr [cited 2014 Aug 13];21(2):121–31. Available from: <http://www.ncbi.nlm.nih.gov/pubmed/21029182>
- EN 15251 European Standard. Indoor environmental input parameters for design and assessment of energy performance of buildings—addressing indoor air quality, thermal environment, lighting and acoustics. 2007.
- Malta Services Division Building Regulations Office. Technical Guidance Document F, Conservation of Fuel, Energy and Natural Resources (Minimum requirements on the energy performance of buildings regulations, 2006) [Internet]. Malta; 2006. Available from: http://www.bicc.gov.mt/bicc/files_folder/Cons Fuel Energy Doc F new.pdf



SBE16
MALTA
INTERNATIONAL CONFERENCE

**Europe and the Mediterranean
Towards a Sustainable Built Environment**

Chapter 6

Renewable Energy Sources

Wind Energy Technology Reconsideration to Enhance the Sustainability Features of Smart Cities

Charalampos Baniotopoulos

University of Birmingham, Edgbaston, Birmingham B15 2TT, United Kingdom

Sustainable development is tightly related to the fate of sustainable energy. According to the Horizon 2020 decisions, EU countries ensured their commitment to reduce greenhouse gas emissions by 20% by 2020 with the objective of a further reduction up to 80-95% by 2050. Along this line, future cities aim at 15% of renewable energy in terms of produced energy by renewable sources. In other words, sustainable energy is energy obtained from non-exhaustible resources and in this sense, sustainable energy by definition serves the needs of the present without compromising the ability of future generations to meet their needs. Technologies that promote sustainable energy include renewable energy sources, such as wind energy, and also technologies designed to improve energy efficiency.

Nowadays, the major contributors of locally produced renewable energy are photovoltaic systems, solar panels and combined heat power systems, and the significant potential from wind energy to complement them. According to the Kyoto Protocol, the latter technology provides one of the most robust technologies to meet the increasing energy demand without compromising the environment.

During the last years the cost of sustainable energy has significantly fallen and continues to fall. Most of the aforementioned technologies are nowadays either economically competitive or close to being so. Increasingly, effective government policies support investor confidence leading to the expansion of these markets. Thus, considerable progress has been observed in the energy transition from fossil fuels to sustainable energies. It seems that it is now the appropriate time for all countries stakeholders to intensively collaborate in order to exchange expertise, to discuss open problems and disseminate the respective outcomes to stakeholders, engineers, designers, researchers, municipalities and governments.

This presentation is focused on two distinct research efforts that effectively contribute to this procedure of the enhancement of sustainable energy and in particular, the wind energy. The first one refers to repowering that is the replacement of the existing old wind turbines with fewer and taller ones being able to yield more energy. Focusing on the UK H2020 strategy, repowering seems to be an efficient and effective approach for the country to obtain the 15% renewable energy target by 2020. As of last year, 25 from the 600 wind farms had applied for repowering aiming to a total number of wind turbines to be reduced from 338 to 188, the average turbine tip height to be almost doubled from 52m to 96m, the average individual turbine capacity to be quadrupled from 0.5MW to 2MW and the total capacity to be almost tripled from 131MW to 385MW. It is therefore, obvious that the next years, repowering will be applied to all Aeolian farms in the UK requesting thorough investigations and robust propositions. In this framework, the enhancement of the structural response of tall wind turbines by improving the structural design and the detailing of the supporting structures will be the key point to reach the target of tip heights between 100-300m for the new tall towers.

Certain recently obtained research outcomes that serve this objective are here presented. As a matter of fact, innovative wind tower connections, new types of wind tower foundations and a variety of tower stiffening schemes contribute towards the success of any repowering process. The other important effort to better establish wind energy harvesting concerns the built environment wind energy technology. The recently launched WINERCOST Action with research groups from 29 EU countries work towards the enhancement of the Future Smart Cities concept by identifying prerequisites and conditions for the adoption of the Built Environment Wind Energy Technology into the urban and suburban habitat constructions. This is promoted by supporting relevant measures and actions, and trying to convince municipal authorities, decision-making groups and local societies themselves about the assets of the application of the Built Environment Wind Energy Technology exploitation in Smart Cities aiming to the enhancement of their sustainability and resilience features.

REFERENCES

Renewable UK: Wind Energy Database <http://www.renewableuk.com>

Offshore Wind Turbines: From Fixed-bottom to Floating Technologies

C. Borri

Dept. of Civil and Environmental Engineering, University of Florence

A. Giusti

Dept. of Civil and Environmental Engineering, University of Florence

E. Marino

Dept. of Civil and Environmental Engineering, University of Florence

G. Stabile

Dept. of Civil and Environmental Engineering, University of Florence

Email: dir-dicea@dicea.unifi.it

Abstract. This paper addresses the main general issues regarding both fixed-bottom and floating wind turbines. For the fixed-bottom technology, higher-order loading effects on the dynamic response of the tower are discussed. Hydro-aero-elastic simulations incorporating fully nonlinear wave models show that the linear wave model not only underestimates peaks in the system response but, even more importantly, it is not able to capture dangerous resonant phenomena triggered by the passage of nonlinear waves. For the floating technology, especially when moored barge-type platforms are considered, large displacements and rotations of the platform become relevant in rough sea states. A numerical approach based on a suitable Lie-group time integrator is here discussed, together with the models used for assessing the hydrodynamic and the mooring-line loads that should be coupled with the dynamic solver. The coupling is still being developed. In the present paper we limit the discussion to the main theoretical and numerical features of the model, leaving validations and applications to a forthcoming paper.

1. INTRODUCTION

Over the last decade, wind energy has become one of the most attractive renewable energy resource. In particular, the offshore wind technology experienced a tremendous growth that requires the development of accurate numerical tools to investigate the effects of the environmental loads on larger and larger wind turbines. Recently, offshore floating wind turbines have attracted increasing interest due to the larger energy potential and the reduced visual impact due to far offshore sites. Nevertheless, the development of fixed-bottom technologies still requires research on key topics for economic, safe and reliable designs. This paper gives a short overview about some of the main general issues regarding both fixed-bottom and floating technologies.

For the fixed-bottom case, we focus on the effects that high-order wave components have in terms of dynamic response and structural loads. The NREL 5-MW wind turbine is used as case study.

For the floating technology we emphasize the importance of large rotations dynamic solver for the platform and the fluid-structure interaction (FSI) problem of the mooring lines.

1.1. Fixed-bottom structure

As shown by Marino et al, standard linear wave theory leads to dangerous inaccuracies - significant peaks in the system response are underestimated causing unacceptable predictions. More importantly, linear wave models are unable to capture important resonant phenomena, such as ringing and springing. In parked condition, resonant vibrations are induced by the interaction of the structure with steep wave front. These phenomena are suppressed in power

production. When a slamming event associated with a breaking wave occurs, the maximum loads undergo an increase that is almost independent of the working condition of the turbine. Very high-frequency oscillations are observed in the tower-base fore-aft shear force and bending moment, whereas, apparently no evident influence on the tower-top displacements is observed. Limitations of weakly nonlinear wave models in capturing these phenomena are highlighted in.

We show that though current aero-elastic models provides an acceptable accuracy level for the numerical simulation of wind turbines, still overly simplistic linear or weakly nonlinear models for wave propagation are routinely used for the prediction of wave-induced loads on offshore wind turbines (OWTs). When severe sea and wind conditions occur, most of the linear or weakly nonlinear wave models fails in predicting the actual loading process, leading to large inaccuracies in the estimation of the global response of the system.

1.2. *Floating platform and mooring lines*

The exploitation of shallow-water wind energy is not always possible and feasible: a lot of available sites all around the Europe, but not only, are characterized by either a continental slope close to the coast or a very steep continental shelf, so that the available shallow-water sites are a very narrow stripe. Considering that generally it is not possible to build an offshore wind farm very close to the shore, mainly for the environmental impact of such constructions, the only chance is to move into the deep-water sites.

Depending on the water depth, several concepts of offshore support structures were proposed for wind engineering purposes. The floating platform concept was evaluated to be the most economical type of support structure for deep-water employments, whereas other concepts such as the bottom-founded wind turbines are only feasible in shallow waters.

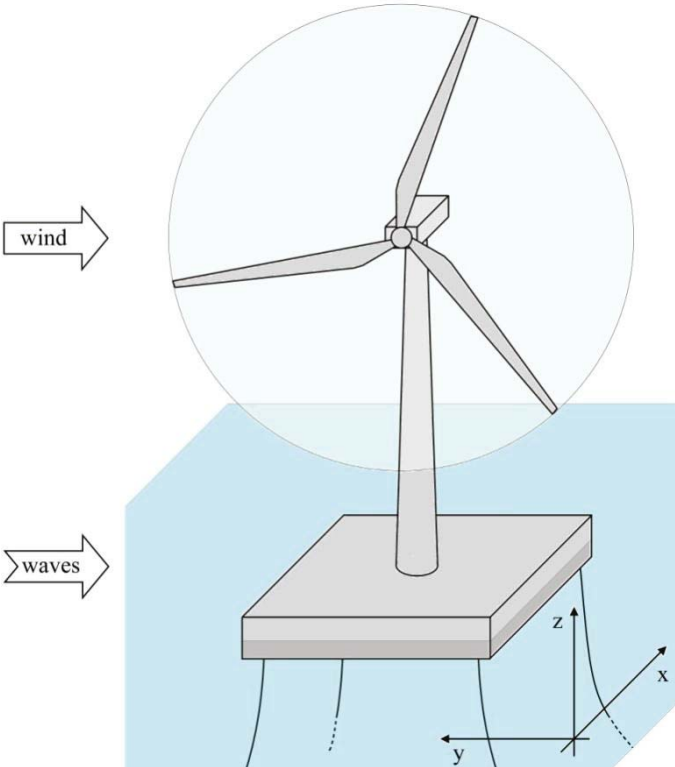


Fig 1. Offshore wind turbine with moored floating platform.

For these reasons, the study of the dynamics of a moored floating platform has a considerable importance and requires tools able to face the complexity of the problem. The

dynamic behavior of such systems depends on the interaction between the body, the fluid and the mooring system (catenary cables but also tension leg) analyzed in the more general case of large displacements. In fact the usual small-displacement assumption could represent a strong limit because it involves the linearization (i.e. first-order approximation) of the rotations that could lead to rough inaccuracies.

2. NUMERICAL SOLVERS

2.1. Fixed-bottom monopile supported WT

We couple a fully nonlinear wave solver with the hydro-aero-elastic simulator FAST of the entire system. FAST is a combined modal and multi-body solver able to model the rigid and flexible components of a wind turbine. Aerodynamic loads acting on the blades are calculated by means of AeroDyn. Hydrodynamic forces are calculated by means of a user-defined subroutine. The subroutine, at each time step, reads the nonlinear wave kinematics (provided by a high-order boundary element in-house solver) as input for the calculation of the hydrodynamics forces. For a detailed description of the numerical model we refer to.

The turbine model used in this study is the 5-MW Reference Wind Turbine for Offshore System Development, whose main characteristics are listed in Table 1. The diameter and the wall thickness vary linearly with the tower height. The base diameter of 6 m is equal to the diameter of the monopile.

Table 1: Main parameters of the baseline wind turbine model.

Rating Power	5 MW
Rotor orientation / conf.	Upwind, 3 blades
Rotor / hub diameter	126 / 3 m
Hub Height	90 m
Cut-in / Rated / Cut-out Wind Speed	3 / 11.4 / 25 m/s
Cut-in / Rated Rotor Speed	6.9 / 12.1 rpm
Rotor Mass	110 t
Nacelle Mass	240 t
Tower base and pile diameter	6 m
Tower top diameter / Wall thickness	3.87 / 0.019 m
Pile length	30 m
Pile mass	190 t
First Fore-Aft monopile natural frequency	0.28 Hz

2.1.1. Numerical simulations

We analyze the case of a severe sea state characterized by a significant wave height $H_s = 7.5$ m and spectral peak period $T_p = 15$ s. These sea conditions would likely occur under wind speeds much higher than the cut-out limit reported in Table 1, therefore the wind turbine is set in parked configuration with blades pitched to feather and the rotor idling. In parked condition, wind turbulence plays a minor role; thus, according to the chosen sea state, characterized by a wind speed of 26.5 m/s at 19.5 m asl, a hub-height constant wind speed of 33 m/s is used.

The effects of the nonlinear hydrodynamics, including breaking waves, are highlighted in Figure 2, where the response obtained using the proposed model are compared with the one based on the standard linear wave theory.

Figure 2 shows that at approximately 3080s, a steep and asymmetric wave triggers a resonant vibration. At about 3095s a steeper wave amplifies (doubles) the oscillations amplitudes for approximately one period T_p . Each of the subsequent nonlinear waves causes resonant vibrations persisting for about one T_p .

An impact event occurs at 3168.5 s; it causes two different effects: (i) a very high-frequency vibration in the tower-base shear force ($TwrBsFxt$) and in the bending moment ($TwrBsMyt$) that

persists for approximately one T_p ; (ii) an amplification of the fore-aft tower-top oscillations amplitudes (TTDspFA) which is about 80% larger than the underlying springing-like vibration. From the TTDspFA we observe that type (i) excitation is filtered out by the dynamical system and no trace is found in the tower-top motion.

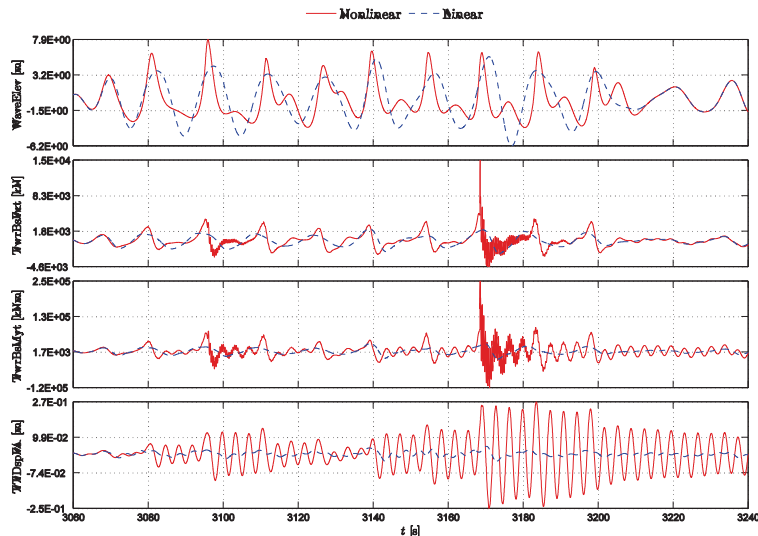


Fig 2. Comparison between the linear (blue dashed) and nonlinear (red solid) solutions of free surface elevation WeveElev (top panel), tower-base shear force TwrBsFxt, tower-base overturning bending moment TwrBsMyt, tower-top displacement TTDspFA.

2.2. Floating platform and mooring lines modelling

The platforms used for offshore wind engineering purposes can usually be sketched as a rigid body without any significant loss of accuracy. Thus the dynamic problem consists of solving the dynamics of a moored floating rigid body forced by the environmental loads. This is a complex problem of wind-wave-structure interaction where the sources of loads are due to the interaction between the structure (support and superstructure, i.e. tower, nacelle, rotor), the waves, the wind and the mooring system. If the wind turbine is considered in parked configuration, the aero-elastic-dynamic problem is simplified and the wind turbine can be considered as a rigid body rigidly connected to the platform. In this case the dynamic problem can be solved by addressing the following issues:

- dynamics of a six degrees-of-freedom rigid body;
- hydrodynamic load problem;
- mooring line load problem.

If the wind turbine is in power production condition, the previous tools should be coupled with the aerodynamic solver.

2.2.1. Dynamic solver

The dynamics of the system is analyzed by using a suitable Lie-group time integrator that solves the equations of motion treating the rotations as elements of the manifold of finite rotations $SO(3)$. This permits to account for large motions. The platform is modeled as a rigid body with all the six degrees of freedom whereas the wind turbine, considered in parked configuration, is represented only in terms of mass and inertia.

The rigid-body dynamic problem consists of solving the motion of the centre of mass and the motion about the centre of mass, considering that translations and rotations can be coupled together, for instance because of the hydrodynamic action (non-diagonal hydrodynamic added mass and damping matrices) or the follower forces. The dynamic solver is formulated by using a mixed reference frame approach, that is at each time step the algorithm works simultaneously with two different reference frames: the motion of the centre of mass is solved (and described)

in an inertial (fixed) frame, whereas the rotations are referred to a body-attached frame (non-inertial). Even if this choice leads to some complications in the formulation of the problem, the approach avoids considering the apparent forces in the translational problem and permits to maintain the time-invariance of the inertia tensor in the body attached frame which simplifies the conservation of the angular momentum. On the other hand some complications arise from the coupling of the translational and rotational problems, which implies, at any time instant, the loss of symmetry of all the main system operators (inertia, damping and stiffness) and their dependence on the actual rotation. However, even using other approaches, such as a total local frame formulation, the loss of symmetry cannot be avoided because of the gyroscopic (apparent) loads in the translation problem.

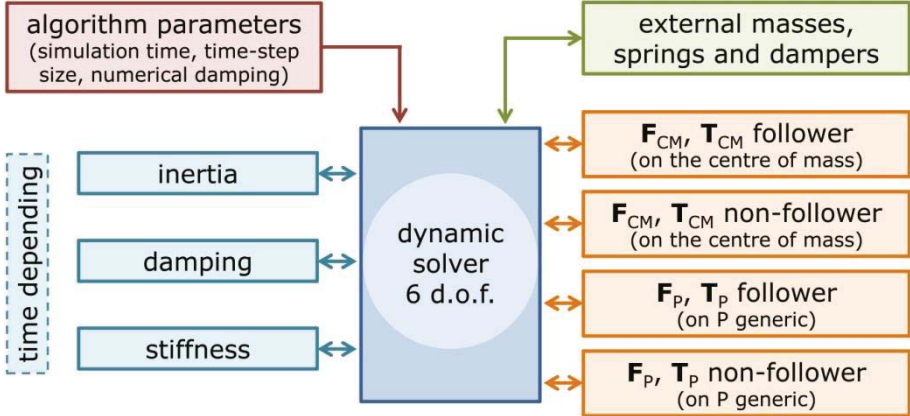


Fig 3. Sketch of the dynamic solver.

The dynamic solver (see Figure 3) is very flexible and permits to analyse a wide range of systems. It can deal with systems whose inertia, damping and stiffness properties vary in time, and can receive as inputs forces and torques (follower or non-follower) and external mass, damping and stiffness matrices. Moreover the loads can be applied both on the centre of mass and in a generic point of the body.

2.2.2. Hydrodynamic problem

The hydrodynamic problem consists in establishing the loads acting on the rigid body due to the interaction with the fluid, in this case the waves. The fluid is supposed incompressible, inviscid and irrotational, thus it is described by the Laplace equation. The fluid-structure interaction problem is solved under the linear assumption, i.e. addressing radiation, diffraction and hydrostatics separately. The first-order wave kinematics is numerically modeled by using a suitable IFFT procedure. The numerical model can simulate both regular and irregular seas and it is coupled with the dynamic solver described in the previous subsection in terms of external loads and added mass and damping matrices. A further step of the research is to include higher-order hydrodynamic effects in the analysis of floating wind turbines.

2.2.3. Mooring line problem

The mooring line system guarantees the constraints to the translations in the water plane and to the rotation about the vertical axis, thus it is fundamental for the functionality of the offshore wind turbine. The cables can be modelled by using a quasi-static theory, i.e. at any time instant each mooring line is considered to be in static equilibrium. This model can be accurate enough if and only if the mass of the cables is small with respect to the overall mass of the system. The quasi-static theory can account for the apparent weight in the fluid, the elastic stretching, the seabed friction (drag force) and the nonlinear geometric restoration of the complete mooring system. On the other hand the model neglects the individual bending stiffness, the inertia of the cables and their damping. These approximations could be a strong limit, especially when higher-order effects are addressed. The only way to account for the cable dynamics is the use of

a fully dynamic model. The equation of motion of the cables is quite complex and an analytical solution cannot be found. An alternative way is to solve the equation of motion with numerical methods that discretize the cable in number of masses linked together by joints either with a multi body or a FEM approach. Here the problem is assessed using a FEM method. Using such an approach the dynamics of the mooring lines can be completely captured. In many existing tools for the modelling of floating offshore wind turbines mooring lines are solved using a separate module. For this reason, the idea here is to use the same approach; each mooring line is structurally modelled using geometrically exact beam elements that can easily assess large displacements and rotations. Hydrodynamic forces acting on each mooring line are evaluated using a reduced order model.

The reduced order model consists of a combination of a state-space model and a forced Van der Pol oscillator. The parameters of the model are deduced from high fidelity analysis involving flexible cylinders undergoing forced vibrations. This model is developed to account the effect of the steady forces acting on the cable and to reproduce also the vortex induced vibration phenomenon.

The idea, as already mentioned, is to keep the platform module and the mooring lines module separated. For this reason, the coupling has to be realized using a partitioned approach. The input information of the whole analysis are the flow velocity profile, the aerodynamic forces acting on the tower and on the rotor, that in this context are considered just as an external applied force, and the mechanical characteristics of the mooring lines and the platform.

Using such an approach, the influence of the mooring lines on the platform is considered as an external restoring force while the influence of the platform on the mooring system is considered as an imposed motion on the top of each mooring line. A sketch which illustrates how the problem is previously decoupled and then re-coupled is shown in Figure 4. An example of a coupling algorithm that could be used for the purpose is represented in Algorithm 1. The algorithm is a block Gauss-Seidel algorithm normally used to couple different models. At each time step of the coupled simulation an iterative problem must be solved. The first step is the prediction of the restoring forces based on their last converged values at the previous time step. The choice of the predictor is not unique and several different orders and expressions could be used. Once the predicted value of the restoring force is determined, it is possible to solve the platform equation in order to get the displacements, velocities and accelerations at the fairlead points. These history of motions are then imposed to the top of the cables so that the mooring line problem is solved and a new restoring force is determined. In general the restoring force obtained during the mooring line computation is different from the predicted one, so an iteration procedure is required. The iteration process continues till the difference between the forces evaluated at two sequential iterations is smaller than a certain tolerance previously defined.

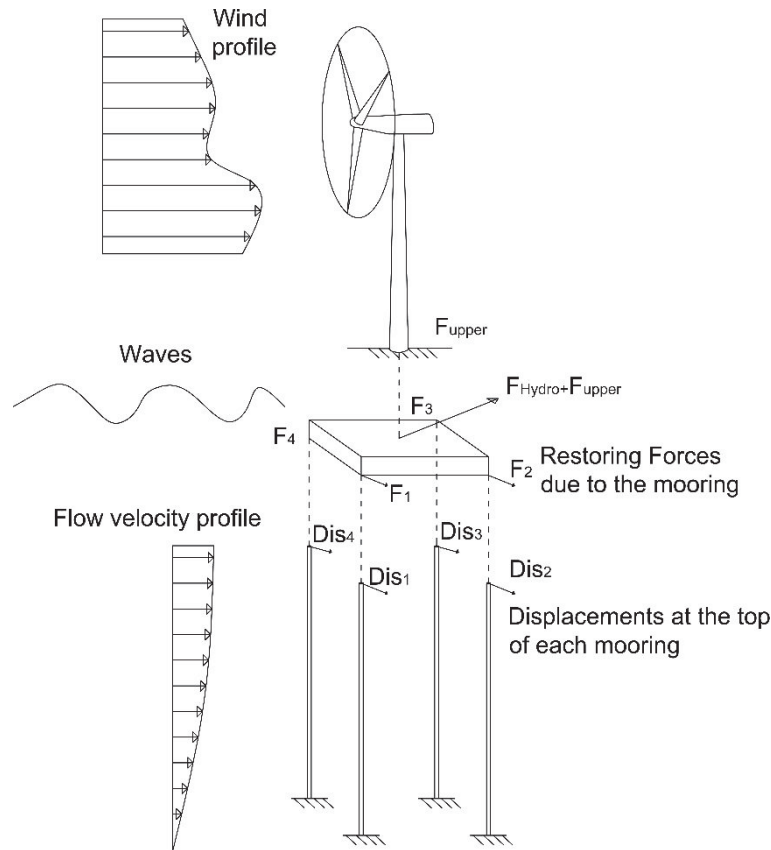


Fig 4. Sketch of the coupled interaction between wind, waves, floating body and moorings.

3. CONCLUSIONS

This paper has given a short overview about some of the main general issues regarding both fixed-bottom and floating technologies for offshore wind turbines.

For the fixed bottom case, a fully hydro-aero-elastic study based on the coupling between FAST for the aero-elastic simulation and an in-house solver for the hydrodynamic solution has been carried out. The hydrodynamic solver permits accounting fully nonlinear wave effects including impacts associated with breaking waves. It is shown that linear wave models (still widely used in the design practice) are unable to capture important resonant phenomena, such as ringing and springing. The significant underestimations of the response are expected to have important implications in terms of both extreme and fatigue loads.

For the floating case the finite rotation approach has been discussed. The dynamics of the floating platform, considered as a rigid body, is solved by using a suitable Lie-group time integration scheme which can account for large displacements without any loss of accuracy. This dynamic solver can be coupled with the set of tools necessary for assessing the environmental loads. In particular the hydrodynamic action is evaluated by means of a first-order theory, but for the future also higher-order theories will be considered. For the mooring system, a more sophisticated FEM model which solves the cables equation of motion. This model is moreover coupled with a hydrodynamic reduced order model capable both to consider the effect of the steady forces acting on the cable and to reproduce the vortex induced vibration phenomenon. The coupling is still under development. Preliminary tests show encouraging results. Validations and applications of the presented model will be discussed in a future work.

Algorithm 1 Coupling algorithm between platform and mooring modules

Given: initial time T_0 , length of the simulation T , time step size of the simulation Δt , the tolerance TOL , Flow Velocity Profile $U(t)$, Forces coming from the upper part $F_{upper}(t)$

```
while  $t < T$  do
   $k = 0$ 
  while  $res_{N+1}^{(k)} < TOL$  do
    if  $k = 0$  then
      for  $i = 1 : N_l$  do
        Predict restoring force:  $\hat{F}_{i,N+1}^{(0)} = P(F_{i,N}^{(k_{max})}, F_{i,N-1}^{(k_{max})}, \dots)$ 
      end for
    end if
    given  $\hat{F}_{1:N_l,N+1}^{(k)}$  solve the platform equation  $\rightarrow Dis_{1:N_l,N+1}^{(k)}$ 
    for  $i = 1 : N_l$  do
      given  $Dis_{1:N_l,N+1}^{(k)}$  solve the mooring problem  $\rightarrow F_{1:N_l,N+1}^{(k)}$ 
    end for
    Evaluate residual  $res_{N+1}^{(k)} = \hat{F}_{1:N_l,N+1}^{(k)} - F_{1:N_l,N+1}^{(k)}$ 
    Update restoring forces  $\hat{F}_{f,N+1}^{(k+1)} = F_{1:N_l,N+1}^{(k)}$ 
     $k = k + 1$ ;
  end while
   $N = N + 1, t = t + \Delta t$ 
end while
```

REFERENCES

- Agarwal, P. and Manuel, L. (2011). Incorporating irregular nonlinear waves in coupled simulation and reliability studies of offshore wind turbines. *Applied Ocean Research*, 33, 215–227.
- Brüls, O. and Cardona, A. (2010). On the Use of Lie Group Time Integrators in Multibody Dynamics. *Journal of Computational and Nonlinear Dynamics*, 5, 031002.
- Cardona, A. and Géradin, M. (1988). A beam finite element non-linear theory with finite rotation. *International Journal for Numerical Methods in Engineering*, 26, 2403–2438.
- Facchinetti, M. L., De Langre, E., and Biolley, F. (2004). Vortex-induced travelling waves along a cable. *European Journal of Mechanics-B/Fluids*, 23(1), 199–208.
- Faltinsen, O. M. (1990). *Sea loads on ships and offshore structures*. Cambridge University Press.
- Jonkman, J.M. (2009). *Dynamics of Offshore Floating Wind Turbines – Model Development and Verification*. *Wind Energy*, 12, 459–492.
- Jonkman, J., Butterfield, S., Musial, W., and Scott, G. (2009). *Definition of a 5-MW Reference Wind Turbine for Offshore System Development*.
- Jonkman, J. M., and Marshall, L. B. J. (2005). *FAST User’s Guide*.
- Marino, E., Borri, C., and Lugni, C. (2011). Influence of wind–waves energy transfer on the impulsive hydrodynamic loads acting on offshore wind turbines. *Journal of Wind Engineering and Industrial Aerodynamics*, 99(6-7), 767–775. doi:10.1016/j.jweia.2011.03.008.
- Marino, E., Borri, C., and Peil, U. (2011). A fully nonlinear wave model to account for breaking wave impact loads on offshore wind turbines. *Journal of Wind Engineering and Industrial Aerodynamics*, 99(4), 483–490. doi:10.1016/j.jweia.2010.12.015.
- Marino, E., Lugni, C., and Borri, C. (2013). A novel numerical strategy for the simulation of irregular nonlinear waves and their effects on the dynamic response of offshore wind turbines. *Computer Methods in Applied Mechanics and Engineering*, 255, 275–288. doi:10.1016/j.cma.2012.12.005.
- Marino, E., Lugni, C., and Borri, C. (2013). The role of the nonlinear wave kinematics on the global responses of an OWT in parked and operating conditions. *Journal of Wind Engineering and Industrial Aerodynamics*, 123, 363–376. doi:10.1016/j.jweia.2013.09.003.
- Marino, E., Lugni, C., Stabile, G., and Borri, C. (2014). Coupled dynamic simulations of offshore wind turbines using linear, weakly and fully nonlinear wave models: the limitations of the second-order wave theory. *Proceedings of the 9th International Conference on Structural Dynamics (EURODYN 2014)*.

- Marino, E., Stabile, G., Borri, C., and Lugni, C. (2013). A comparative study about the effects of linear, weakly and fully nonlinear wave models on the dynamic response of offshore wind turbines. In A. Zingoni (Ed.), *Research and Applications in Structural Engineering, Mechanics and Computation SEMC 2013*. Cape Town: Taylor and Francis Group, London, UK CRC Press.
- Moriarty, P. J., and Hansen, A. C. (2005). *AeroDyn Theory Manual*, NREL.
- Morison, J. R., O'Brien, M. P., Johnson, J. W., and Schaaf, S. A. (1950). The force exerted by surface wave on piles. *Petroleum Transactions (American Institute of Mining Engineers)*, 189, 149–154.
- Simo, J.C. and Vu-Quoc, L. (1988). On the dynamics in space of rods undergoing large motions – A geometrically exact approach. *Computer Methods in Applied Mechanics and Engineering*, 66, 125–161.
- Stabile, G., Matthies, H.G., and Borri, C. (2015). A Reduced Order Model For The Simulation Of Mooring Cable Dynamics, In: *Computational Methods in Marine Engineering VI – MARINE2015*, Salvatore, Francesco; Broglia, Riccardo; Muscari, Roberto, 387–400.
- Wienke, J., and Oumeraci, H. (2005). Breaking wave impact force on a vertical and inclined slender pile — theoretical and large-scale model investigations. *Coastal Engineering*, 52, 435–462. doi:10.1016/j.coastaleng.2004.12.008.

Variable Winds and Aerodynamic Losses of Transport Systems: A New Wind Energy Technology for Future Smart Cities

Tommaso Morbiato,

WindCity c/o Incubatore Fondazione Primo Miglio 1609 Vicenza, Italy

Claudio Borri,

University of Florence, Italy

Simone Salvadori,

University of Florence, Italy

Abstract: The main feature investigated is wind variability, focusing on its potential role as a "novel" resource, due to the fact that existing wind turbines tend to ignore turbulent components. Careful consideration is needed for those scenarios where variability is the main feature in wind, as in intensive traffic flows, where the continuous and rapid transit of vehicles in clusters, results in cycling and superposition of simple aerodynamic losses pulses is possibly able to energize the conversion device. Existing turbines are unlikely to be fitted for this unconventional wind source, that is highly unsteady just as the turbulent atmospheric flows found in urban/suburban sites, that are of particular interest for smart-cities and their sustainable development applications. In particular, the two winds have in common a major component in the large scale of eddies (0.015 Hz range), whose high energy content is well known, together with its harvesting challenges.

Keywords: VAWT, urban boundary layer, smart-cities, LCOE

1. OBJECTIVES IN THE SCOPE OF SUSTAINABLE ENERGY POLICIES

The objective for Future Smart Cities of EU Programme H2020 aims at 20% of renewable energy in terms of produced electricity by renewable sources. The project will contribute to develop an innovative wind energy conversion system that is fully integrated in the built environment sustainable development concept, arriving to comply with emerging energy & transport integrated policies worldwide (e.g. FHWA). The state of the art in flows past moving vehicles [Mat], and a recent study funded by Progetti di Eccellenza Fondazione Cariparo about resource assessment and harvesting feasibility in the road case study [Mor2], stand as a solid rationale for the project. Both the two main goals of our Proposal comply with Project topics in the European Programme for Environment and Climate Action (LIFE Regulation 2014-2020): in fact wind energy conversion from the aerodynamic losses of ground vehicles will reduce the carbon footprint of the transport systems, and the net gain from prior-art obtained by our new SMWT concepts in generic variable winds will re-insert energy in the circular economy principle: turbulent flows nowadays neglected as waste will be turned into a resource. Contrary to other renewables, the aerodynamic losses belong to a source of costs, that will still be present in the horizon of the next-generation transports fossil-fuel free. Our latest studies [Mor1] show that the capacity factor of state-of-the-art SMWT can arrive up to a 20% gain for a coupled application of atmospheric wind and aerodynamic losses, making them a remarkably sustainable potential energy resource.

Based on our previous results for the simple road case [Mor3], as a first milestone, energetic balance has to be reconsidered in relevant transport systems schemes: (a) railway; (b) more complex confined spaces, i.e. flow acceleration at road tunnel exits (natural ventilation typology); (c) by introducing the energy conversion device in the above case s; (d) vehicles

classes and carrier types conveying major aerodynamic losses shall be pointed out for both SMWT applications: (d.1) on-site and (d.2) embedded in the vehicle, the corresponding dragged flows shall be characterized in space/time, and turbulent structures shall be identified in the systems.

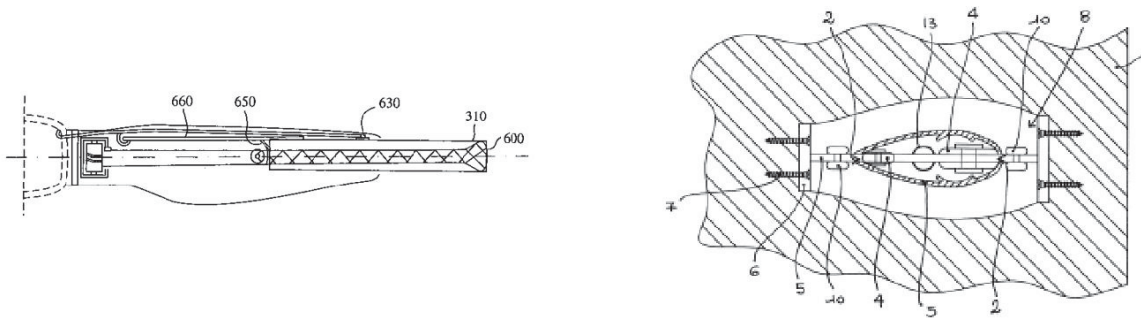


Fig 1. An innovative adaptable rotor concept for a HAWT with variable diameter (top) from P. Jamieson (DNV-GL), and a sketch of the adaptable radial arm from the patenting VAWT rotor of the Propos al (bottom).

The main feature of this novel wind resource is variability: careful consideration is needed for intensive traffic flows, where the continuous and rapid transit of vehicles in clusters, results in cycling and superposition of simple pulses is able to energize the conversion device. Existing turbines are unlikely to be fitted for this unconventional wind source, that is highly unsteady just as the turbulent atmospheric flows found in urban/suburban sites. In particular, the two winds have in common a major component in the large scale of eddies (0.015 Hz range), whose high energy content is well known, together with its harvesting challenges.

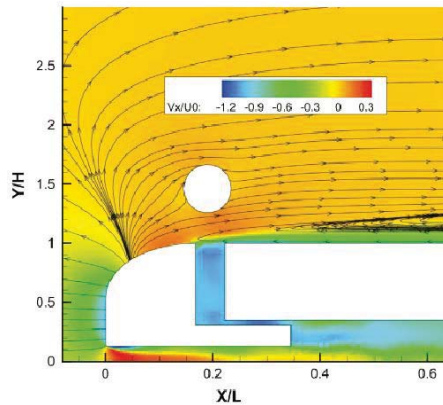
In particular, drag and lift drive n vertical-axis wind turbines (VAWT) will be considered for their omni-directional features. Variable speed operation of wind turbines is a technology that, through power electronics, allows for high performance in a wide range of wind speeds, while fixed speed operation only allows for maximum power extraction at the rated wind speed. High costs of the electronic components in large WT limited its application, while the relatively low costs in SMWT potentially favor its realization. Therefore, assuming electrical power feasibility, the project research and development will focus on maximizing the input mechanical power in variable speed operation, aiming to test new mechanical and aerodynamic concepts of adaptable rotors, suitable for transport systems losses harvesting, and thus generally as a novel turbine that is variable-wind specific. Adaptable rotors are on the cutting edge of innovation in wind turbines technology as they enable a power extraction gain from baseline, and the Research Group has already the opportunity to test such features on a new VAWT concept currently in Patent Cooperation Treaty filed Nov 2014 (Figure 1).

2. STATE-OF-THE-ART AND PRELIMINARY RESULTS

Given the trans-disciplinary nature of our Project, its scientific rationale shall develop from the state-of-the-art of different disciplines. The study of flows induced by transport systems with the corresponding aerodynamic losses, and of flows in confined spaces (e.g. natural ventilation tunnels and urban canyons) allows the calculation of the Energy Balances for the physical systems of interest. Many recent patents address the idea of harvesting wind energy from aerodynamic losses in motorways and railways, however a specific SMWT concept dedicated to the task has never been described nor claimed. The new trends in Built Environment Wind Energy Technology for the Smart-cities, and the challenging research in the energy content and harvesting from largest eddies range of turbulent flows, will indicate the path for the innovation proposed in turbine mechanics and aerodynamics. Up-to-date SMWT Power Electronics [Zar] for Energy Storage or grid integration will guide the development of the power train to be associated with our turbine project. Finally, Renewable Energy Economics provide the framework to analyze capacity factor gains and corresponding levelised cost of electricity parameters (LCOE) for the new applications business ideas & plans. The most recent results in some of the aforementioned parent disciplines were obtained by the research group of this

Proposal, in many cases thanks to the Progetti di Eccellenza Grant (2010-2013) funded by FCRPR:

Energy balance [Mat] for the case of single and multiple truck-panel interaction: a 3D CFD simulation restricted to the cylinder/wind turbine shape interaction demonstrate that the truck drag coefficient is unaffected by the passage of the obstacle upon the roof, giving chances for the application of an energy device near the vehicle (Figure 2), as the extra energy loss is negligible;



Type	Name	L_p^*/L	Energy loss ratio (%)
Rectangular	P_{n1}	0.02	+1.42
	P_{n2}	0.04	+1.95
	P_{n3}	0.08	+3.47
Circular	P_{n4}	0.08	+0.37
	P_{n5}	0.1	+1.23
	P_{n6}	0.14	+1.47

Fig 2. Flow field rounding the cylinder ($Z=0$, $tU_0/L=0.12$) and Required energy boost to keep the speed constant, where L_p^* is the panel dimension, and L the truck reference dimension

Resource assessment for the open-road case [Mor1]. An in-situ anemometry campaign provided the gross wind energy harvestable from a typical daily traffic on a motorway, and the main unsteady feature of aerodynamic losses i.e. the wind drops between two passages of carriers. The associated power reduction factor has been detected by numerical simulations with a blade-element momentum (BEM) code that is validated via wind-tunnel tests, allowing the estimation of the traffic-induced capacity factor gain from baseline for a SMWT (Figure 3) that is remarkably up to a +20%.

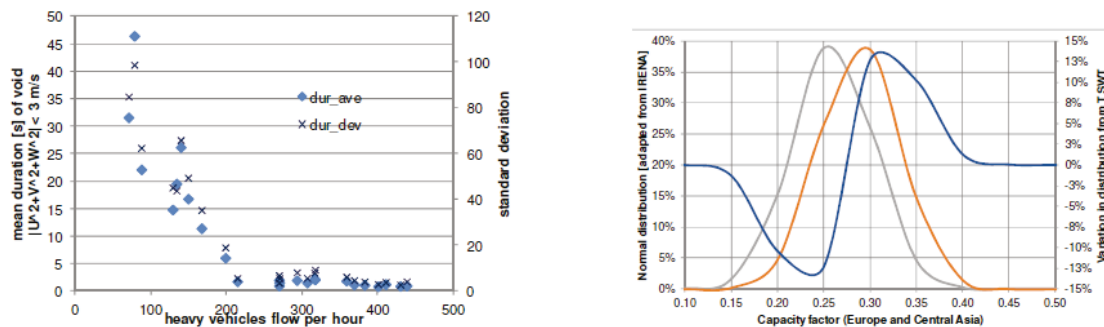


Fig 3. Unsteady features of traffic-induced wind and its capability to increase the capacity factor of a mini-VAWT

Preliminary transient BEM simulations of a new concept of mini-VAWT show a promising increase in energy conversion from variable winds respect to the prior-art: the novel adaptable rotor concept might be capable not only to envelop the power curve of the corresponding fixed geometry rotors, but also to extract power during wind drops where prior-art rotors cannot.

3. EXPECTED RESULTS FOR INNOVATIVE VAWT ROTORS

The project will demonstrate how is possible to extract energy from the largest scales of turbulent flows by means of an innovative concept of passively adaptable rotor VAWT. The energy containing range of the variable part of the wind will be considered for harvesting: as a

reference, will be studied also the bio-mechanical systems such as the albatross flying in dynamic soaring, where the energy lost to overcome drag is successfully recovered by the wings from a variation in wind speed (Figure 4). The research to extract energy from turbulent wind is also active in the field of sailplane studies and piezoelectric conversion.

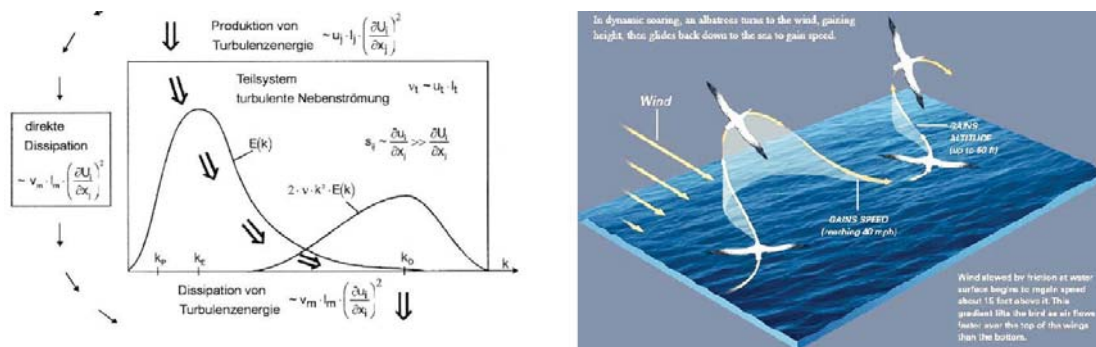


Fig 4 A bio-mechanical system extracting energy from variable wind, and a conceptual vision from Schatzmann of the energy transfer in turbulent flows spectra from large scales (small k) to dissipation in small scales.

Having different possibilities for application of the new rotor shall be a key to diversify and success. The focus on atmospheric variable winds will contribute to the built-environment wind energy technology, fostering smart-cities concepts. The focus on transport systems induced winds at low for a series of on-site energy conversion case studies along roadways, tunnel-exits, railways... but also for a different series of “relative motion” case studies, i.e embedding the mini-VAWT in the vehicle (truck, trailer, train, boat...). All of them foster sustainable development in the H2020 circular economy objectives.

For ground installations, borrowing the same testing approach used for open-road, the traffic-induced resource will be also assessed for a road confined space (flow acceleration at a tunnel exit) and a railway (high-frequency passages at lines confluence). Thus the complete picture for transport on-site installations will be achieved.

The support of CFD simulations will be of great benefit also to evaluate embedded installations, both prior-art ideas and our new concepts : the top of a truck or a train (freight/passenger) are both case studies where variation of inlet is relevant, and thus the adaptable rotor is suitable. A preliminary assessment to choose a fitting set of CFD models can be performed via our BEM transient code (a software already implemented and calibrated with wind tunnel tests). The estimation of the net energy harvested by the rotor, i.e. taking into account the power reduction factor associated to wind-drops (distance between passages in ground installations, or vehicle speed variation in embedded) will be also possible through the transient BEM code. Simulation is feasible in general for any transport system: in fact it is sufficient to choose the correct wind inlet and generator/power train models. The final performance assessment will come from the design, prototyping and experimental testing of the new VAWT, where preliminary estimations could be validated. At least two adaptable rotor prototypes (H-Darrieus and Savonius families) will be tested both in our boundary layer wind tunnel (BLWT) facilities and finally as a pilot on-site (road tunnel exit or railway).

Finally, business ideas and models of the best performing application cases will be evaluated for feasibility in the framework of Energy Economics, including the Levelised Cost of Electricity (LCOE) parametrization, comparing investments to effective energy production. It is worth noting that most recently SMWT applications as the ones in this Proposal display optimum LCOEs compared to giant off-shore wind turbines, photovoltaic, and concentrated solar power. SMWT share with biomass (anaerobic digestion), hydropower, and geothermal applications the outstanding achievement of competing in LCOE with fossil fuel power (source IRENA). Other parametric studies will also include health and climate damage savings, valuable for novel and upcoming energy mix policies. Following EU energy policy, also in Italy the DM 6/7/2012 applies the feed-in tariff (FIT) to SMWT (1-20 kW): the energy extracted by SMWT is paid by FIT about 153% of the normal electricity cost. This reflects in SMWT worldwide annual growth is +27.5% in forecast until 2020.

REFERENCES

- Morbiato T., Vitaliani R., Colladet S., Allori D., Gallo A., Aerodynamic Losses of Transport Systems as a New Wind Energy Market: Evaluation of the Behaviour of a mini-VAWT, Proc. of the 1st Workshop Trends and Challenges for Wind Energy Harvesting, COST Coimbra 2015
- Morbiato T., Borri C., Vitaliani R., Wind Energy Harvesting from Transport Systems: A Resource Estimation Assessment, J. Applied Energy 133 (2014) 152–168
- Morbiato T., Vitaliani R., Wind Energy from Road Traffic: a Resource Estimation, Proc. of the European Wind Energy Association Annual Event, Barcelona 10-13 March 2014
- Mattana A, Salvadori S., Morbiato T., Borri C., On the Ground-vehicle Induced Flows and Obstacle Interaction for Energy Harvesting Purposes, J. Wind Eng. and Industrial Aerodyn., 124: 121-131, 2014
- Zaragoza J., Pou J., Arias A., Spiteri Staines C., Robles E., Ceballos S., Study and experimental verification of control tuning strategies in a variable speed wind energy conversion system, J. Renewable Energy (2011) 1421-1430, Elsevier 2011.

Wind Energy Potential in Venturi-shaped Roof Constructions

B. Blocken

Department of the Built Environment, Eindhoven University of Technology, P.O. Box 513, 5600 MB Eindhoven, the Netherlands

Department of Civil Engineering, Leuven University, Kasteelpark Arenberg 40 – bus 2447, Leuven, Belgium

T. van Hooff

Department of the Built Environment, Eindhoven University of Technology, P.O. Box 513, 5600 MB Eindhoven, the Netherlands

Department of Civil Engineering, Leuven University, Kasteelpark Arenberg 40 – bus 2447, Leuven, Belgium

L. Aanen

Peutz BV, P.O. Box 66, 6585 ZH Mook, the Netherlands

B. Bronsema

Bronsema Consult, Prof. Boerhaaveweg 37, 2251 HX Voorschoten, the Netherlands

Email: b.j.e.blocken@tue.nl

Abstract. A venturi-shaped roof for integration of a Vertical Axis Wind Turbine (VAWT) in the narrowest part of the roof contraction is analyzed with 3D Computational Fluid Dynamics (CFD). Three roof types are considered: a roof with 36 vertical guiding vanes, a roof with 4 vertical guiding vanes and a roof without vertical guiding vanes. The roof is positioned on top of a 50 m high isolated building. The CFD simulations are performed with the steady Reynolds-Averaged Navier-Stokes equations and the RNG k - ϵ turbulence model and validated with reduced-scale wind tunnel measurements. The simulations show that adding vertical guiding vanes does not improve the performance of the roof, but actually cancels its effect and reduces its wind energy performance to values that are equal to or even lower than those of a free-standing VAWT at the same height, which is a counter-intuitive result. The simulations also show that, of the configurations investigated, a contraction ratio of 6.3 provides the largest improvement of wind energy potential (260% compared to free-standing VAWT), although the absolute value of energy yield is limited due to the limited contraction height.

1. INTRODUCTION

Campbell and Stankovic distinguish between three categories of possibilities for integration of wind energy generation systems into urban environments: (1) siting stand-alone wind turbines in urban locations; (2) retrofitting wind turbines onto existing buildings; and (3) full integration of wind turbines together with architectural form. The present paper focuses on category 3. Well-known examples of buildings designed for integration of large-scale wind turbines are the Bahrain World Trade Center, the Strata Tower in London and the Pearl River Tower in Guangzhou, China.

Sharpe and Proven mention the following six desirable characteristics for building-integrated wind turbines: (1) Building integrated for visual performance; (2) Building integrated for augmented flow; (3) Scalable and economic through modularity; (4) Good power output in turbulent and gusting sites; (5) Ease of installation; and (6) Applicable in a wide variety of locations.

Driven by the concept of building-integrated wind energy systems (category 3) and by the six desirable characteristics, the present paper addresses the assessment and optimization of the wind energy potential of a venturi-shaped roof for integration of a VAWT. This roof was designed by Bronsema in 2005 and later further developed by him (figures 1 and 2). It consists of a disk-shaped roof construction that is positioned at a certain height above the actual

building, creating a contraction that should provide significantly increased wind speed in the center of the contraction, where the VAWT is positioned to harvest wind energy. For assessment and optimization of its wind energy potential, the wind flow around the building and through the roof need to be analyzed in detail.

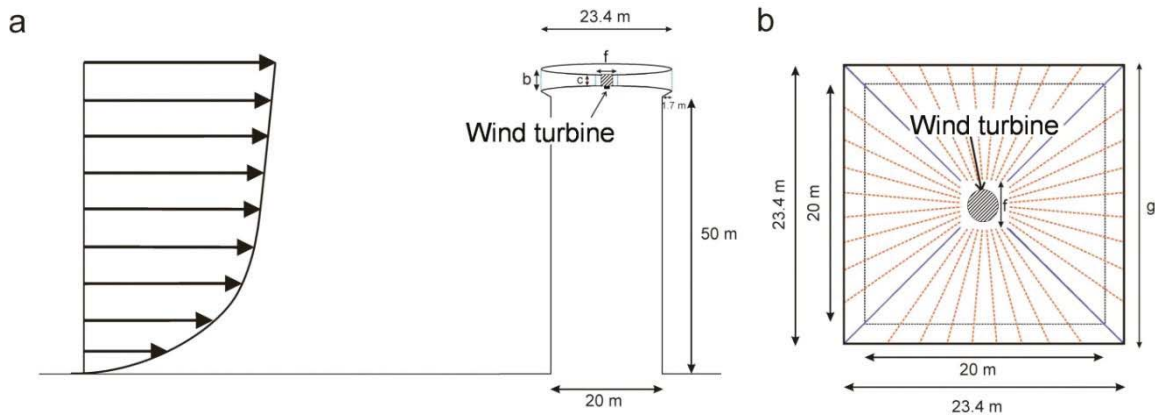


Fig 1. Geometry of the building under study. (a) Vertical cross-section showing the building with the disk-shaped roof and the parameters b and c (not to scale). (b) Horizontal cross-section and position where the turbine will be positioned. The solid blue lines represent the guiding vanes positioned at every 90° interval, the dashed orange lines represent the guiding vanes at every 10° interval.

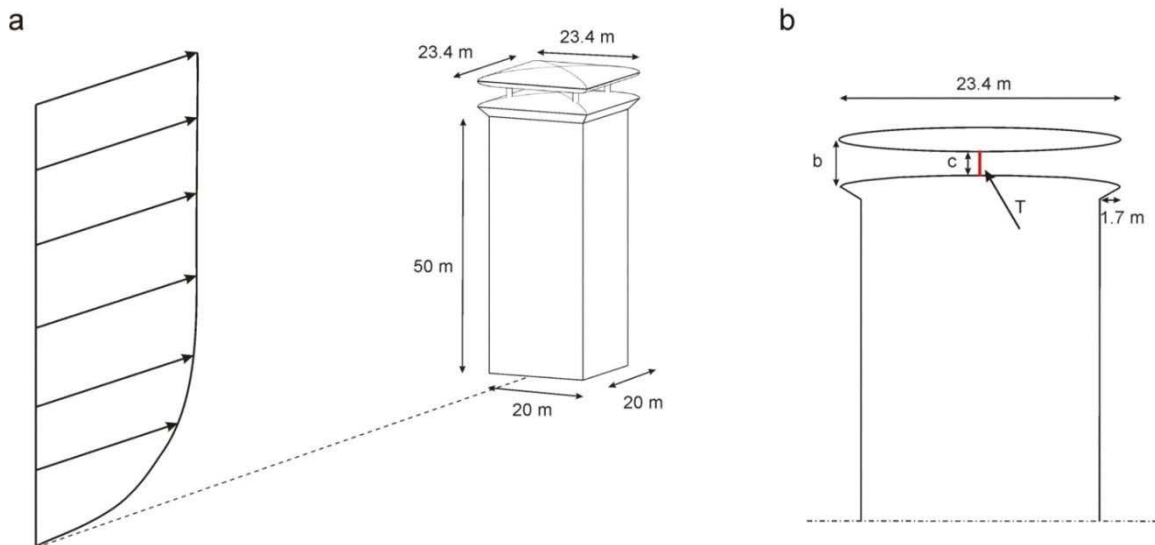


Fig 2. Geometry of the building under study. (a) Perspective view. (b) Vertical cross-section with line T at which wind speed and wind energy potential will be evaluated.

2. BUILDING AND ROOF GEOMETRY

The analysis is performed for a similar building as in. The building has a rectangular (20 m x 20 m) floor plan and a height of 50 m, measured up to the edge of the roof (figure 1a). The venturi-shaped roof consists of two parts (figure 2). The lower part is constructed from half a “square disk” with dimensions 23.4 m x 23.4 m x 2 m (L x W x H) and it is positioned directly on top of the building, this way creating a roof overhang of 1.7 m on each side of the building. At a distance ‘ c ’ above this part of the roof a full “square disk” is positioned with dimensions 23.4 m x 23.4 m x 4 m (L x W x H), resulting in a nozzle-shaped roof entrance from all four sides of the building. This part of the roof can be supported by e.g. a set of slender vertical columns or by vertical guiding vanes. The position of interest is that of the VAWT in the center of the roof

contraction (figure 1). The wind speed amplification factor and wind energy potential will be evaluated along line T (figure 2b). Two sets of geometrical roof configurations are considered, each of which corresponds to one stage in the two-stage optimization procedure. The first set consists of roof configurations with a varying number of vertical guiding vanes, as shown in figure 1b. From this set, the best configuration is selected to build the second set. The roof configurations in the second set differ from each other by the contraction height c and the contraction ratio b/c (see figure 1, 2).

3. CFD SIMULATIONS: COMPUTATIONAL SETTINGS AND PARAMETERS

The building is isolated and positioned on rough suburban terrain with an aerodynamic roughness length $z_0 = 0.5$ m. The computational domain has dimensions $L_D \times W_D \times H_D = 1020$ m \times 1020 m \times 300 m. High-quality and high-resolution computational grids are constructed using the grid generation technique presented by van Hooff and Blocken and taking into account best practice guidelines. The grids are block-structured and are discussed in more detail in section 5. The inlet boundary conditions are the vertical profiles of mean wind speed U , turbulent kinetic energy k and turbulence dissipation rate ε . The profile of U is a logarithmic law $U = (u^*/\kappa)\ln((z+z_0)/z_0)$ with $u^* = 0.956$ m/s the friction velocity, κ the von Karman constant ($\kappa = 0.42$) and z the height coordinate. Turbulent kinetic energy k is calculated from the longitudinal turbulence intensity I_u using $k = 0.5(I_u U)^2$. Turbulence dissipation rate $\varepsilon = (u^*)^3/(\kappa(z+z_0))$. Simulations are made for four wind directions: 0° , 15° , 30° and 45° . At the ground and building surfaces, the standard wall functions by Launder and Spalding are used with the sand-grain based roughness modification by Cebeci and Bradshaw. For the ground surface, the parameters k_S and C_S are determined using their appropriate consistency relationship with z_0 : $k_S = 9.793z_0/C_S$. The building surfaces are assumed to be smooth ($k_S = 0$ m and $C_S = 0.5$). Zero static pressure is imposed at the outlet of the domain and the top of the domain is modeled as a slip wall (zero normal velocity and zero normal gradients of all variables). The commercial CFD code Fluent 6.3.26 is used to solve the 3D Reynolds-Averaged Navier-Stokes (RANS) equations in combination with the Renormalization Group (RNG) k - ε turbulence model. Pressure-velocity coupling is taken care of by the SIMPLE algorithm, pressure interpolation is standard and second-order discretization schemes are used for both the convection terms and the viscous terms of the governing equations.

4. CALCULATION PROCEDURE FOR WIND ENERGY POTENTIAL

For assessment of the wind energy potential, a VAWT is selected. The basic features of the VAWT analyzed in this paper are identical to that studied by Balduzzi et al., but where the height of the VAWT is adjusted to fit the height of the contraction (i.e. the value of the parameter c , see figure 1). The main characteristics of the VAWT and its power output curve can be found in. For other c values, the turbine characteristics remain the same, only the turbine height is adjusted, and the power output curve scales linearly with the turbine height. The assessment of the yearly wind energy potential should be performed based on the wind speed statistics of the location of interest. The present study uses the 30-year wind speed statistics of Eindhoven airport which are described by Weibull distributions for each of the 12 wind direction sectors. These statistics refer to the wind speed U_{10} at a height of 10 m over terrain with $z_0 = 0.03$ m. Because all values of wind speed and wind energy potential in this paper are related to the wind speed at building height (= 50 m) U_{50} , the statistics are converted from wind speed at 10 m to wind speed at 50 m over terrain with $z_0 = 0.5$ m based on the logarithmic profiles of mean wind speed. This yields: $U_{50} = aU_{10}$ with $a = 1.276$. In addition, the venturi-shaped roof is expected to increase the free-stream wind speed U_{50} in the narrowest part of the roof contraction with a factor AF (the wind speed amplification factor), which is the ratio of the mean wind speed averaged along line T (figure 2b) to the undisturbed wind speed U_{50} . Both factors a and AF are integrated in the Weibull distributions, to provide the exceedance probabilities of mean wind speed at the position of the VAWT. The wind energy potential is calculated based on the Weibull distributions and the method of bins and is expressed both as a

wind energy enhancement factor (EF) and as yearly wind energy production in kWh. EF is defined as the yearly wind energy potential of the VAWT in the venturi-shaped roof, divided by the yearly wind energy potential of the same VAWT in undisturbed flow conditions (i.e. without building and without venturi-shaped roof, but at the same height of 50 m).

5. FIRST OPTIMIZATION STAGE: INFLUENCE OF VERTICAL GUIDING VANES

In the first optimization stage, the influence of vertical guiding vanes is investigated. Configuration A has 36 guiding vanes (one at every 10° interval), configuration B has 4 guiding vanes (one at every 90° interval), and configuration C has no guiding vanes. These configurations are schematically indicated in Figure 1b. They were tested for two different set of values of the parameters c and b (i.e. four different contraction ratios): (a) $c = 1$ m, $b = 5$ m, $b/c = 5$; (b) $c = 4$ m, $b = 8$ m, $b/c = 2$. The computational geometries and computational grids for the three configurations for $c = 1$ m are shown in figure 3. A detailed grid-sensitivity analysis was performed indicating that the grids shown in figure 3 provide nearly grid-independent results. The grid-sensitivity analysis is reported in and will not be repeated here. Wind tunnel measurements were performed for the three configurations A, B and C for $b = 5$ m and $c = 1$ m. The details can be found in. Figure 4 compares the numerically simulated and measured mean wind speed ratios U/U_{50} in the middle point of line T in the center of the roof contraction for each of the four wind directions 0° , 15° , 30° and 45° . The deviations between simulations and measurements are generally equal to or smaller than 10%, which is considered a very close agreement. Note that the values of the ratio U/U_{50} in this figure are not equal to the wind speed amplification factors AF, because the latter are values that, in this paper, are averaged along line T and averaged over the four wind directions. These averaged values are considered in the remainder of this paper. Table 1 shows that the wind speed amplification factor (AF) for configurations A and B (with vertical guiding vanes) is in the range 0.8-1.0, while that for configuration C (without vertical guiding vanes) is in the range 1.2-1.3. This implies that a fairly high AF can be achieved with this venturi-shaped roof, on condition that no vertical guiding vanes are added. Indeed, adding vertical guiding vanes strongly reduces the AF.

Table 1. Results of CFD analysis for roof configurations with and without vertical guiding vanes. AF is the wind speed amplification factor and EF the wind energy enhancement factor, both defined with reference to undisturbed/free-stream conditions at the same height.

Configuration	Number of guiding vanes	c (m)	b (m)	b/c	A (m^2)	AF (-)	E (kWh)	Eref (kWh)	EF (-)
A_c_1	36	1	5	5	2	0.87	336	554	0.61
B_c_1	4	1	5	5	2	0.83	282	554	0.51
C_c_1	0	1	5	5	2	1.31	1335	554	2.41
A_c_4	36	4	8	2	8	1.00	2218	2218	1.00
B_c_4	4	4	8	2	8	0.97	1991	2218	0.90
C_c_4	0	4	8	2	8	1.20	4101	2218	1.85

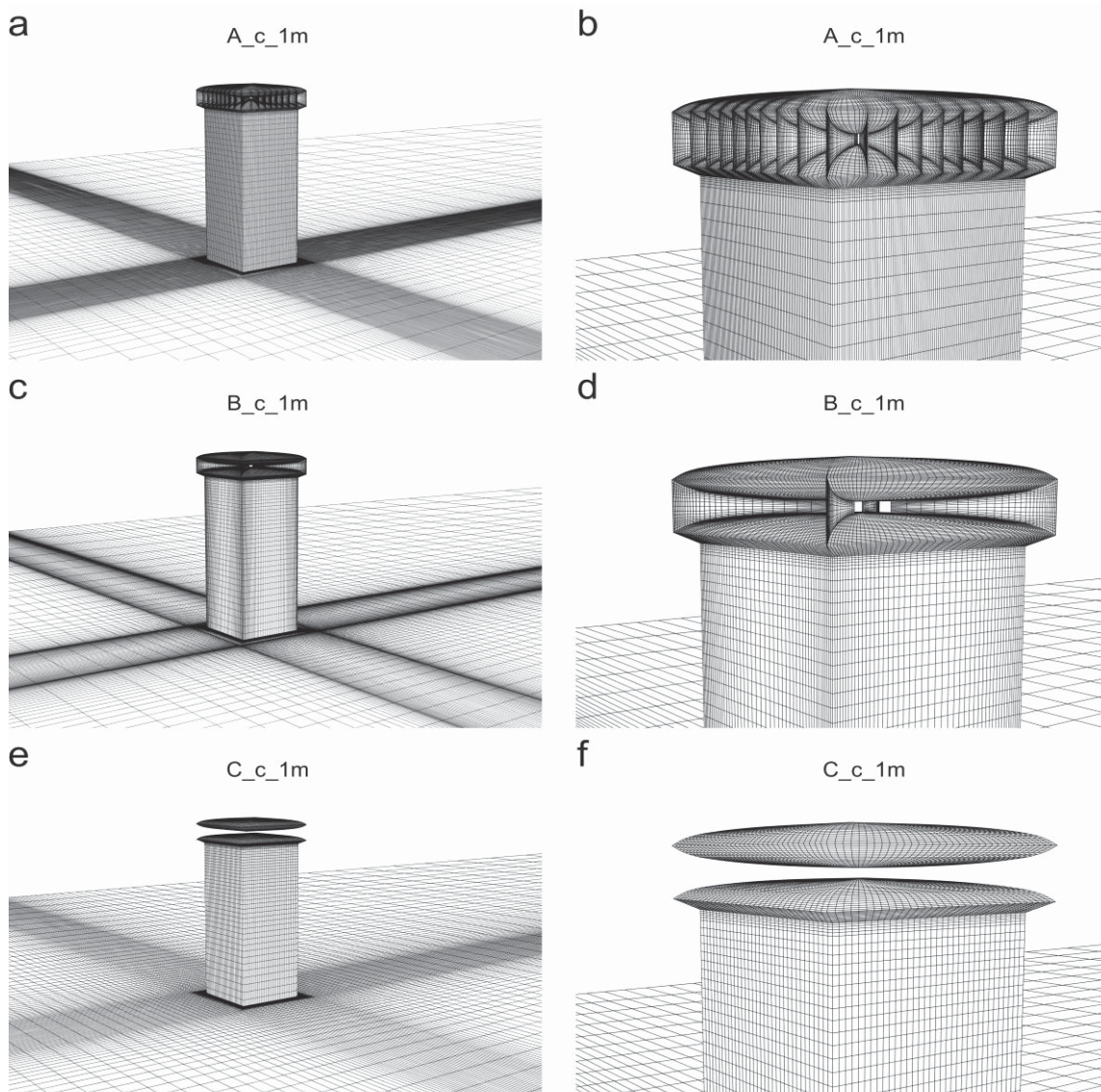


Fig 3. Computational grids for three different design configurations A, B and C (for $c = 1$ m): (a,b) guiding vanes every 10° (3.3 million cells); (c,d) guiding vanes every 90° (2.4 million cells); (e,f) no guiding vanes (2.0 million cells).

The reason is the large resistance of the funnels, which completely cancels the positive effect due to the venturi-shape of the roof. Furthermore, the configuration C without vertical guiding vanes provides the additional advantage that a much larger area is available for wind energy harvesting, because AF is larger than one over a large area of the roof as can be seen in. As a result, several VAWTs could be positioned in the roof. The large resistance of the funnels has an even stronger negative effect on the wind energy potential of the roof. While configuration C without guiding vanes provides values of EF that rise up to 2.41 for $c = 1$ m, adding vertical guiding vanes reduces EF to 0.61 or even 0.51 (see Table 1). This is due to the shift of the wind statistics to lower wind speeds, and partly below the cut-in wind speed of the VAWT. For $c = 4$ m, a similar trend is found, although somewhat less pronounced. Again the negative effect of adding vertical guiding vanes is shown. The results of optimization stage 1 are graphically summarized in Figure 9. Configuration C not only provides more wind energy than configurations A and B for the single VAWT in the center of the contraction, but its wind energy potential might very well become a multitude of that in configurations A and B, when several VAWT would be positioned in the contraction.

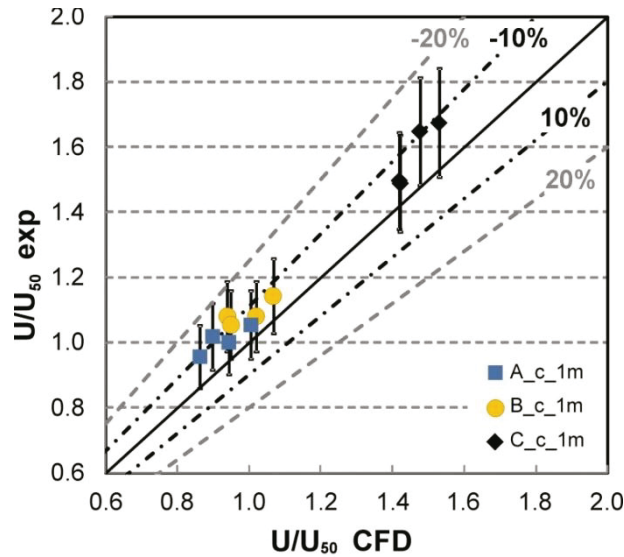


Fig 4. Validation of CFD simulations: comparison between numerical results and wind tunnel measurements in terms of the ratio U/U_{50} in the middle point of line T in the center of the roof contraction for $b = 5$ m, $c = 1$ m, for the three configurations A, B and C and the four wind directions.

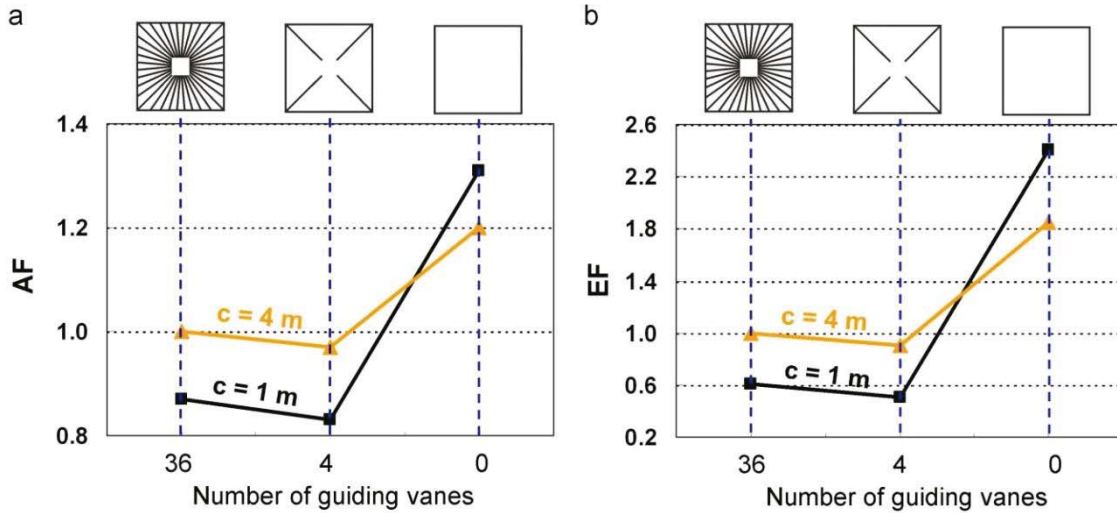


Fig 5. Results of optimization stage 1: (a) wind speed amplification factor AF and (b) wind energy enhancement factor EF for configurations A, B and C and for $c = 1$ m and $c = 4$ m.

6. SECOND OPTIMIZATION STAGE: INFLUENCE OF CONTRACTION RATIO

In the second optimization stage, eleven computational geometries are analyzed. They are all based on the result of optimization stage 1, i.e. configuration C without vertical guiding vanes. The parameters ‘b’ and ‘c’ in Figure 1 and 2 are varied to find an optimum contraction ratio with maximum increase in wind energy enhancement factor EF. The following eleven values for c are analyzed: $c = 0.25$ m, 0.375 m, 0.5 m, 0.75 m, 1 m, 2 m, 3 m, 4 m, 5 m, 6 m and 8 m. The corresponding contraction ratios b/c are 17, 11.7, 9, 6.3, 5, 3, 2.3, 2, 1.8, 1.7 and 1.5, respectively. Table 2 shows that amplification factor (AF) ranges from 0.93 to 1.34. There is a clear maximum for $c = 0.75$. For lower c values, the increased resistance (wind-blocking effect) in the venturi-throat causes lower AF. For higher c values, the venturi acceleration itself is lower. Table 2 also shows the wind energy enhancement factor (EF) for the different values of c. Note that, because power is a function of wind speed cubed, and because of the shift of the wind speed statistics due to the value of AF, even a relatively small difference in AF can result

in a large difference in EF. Table 2 also presents the total yearly wind energy production, based on the assumption that the height of the VAWT is equal to “c”. It is important to note that the optimum configuration in terms of highest EF is not the configuration that yields the highest yearly wind energy. The reason is that higher c values (lower contraction ratios) allow fitting a larger VAWT, yielding larger wind energy potential.

Table 2. Results of CFD analysis for roof configurations without vertical guiding vanes and with different contraction ratios b/c. AF is the wind speed amplification factor and EF the wind energy enhancement factor, both defined with reference to the undisturbed/free-stream conditions at the same height.

Number of vertical guiding vanes	c	b	b/c	A	AF	E	E _{ref}	EF
	(m)	(m)		(m ²)	(-)	(kWh)	(kWh)	(-)
0	0.25	4.25	17	0.5	0.93	107	139	0.77
0	0.375	4.375	11.7	0.75	1.22	405	208	1.95
0	0.5	4.5	9	1	1.32	682	277	2.46
0	0.75	4.75	6.3	1.5	1.34	1067	416	2.57
0	1	5	5	2	1.31	1335	554	2.41
0	2	6	3	4	1.27	2440	1109	2.20
0	3	7	2.3	6	1.24	3406	1663	2.05
0	4	8	2	8	1.20	4101	2218	1.85
0	5	9	1.8	10	1.14	4344	2772	1.57
0	6	10	1.7	12	1.10	4627	3326	1.39
0	8	12	1.5	16	1.02	4756	4435	1.07

7. DISCUSSION AND CONCLUSIONS

This study is only a first step in the analysis of the wind energy potential of this type of venturi-shaped roof. The following important limitations need to be mentioned, which simultaneously indicate directions for further research:

- Although a fairly wide range of roof configurations were analyzed, the geometry of all configurations satisfy the relationship $(b - c = 4)$. Further work should focus on different building configurations with different values of $(b-c)$, i.e. different curvatures of the venturi-shaped roof.
- In this study, only a single building configuration and a single approach-flow atmospheric boundary layer (ABL) were considered.
- Only an isolated building was considered. Future work will include analysis of the roof performance in a variety of urban environments, with low-rise, medium-rise and high-rise buildings. This can include generic urban configurations as well as actual practical case studies.
- The present numerical and experimental (wind tunnel) results did not explicitly consider the presence of the resistance of the VAWT itself in the roof contraction, although this effect is partly and implicitly taken into account by the use of a cut-in wind speed.
- Also the performance of multiple VAWTs, positioned within the same contraction, can be investigated further, in an attempt to arrive at higher wind energy potential.
- Finally, this study was explicitly focused on the aerodynamic aspects of the venturi-shaped roof. Additional research efforts should focus on structural aspects, noise and safety issues.

The following conclusions are made:

- The CFD simulations have been successfully validated by comparison with reduced-scale atmospheric boundary layer wind tunnel measurements. The difference between numerical and experimental results is generally lower than 10%, which is considered a very good agreement.

- The first optimization stage has shown that adding vertical guiding vanes does not improve the performance of the roof, but actually cancels its effect and reduces its wind energy performance to values that are equal or even lower than those of a free-standing VAWT at the same height, which is a counter-intuitive result.
- The second optimization stage has shown that, of the configurations investigated, a contraction ratio of 6.3 provides the largest AF (= 1.3) and EF (= 2.6), although other contraction ratios can give larger absolute energy output due to the larger space that can accommodate a larger VAWT.
- The large EF (energy increase up to 260%) is attributed to three reasons: (1) the absence of vertical guiding vanes; (2) the optimum contraction ratio of 6.3; and (3) the fact that the roof performance is nearly wind-direction independent.

8. ACKNOWLEDGMENTS

Twan van Hooff is currently a postdoctoral fellow of the Research Foundation e Flanders (FWO) and acknowledges its financial support (project FWO 12R9715N).

REFERENCES

- Campbell NS, Stankovic S. Wind energy for the Built environment–Project WEB, A report for Joule III Contract No JOR3-CT98-01270 2001.
- Bahrain World Trade Centre, in <http://bahrainwtc.com/> (accessed August 2011).
- Strata Tower, in <http://inhabitat.com/first-skyscraper-with-built-in-windturbinesopens-in-london/> (accessed August 2011).
- Pearl River Tower, in [http://smithgill.com/#/work/pearl river tower](http://smithgill.com/#/work/pearl%20river%20tower) (accessed August 2011).
- Sharpe T, Proven G. Crossflex: concept and early development of a true building integrated wind turbine. *Energy Buildings* 2010;42(12):2365–2375.
- Bronsema B. Earth, Wind & Fire – Towards new concepts for climate control in buildings. CIB W096 Meeting Lyngby, November 2-4, 2005.
- Bronsema B. Earth, Wind & Fire – Air-conditioning powered by nature. 10th REHVA World Congress CLIMA 2010, 9-12 May, Antalya, Turkey, 2010
- van Hooff T, Blocken B. Coupled urban wind flow and indoor natural ventilation modelling on a high-resolution grid: A case study for the Amsterdam ArenA stadium. *Environ Modell Softw* 2010;25:51-65.
- Casey M, Wintergerste T. Best Practice Guidelines, ERCOFTAC Special Interest Group on Quality and Trust in Industrial CFD, ERCOFTAC, Brussels; 2000.
- Franke J, Hellsten A, Schlünzen H, Carissimo B. Best practice guideline for the CFD simulation of flows in the urban environment; 2007.
- Tominaga Y, Mochida A, Yoshie R, Kataoka H, Nozu T, Yoshikawa M et al. AIJ guidelines for practical applications of CFD to pedestrian wind environment around buildings. *J Wind Eng Ind Aerodyn* 2008;96:1749-61.
- Blocken B. 2015. Computational Fluid Dynamics for Urban Physics: Importance, scales, possibilities, limitations and ten tips and tricks towards accurate and reliable simulations. *Build Environ* 91: 219-245.
- Launder BE, Spalding DB. The numerical computation of turbulent flows. *Comput Methods Appl Mech Eng* 1974;3:269-89.
- Cebeci T, Bradshaw P. Momentum transfer in boundary layers. New York: Hemisphere Publishing Corp, 1977.
- Blocken B, Stathopoulos T, Carmeliet J. CFD simulation of the atmospheric boundary layer: wall function problems. *Atmos Environ* 2007;41:238-52.
- Yakhot V, Orszag SA, Thangam S, Gatski TB, Speziale CG. Development of turbulence models for shear flows by a double expansion technique. *Phys Fluids* 1992;4:1510-20.

- Blocken B, Carmeliet J, Stathopoulos T. CFD evaluation of wind speed conditions in passages between parallel buildings-effect of wall-function roughness modifications for the atmospheric boundary layer flow. *J Wind Eng Ind Aerodyn* 2007;95:941-62.
- Balduzzi F, Bianchini A, Carnevale EA, Ferrari L, Magnani S. Feasibility analysis of a Darrieus vertical-axis wind turbine installation in the rooftop of a building. *Appl Energ*97: 921-929.
- Manwell JF, McGowan J, Rogers AL. *Wind Energy Explained: Theory, Design and Application*. Second Edition, Wiley; 2009.
- van Hooff T, Blocken B, Aanen L, Bronsema B. A venturi-shaped roof for wind-induced natural ventilation of buildings: Wind tunnel and CFD evaluation of different design configurations. *Build Environ* 2011;46:1797-807.

The Effect of Pitch Angle on the Performance of a Vertical-Axis Wind Turbine

Abdolrahim Rezaeiha

Building Physics and Services, Department of the Built Environment, Eindhoven University of Technology, P.O. Box 513, 5600 MB Eindhoven, The Netherlands

Ivo Kalkman,

Building Physics and Services, Department of the Built Environment, Eindhoven University of Technology, P.O. Box 513, 5600 MB Eindhoven, The Netherlands

Bert Blocken

Building Physics and Services, Department of the Built Environment, Eindhoven University of Technology, P.O. Box 513, 5600 MB Eindhoven, The Netherlands

Building Physics Section, Department of Civil Engineering, Leuven University, Kasteelpark Arenberg 40 – Bus 2447, 3001 Leuven, Belgium

Email: a.rezaeiha@tue.nl

Abstract. Wind energy is a highly promising resource to approach a sustainable built environment. Vertical axis wind turbines (VAWT) offer the advantage of omni-directional operation over horizontal axis wind turbines (HAWT). This makes them ideal for utilization in urban environments which are characterized by frequently varying wind direction. However, a comparatively small amount of research on VAWTs has resulted in low power coefficients (C_p) compared to HAWT. The pitch angle (β) is a parameter which is commonly used in HAWTs to enhance their performance and is a potential optimization parameter for VAWT as well. However, a recent study based on inviscid modelling states that it will not have any significant effect on C_p . Therefore, in order to elucidate this claim using a viscous calculation, performance optimization of VAWTs by varying β is investigated in the current paper. C_p , moment and thrust coefficient (C_m and C_T) and angle of attack are obtained from a CFD simulation of a straight-bladed H-type VAWT using 2D Detached Eddy Simulations (DES). The turbine is operating at a tip speed ratio (TSR) of 4 and β -values of 0° , $+3^\circ$, and -3° are investigated. The results show that unlike the inviscid results, increasing β from 0° to $+3^\circ$ would increase C_p by 4% while decreasing it to -3° will result in a 16% reduction in C_p .

1. INTRODUCTION

Wind energy is a highly promising alternative to fossil fuels which offers great potential for a sustainable planet in terms of availability, renewability and land use. There has been a significant global growth of installed wind power in the last decade. In the quest for a sustainable built environment there is also a growing interest in wind energy harvesting in urban environments. Due to frequently-changing wind directions in urban environments, VAWTs have received interest as a result of their omni-directional capabilities. They also offer some additional advantages over their horizontal counterparts, namely no need for a yaw and pitch system; simple blade geometries (no twist or taper); low manufacturing and maintenance costs due to having a direct-driven generator installed at ground level; and low noise level due to low tip speed ratios (TSR).

After early research on VAWT in the 1970s-1980s they suffered from a lack of interest until the mid-2000s. The research gap in the intervening period has contributed to low C_p values in comparison with HAWTs. Additionally, the flow around a VAWT is very complex due to phenomena such as dynamic stall, flow curvature effects, blade-vortex and vortex-vortex interactions, viscous effects, 3D wake characteristics, and azimuthal variations of vortex shedding. This complexity has demanded a great amount of research in order to optimize VAWT performance. Recent modeling and experimental research have contributed to our understandings of these complexities. A recent inviscid study using a moderate-fidelity vorticity-transport model stated that introducing a fixed pitch angle (β) to the blade only shifts the instantaneous loads between the upwind and downwind halves of the turbine and does not have any significant effect on the C_p and C_T of the turbine as they are averaged values over one

revolution. As this conclusion can be generalized to the introduction of any constant circulation on the blade it is very important to verify this effect using high-fidelity viscous methods and/or experiments. Therefore, a viscous CFD simulation using 2D Detached-eddy simulation is performed and instantaneous loads, angle of attack, CP, CT and Cm values are calculated for three different pitch angles (0° , $+3^\circ$ and -3°) in order to further study the inviscid finding. The result of this study can help the optimization of VAWTs.

2. VAWT GEOMETRY, MESH AND COMPUTATIONAL SETTINGS

A straight-bladed H-type vertical axis wind turbine is simulated. The turbine has three blades with the symmetric NACA0015 airfoil shape and a chord-to-radius ratio (c/R) of 0.115. The diameter (D) of the turbine is 1 m and it is operated at a moderate tip speed ratio (λ) of 4 where tip speed ratio is defined as the ratio between the turbine rotational speed ($R\omega$) to the freestream velocity (U_∞) (see Equation 1). The freestream velocity is 7 m/s which is a reasonable mean value for a VAWT. The approach-flow and incident-flow turbulence intensities are 5% and 3.96% respectively and the turbine rotational speed (ω) is 56 rad/s.

$$\lambda = \frac{R\omega}{U_\infty} \dots \dots \dots (1)$$

A schematic of the VAWT illustrating the directions of rotation and wind, azimuth (θ) and an illustration of the circle for the calculation of experienced velocity is shown in Figure 1. Another schematic depicting VAWT blade cross-section showing the flow angle (φ), angle of attack (α), pitch angle (β) and the freestream, induced and experienced velocity vectors is shown in Figure 2. The arrow for pitch angle in Figure 2 shows the positive direction, corresponding to the blade leading edge pitched inwards towards the center of rotation of the turbine.

The fluid domain for the simulation is divided into a rotating core of two times the diameter (D) of the turbine, and a non-rotating part ($20D$ length \times $10D$ width) surrounding the rotating core where the distance from the inlet and outlet of the domain to the center of rotation is $5D$ and $15D$ respectively.

A hybrid mesh consisting of triangular cells in the rotating core and quadrilateral cells elsewhere is generated which consists of 673,471 cells (see Figure 3). The mesh has an average orthogonal quality, skewness and aspect ratio of 0.96, 0.1 and 1.6 and a minimum orthogonal quality of 0.23. A smooth interface between the rotating and non-rotating domains is provided in terms of cell size and stretching ratio, and the near wall cell edges are made normal to the wall.

A mesh sensitivity analysis was done by performing calculations using URANS with the transition SST turbulence model on a coarser mesh (289,397 cells) and a finer one (921,185 cells) to investigate whether the mesh is sufficiently fine. The analysis showed that the key parameter in the simulation, C_m , shows a negligible change when the mesh is further refined from the medium to the finer mesh. The grid convergence index (GCI) was utilized in order to quantify the error and the GCI_{fine} and GCI_{coarse} for the medium-fine mesh pair were found to be 0.75×10^{-2} and 1.02×10^{-2} , respectively. Safety factor (F_s) of 1.25 was used in the calculation of GCI. Therefore, the medium mesh was deemed to be sufficiently fine and the rest of the calculations were performed on this mesh.

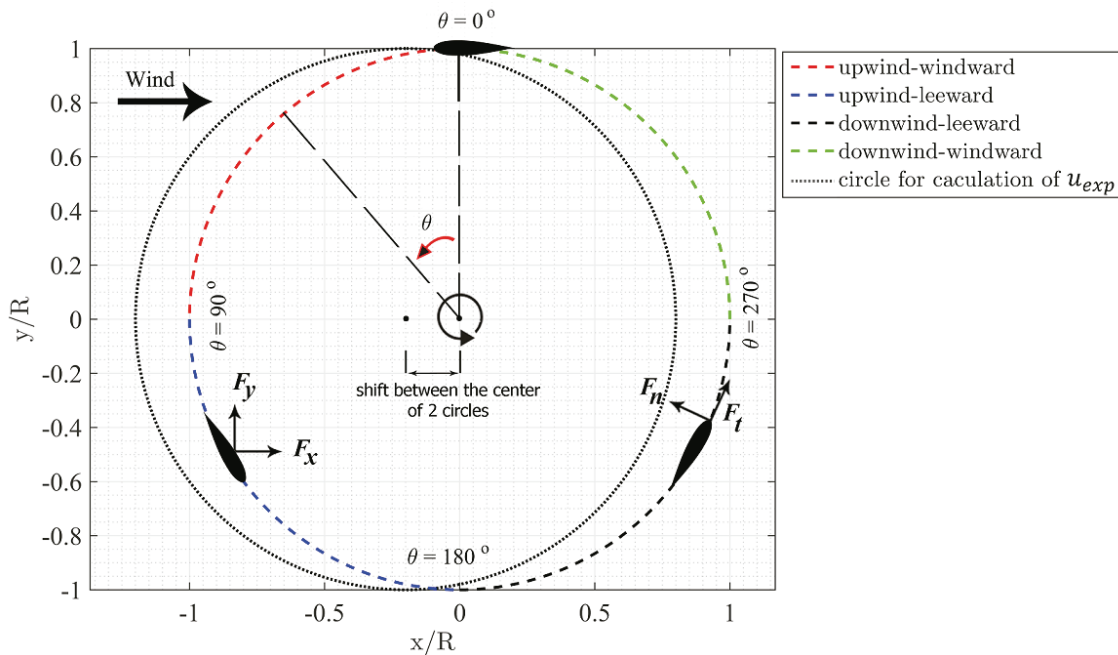


Fig 1. Schematic of the VAWT from top view showing the directions of rotation and wind, azimuth (θ), and an illustration of the circle for the calculation of experienced velocity.

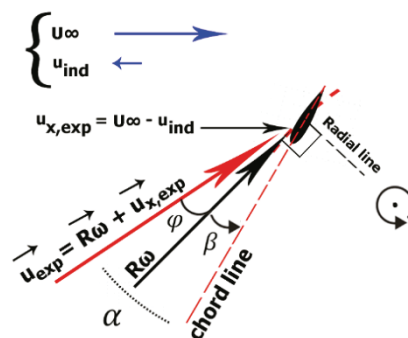


Fig 2. Schematic of the VAWT blade cross-section showing the flow angle (φ), angle of attack (α), pitch angle (β) and the freestream, induced and experienced velocity vectors. The arrow for pitch angle shows the positive direction.

The CFD simulation was performed using the commercial CFD software package ANSYS Fluent 16.1 based on the finite volume method (FVM). The method discretises the computational domain into finite volumes and solves the governing equations of fluids for continuity and momentum. The SIMPLE pressure-velocity coupling and 2nd order discretization schemes were utilized. The side walls were represented as symmetry boundary conditions along with a constant velocity inlet, a zero-pressure outlet and no-slip condition for the airfoil walls. A sliding mesh interface was defined between the rotating core and the non-rotating domain. The solution was initialized using a steady-state solution of the RANS equations using the realizable $k-\epsilon$ turbulence model with enhanced wall treatment. The simulation was performed for 30 revolutions of the turbine. No data were sampled during the first 5 revolutions in order to assure elimination of the transient effects. Over the remaining 25 revolutions which were used for data sampling the change in CP between successive revolutions was well below 1%. A time step of 1.56×10^{-4} s was employed which corresponds to an angular rotation of 0.5° per time

step; CFL number between 5-20 in the airfoil region. 20 iterations per time step were employed in order to obtain scaled residuals on the order of 10^{-5} .

Turbulence was modeled using the Detached-Eddy Simulation (DES) hybrid RANS-LES model. In this approach an LES model is used for the main region of the flow where large turbulent structures are dominant while for the sub-grid turbulent scales in the near-wall region a URANS approach is employed. Both the Delayed DES (DDES) shielding function and curvature correction were employed in the LES domain. In the RANS domain the transition SST model was selected as this model couples the $k-\omega$ SST transport equations with two other equations, i.e. an equation for prediction of the transition onset based on the momentum-thickness Reynolds number and a second equation for intermittency and can give a better prediction of the transition onset in the boundary layer. Therefore, this can result in more accurate results for VAWT flow types where the flow behavior is dependent on the development of the boundary layer on the airfoils.

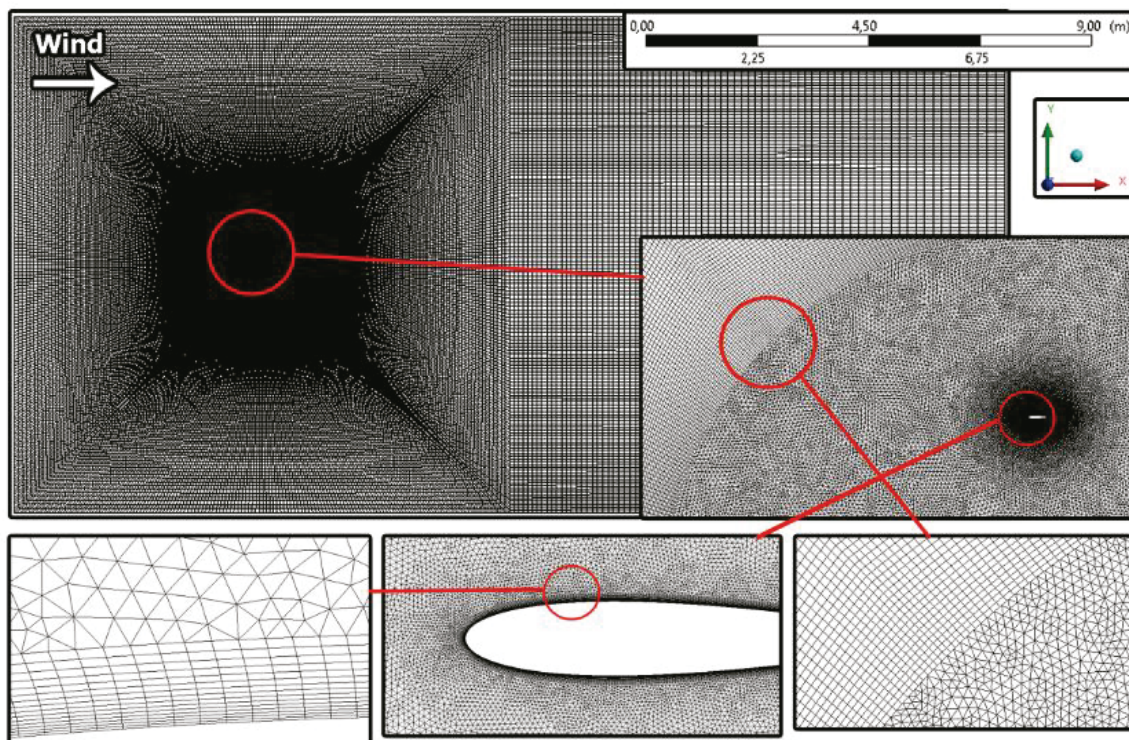


Fig 3. Medium mesh for the VAWT simulation.

The geometrical angle of attack (α_{geo}) is usually used for VAWTs in order to provide a first estimate for variation of angle of attack. As the name implies the geometrical angle of attack is defined based on geometrical relations while assuming zero induced velocity (u_{ind}): see Equation 2. This means it assumed that the blade experiences the freestream velocity in x -direction and the operation of the turbine has no effect on slowing down the flow. This is not physical as the turbine exerts a thrust force opposite to the direction of the flow which extracts energy from the flow and slows it down (the kinetic energy is transferred from the flow to the turbine; see Figure 2). This means that for a correct determination of the angle of attack the induced velocity is required, after which the experienced x -velocity ($u_{x,exp}$) can be obtained.

$$\alpha_{geo} = \tan^{-1} \left(\frac{\cos \theta}{\sin \theta + \lambda} \right) \dots \dots \dots (2)$$

Due to the presence of a local stagnation area near the airfoil it is very challenging to determine the experienced x -velocity and experienced angle of attack. It therefore needs to be

sampled at a finite distance from the airfoil. The current study approximated the experienced x-velocity on a circle with the same radius as the turbine but with the center shifted 0.2D upwind. This way, a constant distance is kept from the blade for the sampling during the whole revolution. The experienced angle of attack (α_{exp}) is calculated based on a vector summation of u_x , u_{xp} and the blade rotational velocity vector $R\omega$ at each value of θ .

3. RESULTS AND DISCUSSION

The variation of geometrical and experienced angle of attack versus azimuth is shown in Figure 4. As anticipated, it is observed that due to the presence of induced velocity the experienced angle of attack is smaller than the geometrical value. As the flow loses energy after passing through the upwind half of the turbine, a much lower experienced x-velocity is found when approaching the downwind half (see Figure 5). The difference between geometric and experienced angle of attack is therefore largest in the downwind region. The effect of the pitch angle on the experienced angle of attack is an almost constant shift of the same magnitude throughout the whole revolution.

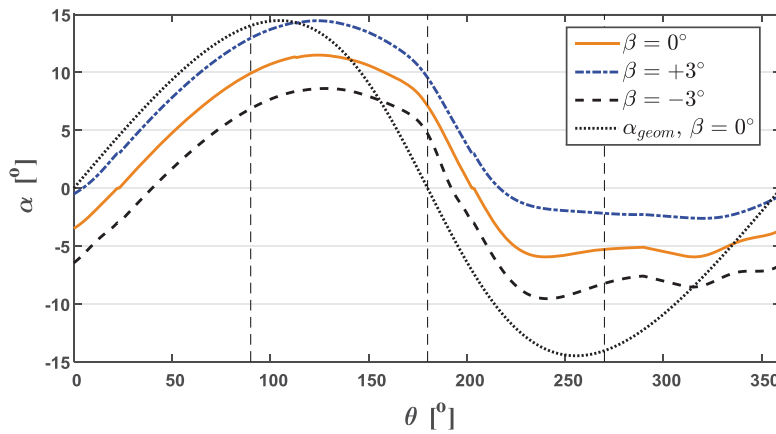


Fig 4. Angle of attack for the three fixed-pitch cases, $\lambda = 4$.

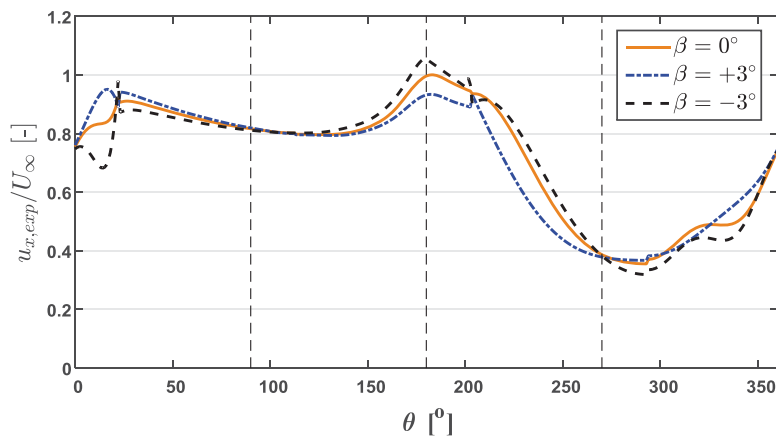


Fig 5. Non-dimensional experienced x-velocity for the three fixed-pitch cases, $\lambda = 4$.

When the pitch angle is increased from 0 to +3, a higher x-velocity in the windward half of the rotation is experienced while this value is lower in the leeward half (see Figure 5). The opposite effect was observed for a decrease in pitch angle. This is in contrary to the finding from the inviscid results which predicted an insignificant effect on induced velocity as a result of adding a constant finite and small circulation to the blade during each revolution. The discrepancy can be a result the presence of the boundary layer due to viscous effects and

subsequent effects on the vortex shedding and the wake. Small ripples around $\theta = 20^\circ$, 220° and 330° (Figure 5) are a local result of passing blades on experienced x-velocity.

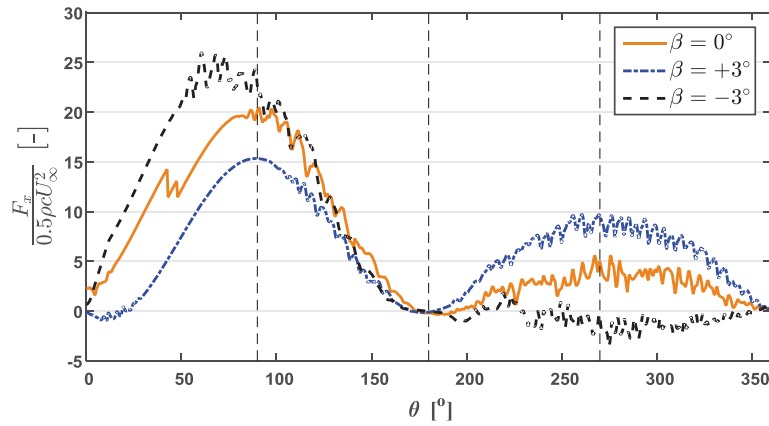


Fig 6. Force in the flow direction versus azimuth for three fixed pitch angles, $\lambda = 4$.

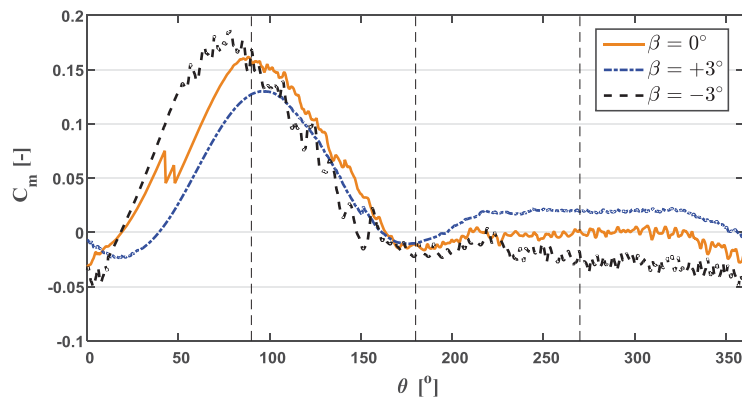


Fig 7. Moment coefficient versus azimuth for three fixed pitch angles, $\lambda = 4$.

In terms of non-dimensional force in flow direction (Figure 6) and moment coefficient (Figure 7), an opposite behaviour to the experienced x-velocity was observed for both the upwind half and the downwind-leeward quartile. This is due to the fact that a lower experienced velocity means higher induced velocity and higher force in the flow direction, and consequently a higher moment coefficient.

Introduction of the pitch angle resulted in a shift of non-dimensional force in flow direction and moment coefficient between the upwind and downwind halves of the turbine. This was also stated in the inviscid results. However, the integral of the moment coefficient over the time times the tip speed ratio, which makes the CP, is significantly affected by varying the pitch angle (see Table 1). Increasing the pitch angle from 0° to $+3^\circ$ will increase the CP by 6% while decreasing it from 0° to -3° will drop the CP by 27% which is a very notable influence. This is in contrast to the result reported by Simão Ferreira et al. A negligible effect on CT was predicted by the current study (Table 1) as well as the inviscid study.

Table 1. Non-dimensional power and thrust coefficient for different fixed-pitch cases, λ

β	$C_P / C_{P,0}$	$C_T / C_{T,0}$
-3°	0.73	0.98
$+3^\circ$	1.06	1.01

4. CONCLUSIONS

In this study the effect of pitch angle on the power coefficient (CP) of a VAWT was investigated using 2D hybrid URANS-LES viscous simulations using the DES approach combined with the transition SST turbulence model. The following conclusions can be drawn:

In qualitative agreement with previously reported inviscid simulation results, the instantaneous loads and moment were shifted between upwind and downwind regions as a result of varying the pitch angle.

In contrast to the inviscid results, introducing a pitch angle to the blade resulted in a significant change in CP.

Although increasing the pitch angle results in higher CP the reduction in CP is much stronger when the pitch angle is decreased.

The difference between the current study and the inviscid results can be a result of development of the boundary layer due to presence of viscosity, and consequent influences on the induced velocity and wake.

A future 2.5D simulation and investigations at different tip speed ratios are planned to further study these effects.

5. ACKNOWLEDGEMENTS

The authors would like to acknowledge support from the European Commission's Framework Program Horizon 2020, through the Marie Curie Innovative Training Network (ITN) AEOLUS4FUTURE - Efficient harvesting of the wind energy (H2020-MSCA-ITN-2014: Grant agreement no. 643167).

REFERENCES

- J. F. Manwell, "Wind energy explained theory, design and application", 2nd ed. ed. Hoboken: Wiley, 2010.
- Global wind report 2014," Global Wind Energy Council (GWEC)2014.
- S. Mertens, Wind energy in built environment. Brentwood, UK: Multi-Science, 2006.
- F. Balduzzi, A. Bianchini, E. A. Carnevale, L. Ferrari, and S. Magnani, "Feasibility analysis of a darrieus vertical-axis wind turbine installation in the rooftop of a building," *Applied Energy*, vol. 97, pp. 921-929, 2012.
- F. Toja-Silva, A. Colmenar-Santos, and M. Castro-Gil, "Urban wind energy exploitation systems: behaviour under multidirectional flow conditions—opportunities and challenges," *Renewable and Sustainable Energy Reviews*, vol. 24, pp. 364-378, 2013.
- S. Gsanger and J. D. Pitteloud, "2015 small wind world report summary," World Wind Energy Association (WWEA), Bonn, Germany2015.
- H. J. Sutherland, D. E. Berg, and T. D. Ashwill, "A retrospective of VAWT technology," Sandia National Laboratories2012.
- M. R. Islam, S. Mekhilef, and R. Saidur, "Progress and recent trends of wind energy technology," *Renewable and Sustainable Energy Reviews*, vol. 21, pp. 456-468, 2013.
- C. Simão Ferreira, C. Hofemann, K. Dixon, G. van Kuik, and G. van Bussel, "3D wake dynamics of the VAWT: experimental and numerical investigation," in 48th AIAA Aerospace Sciences Meeting Including the New Horizons Forum and Aerospace Exposition, Orlando, Florida, 2010.
- M. Elkhoury, T. Kiwata, and E. Aoun, "Experimental and numerical investigation of a three-dimensional vertical-axis wind turbine with variable-pitch," *Journal of Wind Engineering and Industrial Aerodynamics*, vol. 139, pp. 111-123, 2015.
- R. Nobile, M. Vahdati, J. F. Barlow, and A. Mewburn-Crook, "Unsteady flow simulation of a vertical axis augmented wind turbine: a two-dimensional study," *Journal of Wind Engineering and Industrial Aerodynamics*, vol. 125, pp. 168-179, 2014.
- A. Rezaeiha, I. M. Kalkman, and B. Blocken, "A short review of recent research activities for aerodynamic optimization of vertical axis wind turbines," in 1st International TU1304 WINERCOST Conference, Ankara, Turkey, 2016.

- C. Simão Ferreira and F. Scheurich, "Demonstrating that power and instantaneous loads are decoupled in a vertical-axis wind turbine," *Wind Energy*, vol. 17, pp. 385-396, 2014.
- B. Blocken, "Computational Fluid Dynamics for urban physics: Importance, scales, possibilities, limitations and ten tips and tricks towards accurate and reliable simulations," *Building and Environment*, vol. 91, pp. 219-245, 2015.
- "ANSYS® Fluent user's guide, release 16.1, ANSYS, Inc.," 2015.
- P. J. Roache, "Quantification of uncertainty in computational fluid dynamics," *Annual Review of Fluid Mechanics*, vol. 29, pp. 123-160, 1997.
- P. R. Spalart, "Detached-Eddy Simulation," *Annual Review of Fluid Mechanics*, vol. 41, pp. 181-202, 2009.

On the Understanding of the Above Roof Flow of a High-rise Building for Wind Energy Generation

Hassan Hemida

Department of Civil Engineering, School of Engineering, University of Birmingham

Email:h.hemida@bham.ac.uk

Abstract. This paper presents a numerical study of the above roof wind flow characteristics of a high-rise building using large-eddy simulation. Two variations of the high-rise buildings were considered; an isolated building in a built environment. In order to increase the velocity of the air in the above roof flow and enhance its turbulence characteristics, a new design of a roof with an umbrella-like structure above it has been suggested and tested. The simulations showed that the umbrella-like shape improved the averaged wind speed and reduced the turbulence intensity significantly and hence could provide a suitable improve to the wind energy harvesting from the above roof flow.

1. INTRODUCTION

Worldwide, existing buildings consume about 40% of the world's energy and are responsible for approximately the same percentage of global carbon emissions (UNEP, 2007). In the UK the situation is even worse with existing buildings consuming about 45% of the country's energy (ESRC, 2009). It is anticipated that by 2050 the UK's population will increase to 72 million and that 88% of this population will be living in cities and towns (UN, 2009), which suggests a significant increase in urban buildings. If current trends in building energy consumption continue, an unprecedented increase in the energy used by buildings will occur. "Buildings worldwide will become the top energy consumer by 2025, and are likely to use as much energy as industry and transportation combined by 2050" (NSTC, 2008). Such a sharp increase in the energy consumed will pose a serious threat to the goal of reducing the UK's carbon emissions to 60% below 1990 levels by 2050 unless low and zero carbon (LZC) energy sources are utilized.

Wind energy is one of the fastest growing LZC energy sectors in the world. It is the most successful and fastest spreading LZC energy source in the UK with an installed capacity of about 7391 MW. Traditionally, wind turbines have been installed in large offshore and onshore wind farms, and the energy generated by wind turbines is carried by transmission and distribution systems to the end user. Due to energy losses in such systems, in situ wind energy generation seems more appealing. One possible way of generating wind energy in situ involves integrating wind turbines in high-rise buildings. With the development of the wind turbine industry over the last decade, there has been increasing global interest in this technique; examples include Strata SE1, London, UK; Bahrain World Trade Centre, Manama, Bahrain; and Pearl River Tower, Guangzhou, China. These projects have demonstrated that building-integrated wind turbines (BIWTs) can utilize the increased wind velocity at higher altitudes to generate energy and thereby reduce building carbon emissions.

Another way of harvesting wind energy from built environment is to install micro-wind turbines on the roof of existing high-rise buildings. The wind flow field above the roof of high-rise buildings is complex with massive flow separation and reattachment and thus the determination of the optimum location of the micro-wind turbine is crucial in order to maximize the generated wind energy. This paper thus presents a numerical study of above roof wind flow characteristics of a high-rise building using large-eddy simulation and different RANS approaches.

2. HIGH-RISE BUILDINGS AND COMPUTATIONAL DOMAIN

The building under investigation is similar in dimension to that of Kim, Yukio et al (2012) used in their investigation of the interference effects on the local peak pressures between two buildings.

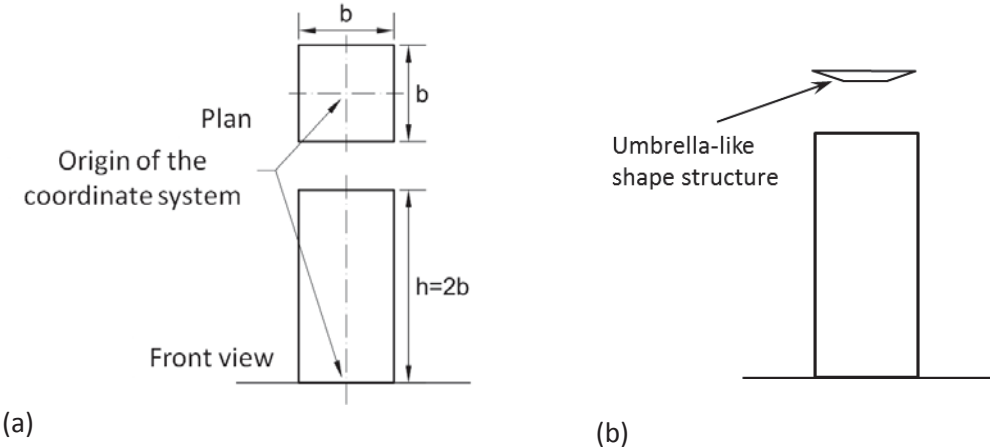


Fig 1 dimensions of the high-rise buildings; (a) flat roof and (b) with an umbrella-like shape .

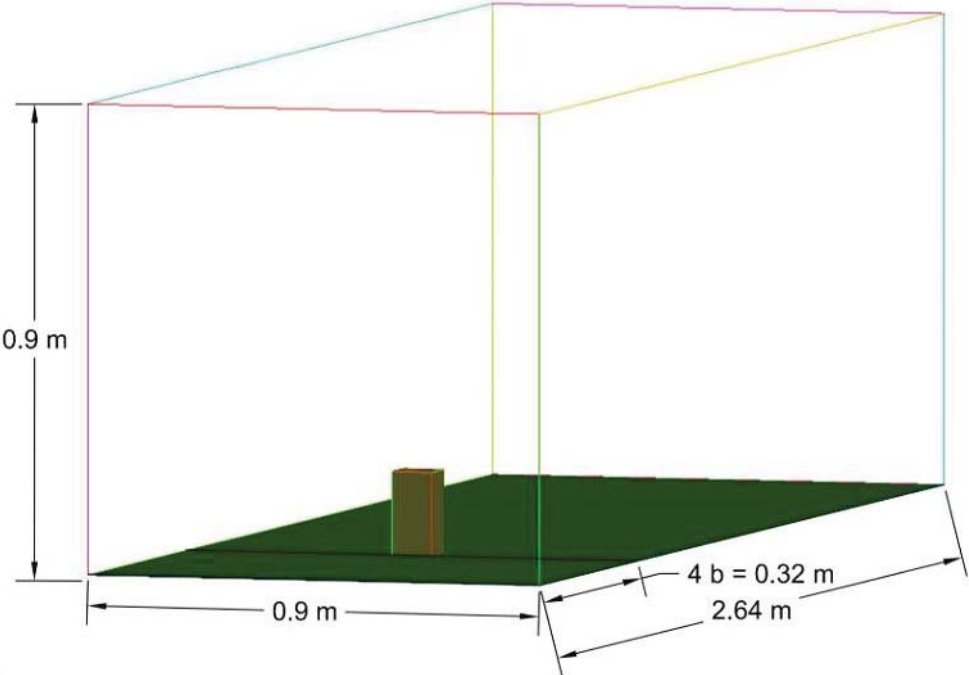


Fig 2 dimensions of the computational domain.

Two variations of the high-rise buildings were considered; an isolated building with a flat roof and a high-rise building with a flat roof and an umbrella-like shape structure above the

roof. Figure 1 (a) shows the dimensions of the base building, where $b=0.08$ m is the width of the building and Fig 1(b) shows the shape of the umbrella-like shape structure. The dimensions of computational domain, which mimics the wind tunnel setup are shown in Fig 2.

3. BOUNDARY CONDITIONS

Similar to that used by Kim et al (2012), the inlet wind profile was simulated through imposing a power law type atmospheric boundary layer profile (Figure 3(a)). Figure 3(b) shows the boundary conditions used and Fig 4 shows the distribution of the mesh in the computational domain.

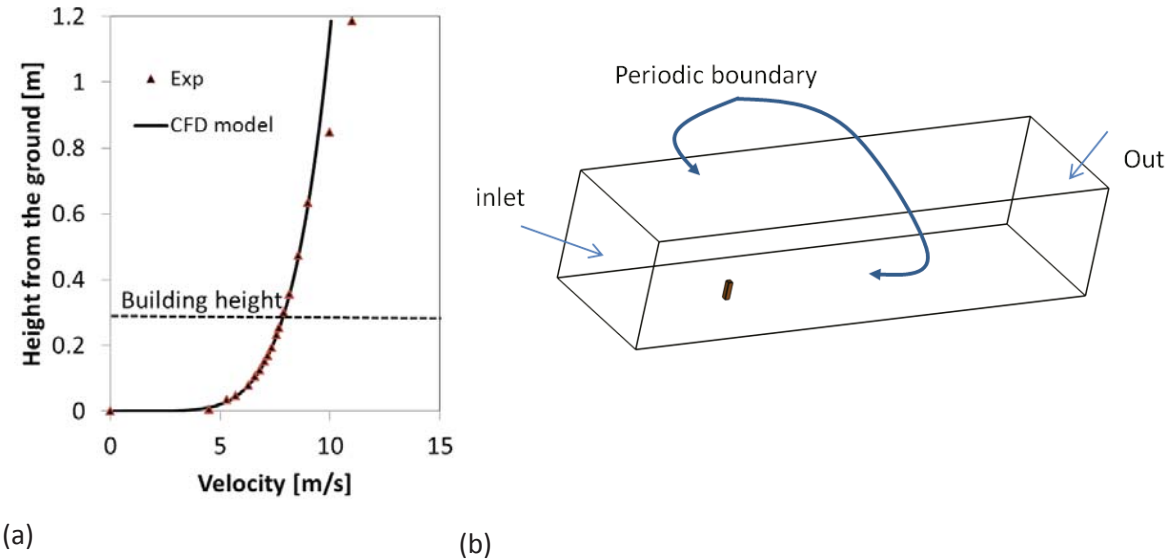


Fig 3: Inlet velocity profile (a) and boundary conditions (b).

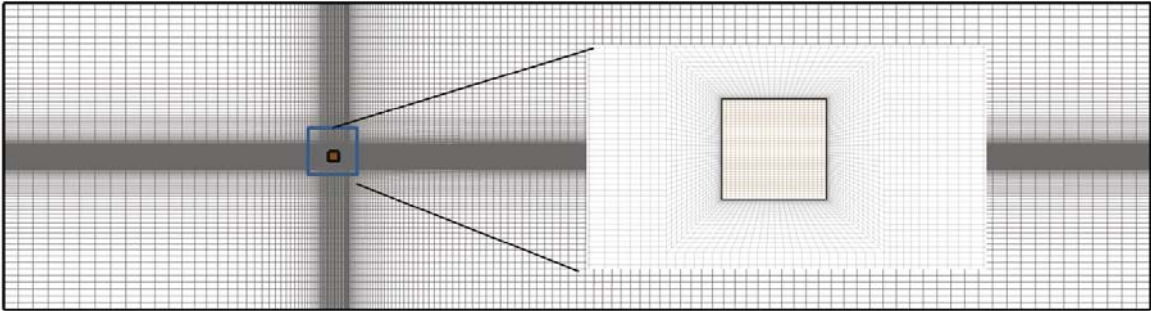


Fig 4: Mesh distribution.

4. BUILDING WITH AN UMBRELLA-LIKE SHAPE STRUCTURE ABOVE THE ROOF

In order to increase the air velocity in the above roof flow, an umbrella-like shape structure has been placed at distance $0.5b$ above the roof as shown in Fig 1(b). The gap between the umbrella-like shape structure and the roof looks like a venturi in shape as shown in Figure 5 (b). Figure 5 shows also the surface mesh on the buildings with and without umbrella-like shape structure.

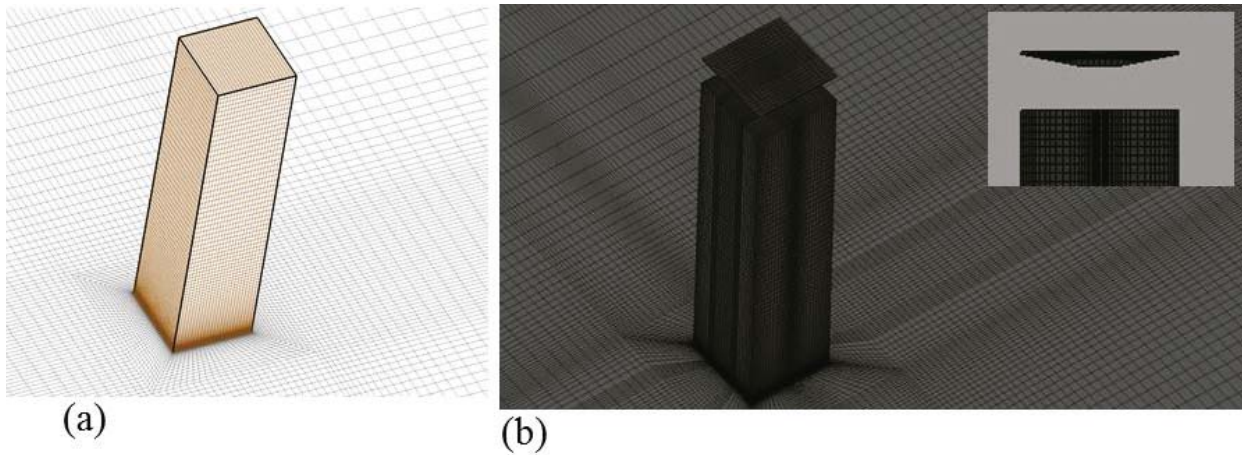


Fig 5: Surface mesh and shape of the umbrella above the roof of the building; (a) base building with a flat roof, (b) with umbrella-like shape structure.

5. COMPARISON WITH EXPERIMENT

Figure 6 shows the location of the lines used in the experiment to find the velocity distributions. Same lines were used in the LES to find the velocity profiles. Figure 7 shows the comparison between LES results and the experimental data at only two locations; (1) and (6). It can be concluded from Figure 7 that the LES results agree well with the experimental data. RANS simulations were also performed using different computations with different number of cells and different turbulent models and the results reasonably agree with the experimental data (not shown here).

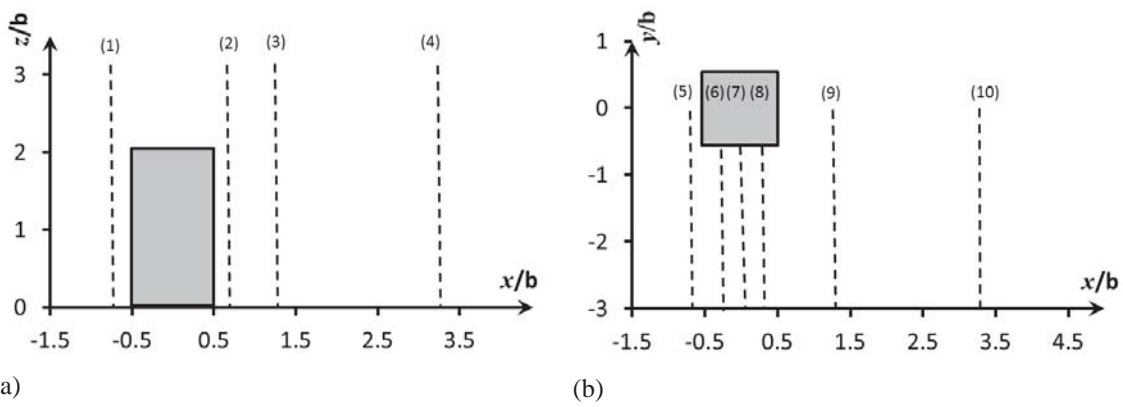


Fig 6 Locations of the experimental velocity profiles

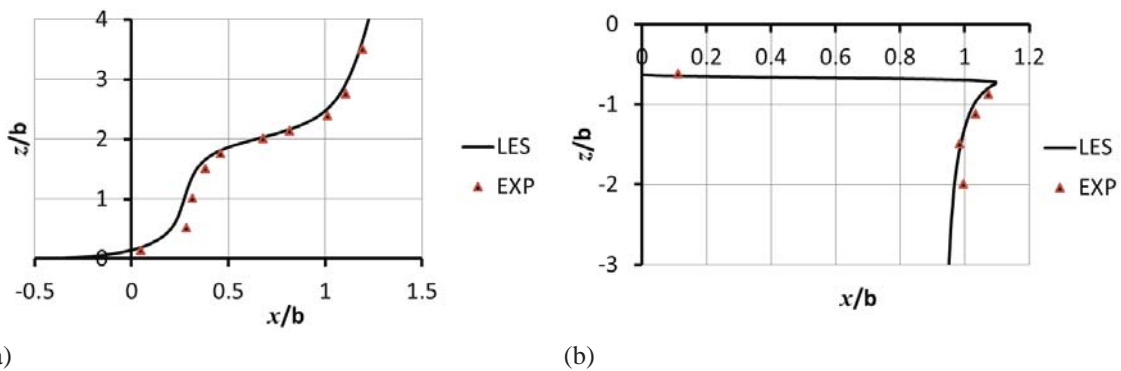


Fig 7 Comparison with the experiment

6. RESULTS

Numerical simulations using the LES approach have been performed on the two building using the boundary conditions shown in Fig 3(b) with a time step 1×10^{-5} sec, which gives a maximum Courant–Friedrichs–Lewy (CFL) number of about 2.0. The simulation takes about 1.5 sec from the start of the simulation until the flow is fully developed turbulent around the building. Fig 8 shows the flow fully turbulent structure around the building colored by the velocity while the ground is colored by the static pressure.

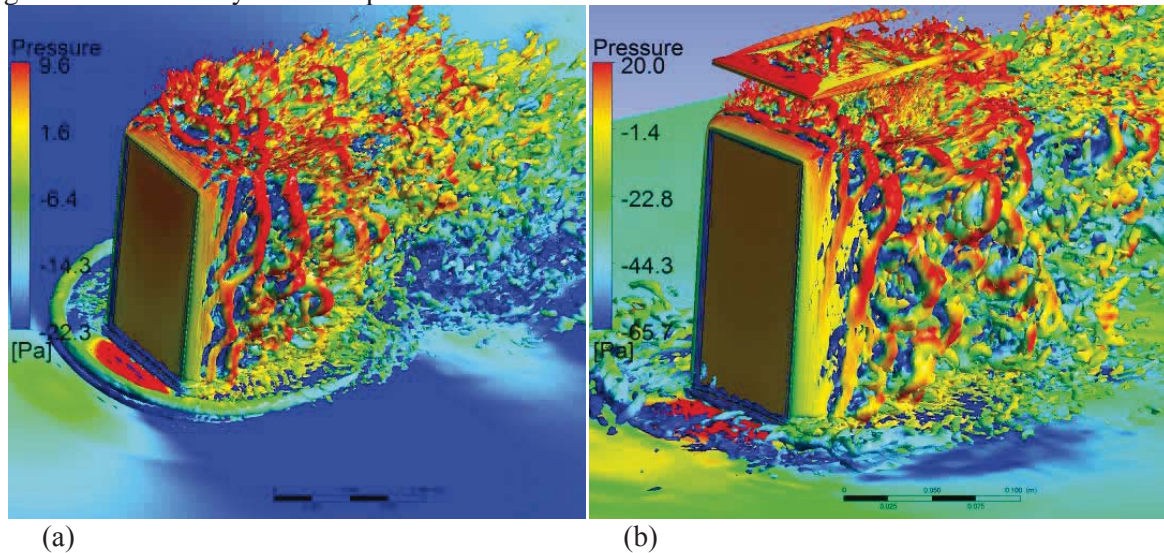


Fig 8: Flow structure around the buildings; (a) flat roof building and (b) with the umbrella-like structure above the roof.

Once the flow is fully developed turbulence, the averaged process started and it takes about 2.0 sec for obtaining an average flow. Fig 12 shows the time-averaged flow around the high-rise buildings (Fig 12(a) if or float roof and Fig 12(b) is with umbrella-like shape) through streamlines projected on a plane passing through the center of the buildings. The figure shows a massive separated flow above the roof. There is also a large effect of the umbrella on the velocity distribution in the above roof flow. The umbrella increases the wind speed close to the roof and thus maximizes the potential of harvesting wind energy from the above roof flow. There is also an increase of the velocity above the umbrella-like shape that can be used for harvesting wind energy.

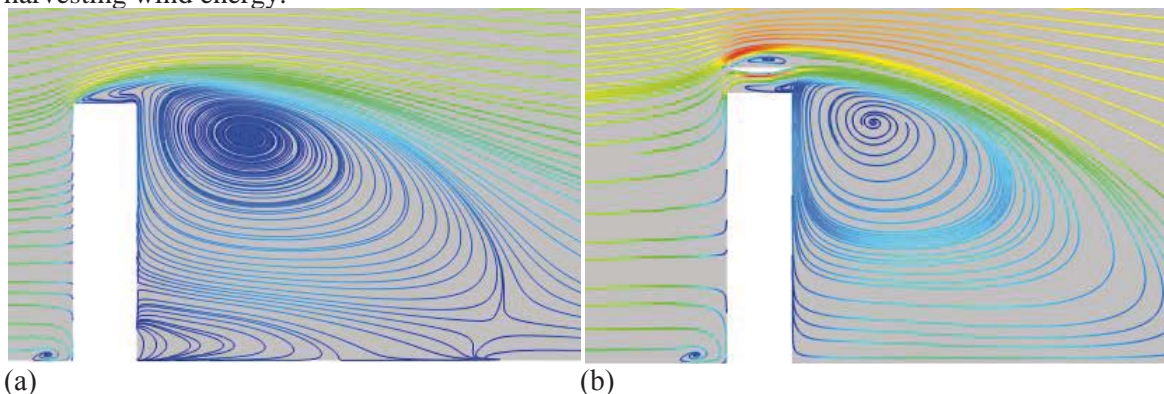


Fig 9: Flow streamlines projected onto a plane at the centerline of the building. (a) flat roof (b) with the umbrella-like structure above the roof.

Fig 10 shows a mid-plane colored by the time-averaged velocity magnitude. The above roof flow can be consisted to three regions; circulation region, shear layer region and core flow region. The circulation region is closest region to the roof of the building and the core region is the further from the roof of the building. The shear layer is the layer between the circulation and

core regions. In order to maximize the wind energy generation, the wind turbine should be placed in the core flow region.

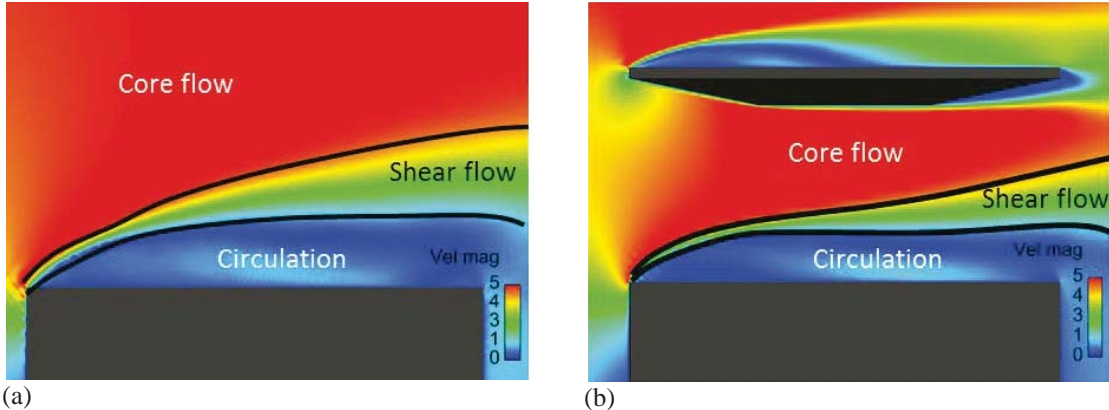


Fig 10 Mid-plane coloured by the time-averaged velocity magnitude; (a) without umbrella and (b) with umbrella.

Fig 11 shows the size of the circulation region above the roof. In case of isolated building without umbrella, the thickness of the circulation region is about $0.3b$, while it is reduced to $0.2b$ due to the umbrella.

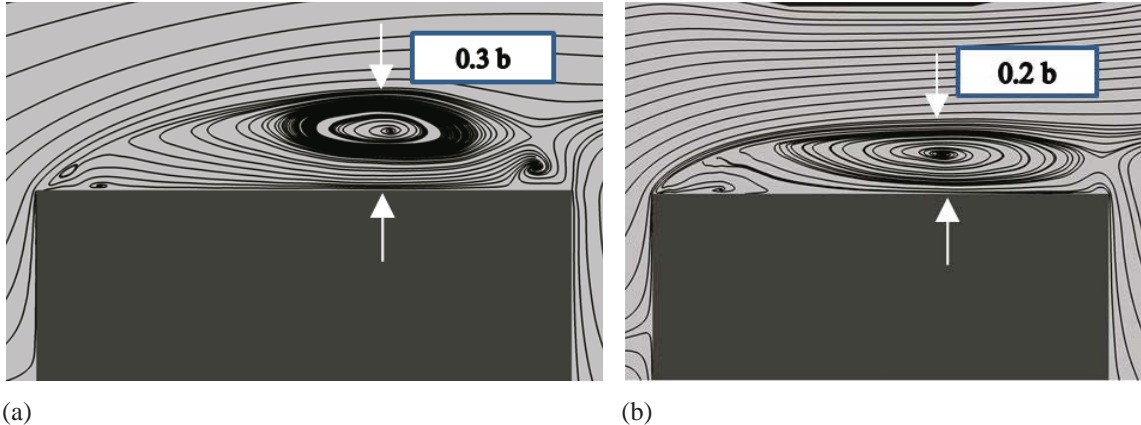


Fig 11 Streamlines show the above roof; (a) without umbrella and (b) with umbrella.

Fig 11 reveals also that the core flow above the building is parallel to the roof in case of the umbrella while it is slightly moves with an upward angle in the case of a building without umbrella.

In order to evaluate the effectiveness of the umbrella, the velocity profiles in the above roof flow and under the umbrella are compared with those without umbrella at the same position as shown in Fig 12. In the first quarter of the width of the building, there is no significant effect of the umbrella on the above roof flow. After the first quarter and along the width of the building, there is a significant reduction in the circulation region height and the thickness of the shear layer. There is also a slight increase in the time-average wind velocity.

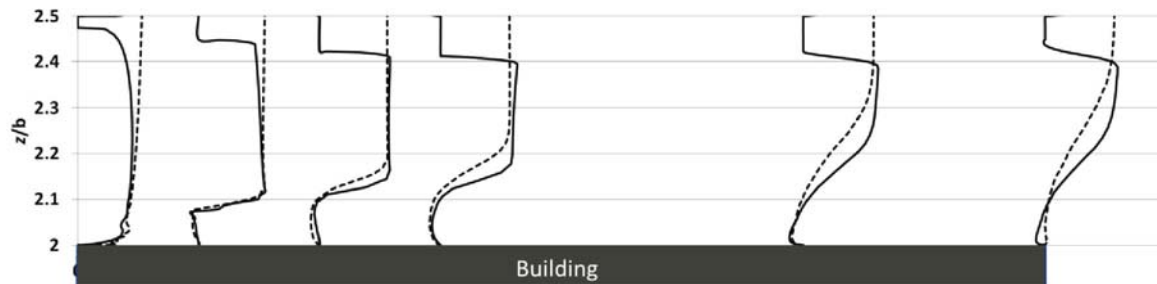


Fig 12 Velocity distribution on the above roof flow; (dashed) without umbrella and (solid) with umbrella.

7. CONCLUSIONS

Large-eddy simulation of the flow above and around high-rise buildings with two roof shapes, with and without umbrella-like shape has been made. The results have been compared with experimental data and good agreement has been obtained. Three different regions have been identified in the above roof flow; circulation region, shear layer and core region. The recirculation region is the closest to the roof of the building, which is characterized by low velocity and high turbulence intensity and not suitable for wind energy generation. The shear layer is characterized by large change in velocity magnitude, which is also not suitable for wind energy generation. The core region is characterized by high velocity and low turbulence intensity, which is ideal for wind energy generation. In general, it could be concluded that attaching an umbrella-like shape above the roof of the building could add positive effect on the flow velocity by decreasing the height of the circulation region and increasing slightly the air velocity in the core region and hence the potential of increasing the energy harvesting.

8. ACKNOWLEDGEMENT

The authors would like to acknowledge the support provided by the COST-Action TU1304. The computational resources provided by the Birmingham Environment of Academic Research (BEAR) are gratefully acknowledged.

REFERENCES

- ESRC (2009) How people use and 'misuse' buildings. Swindon: Econ. & Soc. Res. Council.
- Kim, W., Tamura, Y. and Yoshida, A. (2011). Interference effects on local peak on local peak pressures between two buildings. *Journal of wind engineering and industrial aerodynamics*.
- UN (2009) World Urbanization Prospects: The 2009 Revision. New York: UN.
- UNEP (2007) Buildings and Climate Change: Status, Challenges and Opportunities. Paris: UN Enviro. Prog.

Monitoring Based Identification for Structural Life Cycle Management of Wind Energy Converters

R Höffer

Ruhr University Bochum, Wind Engineering and Fluid Mechanics, Bochum, Germany

S Tewolde

Ruhr University Bochum, Wind Engineering and Fluid Mechanics, Bochum, Germany

Airwerk GmbH, Essen, Germany

S Bogoevska

St Cyril & Methodius University Skopje, Macedonia

M Baitsch

Hochschule Bochum, Bochum, Germany

S Zimmermann

University of Florence, Department of Civil and Environmental Engineering, Florence, Italy

G Barbanti

Ruhr University Bochum, Wind Engineering and Fluid Mechanics, Bochum, Germany

Email: Ruediger.Hoeffler@ruhr-uni-bochum.de

Abstract. Wind energy is becoming increasingly favorable and reliable energy source. But in order to make it more efficient and costly competitive with the other energy sources, wind turbines are continuously getting bigger, taller and positioned in more challenging environments for higher power generation. But with higher output also comes higher risks, which need to be identified and mitigated. So as to be able to ensure the operational safety and functionality of the Wind Energy Converters (WECs) with minimum operational and maintenance costs throughout its life time. For an efficient life cycle management of WECs, it is very important to implement smart monitoring systems that are able to effectively track the structural health condition of the operating wind turbine. With such systems the operation and maintenance cost of the wind turbines will significantly decrease, resulting in an affordable cost per KWH of the energy generated from wind turbines. The implementation of such techniques needs a careful planning and consideration of various prerequisites, with which this paper deals.

Keywords: Life cycle management; wind energy converters; structural health monitoring; OMA

1. INTRODUCTION

Wind Energy Converters (WECs) contain many electrical, mechanical and structural components, which may fail and result in interruption of power generation. And larger wind turbines may potentially have higher failure rates, which result in more downtime compared to smaller turbines. To avoid this situation from happening, it is important to have reliable information about how the components are performing. Having this information will minimize the uncertainty on the decisions made.

According to ISO 31000“risk” is defined as, the effect of uncertainty on achieving objectives. In the case of WECs, the objective is to get a continuous power generation. But the failure of one or more components can lead to power generation interruption (down time). Therefore, for an efficient life cycle management of wind energy converters, it becomes very important to know the status of the wind turbine components, in this paper the structural components, so as

to be able to plan and implement a strategy for avoiding down time or resuming power generation with as minimum down time as possible.

This knowledge can also be utilized for planning preventive maintenance rather than the more expensive corrective maintenance. The concept of preventive maintenance is that damages are detected in their early stages and actions taken before damage propagation, which may result in total failure. While in the case of corrective maintenance, maintenance is done after damage already occurred, which leads to much higher maintenance cost and longer down time.

Therefore, preventive maintenance is preferable due to the cheaper repair costs for the small damages and most importantly the WEC can in minor cases be repaired while in operation or with very short and controlled down time. But to implement preventive maintenance, the need arises to have information of the structure's status, because having more knowledge (information) reduced the uncertainty and thus reducing the risk. And this can be achieved in wind energy sector through Structural Health Monitoring (SHM) of the wind energy converters.

The benefits of incorporating the structural health monitoring in life cycle management for operating WECs can be summarized as: contribution to improved safety and functionality of structures, minimizing the number of inspection visits, timely and cost effective maintenance, possible service life time extension with less and controlled risk and positive contribution for future innovative designs. However the implementation of such scheme needs detailed planning and tackling of several prerequisites.

2. PREREQUISITES FOR LIFE CYCLE MANAGEMENT OF OPERATING WECS

The life cycle management of wind energy converters mainly involves decisions concerning inspection and maintenance scheduling. Generally, inspection strategies can be classified as Prescriptive (rule based) and Risk based. In the case of rule based inspection, all joints (hot spots) of a structure are inspected at a predetermined fixed time interval. This method is much simpler to implement with no need of risk analysis and a routine like allocation of resources every time inspection is made. But it is not effective, as some of the joints might be unnecessarily inspected or it might be too late for some of them, which might lead to corrective maintenance.

The second strategy called, Risk Based Inspection (RBI), develops an inspection model by making use of the Bayesian decision theory and structural reliability analysis. The structural reliability analysis makes use of fracture mechanics to investigate the life time development of a crack from its initiation to propagation and failure stages. Then these stages are calibrated against corresponding S-N curve, so that the model can roughly predict the crack size at a time t . As a result, inspections of joints (hot spots) are then planned at a time between detectable crack size and failure stage. But the detection of a crack is not easy, the earlier the crack is needed to be detected then the more sophisticated tools are required to detect it which will increase the inspection cost. Generally the probability of detection (PoD) of a crack is directly proportional to the inspection quality used.

The presence of many uncertainties in many of the parameters of the models involved need to be addressed by random variables characterized by corresponding probability density functions to be incorporated in the Bayesian network. These parameters are to be updated with new information obtained at, for example, every inspection outcomes. But the number of parameters involved makes the computational effort very demanding, as a result a generic approach for risk based inspection was developed by Straub (2004). In this method representative hot spots are selected from the structure and used for the model. Then the inspection plan for the unselected hot spots is obtained by interpolating the result obtained from the representative hot spots. This very significantly decreases the computational demand for implementing RBI in industries. RBI is much more effective from the rule based inspection, because the next inspection is scheduled based on the outcomes of the previous inspection.

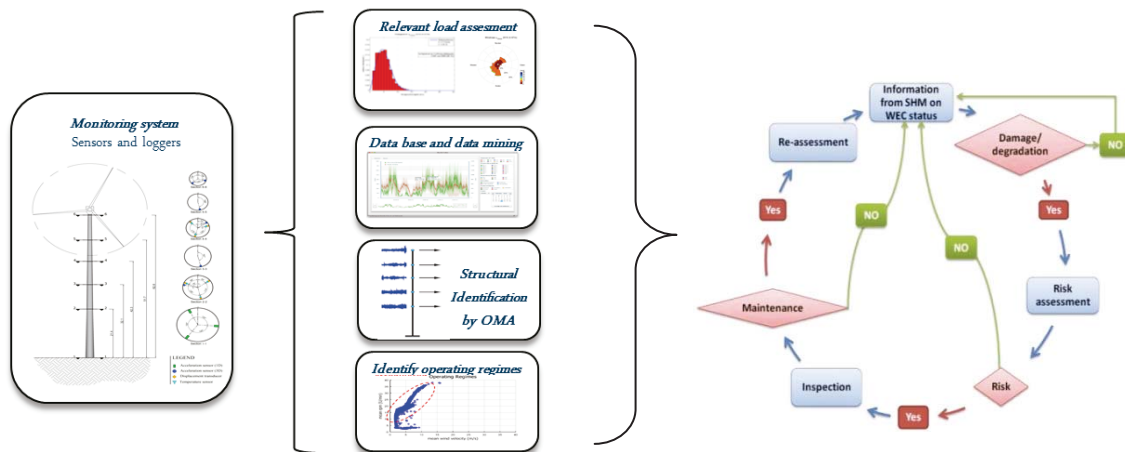


Fig 1. General overview of prerequisites for a successful Life cycle management strategy

Nevertheless, the second method (RBI) still fully depends on the design assumptions for the loads, which in most cases are too conservative compared to the actual condition the structures are exposed to during their lifetime. In addition, it fully depends on the fatigue deterioration of the structures with the risk that unexpected sudden events between inspection periods can result in failure of structures, which then might still lead to corrective maintenance.

This and similar monitoring based life cycle management strategies can be taken one step forward in the case of WECs, by making use of the real time continuous structural health monitoring systems and fed with updated valuable information from automated structural identification techniques. The scheme and the techniques required for successfully implementing this strategy are summarized in figure 1 and discussed in detail in this paper.

2.1. Assessment of relevant load based on actual location specifics

The towers of wind energy converters (WEC) are affected by wind, which is the most significant meteorological influence for this type of structures. It is anticipated that wind farms are systematically located at sites with especially high mean values of the complete ensemble of wind speeds. Therefore, in order to estimate the residual lifetime of WEC structures, the extremes of the wind quantities on one side and its values at service conditions at the other side are required. The wind field at a certain location is due to the large scale synoptic weather phenomena and due to the roughness in the surrounding of the wind turbines, the orography and thermal stratification.

The description of the wind climate at a site of interest is based on the mean values of statistical time series. The mean values form an own ensemble and can be represented as a histogram. The most frequently applied probability density distribution for the analytical description of the histogram is the Weibull function. Wind rosettes are used for the statistical evaluation of the monitored wind directions.

An example of a measurement based, evaluated histogram of mean wind velocities at the site of a WEC at Dortmund in a geodetic height of 67m is shown in Figure 2 below.

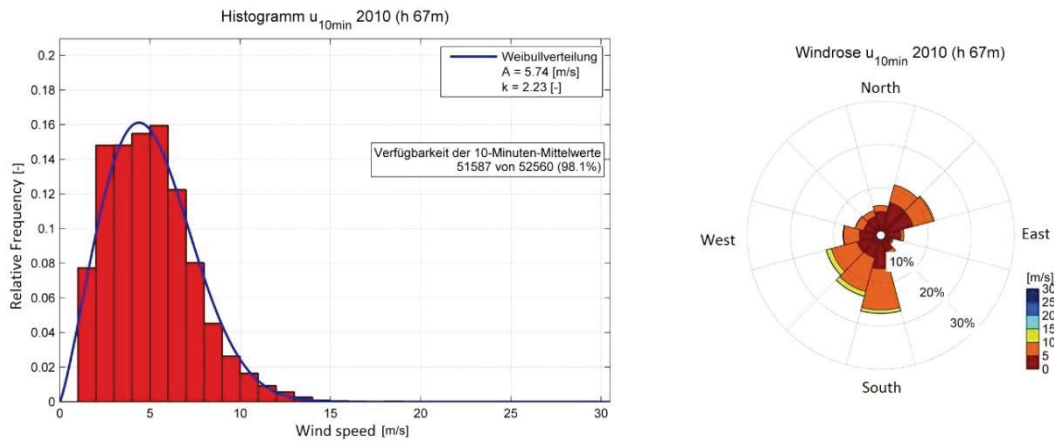


Fig 2. Left: histogram of the measured mean wind velocities in a height of 67m above ground level, analytical approximation using a Weibull distribution. Right: measured distribution of wind directions at a height of 67m above ground level

Information about the apparent roughness and orographic structures at an arbitrary location can be taken from suitable geo-information systems including the relation to the wind direction. A world-wide digital terrain model exists which is based on data from the Space Shuttle Radar Topography Mission (SRTM). The required land use data for the roughness description is provided by the CORINE data base (Coordination of Information of the Environment) of the European Environment Agency. Fig 3. represents the sectorial distribution of the land use over a radius of 5km around the site of a WEC at Dortmund (Figure 5) with numerically approximated lines of equal geodetic heights. Such detailed information about the local situation together with introduced procedures provides a possibility to derive estimations of the effect of roughness and orography on the wind field characteristics.

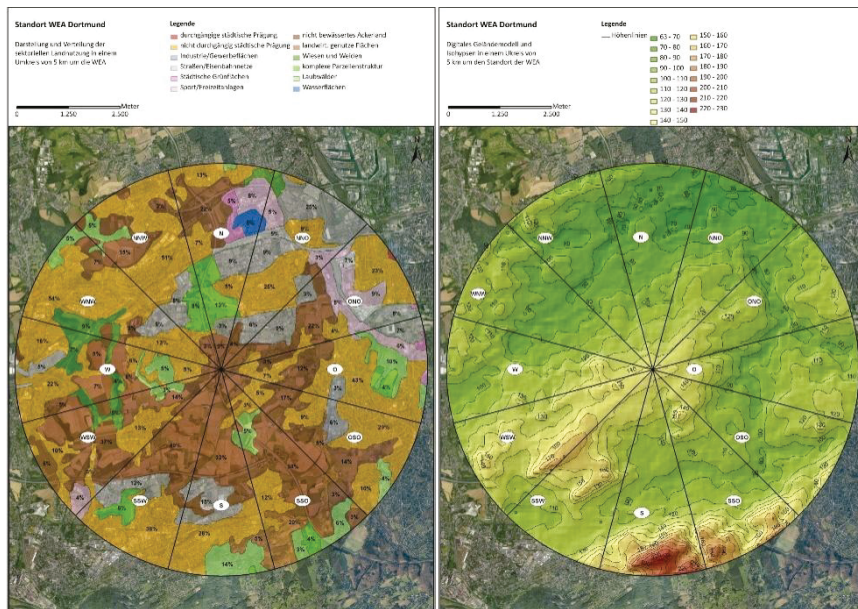


Fig 3. Left: Sectorial distribution of land use in the investigated area based on the CORINE land register. Right: Digital model of the investigated area based on geodetical SRTM data and numerically approximated lines of equal geodetic height.

To date information about the wind field for the situation of a non-neutrally stratified atmosphere can only be collected through wind velocity measurements at the location of interest. The stability of the stratification has a decisive influence on the vertical mixing within the atmospheric boundary layer. The vertical transport of air volumes is fostered in the case of labile at-

mospheric stratification, and blocked in the case stable stratification. In the mean labile stratification appears during the day whereas stabile stratification appears during the night. Fig shows an example about the distribution of the exponents of the wind profiles (Hellmann exponent) and of the mean wind velocities at the site of a WEC at Dortmund. On the right hand side the figure shows the development of the mean Hellmann exponent with changing wind velocities evaluated for the location.

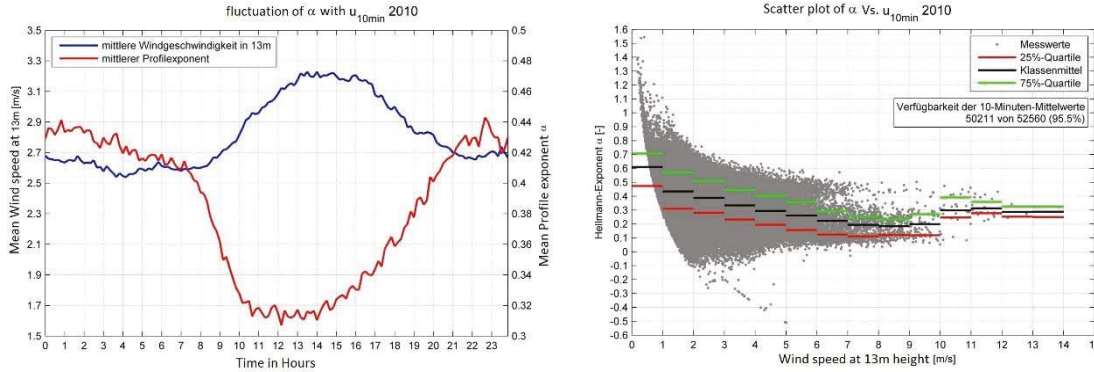


Fig 4. Left: mean measured distribution of the exponent of the wind profile in the course of a day; right: distribution of the exponents of the wind profiles (Hellmann exponent) and of the mean wind velocities at the site of a WEC at Dortmund.

2.2. Optimization of Sensor positions

The purpose of the strategic sensor positioning is to track the changes in structural vibration responses, so as to be able to determine from the changes in dynamic parameters, when deterioration or damage occurs. Sensor position for an actual operating wind turbine in Dortmund, Germany which is in operation since 1997 and being monitored since 2010 is presented on figure 5 below.

Table 1. List of sensor types and sampling rates

Sensor Types	Number of Sensors	Sampling Rate (Hz)	Remark
3D Accelerometer	6	100	Along the tower at five levels
1D Accelerometer	3	100	On top of the tower's concrete foundation
Displacement Transducer	6	50	Along tower at two levels
Temperature	6	1	Together with Displacement sensors
Temperature	2	1	Inside tower at 3m and 20m heights
Temperature	2	1	Outside tower at 3m and 20m heights
Ultrasonic Anemometer	1	50	On top of a separate nearby tower, at 13m height. Measures: Horizontal and Vertical wind speed, Wind direction and Air temperature

The wind turbine in Dortmund shown in Figure 5 is an Enercon type (E-40-500 kw), with hub height of 65m and rotor diameter 40m. The tower is conical with an outer diameter of 2.99m at the bottom and 1.20m at the top. The type and number of sensors used along with their sampling rates are summarized in table 1 below.

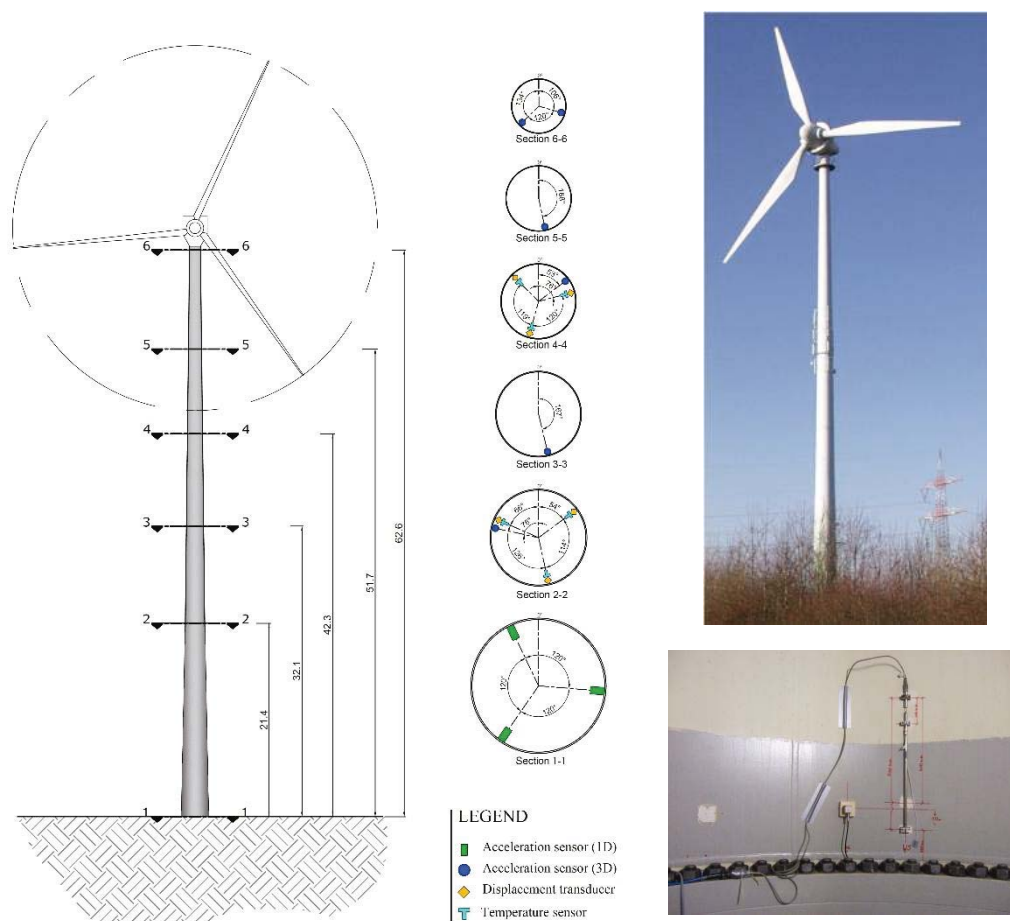


Fig 5. Sensor layout scheme (left) for the AIRWIN WEC (top) and displacement transducer (bottom)

2.3. Data management and storage planning

Analog signals from sensors are converted to digital data streams by several data logging devices. Specialized programs write the data to disk, in various formats either in binary or ASCII form. According to the number of sensors and logging frequencies, approx. 120 GB of data are generated per year. For efficient further processing in the lifecycle management of the wind turbine, this large amount of heterogeneous data is processed and stored in a relational database. From there, information can be retrieved either directly by an application which supports import from databases (such as MS Excel or Matlab) or be exported to various formats via a web application. Fig 6. shows an outline.

On-site server: All logging devices are connected to the on-site server located on the ground floor of the wind turbine tower. Because the logging devices require vendor specific software which is only available for Windows, this computer runs Windows XP. The system is connected to the Internet by a German Internet service provider; in order to enable remote system administration, a dynamic DNS service is being used. The following tasks are performed on a regular basis:

- Temperature data from the PT104 logger is stored in binary files. For consistent processing these are first converted into ASCII using a small Java program.
- The files written in the last time interval are renamed such that the name reflects the create date. This greatly simplifies ordered further processing and management.

- Finally, the renamed files are transferred to the database server using the rsync program for efficient file synchronization. After transmission, integrity of the transferred files is verified using MD5 checksums.
- Files which have already been transferred to the database server are removed after a safety period.

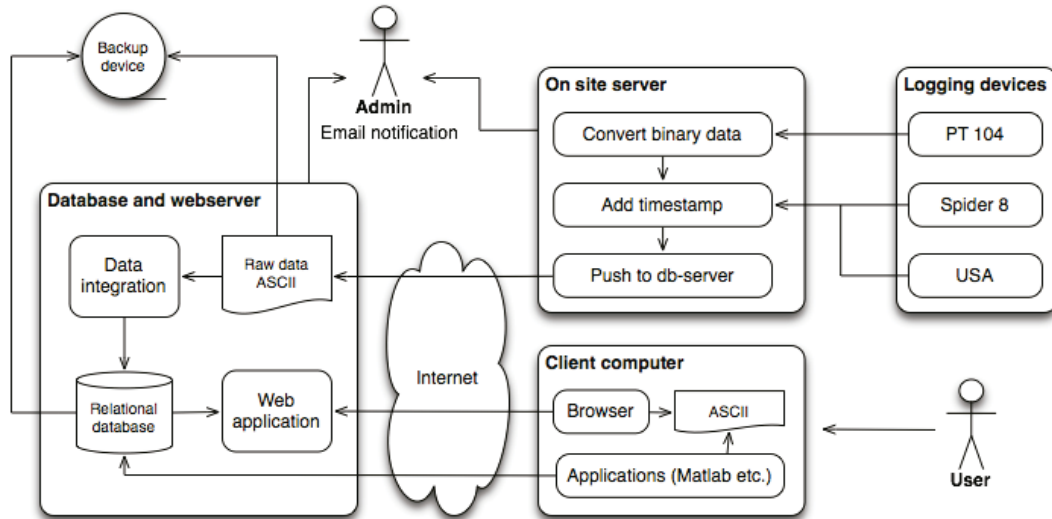


Fig 6. Processing of monitoring data

Data processing is operated by a set of shell scripts running in a Cygwin environment. In order to avoid concurrent access to unprocessed data by different processes, sensitive folders are locked by semaphore files. In the case, a process exits abnormally; expired semaphore files are removed automatically after a certain time interval in order to avoid deadlocks.

Database and web server: The database server is a Linux-computer located at Ruhr-University Bochum. On this computer, the content the raw data files (primary data) from the on site server is stored in a MySQL database (secondary data). The layout of the database is straight forward; each logging device has its own table with columns for each connected sensor. The process of transferring raw data into the database is performed by the well established data integration tool by Pentaho. For example, acceleration is logged at a frequency of 100Hz which results in more than 8 million data points per sensor (one channel)per day. For the graphical representation of an overview for several days or weeks in a web-based user interface, this amount of data cannot be handled. For this reason, high-frequency logging data is statistically down sampled for further processing. In this step, the median value, 50% quartiles and the smallest and largest non outlier values are computed for the down sampling time interval and stored in an additional table (tertiary data). Users can either access the data directly from the database or via a web application [9]. On the server side, a web service running inside an application server (JBoss) provides data using the SOAP protocol. The client application (see) runs in a web browser and allows users to conveniently inspect logged data and to export data in various formats.

Error handling: The described system is expected to operate continuously without any user interaction. However, a wide variety of exceptional situations can occur: Loggers might write corrupted files, sensors may fail or the Internet connection may be interrupted. Some of these situations require the system administrator to take fix problems manually. The system sends an email to persons in charge when one of the programs involved in the conversion pipeline terminates abnormally. A program periodically examines the database based on several heuristic rules encounters a problem.

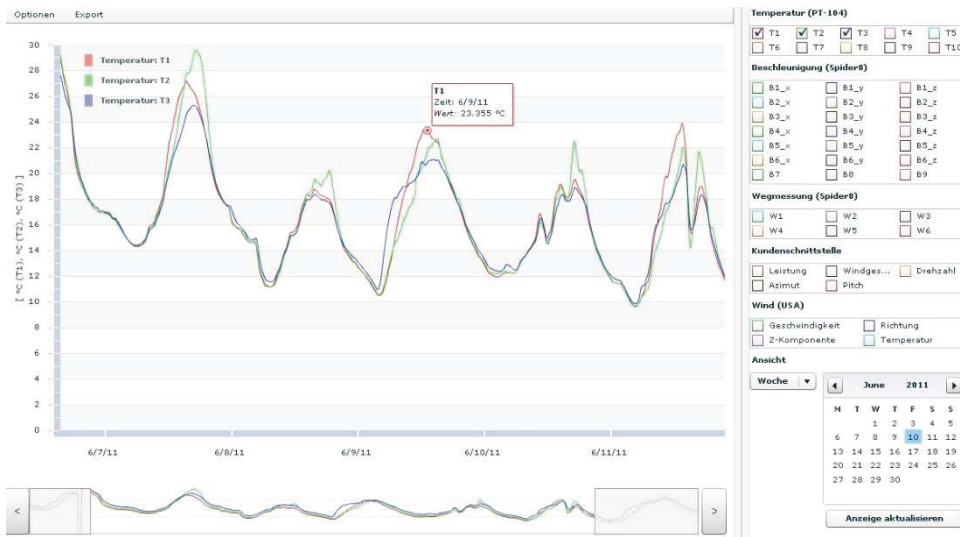


Fig 7. Client-application

2.4. Identification of wind turbine's operating regimes

Wind is a naturally varying resource, therefore wind turbines are designed in such a way that they can make the best of the available wind. That is, they are equipped with a controller inside the nacelle which constantly rotates the rotor in such a way that they can face the direction. And the blades are pitch controlled, so that their pitch angle can be automatically adjusted to make the best of a small wind speed or to decrease the uplift force in cases of extreme wind speeds (above cutoff wind speed). Wind energy converters mainly operate in one of the three main states presented in Table 2 below. These working regimes have important influence on the outcome of the employed operational modal analysis and structural identification approach and hence need to be identified.

Table 2. Operating regimes of the wind turbine

Parked Regime (no wind, maintenance or safety stop)	RPM-regulated Regime (weak or moderate wind)	Pitch-regulated Regime (strong wind)
<ul style="list-style-type: none"> • Pitch angle set to maximum to reduce wind load • No power production and non-working rotor • The most simple case from analysis point of view 	<ul style="list-style-type: none"> • The pitch angle is minimal and the blades exploit all available wind energy • The RPM increases with the wind speed • Does not affect the natural frequencies as the pitch-regulated regime 	<ul style="list-style-type: none"> • The RPM is kept constant by the control system by changing pitch angle • The pitch changes with wind turbulence • Seriously affects the in-plane and out-of-plane rotor modes

On figure 8 below, the analysis of an operational data for one month is presented. Obviously, the structure is working in RPM-regulated regime.

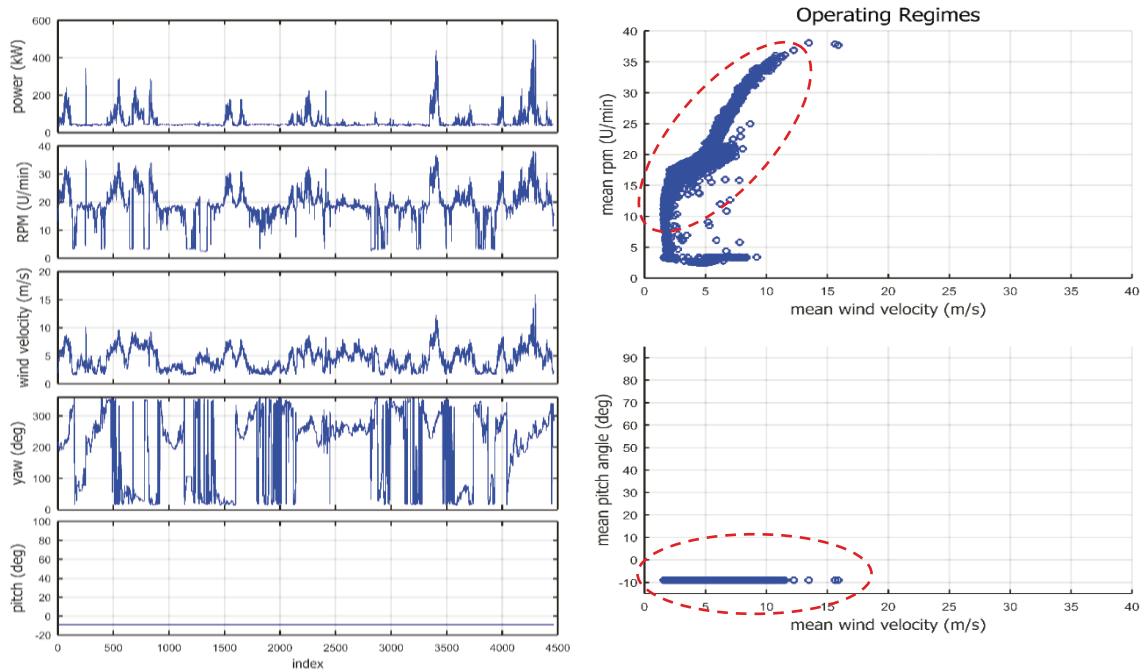


Fig 8.10min mean values of operational data (left) and identified operating regime (right) for May 2010

2.5. Structural identification – applicability limitations

The main goals of the monitoring system are the characterization of the wind turbine tower vibrations and the assessment of the structure’s most relevant modal parameters, in order to evaluate its structural status, detect damages and eventual abnormal behaviors that may reduce its lifetime. And by performing fatigue analysis of the stress time history, it is possible to estimate the residual life time of the structure and evaluate in more detail the extended safe years that it can stay in operation.

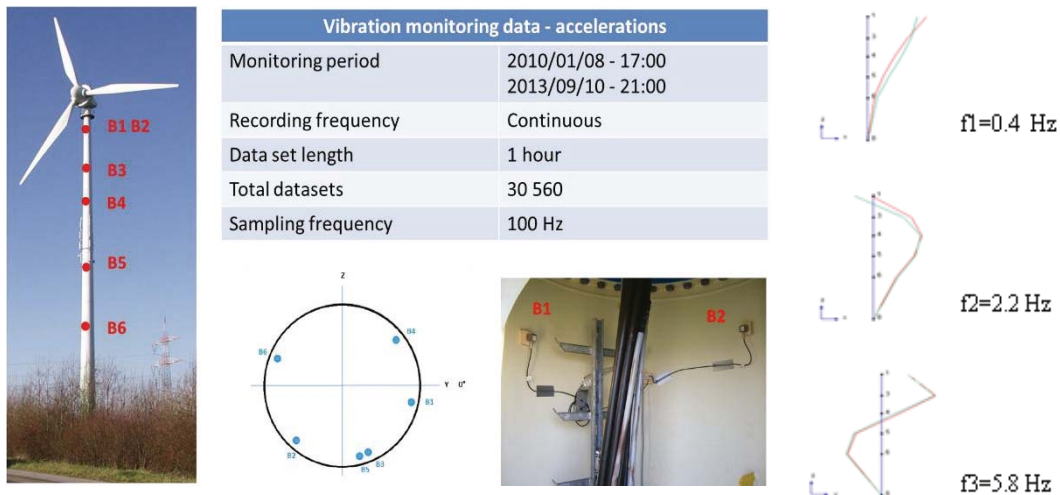


Fig 9. Vibration monitoring sensors, data and preliminary stationary- OMA results

Operational Modal Analysis (OMA) is an ideal tool to perform modal analysis and estimate the modal parameters of large civil engineering structures. Unlike the classical experimental modal analysis, which requires measurement of the inputs forces, OMA uses only the response measurements of the structure being monitored to estimate modal parameters. But identification

of the modal parameters for a full-scale operating wind turbine is particularly difficult, and a lot of research has been done to try to develop suitable methods to tackle this problem.

A structural damage will modify the stiffness, mass or energy dissipation properties of a system which will then result in different measured vibration response (different modal parameters). The inherent problems in operating wind turbine structures originate from the complexity of the structure, uncertainty of the loads and environmental factors, which violate the basic OMA assumptions that the excitation force is a random white noise. And this violation could result in spurious structural identification (non structural false modes).

Furthermore, not considering the randomly changing environmental and operational conditions could yield false structural damage identification. Hence, to capture the time variable behavior of wind energy convertors and identify a comprehensive dynamic model of the structure is necessary for the successful implementation of an effective life cycle management strategy. In order to achieve this, the time varying behavior of wind energy convertors and non-stationarity of response data need to be considered.

2.6. *Damage detection*

The strategically positioned sensors can detect the changes in structural vibration response as a result of damage or significant deterioration, which is reflected by the variation of the modal parameters. But in order to be able to detect damage it is very important to have the reference dynamic parameters of the healthy structure, against which the newly computed dynamic parameters are compared. Generally, damage is directly proportional to damping and inversely proportional to natural frequency. Therefore by tracing the variation of the modal parameters in time, a damage index can be developed against which the newly computed modal parameters are compared, so that it is used as an input for the reliability based inspection decision making.

Table 3. Summary of information that can be extracted from sensors

Sensor type	Information obtained (used for)
Accelerometer	Natural frequencies, Mode shapes and Damping Generally – Damage is inversely proportional to Natural frequency and directly proportional to damping.
Strain gauge (Displacement transducer)	Fatigue analysis for remaining life time estimation
Temperature	Environmental effect compensation

3. APPLICATION

All data obtained from the SHM is interpreted in such a way that it assures the safe operation of the structure and aids the decision makers for inspection and maintenance planning of the wind turbines. That is, Instead of waiting for the damage until failure occurs and apply corrective maintenance, which is more expensive and most of the time needs stopping the operation of the wind turbines, it is more preferable to implement preventive maintenance through SHM which can detect the damage during its initial stages or prevents the damage from occurring by taking mitigation actions in good time. By incorporating the continuous information about the structural status obtained from SHM, corrective maintenance will be avoided as much as possible.

In this method it is proposed to develop degradation and damage indices of the healthy structure so that they can be used as reference thresholds for inspection planning during the life time of the WEC, of course they need to be calibrated for deterioration with age of the WEC. Also it is very important to consider the environmental and operation condition of the wind turbine; because the response of the wind turbine greatly varies in what condition it is happening. A normal response for a certain scenario might be a critical situation for another scenario. There-

fore, it is very crucial to consider the environmental and operational conditions of the wind turbine for realistic interpretation of the vibration responses and effective life cycle management.

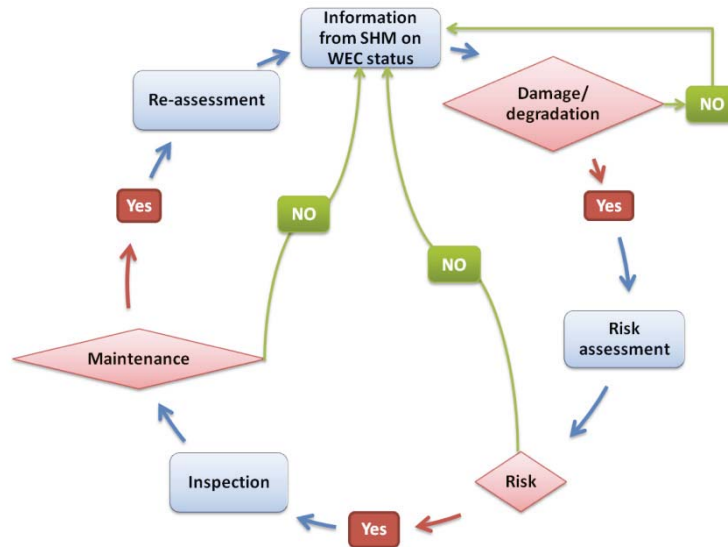


Fig 10. Incorporation of SHM in the life cycle management of WECs for inspection and maintenance planning

4. CONCLUSION

Monitoring can be a qualified basis for continuous strength checking of the structure of wind converters. In recent years, structural elements of wind energy converters have been monitored in order to control and steer the blade and gear configuration during power production, to alert about dynamic overloading, and to detect dangerous conditions such as icing. New and modern monitoring concepts aim more at the identification of present or developing damages to provide an advanced estimation of the residual lifetime of the structure of the wind turbine. To this, the applied sensor systems for periodical and/or continuous monitoring are predominantly acceleration sensors, cycle transmitters, strain-gauges, and inductive displacement transducer, where the accuracy of such systems depends strongly on the local peculiarities. Previous sensor systems have mainly been used for sensing purposes within a specified recording concept. By contrast, relatively new applications employ optical displacement detectors or radar interferometers. Both devices are mostly based at an outside reference positions adjacent to the wind energy converter (WEC).

The benefits of incorporating the structural health monitoring for life cycle management of wind energy converters can be summarized as:

- Improve safety and functionality of structures
- Minimize number of Inspection visits and down time
- Timely and cost effective maintenance
- Service life time extension with minimum risk

5. ACKNOWLEDGEMENT

The support of the German Research Foundation (Deutsche Forschungsgemeinschaft DFG) in the framework of the research projects no. HA 463/20-1 and HO 3286/1-2 as well as the support of the Innovative Training Network “Aeolus4Future” granted as a Marie Skłodowska-Curie action within HORIZON 2020, grant agreement no. 643167, is gratefully acknowledged.

REFERENCES

- Ribrant, J. and Bertling, L.R.: Survey of failures in wind power systems with focus on Swedish wind power plants during 1997-2005, Proceedings of the IEEE Power Engineering Society General Meeting 2007. Tampa, FL, USA, June 24-28, 2007.
- ISO 31000: 2009, Risk management - Principles and guidelines
- D. Straub, J. Goyet, J. D. Sørensen, M. H. Faber: Benefits of risk based inspection planning for offshore structures. Proceedings of 25th International Conference on Offshore Mechanics and Arctic Engineering. June 4-9, 2006, Hamburg, Germany.
- Daniel Straub: Generic approaches to risk based inspection planning for steel structures. PhD thesis. Eidgenössische Technische Hochschule ETH Zürich, Zürich. 2004
- D. Straub, M. H. Faber. Computational aspects of risk-based inspection planning. Institute of Structural Engineering, Swiss Federal Institute of Technology, ETH- Hönggerberg, Switzerland. 2006
- Lachmann, S.: Kontinuierliches Monitoring zur Schädigungsverfolgung an Tragstrukturen von Windenergieanlagen. Dissertation, Fakultät für Bau- und Umweltingenieurwissenschaften der Ruhr-Universität Bochum, 2014
- Liu, X.: System Identification of a Wind Energy Converter using Wavelet-based Damage Detection and Robust Model Updating Strategy”, Ruhr-Universität Bochum, Dissertation, 2013.
- Höffer R., Tewolde S., Haardt H. and Bogoevska S.: Monitoring techniques for the detection of fatigue damages at Wind Energy Converters, WINERCOST Workshop ‘Trends and Challenges for Wind Energy Harvesting’, Coimbra, March, 2015.
- Hilfert, T.: Konzeption und Erstellung eines Webinterfaces zur Darstellung der Monitoring daten einer Windkraftanlage, Bachelorarbeit, 2009, Lehrstuhl für Ingenieurinformatik im Bauwesen, Ruhr-Universität Bochum
- Brincker R, Zhang L and Andersen P.: Modal identification of output only systems using frequency domain decomposition, Smar Mat. St., 441–445, 2001.
- Cauberghe B.: Applied frequency-domain system identification in the field of experimental and operational modal analysis, PhD Thesis, Vrije Universiteit Brussel, Brussels, 2004.
- Carne TG and James GH.: The inception of OMA in the development of modal testing technology for wind turbines, Mech Syst Signal Pr, 1213–1226, 2010.
- Dmitri Tcherniak et al. ; Output-only Modal Analysis on Operating Wind Turbines: Application to Simulated Data, European Wind Energy Conference (20-23 April 2010, Warsaw, Poland)
- Muammer Ozbek, Fanzhong Meng , DanielJ.Rixen: Challenges in testing and monitoring the in-operation vibration characteristics of wind turbines, Mechanical Systems and Signal Processing August 2013
- L.D. Avendaño-Valencia, S.D.Fassois , Stationary and non-stationary random vibration modelling and analysis for an operating wind turbine, Mech. Syst. Signal Process. (2013)
- M. Spiridonakos, E. Chatzi: Polynomial chaos expansion models for SHM under environmental variability, Proceedings of the 9th International Conference on Structural Dynamics, EUROLYN 2014
- Airwerk GmbH, Essen

Design and Construction of a Small Multi-Bladed Wind Turbine for the Suburban and Rural Environments

M. Muscat

University of Malta, Faculty of Engineering, Msida, MSD 2080, Malta.

T. Sant

University of Malta, Faculty of Engineering, Msida, MSD 2080, Malta.

R. N. Farrugia

Institute for Sustainable Energy, University of Malta, Marsaxlokk MXK1531, Malta

C. Caruana

University of Malta, Faculty of Engineering, Msida, MSD 2080, Malta.

R. Axisa

University of Malta, Faculty of Engineering, Msida, MSD 2080, Malta.

Email: martin.muscat@um.edu.mt

Abstract. The Maltese countryside is still dotted with a number of American style wind-driven water pumps which were used to extract water from the aquifer for irrigation purposes. Many of these machines have fallen into disuse as electrification has taken over. In some cases, the only remaining component is the lattice tower. These machines are now acknowledged landmarks of the Maltese rural landscape. The idea behind this current initiative is to use the existing wind pump towers and to replace their old rotors with a new turbine design. Field surveys were carried out in order to estimate the structural integrity of the existing towers, the number of towers available and their distribution over the Maltese islands. A multi-bladed, 3.4 metre rotor diameter wind turbine capable of generating electricity and having a higher aerodynamic efficiency was designed to aesthetically resemble the original wind driven water pumps. The new wind turbine blades were fabricated from glass fibre reinforced polyester composite and have been tested to MSA EN 61400 Part 2:2006. The rotor is aligned to face the wind direction by means of a tail vane. The yaw shaft is slightly misaligned from the longitudinal axis of the main driveshaft in order to protect the turbine in high winds through passive yaw control.

1. INTRODUCTION

The Chicago type wind pump was introduced in the Maltese countryside with the main purpose of pumping water from the aquifer for agricultural purposes. Nowadays this particular type of wind pump is considered to be part of the Maltese national heritage. Over the past decades, with the introduction of the electric water pumps, most of these wind pumps were neglected and left to deteriorate. Nowadays, there is a drive to gradually change the energy supply infrastructure to one that integrates renewable energy technologies. The European Union has a target to cut green house emissions by 20% and to supply 20% of the final energy consumption from renewable energy sources by 2020. The two most common sources of renewable energy in Malta are wind and solar energy.

In 2007, the Ministry for Resources and Rural Affairs funded the Faculty of Engineering and the Institute for Sustainable Energy within the University of Malta to design a new and significantly higher aerodynamic efficient wind turbine rotor to replace the traditional Chicago style windmills, while at the same time retaining, as far technically possible, the original visual characteristics of the multi-bladed rotor. The concept was to use the existing wind pump towers and to replace their old rotors with the new wind turbine/generator design in order to feed electrical energy into the national grid. The aim of the project was to revive the unused windpumps and help conserve the national heritage. In January 2008 field surveys were carried out in order to estimate the structural integrity of the existing towers, the number of towers available and their distribution over the Maltese islands. A representative sample of about 50

wind driven water pumps was used to assess the tower structure above ground level. It was concluded that about 41% of the existing towers were structurally fit to have the new wind turbine mounted on them. However 47% required moderate repairs to regain the structural integrity required, while the remaining 12% required full reconstruction. Based on the results of the survey it was concluded that the majority of the existing wind pump towers were capable of carrying the new wind turbine so that the system can be converted to generate electricity. The design of the wind turbine system was based on European and British standards. Figure 1 and Figure 2 show photographs of a typical original Chicago windpump and of the designed, manufactured and installed prototype wind turbine electricity generator and tower.



Fig 1: A typical original Chicago windpump.



Fig 2: The designed, manufactured and installed prototype wind turbine generator.

2. EUROPEAN CODE OF STANDARDS FOR SMALL WIND TURBINES

The aerodynamic and structural designs of the main components of the wind turbine system followed the European standard MSA EN 61400-2:2006 which was especially written for small wind turbines. The standard deals with the design, manufacture, installation and maintenance of the small wind turbine. Each wind turbine design starts with consideration of the environmental conditions that exist at the installation site. Reference defines a number of small wind turbine (SWT) classes in terms of wind speed and turbulence parameters. For the island of Malta the SWT class III was chosen. This gives V_{ref} as 37.5m/s and V_{ave} as 7.5m/s as well as a number of other parameters such as the dimensionless characteristic value of the turbulence intensity at 15m/s. MSA EN 61400-2:2006 further provides equations that characterise normal and extreme wind conditions. These equations cover wind speed distribution at hub height, the wind profiles both for normal and extreme wind conditions, the normal turbulence model, the extreme wind speed model, wind speed at extreme operating gust, extreme wind direction change, wind extreme coherent gust and extreme coherent gust with direction change.

Reference presents three different methods in order to predict wind loads on the wind turbine. These involve simplified load equations, aeroelastic modelling and mechanical loads testing procedures. Each of the methods has different uncertainties so that different load safety factors are applied to each load estimation method. In this work the authors used the simplified load equations to calculate wind actions since the turbine satisfied a number of conditions. These conditions were that the turbine has a horizontal axis, it has two or more cantilever blades and it has a rigid hub. The simplified load model considers 10 load cases as listed in Table 1. The loads calculated using the simplified load equations need to be multiplied by a factor of safety of 3.

Table 1: Design load cases used for the turbine design (adapted)

Design situation		
Power production	Load case A	Normal operation
	Load case B	Yawing
	Load case C	Yaw error
	Load case D	Maximum thrust
Power production plus the occurrence of a fault	Load case E	Maximum rotational speed
	Load case F	Short at load connection
Shutdown	Load case G	Turbine braked
Parked idling or standstill	Load case H	Wind loading
Parked and fault conditions	Load case I	Wind maximum exposure
Transport assembly maintenance and repair	Load case J	Agreed upon

3. AERODYNAMIC AND STRUCTURAL DESIGN OF THE WIND TURBINE BLADES

The nine bladed rotor was designed with a tip radius of 1.7 metres and for an optimum design tip speed ratio of 3.2. This resulted in a slower design speed than conventional three-bladed rotors, but one still high enough to drive a permanent magnet generator without the need for a high gearbox ratio. The blade chord and twist distributions were derived using the Betz optimal rotor model defined by the following relations [9]:

$$\varphi = \frac{2}{3} \tan^{-1} \left(\frac{1}{\lambda_r} \right) \quad [1]$$

$$c = \frac{8\pi r}{BC_L} = (1 - \cos\varphi) \quad [2]$$

$$\lambda_r = \lambda \frac{r}{R} \quad [3]$$

The above model for the ideal blade shape was derived from the Blade-Element-Momentum (BEM) relations, taking the axial induction factor a_1 to be equal to the Betz optimal value of 1/3. The drag on the blades was ignored. The current design was based on the Eppler E197 aerofoil with the optimal angle of attack for the design tip speed ratio assumed to be 8 degrees. The Betz optimal blade design model yielded a blade twist that increases continuously towards the blade root. The blade twist angle was modified for the inboard sections with $r < 0.45m$, decreasing it gradually to zero at the root ($r = 0.25m$) to allow for a robust assembly at the rotor hub. The actual chord and twist distributions for the blades are presented in Figures 3 and 4. The blade cross-sectional geometry was also allowed to deviate at the inboard sections from that of the E197 aerofoil to gradually end up with a rectangular cross-sectional profile at the root. Apart from facilitating mounting at the rotor hub, the modified profile provided higher strength to cater for the high bending moments occurring in this region. The blade tip part ($r/R > 0.91$) was also modified to result in a decreasing chord culminating in a pointed tip similar to the tip shape of seabirds' wings. Apart from reducing the aerodynamic tip losses, the design improves the acoustic characteristics of the rotor.

The BEM theory was used to estimate the variation of the power coefficient of the actual nine-bladed rotor design with the tip speed ratio. The curves for three different blade pitch angles are shown in Figure 5. Despite the rotor overall solidity being high (20.6%), the estimated optimal power was found to be around 45% with the optimal tip speed ratio in the range $3 < \lambda < 4$. The maximum axial thrust coefficient was found to reach 0.85. In such computations, only 2D aerofoil data for the E197 aerofoil were used and the presence of 3D stall delay phenomena, known to augment power yields at low tip speeds, were ignored.

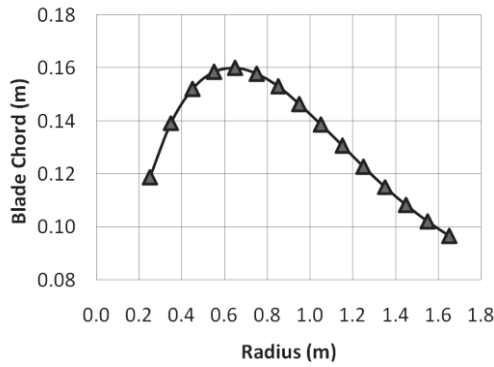


Fig 3: Blade Chord Distribution.

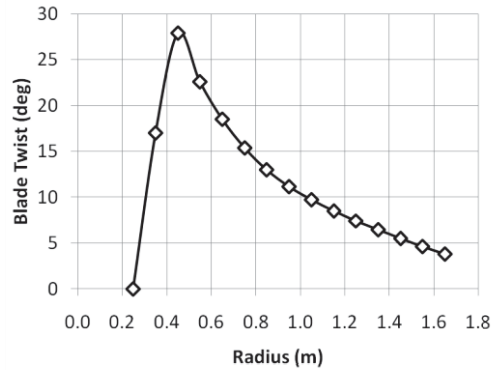


Fig 4: Blade Twist Distribution (Blade Pitch Angle is 0 deg).

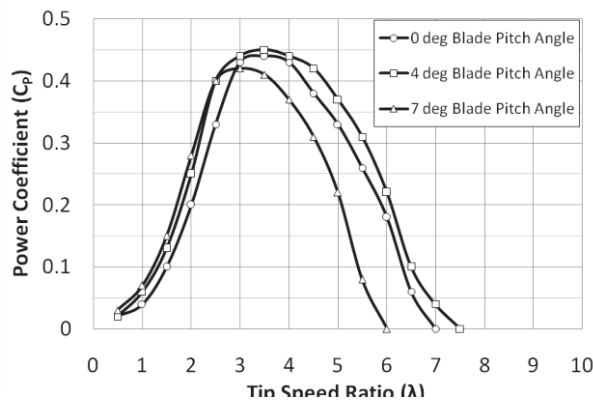


Fig 5: Predicted Rotor Power Coefficient at Different λ and Blade Pitch Angles.

4. STRUCTURAL DESIGN AND CONSTRUCTION OF THE WIND TURBINE BLADES

The blade span was divided into four different sections and a different design was adopted for each section (Figure 6). The loads and stress computations on the turbine blade were based on *MSAEN 61400-2:2006* for small wind turbines. All the load cases were assessed for the rotor design and the maximum load was obtained for Load Case H (Parked wind loading). Reference [3] only provides equations to compute the blade loads at the root. Using basic beam theory, the aerodynamic forces and moments along the entire blade span were computed. The selected material was GRP composed of E-Glass fibre laminates reinforced with a polyester resin matrix. The dimensions of the structural members at the different blade sections (Figure 6) were computed to ensure that the composite blades can withstand the extreme loads without failure. To manufacture the nine blades, a mould was constructed from GRP. Initially a plug was carved by hand from a solid rectangular piece of lime wood. Its surface was smoothed using a fine grain filler together with lacquer spray to seal and produce a fine finish. The plug was then used to produce the GRP mould, divided in two separate halves: the upper camber mould and the lower camber mould. Guide pins were introduced to keep the mould in position during the composite lay-up process.

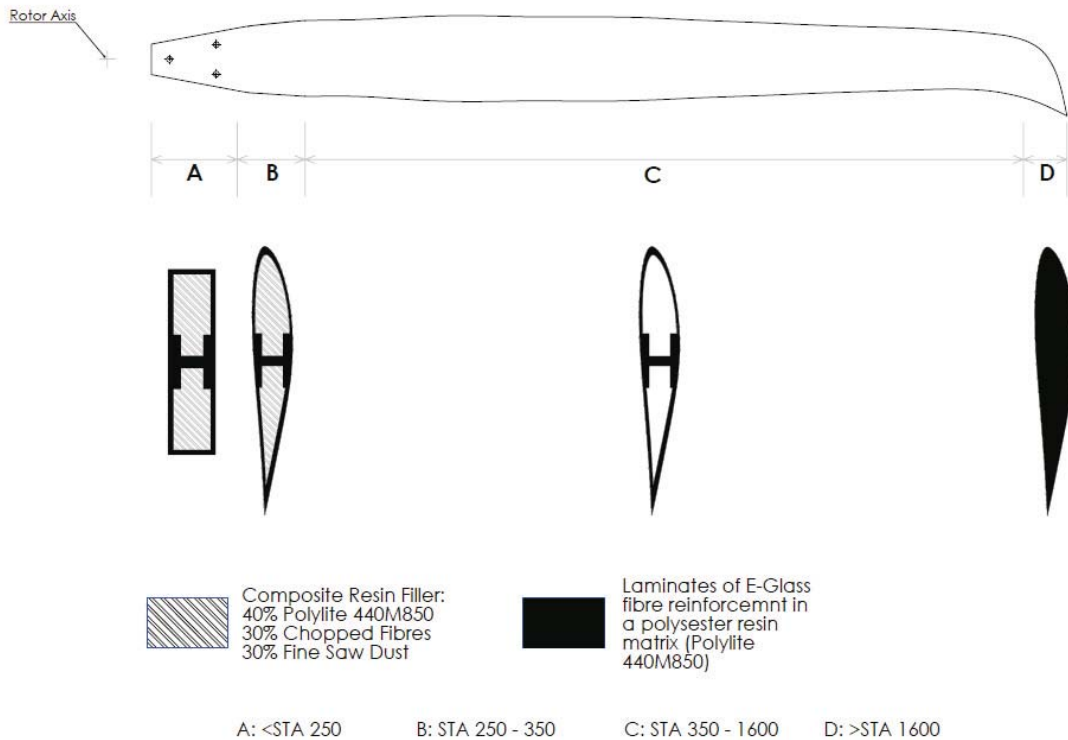


Fig 6: The Blade Profile with Different Sectional Geometries.

5. STRUCTURAL DESIGN OF THE NACELLE AND TOWER

For the structural design of the nacelle and tower, the most important load action comes from the wind. Other environmental conditions that can affect the structural integrity of a wind turbine system include rain, hail, snow and ice loading. These were not considered in this work since Malta's geographic position excludes heavy loads resulting from these conditions. On the other hand, temperature, humidity, solar radiation and lightning were taken into consideration in various aspects of the designed components. An example of this is that the generator, generator/rotor shaft and bearings and the slip rings that connect signal and power cables are all enclosed in the nacelle that offers protection against the latter environmental conditions in Malta.

Load case A is regarded to be a fatigue load case so that fatigue assessment is taken into consideration at the design stage. The other load cases, load cases B to J, are considered to be of the limit type, so that the analysis required the prevention of excessive strain, excessive deflection and static instability. The loads calculated using the simplified load model were used to calculate the important dimensions for the root of the blades, blade hub/shaft assembly, turbine shaft, nacelle bearings, nacelle frame and lifting lugs, main mast flanges, yaw shaft and supporting tower. Code compliant material safety factors were used for the turbine blades, for the turbine shaft, for the nacelle and for the supporting mast and tower. At the design stage all components passed the design checks as stipulated in EN 61400-2. In addition to the design checks required by buckling, modal and limit state analyses were carried out on the turbine tower and mast to ensure that the supporting structure does not suffer a buckling load failure or a limit load failure during turbine operation and to ensure that the natural frequency of the system is not in the range of the rotational speeds (or in multiples) of the turbine. Structural stresses at various points in the nacelle were calculated using the finite element software ANSYS Mechanical in order to perform a fatigue check on the frame of the nacelle. The design of the tower gusset plates and structural joints is not covered in EN 61400-2:2006 so that these

components were designed using BS 8100-1-1999. Figures 7 and 8 show ANSYS Mechanical graphic outputs for some of the various analyses that were carried out.

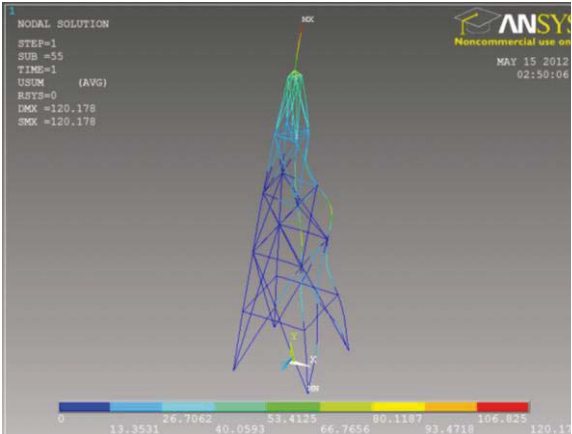


Fig 7: Buckled tower structure for Load Case A.

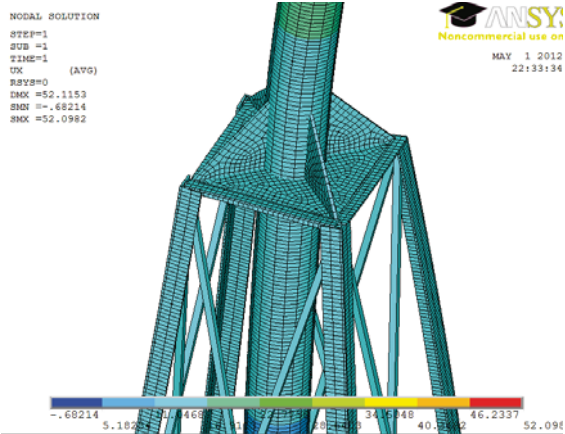


Fig 8: Finite element analysis detail of the mast/tower connection.

6. STRUCTURAL TESTING OF TURBINE BLADES AND TOWER

The nine blades were tested by performing a static load test to validate the design calculations. Each blade was mounted as a cantilever, in a similar way to that for mounting the blades at the rotor hub. Weights were applied at different radial locations to generate the maximum bending moment for load Case H: Parked wind loading with a factor of safety of 3 (Figure 9). The blade tip deflection was found to be much less than the distance between the blade tip and the tower. It is therefore not expected that the blade would hit the tower under extreme wind conditions. Also, no signs of cracking, de-bonding or de-lamination were found on the blades after the test.

MSA EN 61400-2:2006 requires a full scale test to validate the numerical models of the turbine tower and confirm that the supporting structure can carry the design load. In this case, the design load was taken to be the largest horizontal wind thrust calculated using the simplified load equations multiplied by a factor of safety of 3. The full scale load test would also check for any manufacturing or materials defects which were not accounted for in the numerical models and theoretical analysis. Figure 10 shows the schematic diagram of the test setup. The wind generated thrust was simulated by the cable going over the sheaves of a mobile crane and loaded as shown almost at ground level. A load cell was used to measure the load being applied and the structural response of the whole structure was visually checked continuously. Tower members in compression were checked for any signs of buckling. The test confirmed that the support structure can resist the loading as per MSA EN61400-2:2006.



Fig 9: Static blade test.

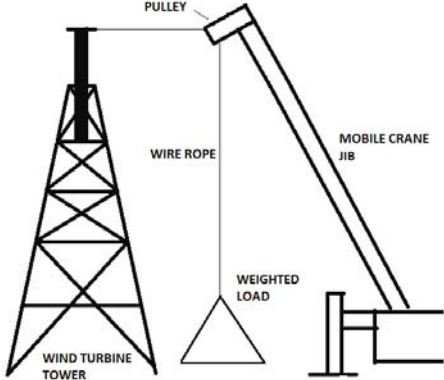


Fig 10: Schematic diagram of the static tower test.

7. WIND MAST DESIGN AND INSTALLATION

Wind resources are a fundamental aspect of long-term wind turbine operation and productivity. Thus they invariably also make up an integral part of a wind machine's performance testing phase. With a proof-of-concept design such as the one in context, controlled testing and fine-tuning, with the possibility of re-design and retesting, was a basic prerequisite. Once installed on the tower, user-intervention and control at all levels would be limited. This requested different, yet concerted approaches, in monitoring of wind resources for wind turbine performance testing.

A wind monitoring mast was designed using the IEC 61400-12-1 standard for wind turbine performance testing as required by. The wind mast was installed very near to the wind turbine site (Figure 2). The mast design was envisaged to enable the raising and lowering of the structure by means of a gin pole. The self-supporting wind mast was guyed in four directions with guy sets at three levels. The upper mast hardware required to support the anemometry consists of a U-shaped piping structure designed to position two anemometers with a horizontal distance separation of 1.5 m at turbine hub height level and a wind vane positioned at a lower level. A dedicated Nomad 1 data logger was installed to enable the compilation of a time referenced data bank of wind speed and direction-related parameters. This dataset was envisaged to enable characterisation of the site-specific wind resources and also to enable wind turbine performance assessment during the field testing phase of the project.

8. DESIGN OF THE ELECTRICAL SYSTEM

In line with the trend for typical small-scale wind turbines, a permanent magnet synchronous generator (PMSG) was considered for generating electricity and feeding it into the national grid. PMSGs allow variable speed operation and relieve the need of dedicated equipment for magnetisation. Such generators also offer the capability to brake the wind turbine in cases of maintenance or emergency. In order to limit the budget, it was opted to go for an off-the-shelf generator. As these are typically designed for three-bladed wind turbines which typically have higher rated speeds, a gearbox was introduced between the wind turbine and the generator. The selection of the generator was based on the expected system's steady-state behaviour at different wind speeds. A range of suitable generator power ratings was identified, based on the expected average power output. The gearbox ratio was then set to fit the operating speed range of the selected generator to the designed wind turbine characteristics.

Following a review of PMSGs available on the market, the Ginlong GL-PMG-1800 was chosen. It is a three-phase generator with a rated power of 1800W at 450rpm. As shown in Figure 11, the PMSG is interfaced to the grid in two stages, with an intermediate DC link. The variable AC output from the generator is converted to DC through a six-pulse rectifier. The DC power is then converted for export to a low-voltage single-phase connection through a grid-tie inverter. The grid-tie inverter allows indirect control of the wind turbine rotor speed through variation of the DC link voltage. It also performs the synchronisation to the grid and provides a number of protection features, most notably anti-islanding protection to disconnect the wind energy system in case of grid failure. A protection circuit is included in the DC link, as illustrated in Figure 11, to protect the generator by diverting the energy to a dump load in cases of grid fault or very high wind speeds.

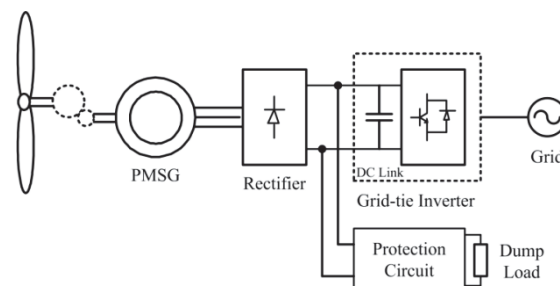


Fig 11: Schematic of the wind turbine electrical system

9. FUTURE WORK

The wind turbine is currently being tested to verify design data most especially wind loads calculated using the simplified load method of analysis. In addition to these, other performance data such as electrical power output and the maximum rotational speed under different wind conditions will be measured. The turbine system's dynamic behaviour will also be documented as part of a duration test as stipulated in EN 61400-2:2006.

ACKNOWLEDGEMENTS

The project was made possible through a 2007 financial grant from the Ministry for Resources and Rural affairs (MRRA) and wish to acknowledge the use of the ANSYS software academic research license and the education edition software SolidWorks provided to the University of Malta by ANSYS Inc. and Dassault Systèmes respectively. Over the recent past years a number of students made valuable contributions towards the project. Albert Borg, Adrian Farrugia, Josianne Cassar, Christian Cordina, Anne Marie Zammit, Ryan Bugeja, Steven Schembri and Ryan Mahoney are being acknowledged for their work on this project undertaken as part of their *B. Eng. (Hons.)* theses. The authors also wish to express their sincere gratitude to Mr Daniel Talma, Professor Charles Pule', engineer Noel Balzan and laboratory officers James Saliba, Daniel Pisani, Andrew Briffa and Kevin Farrugia for their technical support during the construction and installation of the prototype.

NOMENCLATURE:

V_{ref}	Reference wind speed averaged over 10 minutes
V_{ave}	Annual average wind speed at hub height
a_l	Axial load induction factor
c	Local blade chord [m]
C_L	Lift coefficient [-]
r	Radial location [m]
R	Rotor tip radius [m]
φ	Local flow angle [deg]
λ	Rotor tip speed ratio [-]
λ_r	Tip speed ratio of blade section [-]

REFERENCES

- E. Commission, Renewable energy: Progressing towards the 2020 target [Online] Available: <http://eur-lex.europa.eu/LexUriServ.do?uri=COM:2011:0031:FIN:EN:PDF>, Accessed on 29th September 2015
- Farrugia A., 'Conversion of the Chicago type wind pump to generate electricity – the structural aspect'. B.Eng. (Hons.) dissertation, University of Malta, Malta, 2011
- MSA EN 61400-2:2006 – Wind turbines – Part 2: Design requirements for small wind turbines
- MSA EN 1993-1-8, Eurocode 3: Design of steel structures – Part 1-8: Design of joints
- MSA EN 1993-1-9, Eurocode 3: Design of steel structures – Part 1-9: Fatigue
- BS 8100-3:1999, Lattice towers and masts – Part 3: Code of practice for strength assessment of members of lattice towers and masts.
- BS 8100-1:1999, Lattice towers and masts – Part 1: Code of practice for loading.
- ANSYS Academic Research Mechanical, Release 14, Ansys Inc., Canonsburg, USA
- Manwell, J. F., McGowan, J.G. and Rogers, A.L., Wind Energy Explained: Theory, Design and Applications, John Wiley and Sons Ltd. , 2nd Edition, ISBN: 978-0-470-01500-1, 2009.
- Borg., A., Design, Construction and Testing of A Multi-Bladed Wind Turbine Rotor, B.Eng. (Hons.) Thesis, University of Malta, June 2011.
- IEC 61400-12-1 Wind turbines - Part 12-1: Power performance measurements of electricity producing wind turbines
- Nomad data logger, Second Wind Inc., Somerville, MA, USA
- Cassar, J., Performance Testing of a Multi-bladed Wind Turbine Rotor, B. Eng. (Hons.) Thesis, University of Malta, Msida, June 2012.
- Cordina, C., Wind Monitoring and Instrumentation Development for the Performance Testing of a Multi-bladed Wind Turbine Rotor, B. Eng. (Hons.) Thesis, University of Malta, June 2012

Reduction of Current Harmonics in Grid-Connected PV Inverters using Harmonic Compensation - Conforming to IEEE and IEC Standards

Daniel Zammit

Department of Industrial Electrical Power Conversion, Faculty of Engineering, University of Malta, Msida, MSD 2080, Malta

Cyril Spiteri Staines

Department of Industrial Electrical Power Conversion, Faculty of Engineering, University of Malta, Msida, MSD 2080, Malta

Maurice Apap

Department of Industrial Electrical Power Conversion, Faculty of Engineering, University of Malta, Msida, MSD 2080, Malta

Email: daniel.zammit@um.edu.mt

Abstract. This paper deals with the reduction of harmonics generated by Grid-Connected PV Inverters to conform to the harmonic limits set by the IEEE and IEC standards. An analysis of the current harmonics present in the output current of a grid-connected inverter will be presented. The inverter will be current controlled by a Proportional-Resonant (PR) current controller. The design and testing of the PR current controller will be presented. This paper will also deal with the application of harmonic compensation to make the inverter compliant to the standards, by using selective harmonic compensators in addition to the Proportional-Resonant (PR) controller. Both simulation and experimental results will be presented. Testing was carried out on a Grid-Connected PV Inverter which was designed and constructed for this research.

Keywords. Inverters; Proportional-Resonant Controllers; Harmonic Compensation; Photovoltaic.

1. INTRODUCTION

Distributed power generation systems connected to the electricity supply grid are always increasing, especially inverter based renewable energy generation systems. This high penetration of inverter based power generation systems can cause a power quality issue due to the harmonics injected into the supply grid. This means that it is very important to control the harmonics generated by these inverters to limit their adverse effects on the grid power quality. IEEE and European IEC standards suggest harmonic limits generated by Photovoltaic (PV) Systems and Distributed Power Resources for the current total harmonic distortion (THD) factor and also for the magnitude of each harmonic. The IEEE 929 and IEEE 1547 standards allow a limit of 4% for each harmonic from 3rd to 9th and 2% for 11th to 15th. The IEC 61727 standard specifies similar limits.

In current-controlled PV inverters the current controller can have a significant effect on the quality of the current supplied to the grid by the inverter, and therefore it is important that the controller provides a high quality sinusoidal output with minimal distortion to avoid creating harmonics. A controller which is commonly used in current-controlled PV inverters is the Proportional-Resonant (PR) controller. The performance of the PR controller has been discussed in a number of papers including among others. Another type of current controller which can be used in grid-connected inverters is the Proportional-Integral (PI) controller, but this type of controller has the drawback of not being able to follow a sinusoidal reference without steady state error. On the other hand, the PR controller is more suited to operate with sinusoidal

references, and does not suffer from steady state error issues. This makes the PR controller an ideal choice for grid-connected inverters. The PR controller has the ability to provide gain at a certain frequency (resonant frequency) and almost no gain exists at the other frequencies. Although the PR controller has a high ability to track a sinusoidal reference such as a current waveform, the output current of the grid-connected inverter is not immune from harmonic content. Harmonics in the output current can result due to the converter non-linearities as well as from harmonics which are already present in the grid. Selective harmonics in the current can be compensated by using additional PR controllers which act at particular harmonic frequencies to be reduced or eliminated such as the 3rd, 5th, 7th and so on. This compensation can be used to reduce the current THD and make the inverter compliant to the IEEE and IEC standards.

This paper presents the design and analysis of the PR current controller. In addition to the fundamental PR current controller, selective harmonic compensators are designed and applied for the 3rd, 5th and 7th harmonics, to make the inverter system compliant to the IEEE and IEC standards. The design of the current controller and harmonic compensators was carried out using Matlab's SISO Design Tool. Test results obtained by simulations and by experimental tests for the PR and the harmonic compensators will be presented. Experimental testing was carried out on a single phase 3kW grid-connected PV inverter, which was designed and built for this research. Figure 1 shows the block diagram of the Grid-Connected PV Inverter system connected to the grid through an LCL filter used for this research.

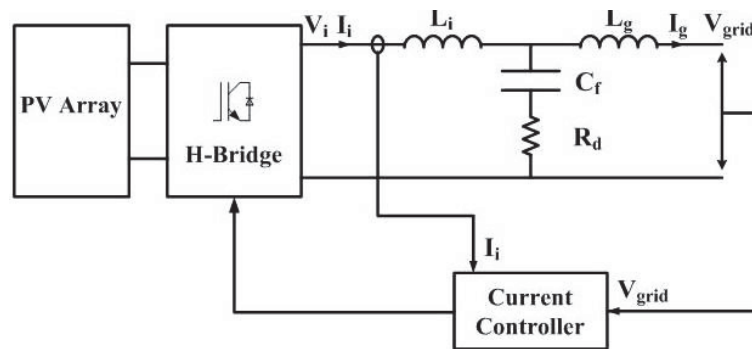


Fig 1. Block diagram of the Grid-Connected PV Inverter with the LCL Filter

This paper is divided into six sections. Section two covers the theory for the LCL filter, the PR current control, as well as the harmonic compensators. Section three covers the design of the LCL filter and the PR current controller including the harmonic compensators. Sections four and five present the simulations and inverter testing, respectively. A comparison of results of the current controllers is covered in section six. Section seven presents the final comments concluding the paper.

2. LCL FILTER AND CURRENT CONTROL

2.1. LCL Filter

The transfer function of the LCL filter of Figure 1 in terms of the inverter current I_i and the inverter voltage U_i , neglecting R_d , is:

$$G_F(s) = \frac{I_i}{U_i} = \frac{1}{L_i s} \frac{\left(s^2 + \left(\frac{1}{L_g C_f} \right) \right)}{\left(s^2 + \left(\frac{L_i + L_g}{L_i L_g C_f} \right) \right)} \quad (1)$$

where, L_i is the inverter side inductor
 L_g is the grid side inductor
and C_f is the filter capacitor

The resonant frequency of the filter is given by:

$$\omega_{res} = \sqrt{\frac{(L_i + L_g)}{(L_i L_g C_f)}} \quad (2)$$

The transfer function in (1) does not include the damping resistor R_d . The introduction of R_d in series with the capacitor C_f increases stability and reduces resonance. This method of damping is a type of passive damping. Whilst there exist other methods of passive damping and also more advanced active damping methods, this particular damping method used was considered enough for the aim and purpose of this research due to its simplicity. The transfer function of the filter taking in consideration the damping resistor R_d is:

$$G_F(s) = \frac{I_i}{U_i} = \frac{1}{L_i s} \frac{\left(s^2 + s \left(\frac{R_d}{L_g} \right) + \left(\frac{1}{L_g C_f} \right) \right)}{\left(s^2 + s \left(\frac{(L_i + L_g) R_d}{L_i L_g} \right) + \left(\frac{L_i + L_g}{L_i L_g C_f} \right) \right)} \quad (3)$$

2.2. PR Control

Figure 2 shows the PR current control strategy. I_i is the inverter output current, I_i^* is the inverter current reference and U_i^* is the inverter voltage reference.

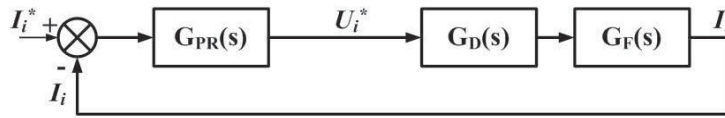


Figure 2. The PR Current Control

The PR current controller $G_{PR}(s)$ is represented by:

$$G_{PR}(s) = K_P + K_I \frac{s}{s^2 + \omega_0^2} \quad (4)$$

where, K_P is the Proportional Gain term, K_I is the Integral Gain term and ω_0 is the resonant frequency.

$G_F(s)$ represents the LCL filter. $G_D(s)$ represents the processing delay of the microcontroller, which is typically equal to the time of one sample T_s and is represented by:

$$G_D(s) = \frac{1}{1 + sT_s} \quad (5)$$

The ideal resonant term on its own in the PR controller provides an infinite gain at the ac frequency ω_0 and no phase shift and gain at the other frequencies. The K_P term determines the dynamics of the system; bandwidth, phase and gain margins.

Equation (4) represents an ideal PR controller which can give stability problems because of the infinite gain. To avoid these problems, the PR controller can be made non-ideal by introducing damping as shown in (6).

$$G_{PR}(s) = K_P + K_I \frac{2\omega_c s}{s^2 + 2\omega_c s + \omega_0^2} \quad (6)$$

where, ω_c is the bandwidth around the ac frequency of ω_0 .

With (6) the gain of the PR controller at the ac frequency ω_0 is now finite and it is still large enough to provide only a very small steady state error. This equation also makes the controller more easily realizable in digital systems due to their finite precision.

2.3. PR Control with Harmonic Compensators

Figure 3 below shows the PR current control with an additional harmonic compensation block $G_H(s)$.

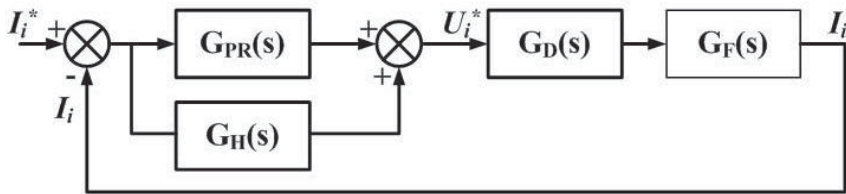


Fig 3. The PR Current Control with Harmonic Compensators

The harmonic compensator $G_H(s)$ is represented by:

$$G_H(s) = \sum_{h=3,5,7,\dots} K_{lh} \frac{s}{s^2 + (h\omega_0)^2} \quad (7)$$

where, K_{lh} is the Resonant term at the particular harmonic and $h\omega_0$ is the resonant frequency of the particular harmonic.

The harmonic compensator for each harmonic frequency is added to the fundamental frequency PR controller to form the complete current controller, as shown in Figure 3.

Equation (7) represents an ideal harmonic compensator which as stated for the fundamental PR controller, can give stability problems due to the infinite gain. To avoid these problems, the harmonic compensator equation can be made non-ideal by representing it using (8).

$$G_H(s) = \sum_{h=3,5,7,\dots} K_{lh} \frac{2\omega_c s}{s^2 + 2\omega_c s + (h\omega_0)^2} \quad (8)$$

where, ω_c is the bandwidth around the particular harmonic frequency of $h\omega_0$.

As for the case of the fundamental PR controller, with (8) the gain of the harmonic compensator at the harmonic frequency $h\omega_0$ is now finite but it is still large enough to provide compensation.

3. LCL FILTER, PR CONTROLLER AND HARMONIC COMPENSATORS DESIGN

3.1. Inverter and LCL Filter Design Parameters

To carry out the tests using the PR control and the harmonic compensation, a 3kW Grid-Connected Inverter was designed and constructed. Designing for a dc-link voltage of 358V, maximum ripple current of 20% of the grid peak current, a switching frequency of 10kHz, filter cut-off frequency of 2kHz and the capacitive reactive power not exceeding 5% of rated power, the following values of the LCL filter were obtained: $L_i = 1.2\text{mH}$, $L_g = 0.7\text{mH}$, $C_f = 9\mu\text{F}$ and $R_d = 8\Omega$.

3.2. PR Controller Design

The block diagram of the system used to design the control is shown in figure 2, with the only difference that an Anti-aliasing filter was introduced in the inverter current feedback path to prevent the aliasing effect when sampling the inverter current. The Anti-Aliasing filter used was a second order non-inverting active low pass filter using the Sallen-Key filter implementation and a Butterworth design with cut-off frequency of 2.5kHz.

The optimal fundamental PR current controller design was carried out using SISO Tool in Matlab. To design the optimal controller, the integral gain K_I at the ac frequency ω_0 must be set large enough to enforce only a very small steady state error, and also set the proportional gain K_P value to obtain sufficient bandwidth accommodating the other harmonic compensators which would otherwise cause system instability. The PR controller was designed for a resonant frequency ω_0 of 314.16rad/s (50Hz) and ω_c was set to be 0.5rad/s, obtaining a K_P of 6.8 and K_I of 1498.72, shown in (9).

$$G_{PR}(s) = 6.8 + 1498.72 \frac{s}{s^2 + s + (2\pi(50))^2} \quad (9)$$

Figure 4 shows the root locus plot in Matlab of the system including the LCL filter, the processing delay, anti-aliasing filter in the output current feedback path and the PR controller. The root locus plot shows that the designed system is stable.

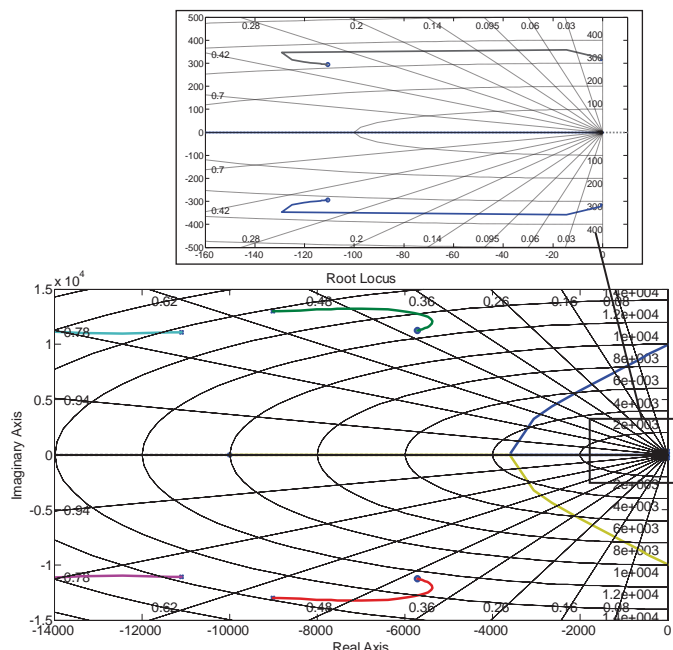


Fig 4. Root Locus of the Inverter with the PR Controller

Figure 5 and figure 6 show the open loop bode diagram and the closed loop bode diagram of the system, respectively. From the open loop bode diagram, the Gain Margin obtained is 13.9dB at a frequency of 9970rad/s and the Phase Margin obtained is 51deg at a frequency of 3300rad/s.

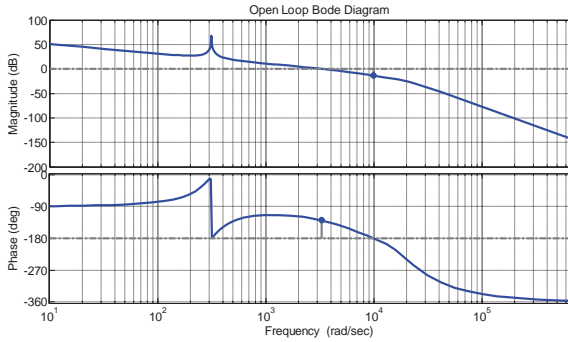


Figure 5. Open Loop Bode Diagram of the System with PR Control

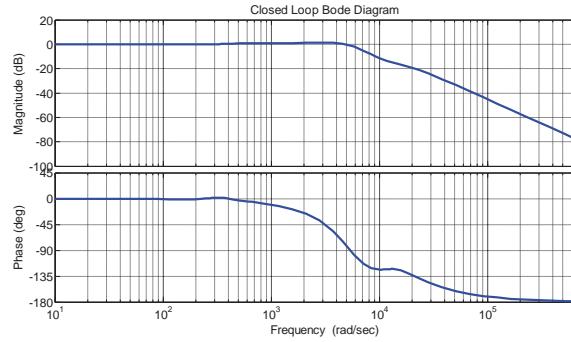


Figure 6. Closed Loop Bode Diagram of the System with PR Control

3.3. Harmonic Compensators Design

The block diagram of the complete system used to design the selective harmonic compensators is shown in figure 3. In the inverter current feedback path the same Anti-aliasing filter as the one used with the PR controller was used to prevent the aliasing effect when sampling the inverter current.

Harmonic compensators were designed for the 3rd, 5th and 7th harmonics. The PR harmonic compensators were designed using SISO Tool in Matlab with the resonant frequency set to the particular frequency to be compensated, i.e. 150Hz for the 3rd harmonic, 250Hz for the 5th harmonic and 350Hz for the 7th harmonic. Similarly to the fundamental PR current control design, the Root Locus, Open Loop and Closed Loop Bode diagrams plotted by SISO Tool were used to achieve the optimal design for each harmonic compensator. Each harmonic compensator was designed on its own and then combined together with the fundamental PR controller at the end in SISO Tool. Ultimately fine tuning of the compensators was performed to obtain the optimum operation of the compensators by varying ω_c and K_I of the corresponding compensator. Care was taken that the system remains stable, by using the gain margin and phase margin stability criteria.

The 3rd harmonic compensator at a resonant frequency $3\omega_0$ of 942.48rad/s (150Hz) was designed with a ω_c of 2.5rad/s and a K_I of 211.208. The 5th harmonic compensator at a resonant frequency $5\omega_0$ of 1570.8rad/s (250Hz) was designed with a ω_c of 4.5rad/s and a K_I of 83.867. The 7th harmonic compensator at a resonant frequency $7\omega_0$ of 2199.11rad/s (350Hz) was designed with a ω_c of 10rad/s and a K_I of 40.834. The transfer function of the complete controller $G_C(s)$ is shown in (10).

$$G_C(s) = G_{PR}(s) + G_{3H}(s) + G_{5H}(s) + G_{7H}(s)$$

$$= \frac{6.8(s^2 + 221.4s + (2\pi \times 50)^2)}{s^2 + s + (2\pi \times 50)^2} + \frac{1056.04s}{s^2 + 5s + (2\pi \times 150)^2} + \frac{754.8s}{s^2 + 9s + (2\pi \times 250)^2} + \frac{816.68s}{s^2 + 20s + (2\pi \times 350)^2} \quad (10)$$

Figure 7 shows the root locus plot in Matlab of the system with the additional harmonic compensators. The root locus plot shows that the designed system is stable.

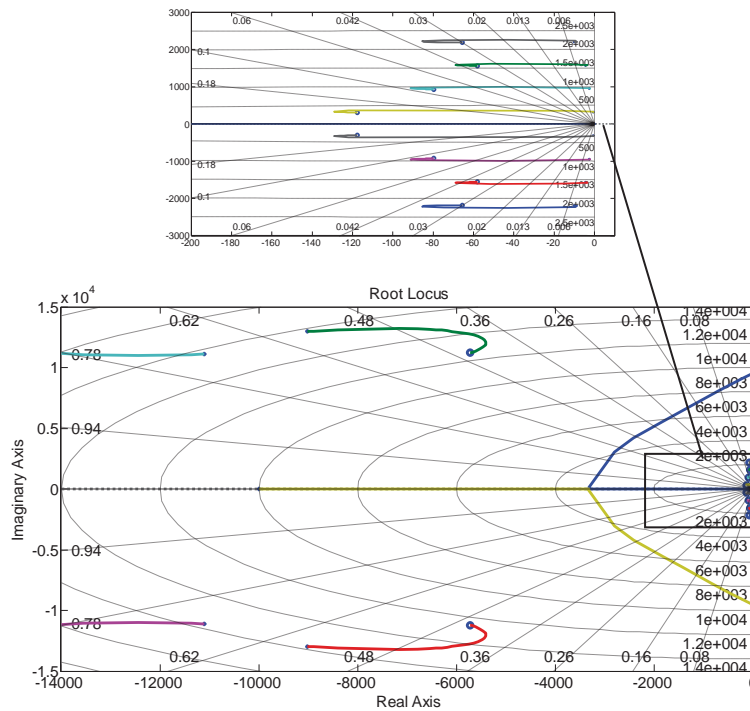


Fig 7. Root Locus of the Inverter with the Fundamental PR Controller and the Harmonic Compensators

Figure 8 and figure 9 show the open loop bode diagram and the closed loop bode diagram of the system, respectively. From the open loop bode diagram, the Gain Margin obtained is 13.2dB at a frequency of 9520rad/s and the Phase Margin obtained is 41.8deg at a frequency of 3310rad/s.

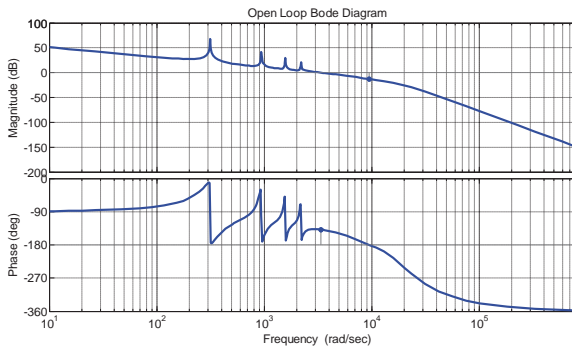


Figure 8. Open Loop Bode Diagram of the System with the Fundamental PR Controller and the Harmonic Compensators

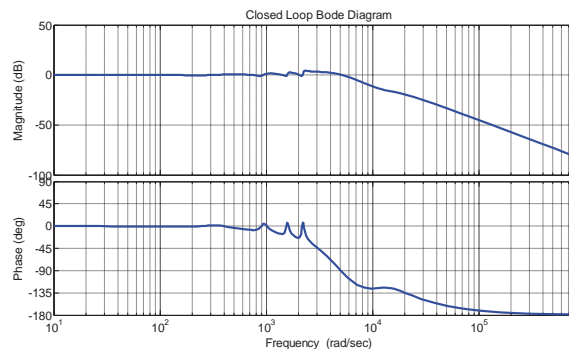


Figure 9. Closed Loop Bode Diagram of the System with the Fundamental PR Controller and the Harmonic Compensators

4. SIMULATIONS

The 3kW Grid-Connected PV Inverter was modelled and simulated in Simulink with PLECS blocksets. The grid voltage was set to 325V peak (230V rms), the dc-link voltage was set to 360V and the reference current was set to 18.446A peak to simulate a 3kW inverter. 3rd, 5th and 7th harmonics were added to the grid voltage corresponding to a Total Harmonic Distortion (THD) of 3.37%, to distort the grid voltage sinusoidal waveform. Simulations were carried out to observe the effect of the harmonics with and without harmonic compensation on the inverter voltage and grid current.

Figure 10 and figure 11 show the inverter voltage (V_{pwm}), the grid voltage (V_{grid}), the capacitor voltage (V_{cap}), the inverter current (I_{inv}), the grid current (I_{grid}) and the reference

current (I_{ref}) from the simulation in the s-domain using the PR controller without and with harmonic compensation, respectively.

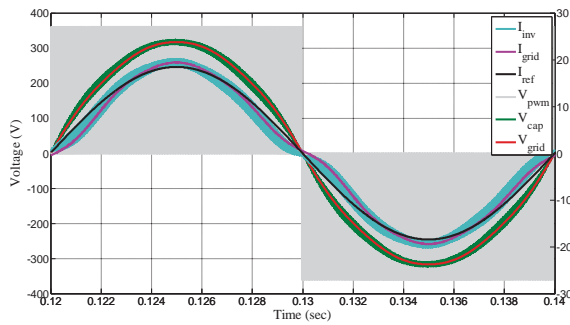


Figure 10. Inverter Operation without Harmonic Compensation (Simulation)

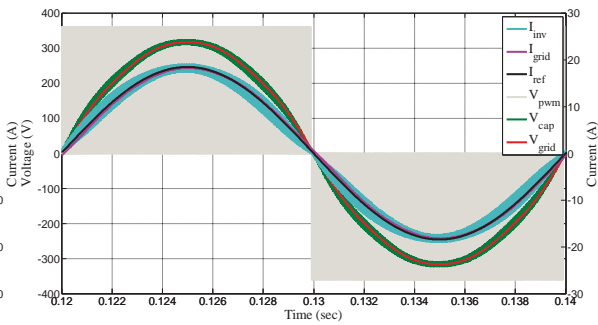


Figure 11. Inverter Operation with Harmonic Compensation (Simulation)

Figure 12 and figure 13 show the harmonic spectrum of the grid current from the simulation using the PR controller without and with harmonic compensation, respectively. From the harmonic spectrum shown in figure 12 it can be seen that the grid current I_{grid} was highly affected by the harmonics present in the grid voltage when no compensation was applied. When considering the harmonics of the grid current as a percentage of the reference current the 3rd, 5th and 7th harmonics were about 8.528%, 3.44% and 1.649%, respectively. When harmonic compensation were applied the 3rd, 5th and 7th harmonics in the grid current I_{grid} were reduced to 0.613%, 0.474% and 0.388%, respectively, as can be observed from figure 13.

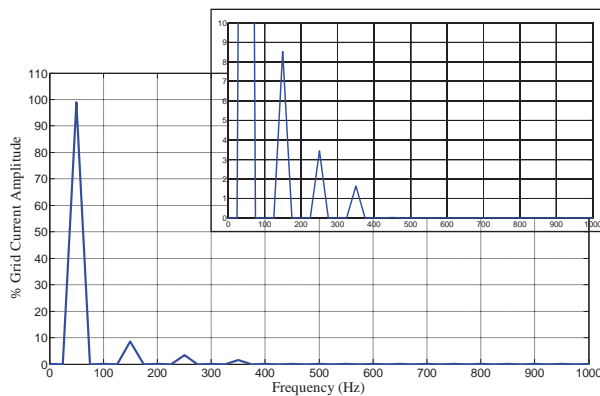


Figure 12. Harmonic Spectrum of the Grid Current without Harmonic Compensation (Simulation)

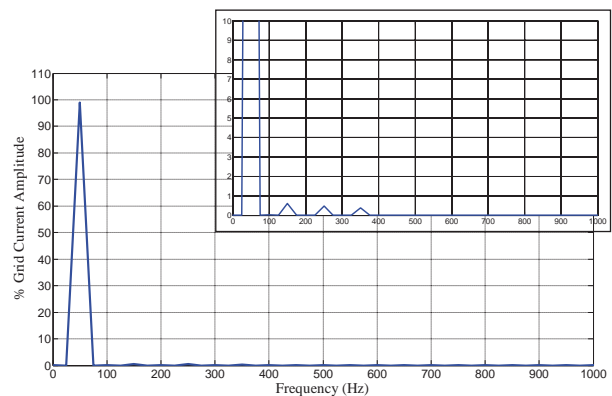


Figure 13. Harmonic Spectrum of the Grid Current with Harmonic Compensation (Simulation)

5. GRID-CONNECTED PV INVERTER TESTING

The constructed 3kW Grid-Connected PV Inverter test rig is shown in figure 14 below. The inverter was operated at a switching frequency of 10kHz and was connected to a 50Hz grid supply. The inverter was controlled by the dsPIC30F4011 microcontroller from Microchip. Testing was carried out using the PR controller without and with the selective harmonic compensators to analyze the performance of the compensators. The inverter was connected to the grid using a variac to allow variation of the grid voltage for testing purposes. A dc link voltage of 300V was obtained from a dc power supply. The grid voltage was set to 154V rms and the preset reference value of the controller was set to 8A peak.



Fig 14. 3kW Grid-Connected PV Inverter Test Rig

Tests were performed to measure the voltage harmonics present in the grid voltage. The 3rd, 5th and 7th harmonics present in the grid voltage were typically about 0.9%, 1.912% and 0.231%, respectively.

Figure 15 and figure 16 show the grid current for the grid-connected inverter with the PR current controller without harmonic compensation and with 3rd, 5th and 7th harmonic compensation, respectively. I_g is the grid current, I_{gr} is the reconstructed grid current up to its 13th harmonic (a reconstruction of the grid current by adding the first 13 lower harmonics) and I_{gfund} is the fundamental component of the grid current.

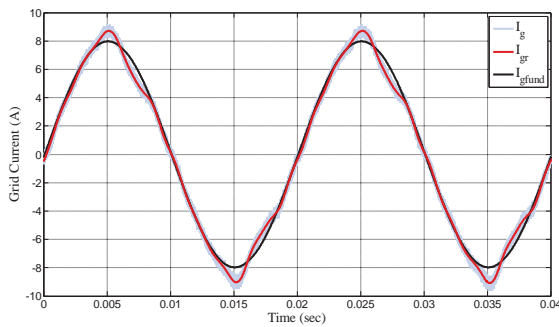


Figure 15. Inverter Grid-Side Current without Harmonic Compensation

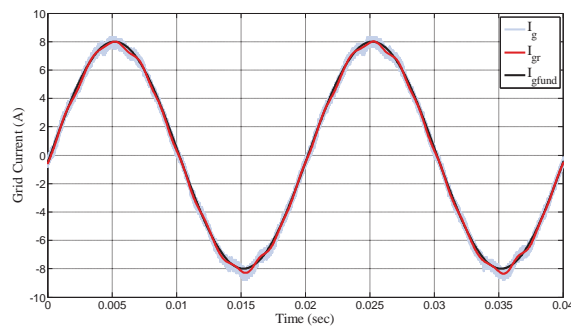


Figure 16. Inverter Grid-Side Current with the 3rd, 5th and 7th Harmonic Compensation

Figure 17 and figure 18 show the harmonic spectrum of the grid current with PR current control without harmonic compensation and with 3rd, 5th and 7th harmonic compensation, respectively. Without harmonic compensation the 3rd, 5th and 7th harmonics resulted about 5.574%, 4.231% and 2.435% of the reference value of 8A peak, respectively. When the harmonic compensators were used the 3rd, 5th and 7th harmonics resulted about 0.378%, 0.641% and 0.24% of the reference value of 8A peak, respectively.

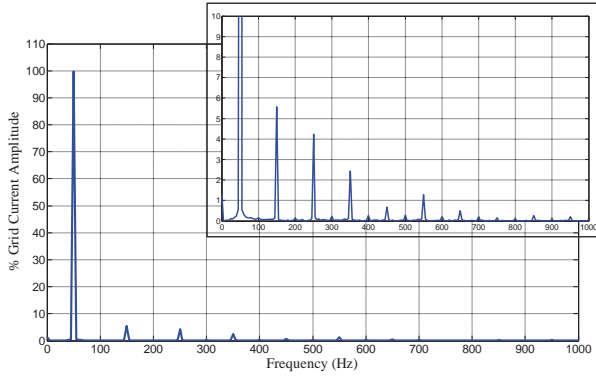


Figure 17. Inverter Grid-Side Current Harmonic Spectrum without Harmonic Compensation

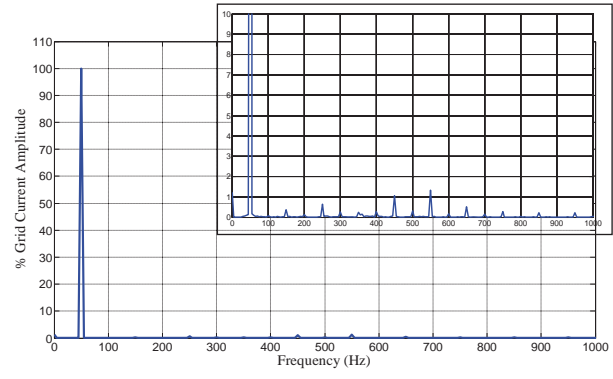


Figure 18. Inverter Grid-Side Current Harmonic Spectrum with the 3rd, 5th and 7th Harmonic Compensators

6. COMPARISON OF EXPERIMENTAL RESULTS

Table 1 Fundamental and Harmonics for the PR Current Controlled Grid-Connected Inverter with Selective Harmonic Compensation

	I_g (Fund.)	I_g (3 rd Harm.)	I_g (5 th Harm.)	I_g (7 th Harm.)
Fund. PR, no compensation	100 %	5.574 %	4.231 %	2.435 %
Fund. PR, 3 rd , 5 th , 7 th Harm. compensation	100 %	0.378 %	0.641 %	0.24 %

The 3rd, 5th and 7th harmonics in the grid voltage were typically about 0.9%, 1.912% and 0.231%, respectively. Table 1 shows the percentage fundamental and harmonic content of the grid current for the PR current controlled grid-connected inverter without and with the selective harmonic compensators. The percentage calculations for the grid current are based on the reference current of 8A peak. The experimental results show the harmonic compensators drastically reduced the 3rd, 5th and 7th harmonics in the grid current. The IEEE 929 and IEEE 1547 standards allow a limit of 4% for each harmonic from 3rd to 9th and 2% for 11th to 15th. The IEC 61727 standard specifies similar limits. As can be observed from the results obtained the 3rd and 5th harmonics were above the limit when no harmonic compensation was applied. These harmonics result from the inverter non-linearities and also from the harmonics already present in the grid supply. The harmonic compensators reduced the 3rd and 5th harmonics within the limits and reduced further the 7th harmonic, thus making the inverter compliant to the standard regulations.

7. CONCLUSION

This paper dealt with the reduction of current harmonics generated by grid-connected inverters to make the inverter compliant to the standard regulations. The procedure to design a Proportional Resonant (PR) current controller with additional selective harmonic compensators was presented. Results from simulations as well as from experimental tests were presented and analysed, which showed the effectiveness of the harmonic compensation technique to reduce the current harmonics in the grid current. Experimental testing was carried out on a 3kW Grid-Connected Photovoltaic (PV) Inverter which was designed and built for this research. The 3rd, 5th and 7th harmonics in the grid current were reduced from about 5.574%, 4.231% and 2.435%, respectively, to about 0.378%, 0.641% and 0.24%, respectively, thus making the grid-connected inverter compliant to the IEEE and IEC standard regulations.

REFERENCES

- IEEE 929 2000 Recommended Practice for Utility Interface of Photovoltaic (PV) Systems.
- IEEE 1547 Standard for Interconnecting Distributed Resources with Electric Power Systems.
- IEC 61727 2004 Standard Photovoltaic (PV) Systems – Characteristics of the Utility Interface.
- R. Teodorescu, F. Blaabjerg, U. Borup, M. Liserre, “A New Control Structure for Grid-Connected LCL PV Inverters with Zero Steady-State Error and Selective Harmonic Compensation”, APEC’04 Nineteenth Annual IEEE Conference, California, 2004.
- M. Liserre, R. Teodorescu, Z. Chen, “Grid Converters and their Control in Distributed Power Generation Systems”, IECON 2005 Tutorial, 2005.
- M. Ciobotaru, R. Teodorescu, F. Blaabjerg, “Control of a Single-Phase PV Inverter”, EPE2005, Dresden, 2005.
- D. N. Zmood, D. G. Holmes, “Stationary Frame Current Regulation of PWM Inverters with Zero Steady-State Error”, IEEE Transactions on Power Electronics, Vol. 18, No. 3, May 2003.
- D. Zammit, C. Spiteri Staines, M. Apap, “Comparison between PI and PR Current Controllers in Grid Connected PV Inverters”, WASET, International Journal of Electrical, Electronic Science and Engineering, Vol. 8, No. 2, 2014.
- R. Teodorescu, F. Blaabjerg, M. Liserre, P. C. Loh, “Proportional-Resonant Controllers and Filters for Grid-Connected Voltage-Source Converters”, IEEE Proc. Electr. Power Appl, Vol. 153, No. 5, 2006.
- M. Castilla, J. Miret, J. Matas, L. G. de Vicuna, J. M. Guerrero, “Control Design Guidelines for Single-Phase Grid-Connected Photovoltaic Inverters with Damped Resonant Harmonic Compensators”, IEEE Transactions on Industrial Power Electronics, Vol. 56, No. 11, 2009.
- D. Zammit, C. Spiteri Staines, M. Apap, “PR Current Control with Harmonic Compensation in Grid Connected PV Inverters”, WASET, International Journal of Electrical, Computer, Electronics and Communication Engineering, Vol. 8, No. 11, 2014.
- V. Pradeep, A. Kolwalkar, R. Teichmann, “Optimized Filter Design for IEEE 519 Compliant Grid Connected Inverters”, IICPE 2004, Mumbai, India, 2004.
- R. Teodorescu, M. Liserre, P. Rodriguez, “Grid Converters for Photovoltaic and Wind Power Systems”, Wiley, 2011.
- M. Liserre, F. Blaabjerg, S. Hansen, “Design and Control of an LCL-Filter Based Three Phase Active Rectifier”, IEEE Transactions on Industry Applications, Vol 41, No. 5, Sept/Oct 2005.



SBE16
MALTA
INTERNATIONAL CONFERENCE

**Europe and the Mediterranean
Towards a Sustainable Built Environment**

Conference Partners

Platinum Sponsors



Silver Sponsors



Bronze Sponsors



Collaborators



UNIVERSITY OF MALTA
L-Università ta' Malta



MINISTRY FOR SUSTAINABLE DEVELOPMENT,
THE ENVIRONMENT AND CLIMATE CHANGE



Building Industry Consultative Council



European Project Collaborations





SBE16 MALTA

INTERNATIONAL CONFERENCE

Europe and the Mediterranean: Towards a Sustainable Built Environment

Edited by Ruben Paul Borg, Paul Gauci, Cyril Spiteri Staines

SBEMALTA



UNIVERSITY OF MALTA
L-Università ta' Malta



MINISTRY FOR SUSTAINABLE DEVELOPMENT,
THE ENVIRONMENT AND CLIMATE CHANGE



Building Industry Consultative Council